DISPERSION OF POLLUTANTS IN ESTUARY TYPE FLOWS

by
Edward R. Holley, Jr. and Donald R.F. Harleman

HYDRODYNAMICS LABORATORY
Report No. 74

Prepared Under
Research Grant No. WP-00071
Division of Water Supply and Pollution Control
Public Health Service
Department of Health, Education and Welfare

JANUARY 1965

MIT

DEPARTMENT OF CIVIL ENGINEERING

SCHOOL OF ENGINEERING
MASSACHUSETTS INSTITUTE OF TECHNOLOGY
Cambridge 39, Massachusetts

T65-02

HYDRODYNAMICS LABORATORY
Department of Civil Engineering
Massachusetts Institute of Technology
Cambridge 39, Massachusetts

DISPERSION OF POLLUTANTS IN ESTUARY TYPE FLOWS

by

Edward R. Holley, Jr. and Donald R.F. Harleman

January 1965

Report No. 74

Prepared Under
Research Grant No. WP-00071
Division of Water Supply and Pollution Control
Public Health Service
Department of Health, Education and Welfare

ABSTRACT

Submitted to the Department of Civil Engineering on September 21, 1964, in partial fulfillment of the requirements for the degree of Doctor of Science

Much of the engineering literature has failed to show an understanding of the mechanism of longitudinal dispersion which arises in the one dimensional representation of pollution transport in turbulent shear flows. In the present work, it is shown that the one dimensional form of the mass balance equation may be obtained by spatially averaging the three dimensional mass balance equation. This averaging indicates that the convective transport cannot be represented in a one dimensional equation solely by the average velocity and average concentration at a section since there is a net transport associated with the variations of velocity and concentration from their averages. This net transport (called longitudinal dispersion) is shown to be diffusive in nature for uniform flow, and it is assumed to be diffusive for non-uniform flow. Thus, the mass transport due to dispersion is proportional to the longitudinal gradient of average concentration. The relative importance of dispersion depends on the relative steepness of the concentration gradient.

A review is given of the procedures which have been used for modeling dispersion in estuaries. Investigation of the model laws, the dispersive mechanism, and model verification procedures indicates that model results on concentration distributions have been incorrectly transferred to prototype scale in the constant density regions of estuaries. It is shown that in distorted models concentration ratios are not numerically the same at geometrically similar points as has been assumed. This assumption has resulted in predicted concentrations which are an order of magnitude too large in many cases.

An analytical method is presented for calculating the dispersion coefficient for uniform oscillating flow of the type found in constant density regions of estuaries. For turbulent estuary type flow in a uniform pipe of radius a, the analytical value of the dispersion coefficient is $10.1\, a u_*$, where u_* is the shear velocity (square root of boundary shear stress divided by fluid density). Since u_* is a periodic function of time, so is the dispersion coefficient. It is shown that after one or two periods of dispersal of mass, a sufficiently accurate concentration distribution may be obtained by use of a constant dispersion coefficient (viz., the time average of the dispersion coefficient during a period of tidal oscillation).

A mass balance equation representing conditions at "slack" times in an estuary is commonly used as a mathematical model for the distribution of a pollutant. The results of this investigation may be used to estimate the time averaged dispersion coefficient in this equation for constant density portions of tidal estuaries. Thus, preliminary estimates of concentration distributions may be obtained for known input conditions.

ACKNOWLEDGEMENTS

The author is grateful for all phases of the guidance given by Professor Donald R. F. Harleman. In particular, Professor Harleman conceived the research topic which was used for this thesis and supervised the thesis work. This was by no means the limit of his quidance.

Gratitude is also due to Professor Norman H. Brooks, of the California Institute of Technology. During the year that he and Professor Harleman held exchange Visiting Professorships, the author gained much from studying and working under him.

Appreciation is expressed to all the staff of the Hydrodynamics Laboratory at M.I.T., especially to the graduate research assistants with whom many beneficial discussions were held. Particular thanks are due to Wayne Huber, for his conscientious work as a graduate assistant; to John Hoopes, for many hours devoted to the discussion of research and academic topics; and to Uri Shamir, for time spent in discussions and in translating foreign articles.

During the author's graduate study at M.I.T., financial assistance was received from the Sloan Foundation, the Ford Foundation, the National Science Foundation, the Humanities Fund, the National Institutes of Health, and the John R. Freeman Fund of the Boston Society of Civil Engineers. Particular thanks are due to B.S.C.E. for their generous support of the author during the major part of the time which was spent on the thesis research. The research project was supported throughout by the Public Health Service, Division of Water Supply and Pollution Control, under research grant No. WP-00071. Above all, the author is indebted to his wife, Peggy, for her willingness to work to provide financial support during part of the graduate study and for her support in many other ways.

The use of the M.I.T. Computation Center, where part of this research was carried out, is achnowledged.

TABLE OF CONTENTS

1) INTRODUCTION

1.1) General Problem of Pollution

Rivers and estuaries are highly important in the disposal of domestic and industrial waste materials. Questions arise as to how a given waste material will be transported by the river, what the distribution of the material will be at a given time, and how rapidly the material will be removed from the river or estuary after having been introduced. These questions fall into the general category of fluid transport problems, and the answers depend both on the hydraulic or flow characteristics of the river under consideration and on the characteristics of the particular material being transported.

The most effective way to analyze such transport problems is in the formation of a mass balance equation (or conservation of mass equation) for the substance of interest. This mass balance equation is essentially a method of bookkeeping which takes account of the various factors which influence the quantity and distribution of the substance. In Section 2, a general mass balance expression is presented as a differential equation. In this general equation, the direct effects of the hydraulic transport mechanisms (i.e., the convection and dispersion) have been represented explicitly. It is possible to do this because the convection and dispersion depend only on the fluid motion and not on the characteristics of the substance which is being transported.

In order to write a conservation equation, it is necessary to also include factors such as decay of the substance being transported, absorption of the substance across the flow boundaries, etc. These factors depend on the characteristics of the substance being transported and, in the general mass balance equation, are represented by general terms. To apply the general conservation equation to any particular substance, information must be available concerning what factors or reactions are to be considered and concerning the rates at which these reactions take place. A substance is said to be conservative if there are none of these additional factors or reactions which must be considered. That is, a substance is considered to be conservative if none of the substance is diffused

across the flow boundaries or produced (or destroyed) within the flow. For example, salinity is generally conservative. Dissolved oxygen is usually non-conservative because it may be consumed by biochemical oxygen demand (BOD) and because it may be absorbed from the atmosphere or produced by algae. Just as oxygen is consumed by BOD, BOD and other industrial wastes may react with dissolved oxygen or may undergo other digestive processes. Thus, these wastes are non-conservative. Radioactive material is non-conservative by virtue of its decay. Tracers, such as dye, may be absorbed by the flow boundaries and thus be lost to the flow. In these cases, it is necessary to know the rates at which these processes and reactions take place in order to apply the general mass balance equation to a specific case.

There is the possibility that various types of reactions may be associated with a particular substance. For the present work, an important fact is that these reactions and the hydraulic transport processes are independent. Hence, a conservative substance may be used to study dispersion, and the information gained in this way may be applied to the dispersion of a non-conservative substance.

One objective of studies of mixing processes in rivers and estuaries is to gain information on dispersion so that concentration distributions may be predicted. The first prerequisite in obtaining this objective is a clear understanding of the mechanism of longitudinal dispersion. A certain amount of confusion exists in the literature in regard to diffusion and dispersion processes in pollution analysis.

Following a discussion of the mechanisms of dispersion, the next step is an investigation of the relation between dispersion and other hydraulic parameters about which information is more readily obtainable. This is desirable so that a direct evaluation of dispersion does not have to be made in every individual situation. There are at least four methods of seeking the relation between dispersion and other parameters: (1) analytical methods, (2) laboratory (experimental) studies in idealized flow situations, (3) scale models of specific situations, and (4) field studies in rivers and estuaries. All four of these enter the present work to varying degrees. Unfortunately, each one of these approaches has its limitations. Analytical and laboratory studies are useful because they may be used to investigate the

basic dispersive process free from secondary and complicating influences. For this very reason, the results of analytical and laboratory work represent only an approximation to most practical cases. On the other hand, the results of model and field studies are influenced by the secondary factors of the particular case being studied, and the application of these results to other cases is often difficult. Also, the use of models assumes that certain laws of similitude between model and prototype have been developed. It will be shown that in some cases incorrect conclusions have been drawn from the model studies of mixing processes.

As shown in Fig. 1-1, the course of a stream from its origin to the ocean may be divided into a region of unidirectional flow (the river) and a region where tidal effects are present (the estuary). The estuary may also be subdivided into a region which contains only fresh water and a region where salinity has intruded from the ocean. Regardless of which region is being considered, the fundamental factors which contribute to dispersion are the same. These factors are the distribution of velocity and the distribution of turbulent diffusivity across the section. Yet, in each region, the general type of distribution of velocity and diffusivity will be different. Thus, it is to be expected that the dispersion coefficient may be related to different hydraulic parameters in the different regions. All of the regions are dealt with to some extent in the present work. However, the primary interest is in the fresh water portion of estuaries.

1.2) Summary of the Present Work

The three dimensional mass balance equation is developed and time averaged to obtain an expression which includes turbulent diffusion. Next, the details are presented to show how the time averaged equation may be spatially averaged to arrive at a one-dimensional mass balance equation for unsteady, non-uniform flow. In this development it is seen that longitudinal dispersion must be considered in order to correctly and completely represent a transport problem in a one dimensional frame work. It is also pointed out that in different situations, the importance of the dispersive transport

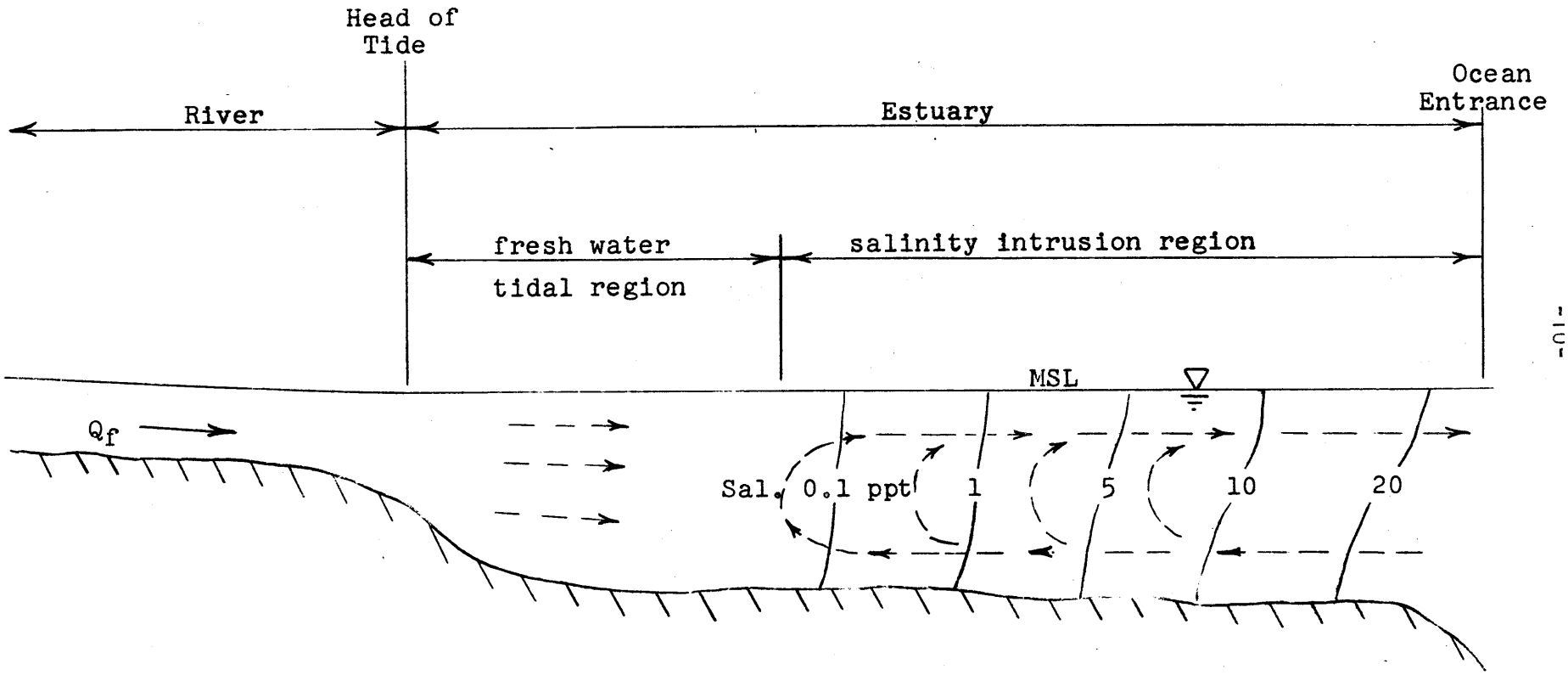

Fig. 1-1: Regions of a natural stream including mean current pattern for estuary

relative to the convective transport may be expected to vary.

In light of the development to obtain the one-dimensional mass balance equation, a discussion is presented of the previous work on dispersion in both steady (river) flow and estuary type flow. It is seen that good analytical predictions of the dispersion coefficient have been made for steady, uniform flow, but not for unsteady, non-uniform flow. This raises the question of modeling longitudinal dispersion. Thus, modeling laws for dispersion are discussed, particularly as they apply to estuary models.

To demonstrate the general manifestations of dispersion, solutions for various boundary conditions are presented and discussed for the one dimensional mass balance equation in steady, uniform flow. Then attention is turned to unsteady estuary type flow. A detailed analysis of dispersion in uniform estuary type flow is presented. This analysis includes the determination of an analytical expression for the dispersion coefficient in estuary type flow. In view of the analysis, an investigation is made into the importance of the time variation of the dispersion coefficient during a period of (tidal) oscillation. Next, some solutions to the one-dimensional equation for uniform estuary type flow are presented.

After discussing some methods for the experimental determination of dispersion coefficients, the experimental program is described. In this program, dispersion coefficients were experimentally determined to check the validity of the analysis for estuary type flow.

2) MASS BALANCE EQUATIONS

2.1) Introduction

In this section, mass balance equations are presented for the case of a substance P which is introduced into and transported by a fluid R. It is assumed that the density of the mixture is independent of the concentration of P in R. This condition is satisfied exactly if P is a fluid with the same density as R. This condition may be satisfied approximately if P is a fluid which differs only slightly in density from R or if the concentration of P is small. First, a general three dimensional conservation equation will be obtained in which the mass transfer by fluid convection is completely and correctly represented in the convective terms. In applying the conservation equation to turbulent flow, it is frequently convenient to write the velocity as a time averaged velocity plus a turbulent fluctuation. It will be shown that time averaging of the general conservation equation leads to an expression where the convection may be written in terms of the time averaged velocity. However, it is seen that there is a net convection associated with the turbulent fluctuations and this transport must be accounted for also. This requirement may be satisfied by representing this net convection as turbulent diffusion. In still other cases where there is a primary direction of flow, it is often convenient to represent the convection as being one dimensional, i.e., convection at a rate given by the spatially averaged velocity at each section. It will also be shown that the conservation equation may be averaged across the flow section to obtain a mass balance with a one dimensional convective term. Just as turbulent fluctuations have a net convection compared to the time averaged velocity, so spatial variations in the velocity and concentration at a given section will be seen to give a net convection compared to the one dimensional velocity. This convection due to the spatial variations may also be represented as a diffusive transport and is called longitudinal dispersion.

2.2) Definitions

Let the concentration c and the density ρ be defined as follows:

$$c = \frac{\text{mass of P}}{\text{mass of solution or mixture of P in R}}$$

$$\rho = \frac{\text{mass of solution}}{\text{volume of solution}}$$

Thus,

$$\rho c = \frac{\text{mass of P}}{\text{volume of solution}}$$

The axes of a Cartesian coordinate system are taken as x, y, z, and the fluid velocities in the three directions are taken respectively as u, v, w. For turbulent flow, the velocity components and the concentration may be written as

$$\begin{aligned} u &= \bar{u} + u' \\ v &= \bar{v} + v' \\ w &= \bar{w} + w' \\ c &= \bar{c} + c' \end{aligned} \qquad 2\text{-}1$$

where the bar indicates a time-averaged quantity and the prime indicates the turbulent fluctuation of a quantity. The time average of any quantity, for example u, is defined by

$$\bar{u} = \frac{1}{T} \int_{t}^{t+T} u \, dt \qquad 2\text{-}2$$

where T is a time which is large relative to the time scale of the turbulence that is present but small compared to any gross unsteadiness which may be present.

To write the differential form of the mass balance equation, an elemental volume will be considered. This volume has sides dx, dy, dz as shown in Fig. 2-1. The mass balance requires that the time rate of increase of mass within the volume be equal to the net rate of influx across the boundaries plus the net rate of production of mass within the volume. For present considerations, the primary mechanisms for flux of mass across the boundaries are convection by the velocities u, v, w and molecular diffusion. According to Fick's first law (Ref. 8), the rate of mass transport due to molecular diffusion may be written as

$$j_x = - \rho A_x D_m \frac{\partial c}{\partial x}$$

$$j_y = - \rho A_y D_m \frac{\partial c}{\partial y} \qquad 2\text{-}3$$

$$j_z = - \rho A_z D_m \frac{\partial c}{\partial z}$$

where j_x, j_y, j_z are the rates of mass transport in the x, y, and z directions, the A's are the areas through which diffusion takes place (A_x perpendicular to x, etc.), and D_m is the molecular diffusion coefficient.

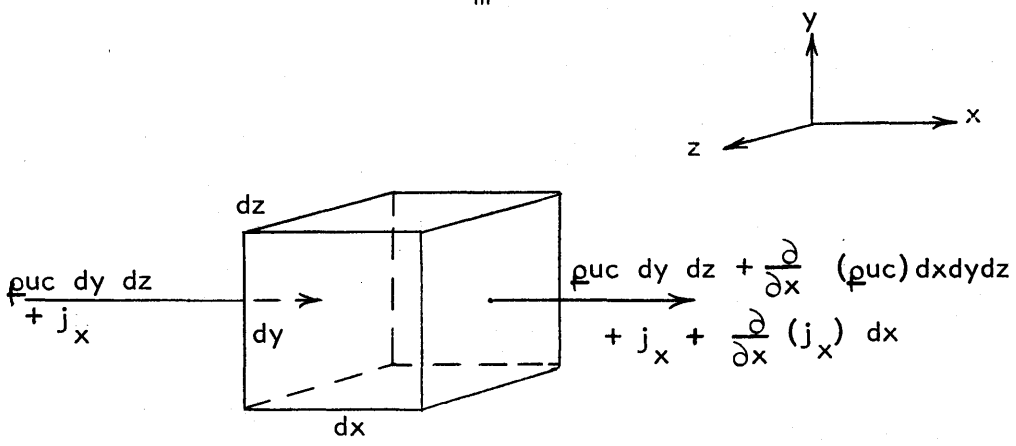

Fig. 2-1: Elemental Volume for Three Dimensional Mass Balance Equation

2.3) General Mass Balance Equation

Fig. 2-1 shows the rates of mass flux due to convection and molecular diffusion through the faces perpendicular to the x direction. Similar expressions may be written for the flux through the other faces. If n_P is written for the rate of production of P per unit volume of solution, then the mass balance for P is

$$\frac{\partial(\rho c)}{\partial t} + \frac{\partial}{\partial x}(\rho uc) + \frac{\partial}{\partial y}(\rho vc) + \frac{\partial}{\partial z}(\rho wc)$$

$$= \frac{\partial}{\partial x}(\rho D_m \frac{\partial c}{\partial x}) + \frac{\partial}{\partial y}(\rho D_m \frac{\partial c}{\partial y}) + \frac{\partial}{\partial z}(\rho D_m \frac{\partial c}{\partial z}) + n_P \qquad 2\text{-}4$$

This equation states that the rate of increase of the mass of P within the elemental volume is equal to the net rate of influx of P plus the rate of production of P within the volume.

Eqn. 2-4 was written as the mass balance of P. A similar equation may be written for the mass balance of R, the fluid which is transporting P. Let the concentration of R be r. Thus, r = 1-c, and by analogy to Eqn. 2-4, the mass balance for R is

$$\frac{\partial(\rho r)}{\partial t} + \frac{\partial}{\partial x}(\rho ur) + \frac{\partial}{\partial y}(\rho vr) + \frac{\partial}{\partial z}(\rho wr)$$

$$= \frac{\partial}{\partial x}(\rho D_m \frac{\partial r}{\partial x}) + \frac{\partial}{\partial y}(\rho D_m \frac{\partial r}{\partial y}) + \frac{\partial}{\partial z}(\rho D_m \frac{\partial r}{\partial z}) \qquad 2\text{-}5$$

By adding Eqn. 2-5 to Eqn. 2-4, one finds

$$\frac{\partial \rho}{\partial t} + \frac{\partial}{\partial x}(\rho u) + \frac{\partial}{\partial y}(\rho v) + \frac{\partial}{\partial z}(\rho w) = 0 \qquad 2\text{-}6$$

which is the general equation of continuity for the solution.

2.4) Mass Balance Equation for Turbulent Flow

Eqn. 2-4 is applicable to turbulent flows as it is written. However, to use it in this form, it would be necessary to use the actual (turbulent) velocities u, v, w. It is usually more convenient to work with time averaged quantities. A mass balance in terms of these time averaged quantities may be

obtained in the following way: Introduce the expressions of Eqn. 2-1 into Eqn. 2-4, and expand the products of sums. Then take the time average of the resulting equation in accordance with the definition contained in Eqn. 2-2. Under this averaging process, all terms having only one primed quantity go to zero. After performing these operations, the mass balance equation may be written as

$$\frac{\partial(\rho\bar{c})}{\partial t} + \frac{\partial}{\partial x}(\rho\bar{u}\bar{c}) + \frac{\partial}{\partial y}(\rho\bar{v}\bar{c}) + \frac{\partial}{\partial z}(\rho\bar{w}\bar{c})$$

$$+ \frac{\partial}{\partial x}(\rho\overline{u'c'}) + \frac{\partial}{\partial y}(\rho\overline{v'c'}) + \frac{\partial}{\partial z}(\rho\overline{w'c'}) \qquad 2\text{-}7$$

$$= \frac{\partial}{\partial x}(\rho D_m \frac{\partial\bar{c}}{\partial x}) + \frac{\partial}{\partial y}(\rho D_m \frac{\partial\bar{c}}{\partial y}) + \frac{\partial}{\partial z}(\rho D_m \frac{\partial\bar{c}}{\partial z}) + \overline{n_p}$$

where the bars indicate the time average defined in Eqn. 2-2. Thus, it is seen that the turbulent fluctuations (u', v', w', c') give rise to a net convection of mass. By analogy to molecular fluctuations which produce molecular diffusion, the convective transport due to turbulent fluctuations is often represented as a diffusive process. Also, by analogy to Fick's first law, the transport due to turbulent fluctuations is assumed to be proportional to the gradient of concentration, i.e.,

$$\rho\overline{u'c'} = -\rho e_x \frac{\partial\bar{c}}{\partial x}$$

$$\rho\overline{v'c'} = -\rho e_y \frac{\partial\bar{c}}{\partial y} \qquad 2\text{-}8$$

$$\rho\overline{w'c'} = -\rho e_z \frac{\partial\bar{c}}{\partial z}$$

where e_x, e_y, e_z are the turbulent diffusion coefficients or the turbulent diffusivities.

The representation of Eqn. 2-8 is also suggested by analogy between mass transport and momentum transport since Navier-Stokes equations may be considered as momentum equations. The turbulent velocities of Eqn. 2-1 may be introduced into the Navier-Stokes equations, and these equations may then be time averaged. When this is done, it is found that there is a net momentum transfer or apparent stress arising from terms like $\overline{u'v'}$. For flow in the x direction, $\rho\overline{u'v'}$ is an apparent shearing stress and is often represented by

$$\tau_{xy} = -\rho\overline{u'v'} = \rho\epsilon_y \frac{\partial \bar{u}}{\partial y} \qquad 2\text{-}9$$

where τ is the shearing stress and ϵ_y is called the eddy viscosity or coefficient of turbulent momentum diffusion. (See Ref. 49 for a more thorough explanation on applying the Navier-Stokes equations to turbulent flow and on representing the turbulent momentum transfer as diffusion of momentum.) Although this analogy exists between turbulent diffusion of mass and momentum, the turbulent (mass) diffusivity (e) is not necessarily equal in magnitude to the eddy viscosity (ϵ). However, both e and ϵ depend strongly on the kinematics of the turbulence which is present in a given situation. Thus, the numerical values of e and ϵ would be expected to be approximately the same and, in many situations, they may be assumed to be equal without introducing appreciable error.

Returning to Eqn. 2-7 and introducing the expressions of Eqn. 2-8, one obtains

$$\frac{\partial(\rho\bar{c})}{\partial t} + \frac{\partial}{\partial x}(\rho\bar{u}\bar{c}) + \frac{\partial}{\partial y}(\rho\bar{v}\bar{c}) + \frac{\partial}{\partial z}(\rho\bar{w}\bar{c})$$

$$= \frac{\partial}{\partial x}\left[\rho(D_m+e_x)\frac{\partial \bar{c}}{\partial x}\right] + \frac{\partial}{\partial y}\left[\rho(D_m+e_y)\frac{\partial \bar{c}}{\partial y}\right] + \frac{\partial}{\partial z}\left[\rho(D_m+e_z)\frac{\partial \bar{c}}{\partial z}\right] + \overline{n_P} \qquad 2\text{-}10$$

This is the mass balance in terms of time averaged quantities. The turbulent diffusion coefficients are many times larger than the molecular diffusion coefficient. Thus, it is usually permissible to drop the molecular diffusion terms from Eqn. 2-10. However, in regions where the turbulence is damped out (e.g., near solid boundaries), it may be necessary to consider molecular diffusion.

2.5) One Dimensional Mass Balance Equation Including Definition of Longitudinal Dispersion

The complex geometries and boundary conditions which exist in most practical cases make the solution of Eqn. 2-10 extremely difficult, if not impossible. The mass balance may be simplified by converting it into an equation containing only quantities which have been averaged across the flow section (i.e., averaged in the lateral direction). Also, let consideration be limited to cases where the flow has a primary direction of motion, and let this be the X direction. The mass balance equation is then one dimentional in that the spatially averaged quantities possess variation only in one dimension, namely the X or flow direction. (In the present sense, the term "spatial" applies only to the cross sectional area.)

Define the spatial average of $\bar{u}$ and $\bar{c}$ as

$$U = \frac{1}{A}\int_A \bar{u}\, dA$$

$$C = \frac{1}{A}\int_A \bar{c}\, dA \qquad 2\text{-}11$$

where A is the cross sectional area. Since only one dimensional flow is being considered, the spatial averages of $\bar{v}$ and $\bar{w}$ (i.e. V and W) are zero. Also define spatial variations of the velocities and concentration by

$$\bar{u} = U + u''$$

$$\bar{c} = C + c'' \qquad 2\text{-}12$$

$$\bar{v} = v''$$

$$\bar{w} = w''$$

Just as u' was a temporal variation from $\bar{u}$, so u'' is a spatial variation from U. Note that v'' and w'' are not necessarily zero even though V and W are zero in one dimensional flows. Introduce the expressions of Eqn. 2-12 into the left-hand side of Eqn. 2-10, expand the products of sums, and take the spatial average of the resulting expression. The details of this operation are presented in Appendix A. From Eqn. A-31, the one dimensional form of the mass balance is seen to be

$$\frac{\partial C}{\partial t} + U\frac{\partial C}{\partial x} + \left[\frac{1}{A}\frac{\partial}{\partial x}(\overline{\overline{u''c''}}A)\right] = \frac{1}{A}\frac{\partial}{\partial x}\left(\bar{\bar{e}}_x A \frac{\partial C}{\partial x}\right) + M_P/\rho + N_P/\rho \qquad 2\text{-}13$$

where $\overline{\overline{u''\,c''}}$ indicates the spatial average as defined in Eqn. 2-11. Also, $\bar{\bar{e}}_x$ is a diffusion coefficient defined so as to represent the average or one dimensional turbulent diffusion in the x-direction. (See Eqn. A-24.) M_P is the rate of influx of mass across the lateral boundaries due to diffusion. (See Eqn. A-22 and the discussion which accompanies it.) As examples, a positive M_P would be the absorption of oxygen in the reaeration of a river, and a negative M_P would be the absorption of dye by a concrete channel. Also, N_P is the spatial average of $\bar{n}_P$. A positive N_P would result from oxygen production by suspended algae while N_P would be negative for

radioactive decay or for the consumption of oxygen by suspended matter possessing biochemical oxygen demand.

In Appendix A it is pointed out that Eqn. 2-13 involves some degree of approximation if the cross sectional area changes with x. However, if the flow area is constant, then no approximations are involved in averaging Eqn. 2-10 to obtain Eqn. 2-13.

It remains to discover the significance of the bracketed term on the left-hand side of Eqn. 2-13. This term is similar to the term which was called the x component of the turbulent diffusion in the time averaged equation. Thus, one might consider writing the transport represented by the bracketed term as a diffusive transport. The u' and c' which gave rise to turbulent diffusion were random variations from the averages $\bar{u}$ and $\bar{c}$. In the present case, u'' and c'' will usually be well defined variations rather than random variations from U and C. Thus one might also question the validity of representing the bracketed term as a diffusive process.

In Eqn. 2-13, the term $U(\partial C/\partial x)$ may be called the one dimensional convection. This term represents the convection due to the average velocity and concentration distributions as shown in Fig. 2-2a. However, the total convection is given by the spatial integral of $\bar{u}\ \partial\bar{c}/\partial x$ where $\bar{u}$ and $\bar{c}$ are the actual (time averaged) velocity and concentration, not the spatial averages. For uniform flow, the distribution of $\bar{u}$ and $\bar{c}$ might be as shown in Fig. 2-2b.

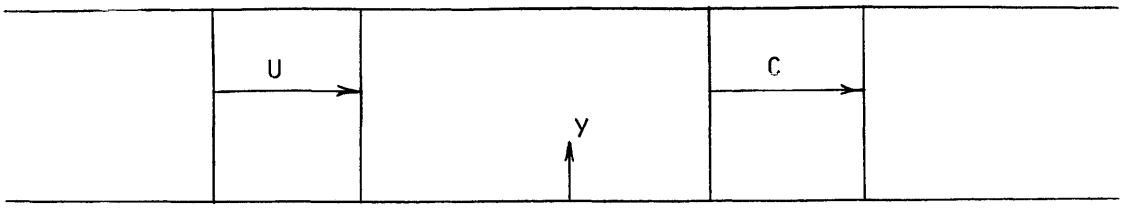

a: One dimensional velocity and concentration

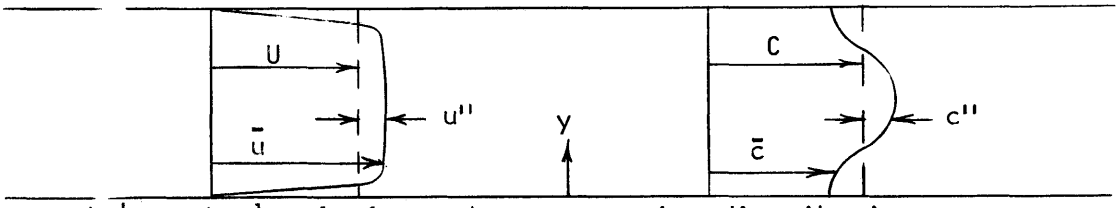

:b: actual velocity and concentration distributions

Fig. 2-2: Velocity and Concentration Distributions

Boundary shear stress causes the velocity distribution to be as shown for uniform flow. As will be seen, the lateral distribution of concentration will be controlled by the lateral turbulent diffusion and the velocity distribution. Thus, it is strictly hydraulic factors which produce the u'' and c'' terms that are shown in Eqn. 2-12 and Eqn. 2-13. This, in turn, means that the net convection represented by the bracketed term in Eqn. 2-13 is a function only of the hydraulics and not of the substance which is being transported.

For steady, uniform flow, Taylor (Ref. 53) and Aris (Ref. 7) have shown that the convection associated with u'' and c'' may be represented as a one dimensional diffusive transport. To distinguish this process from turbulent diffusion, the transport due to the spatial variations u'' and c'' is called longitudinal dispersion. On the basis of the work of Taylor and Aris and by analogy to turbulent diffusion, define E_1 as a coefficient of longitudinal dispersion so that

$$\int_A u''c''dA \equiv \overline{\overline{u''c''}}A = - E_1 A \frac{\partial C}{\partial x} \qquad 2\text{-}14$$

Thus, the bracketed term in Eqn. 2-13 may now be written as

$$\frac{1}{A}\frac{\partial}{\partial x}\left(\overline{\overline{u''c''}}A\right) = - \frac{1}{A}\frac{\partial}{\partial x}\left(E_1 A \frac{\partial C}{\partial x}\right) \qquad 2\text{-}15$$

With this definition of dispersion, the mass balance equation (Eqn. 2-13) becomes

$$\frac{\partial C}{\partial t} + U \frac{\partial C}{\partial x} = \frac{1}{A} \frac{\partial}{\partial x} \left(\bar{\bar{e}}_x A \frac{\partial C}{\partial x}\right) + \frac{1}{A} \frac{\partial}{\partial x} \left(E_1 A \frac{\partial C}{\partial x}\right) + M_P/\rho + N_P/\rho \qquad 2\text{-}16$$

Due to the similarity between the terms representing the average turbulent diffusion and the longitudinal dispersion, it is convenient to include the average turbulent diffusion with the longitudinal dispersion. Thus, define E as the dispersion coefficient so that

$$E = \bar{\bar{e}}_x + E_1 \qquad 2\text{-}17$$

It will be seen in Section 3 that E_1 is much greater than $\bar{\bar{e}}_x$. With this new definition of dispersion, the one-dimensional mass balance equation may finally be written as

$$\frac{\partial C}{\partial t} + U_{xt} \frac{\partial C}{\partial x} = \frac{1}{A} \frac{\partial}{\partial x} \left(E_{xt} A \frac{\partial C}{\partial x}\right) + \frac{M_P}{\rho} + \frac{N_P}{\rho} \qquad 2\text{-}18$$

(The subscripts on U and E are explained below.)

Under the assumptions which have been made, Eqn. 2-18 applies to either steady or unsteady, uniform or non-uniform flows. In any of these cases, the dispersive transport is defined as the difference between the true convective transport and the one dimensional convection represented by $U(\partial C/\partial x)$. In general, the velocity U, the velocity distribution, and the turbulent diffusion may vary with both x and t. Thus, due to the relation between these factors and the dispersion process, the dispersion coefficient may also be expected to vary with x and t. From this point forward, the subscripts x and t will be used on U and E to emphasize the variable or variables on which U and E may depend in a given situation. (Note that the very presence of A in an equation such as Eqn. 2-18 indicates that A varies

with x. Otherwise, the A inside the derivative could be taken out and cancelled.)

2.6) Importance of Dispersion in Various Situations

It has been shown that longitudinal dispersion must be considered if it is desired to completely and correctly represent mass transport in a one dimensional equation. However, in different situations, the importance of dispersive transport relative to one dimensional convection will vary. The relative importance of dispersion depends not only on the magnitude of the dispersion coefficient but also on the longitudinal concentration gradients for the substance which is being transported. This can be seen from the fact that the rate of convective transport is proportional to UC while the rate of dispersive transport is proportional to $E(\partial C/\partial x)$. For given values of U and E, the flatter the concentration distribution is, the less important the dispersion process will be. For example, consider the case of an oxygen balance for a river into which polluted water is being added. In the simplest case, the pollution consumes dissolved oxygen and more oxygen is absorbed from the atmosphere. This leads to the well-known oxygen-sag curve where the oxygen concentration may change by only a few parts per million in several miles. As a result, the derivative of the oxygen concentration is extremely small, and the dispersive transport is negligible in most problems of oxygen balance in rivers. On the other hand, in the same river and under the same flow conditions, dispersion may be very important in describing the transport of another substance. For example, if a slug of some substance, say radioactive wastes, is discharged into the river, the concentration gradients will be steep and the consideration of dispersion will be imperative in describing how the radioactivity is transported downstream.

In a river, the same velocity distribution leads to the one dimensional convection (U) and plays a large role in determining the dispersion coefficient (E). Thus, E should be expected to be a function of U for a river, and this relationship is borne out. (See Section 3.) This means that there is a limit on how large E can be relative to U in a river. This relationship between E and U is one factor which helps to render dispersion negligible in some cases. On the other hand, in an estuary, the net

convection is due to the fresh water velocity (U_f) while the primary velocity distribution which influences dispersion is that associated with the tidal velocities. Hence, there is no limit on how large E can be relative to U_f. Thus, if a given concentration gradient exists in both a river and an estuary, dispersion may be negligible in the river and not negligible in the estuary compared to the net convection.

2.7) The One Dimensional Equation for Some Specific Cases

The one dimensional mass balance relation of Eqn. 2-18 may be written in simpler form for certain specific cases. In all the following cases, it is assumed that a conservative substance is being considered so that M_P and N_P are zero.

If the flow is uniform, then U, A, and E are all independent of x. In general, they may still be time dependent. For example, an unsteady but uniform flow may exist in a uniform pipe line. In certain situations, it might be reasonable to assume that an open channel flow was unsteady but uniform. For uniform, unsteady flow Eqn. 2-18 becomes

$$\frac{\partial C}{\partial t} + U_t \frac{\partial C}{\partial x} = E_t \frac{\partial^2 C}{\partial x^2} \qquad 2\text{-}19$$

If the flow is steady as well as uniform, then U and E are constant:

$$\frac{\partial C}{\partial t} + U \frac{\partial C}{\partial x} = E \frac{\partial^2 C}{\partial x^2} \qquad 2\text{-}20$$

If, still further, a steady state concentration distribution is obtained, then $\partial C/\partial t = 0$:

$$U \frac{\partial C}{\partial x} = E \frac{\partial^2 C}{\partial x^2} \qquad 2\text{-}21$$

This shows that there must be a balance between one dimensional convection and longitudinal dispersion if a steady state is to be obtained.

In dealing with non-uniform flows, it will generally not be possible to give the longitudinal variation of U, A, and E as closed-form mathematical expressions. Thus, to take account of the variation of these parameters, Eqn. 2-18 may be written in finite difference form. This difference equation can be written so as to include the $\partial C/\partial t$ term. (See Section 5.2.) However, if a steady state concentration distribution exists so that $\partial C/\partial t$ equals zero, then the finite difference form is much simpler. For $\partial C/\partial t = 0$, Eqn. 2-18 may be integrated once without specifying the variations of U_x, A, and E_x provided that UA (i.e., the discharge) is constant:

$$U_x C = E_x \frac{dC}{dx} \qquad 2\text{-}22$$

The constant of integration has been set equal to zero. This will be the case if C and dC/dx are both zero at a large distance upstream. If the derivative is written as a central difference with constant Δx between x_i and x_{i+1}, then

$$U_{x_i} C_i = E_{x_i} \frac{C_{i+1} - C_{i-1}}{2(\Delta x)} \qquad 2\text{-}23$$

The subscript i indicates the value of x at which U_x, C, and E_x are to be evaluated.

Estuary type flows (i.e. the type of flow found in the constant density regions of estuaries) are of particular interest in the present work. In these flows the velocity may be represented one dimensionally as

$$U_{xt} = U_{f_x} + U_{T_x} \sin \sigma (t - \delta) \qquad 2\text{-}24$$

where σ is the frequency of oscillation associated with the tidal velocity ($\sigma = 2\pi/T$ where T is the period of oscillation), t is time measured from an arbitrary origin, and δ is a constant representing the time shift between this arbitrary origin and the time of zero oscillatory velocity. In a natural estuary, U_f is the velocity associated with the river flow into the estuary and U_T is the maximum velocity due to tidal motions. Hence, both U_f

and U_T would be expected to vary with longitudinal position due to the changing geometry of the estuary. U_T would also decrease in the upstream direction due to frictional damping. In the present laboratory investigation, a uniform velocity of the type given by Eqn. 2-24 was obtained for studying dispersion in a pipe line. For uniform flows of this type, U_f and U_T are constant while E is time dependent but independent of x. Eqn. 2-19 then becomes

$$\frac{\partial C}{\partial t} + [U_f + U_T \sin \sigma (t-\delta)] \frac{\partial C}{\partial x} = E_t \frac{\partial^2 C}{\partial x^2} \qquad 2\text{-}25$$

In Section 6.5 it will be shown that, if the concentration distribution is observed at one period intervals (i.e., at $t - \delta = nT$ where $n = 1, 2, 3, \ldots$), then the equation

$$\frac{1}{T} \frac{\partial C_s}{\partial n} + U_f \frac{\partial C_s}{\partial x} = E_A \frac{\partial^2 C_s}{\partial x^2} \qquad 2\text{-}26$$

describes the observed concentration. In this expression E_A is the time averaged value of E_t during a period and $\frac{1}{T} \frac{\partial C_s}{\partial n}$ indicates the temporal changes in concentration from one period to the next. Note that the form of Eqn. 2-26 is identical to that of Eqn. 2-20, which was obtained for steady, uniform flow.

For non-uniform flows, the equivalent of Eqn. 2-26 is

$$\frac{1}{T} \frac{\partial C_s}{\partial n} + U_{f_x} \frac{\partial C_s}{\partial x} = \frac{1}{A} \frac{\partial}{\partial x} (AE_{A_x} \frac{\partial C_s}{\partial x}) \qquad 2\text{-}27$$

If a quasi-steady state is obtained so that $\partial C_s/\partial n = 0$, then Eqn. 2-27 may be integrated once provided $U_f A$ (the fresh water discharge) is constant:

$$U_{f_x} C_s = E_{A_x} \frac{\partial C_s}{\partial x} \qquad 2\text{-}28$$

(See Eqn. 2-22.) This may be written in finite difference form as was done to obtain Eqn. 2-23:

$$(U_{f_x})_i C_{s_i} = (E_{A_x})_i \frac{C_{s_{i+1}} - C_{s_{i-1}}}{2(\Delta x)} \qquad 2\text{-}29$$

It must be remembered that Equations 2-27, 2-28, and 2-29 only represent the concentrations at times which differ by a full period.

3) DISCUSSION OF PREVIOUS WORK ON LONGITUDINAL DISPERSION

3.1) Steady Flow

For steady, uniform flow in circular pipes and in two dimensional channels, it is possible to write analytical expressions for the variation of velocity ($\bar{u}$) and eddy viscosity (ϵ) across the flow section. It may also be assumed that the turbulent diffusivity (e) is equal to the eddy viscosity (ϵ). Then, it should be possible to use these expressions in a three dimensional mass balance equation (e.g. eqn 2-10) to solve for the concentration $\bar{c}$ and thus for c'' which is the variation of $\bar{c}$ from its average value, C. Then, by using eqn. 2-14, eqn. 2-17, and the expressions for u'' (i.e., $\bar{u}$ - U) and for c'', it should be possible to arrive at an analytical representation for the rate of longitudinal dispersion and for E, the dispersion coefficient for steady uniform flow.

Taylor (ref. 53) was evidently the first to successfully carry out such an analysis. He considered steady flow in a uniform pipe and used a universal velocity distribution of the form (Table B-1)

$$\frac{\bar{u}_{max} - \bar{u}}{u_*} = f\,(r/a) \qquad 3\text{-}1$$

where $\bar{u}$ is the longitudinal velocity, $\bar{u}_{max}$ is the maximum (or centerline) value of $\bar{u}$, u_* is the shear velocity (i.e., $\sqrt{\tau_o/\rho}$ where τ_o is the boundary shear stress and ρ is the fluid density), r is the radial coordinate, and a is the pipe radius. It was assumed that the lateral turbulent diffusivity was equal to the eddy viscosity and is thus given by

$$e_r = \frac{\tau}{-\rho \frac{\partial \bar{u}}{\partial r}} \qquad 3\text{-}2$$

where τ is the shear stress at radius r. Taylor also assumed that $\bar{c}$ could be written as $(\bar{c}_x + \bar{c}_r)$ where $\bar{c}_x$ is a function of x only and $\bar{c}_r$ is a function of r only. He further assumed that $\partial \bar{c}_x/\partial x$ was independent of x.

The three dimensional mass balance equation (Eqn. 2-10) may be written in radial coordinates for the case treated by Taylor as

$$\frac{\partial \bar{c}}{\partial t} + \bar{u}\frac{\partial \bar{c}}{\partial x} = e_x \frac{\partial^2 \bar{c}}{\partial x^2} + \frac{1}{r}\frac{\partial}{\partial r}\left(e_r \frac{\partial \bar{c}}{\partial r}\right) \qquad 3\text{-}3$$

Using this equation and the assumptions mentioned above he arrived at an expression for the equivalent of c'' (eqn. 2-12) in terms of the velocity distribution and the lateral diffusivity. Then by finding u'' from the velocity distribution and carrying out the integration indicated by eqn. 2-14, E_1 was found to be 10.06 au_*. By assuming that e_x equals e_r, the average value of $\bar{e}_x$ was found to be 0.05 au_*. In accordance with eqn. 2-17, it was concluded for the case under consideration that E is given by

$$E = 10.1\ au_* \qquad 3\text{-}4$$

where $u_* = \sqrt{\tau_o/\rho}$. Notice that the longitudinal turbulent diffusion contributes about one half percent to the dispersion coefficient given by eqn. 3-4.

Taylor also conducted experiments in both smooth and rough pipes of 3/8'' inside diameter. The experimentally measured dispersion coefficients varied from 10.5 au_* to 12.8 au_*. For experiments in a 40'' dia. pipe as reported in ref. 1, Taylor found values of 10.6 and 11.7 for E/au_*.

To investigate the effects of flow through bends, Taylor bent a 3/8'' pipe into a circle of 3' dia. Values of 21.9 and 15.0 were found for E/au_*, and thus it was concluded that curvature increases dispersion more than it increases resistance to flow. Also, for 10'' dia. cross-country pipe lines (which follow the topography), values from 12.3 to 23.4 were found, with most of the values being about 20. These calculations were based on data reported in ref. 25.

From the definition of the dispersion coefficient as given in eqn. 2-17 and eqn. 2-14, it can be seen why E for curved pipes differs from that for straight pipes. Recall that a particular velocity distribution was assumed in the calculation that led to 10.1 in eqn. 3-4. However, the helical secondary flow which develops due to bends (see, for example, ref. 47, p. 523) causes the velocity distribution to be different from that assumed by Taylor's calculation. Thus, one might expect that eqn. 3-4 would not apply to curved flow. In general, the same thing may be said about other non-uniformities. Separation zones, pockets in the sides of the flow boundaries, etc. change the velocity distribution and lateral diffusivity and thus the dispersion coefficient.

Elder (ref. 12) carried out a computation similar to Taylor's, but for uniform, two dimensional, open channel flow. Using the same

assumptions and the same general approach as Taylor, he obtained

$$E = 5.93\ hu_* \qquad 3\text{-}5$$

where h is the depth of flow. Of the 5.93, E_1 accounts for 5.86 and $\bar{\bar{e}}_x$ for 0.07.

Elder pointed out that the longitudinal distribution of tracer after a slug injection should be normal or Gaussian. (See section 5.) However, in his experiments, it was observed that the concentrations in the upstream part of the distributions were higher than the normal distribution would predict. This effect was attributed to the influence of the viscous sublayer which was neglected in developing eqn. 3-5 (and eqn. 3-4), but which was present in his experiments. It was pointed out that tracer which enters the sublayer will be returned to the central part of the flow more slowly than the turbulent transfer rate which was assumed in the analysis. This would mean that, in effect, the lateral diffusivity assumed by Taylor and Elder does not completely represent the physical situation when a laminar sublayer is present.

If the effects which Elder observed are due to influence of the sublayer, then these effects should be reduced as the Reynolds number increases for flows which are not in the hydraulically rough region. Also, the effects should not be present for flows in the rough region since no laminar sublayer exists for these flows. Results presented in section 8 are consistent with these trends. Notice also that the sublayer effectively increases longitudinal dispersion since it causes mass to become more spread out than is predicted by the coefficient of eqn. 3-5.

In some applications (e.g. the Darcy-Weisbach friction factors), the same expressions apply to pipes and open channels if the hydraulic radius (R_H) is used as the characteristic lateral dimension in place of the pipe radius (a) or the channel depth (h). Thus, one might expect that eqn. 3-4 would apply to uniform open channels if the pipe radius were replaced by $2R_H$ so that

$$E = 20.2\ R_H u_* \qquad 3\text{-}6$$

or for two dimensional channels where R_H equals h

$$E = 20.2\ hu_* \qquad 3\text{-}7$$

This expression is obviously different from eqn. 3-5. The reason for this difference may be seen from the following considerations: In terms of the lateral coordinate (i.e., r/a and y/h), the velocity distributions used by Taylor and Elder were slightly different. Also, Taylor took von Karman's constant as 0.40 while Elder used 0.41. If Elder's computation is carried out using the same velocity distribution as Taylor and using von Karman's constant of 0.40, one obtains

$$E = 6.6\ hu_* \qquad 3\text{-}8$$

Thus it is seen that these differences do not account for the difference between the coefficients 20.2 and 5.93 of equations 3-5 and 3-7.

There is another difference which exists between pipes and two-dimensional channels, namely the difference between three dimensional and two dimensional variations of velocity and diffusivity across the section (i.e., side wall effects). This difference and its influence on the spatial averaging which was performed to obtain an expression for E must therefore be the primary cause of the difference between equations 3-5 and 3-7.

The importance of the side-wall effects and the three-dimensional variations which they produce is borne out by experiments reported by Glover (Ref. 13). These experiments were conducted in a rectangular flume 8 ft. wide with flow depths of about 0.5 ft. When the bottom and the sides of the flume were the same material (plywood, Manning's n = 0.010), $E/R_H u_*$ was 20 and 24 for two experiments. The flume was then roughened by laying reinforcing bars just on the bottom. (Manning's n = 0.025.) This effectively reduced the relative side-wall influence, and $E/R_H u_*$ was found to be 13 and 19 for two runs. Also, in a 90° triangular flume, $E/R_H u_*$ was found to be 19, 20, and 25 for three runs. Thus it is seen that varying degrees of side wall effects may be expected to change the value of $E/R_H u_*$.

Harleman (Ref. 29, pp. L-10 and N-8) showed that Eqn. 3-6 could also be written in the following forms:

$$E = 14.3\ R_H \sqrt{2g\ R_H\ S_e} \qquad 3\text{-}9$$

$$E = 77\ \frac{n}{R_H^{1/6}}\ UR_H \qquad 3\text{-}10$$

$$E = \left[\frac{20.2 g^{1/6}}{C_c^{1/3}}\right] R_H^{4/3} G^{1/3} \qquad 3\text{-}11$$

where g is the acceleration of gravity, S_e is the slope of the energy gradient, n is Manning's roughness parameter, U is the mean velocity of flow, R_H is the hydraulic radius, C_c is the Chezy coefficient, and G is the rate of turbulent energy dissipation per unit mass of fluid. It is interesting to note that Eqn. 3-11 shows that dispersion in uniform shear flow follows a relationship similar to Kolmogoroff's similarity hypothesis for diffusion (Ref. 23,45). This hypothesis states that

$$e \sim L^{4/3} G^{1/3} \qquad 3\text{-}12$$

where e is the turbulent diffusivity and L is a characteristic length scale of the turbulence.

Krenkel and Orlob measured longitudinal dispersion coefficients in a uniform, wide, open channel in the laboratory (Ref. 32). For their data, $E = 9.2\, hu_*$. They worked with flow depths from 1" to 2" in a 12"-wide channel which had roughness elements (expanded metal) 0.24" high. In view of this extreme roughness, it might be expected that the velocity distribution would not be the same as that used by Elder to obtain eqn. 3-5. Also, the side walls caused the flow not to be truly two-dimensional. Thus, it is not surprising that their data gives a factor different from Elder's 5.93.

Aris (Ref. 7) presented a general mathematical analysis of longitudinal dispersion in steady, uniform flow. Recall that Taylor (and Elder) assumed that the concentration $\bar{c}$ could be written as $\bar{c}_x + \bar{c}_r$ where $\bar{c}_x$ was a function of x only, $\bar{c}_r$ was a function of r only, and $\partial \bar{c}_x / \partial x$ was independent of x. Taylor also assumed axial symmetry for the case of flow in a pipe. Without any of these assumptions and for a general lateral boundary configuration with any distribution of velocity and turbulent diffusivity, Aris showed that longitudinal dispersion is a diffusive transport. For the case which he considered, the dispersion coefficient may be written as

$$E = \bar{\bar{e}}_x + \frac{U^2 a^2}{e_o}\left[\frac{1}{A}\int_A \lambda\, \phi\, dA\right] \qquad 3\text{-}13$$

where $\bar{\bar{e}}_x$ is the spatial average of the longitudinal turbulent diffusivity, U is the one dimensional velocity, a is a characteristic length related to the lateral boundary geometry, e_o is a characteristic value of the lateral diffusion coefficient and is used so that the distribution of lateral diffusivity may be written in dimensionless form as ψ (i.e., $\psi = e/e_o$), A is the cross sectional area, and λ is the dimensionless velocity distribution (i.e., $(\bar{u} - U)/U$). ϕ is a function related to the lateral distribution of concentration and is defined as the solution of

$$\nabla \cdot (\psi \nabla \phi) = - \lambda \qquad 3\text{-}14$$

under the condition that

$$\psi \frac{\partial \phi}{\partial \nu} = 0 \qquad 3\text{-}15$$

on the lateral boundary where ν is the normal to the boundary. Notice that the second term on the right-hand side of Eqn. 3-13 is in accordance with the definition of E_1 (Eqn. 2-25) since λ is related to u'' and ϕ is related to c''. Also, Eqn. 3-14 shows that ϕ (and therefore c'') is a function only of hydraulic parameters, namely the velocity distribution and the lateral diffusivity. Aris points out that the calculation which Taylor made to obtain Eqn. 3-4 is equivalent to the calculation indicated by Eqn. 3-13. In effect then, the assumptions which Taylor made concerning the concentration distribution did not limit the generality of his result for dispersion in uniform pipes. Because of the generality maintained in developing Eqn. 3-13, it may be used to calculate the dispersion for uniform flow in any boundary configuration provided that the velocity distribution and the turbulent diffusivity are known.

3.2) Rivers

The question arises as to whether Eqn. 3-5, Eqn. 3-6, or perhaps some other expression should be used for a river. The lateral geometry of a river is somewhere between that of a truly two dimensional channel as Eqn. 3-5 would imply and a semi-circle as Eqn. 3-6 would imply. Thus, for a uniform river, the dispersion coefficient would probably be somewhere

between that of eqn. 3-5 and eqn. 3-6. But no river is uniform and it can be seen from the experimental work referred to in this section that the non-uniformities increase dispersion. In general, it is not possible to write analytical expressions for the effects of non-uniformities. Hence any calculated dispersion coefficient for a river will only be an estimate. As will be seen, eqn. 3-6 provides the best estimate from those analytical expressions which are available but this estimate is probably a minimum value.

The references mentioned above have been primarily concerned with dispersion in uniform flow. References which contain data on dispersion in pipe lines having bends and in natural streams and rivers indicate that the bends and non-uniformities cause an increase in dispersion over that predicted by the analyses summarized above. For cross-country pipe lines (which follow the topography) and for laboratory pipe lines with bends, the average of the experimental values found for E/au_* is about 20, with most of the values being between 12 and 25. (See ref. 1,25, 39, 52, 53.) Most of these pipes were of a constant diameter. Thus, it appears that the effects of bends is to cause dispersion to be about twice that predicted by Taylor.

Unfortunately, in most cases where dispersion data is presented for rivers, not enough hydraulic data is given for a value of the shear velocity (u_*) to be calculated. For those cases where $R_H u_*$ may be calculated, $E/R_H u_*$ has a wider range of scatter than for pipes. This is understandable since rivers have not only bends but also varying degrees of "side wall" effects and non-uniformities.

Patterson and Gloyna (ref. 40) conducted some dispersion experiments in the Colorado River near Austin, Texas. However, the dispersion process which they measured is not the same as the one being considered in the present work. Thus, the dispersion coefficient is written as E_a in eqn. 3-16 below. The present work is concerned with one dimensional dispersion or dispersion when the substance which is being transported is distributed across the entire area of flow. In the Colorado tests, the tracer was injected as a point source near the center of the river's cross section. Most of the test reaches were less than 1/3-mile long, and the data shows that the tracer did not mix across the full section within this length. Because of the lateral mixing that was taking place, a one

dimensional equation could not be used for the mass balance. As a result, the equation

$$\frac{\partial C}{\partial t} + U \frac{\partial C}{\partial x} = E_a \frac{\partial^2 C}{\partial x^2} + e_y \frac{\partial^2 C}{\partial y^2} \qquad 3\text{-}16$$

was used in the data analysis. Since y was the lateral horizontal coordinate, eqn. 3-16 assumes that the tracer was completely mixed vertically, but even this condition is not realized for a point source until some distance downstream from the source.

It was observed in some cases that the measured longitudinal dispersion coefficient increased with distance from the injection point. This was probably due to the fact that, as the tracer spread out, an increasing percentage of the velocity distribution was contributing to the dispersion process. However, the test reach used for these experiments was immediately downstream from a bend of about 130° in the river. The secondary flow due to this bend very well may have had a strong influence on the experimental results.

In most practical cases, one would be interested in the dispersion in reaches which are much longer than those used by Patterson and Gloyna. Then, even if the tracer or pollutant is injected as a point source, the distance required for mixing to take place across the section is a small part of the region of interest. In such cases, it may be sufficient to assume that the tracer is mixed across the full section beginning at the injection point.

Glover (ref. 13) conducted a dispersion test in a natural stream. The test reach was about 5 miles long, and the tracer was injected as a distributed source across the stream. Thus, the time required for the tracer to become distributed across the section was probably insignificant. The experiment gave a one dimensional dispersion coefficient of 174 ft^2/sec or $E/R_H u_*$ of 500. The analysis assumed that E was not a function of longitudinal distance. It seems that this value of E does not represent dispersion due to a normal velocity distribution or normal type of non-uniformities found in most rivers. The river used for the experiment followed as many as five channels within the test region. Thus, it seems likely that a large part of the longitudinal spreading may have resulted frpm different rates of mean convection in the various channels. Glover

also reported a value of $E/R_H u_*$ of 800 for the Mohawk River. (See also ref. 38, 51, 54.) Again, this is an extreme value since the test reach included dams, locks, small reservoirs, and density currents. It appears that the experimental values discussed in the following paragraphs give a better indication of the rates of dispersion to be expected in natural streams.

These values come from the work of Godfrey and Frederick (ref. 15). Again, the tracer was injected as a distributed source across the width of the rivers which were investigated. The test reaches were about 4 miles long. Some of the observed concentration distributions were highly skewed compared to that to be expected after an instantaneous injection of tracer. (See section 5.) The method of analysis used by the authors must have been highly sensitive to this skewness since values up to 650 were reported for $E/R_H u_*$. Values of this magnitude seem unexplainably large. On re-analyzing the less skewed data by the modified semi-log plot as described in section 7 (eqn. 7-10), values of $E/R_H u_*$ from 36 to 80 were found. To make this analysis, the flow was assumed to be uniform. In fact, the area and velocity changed by as much as 35% in the test sections. At each section for which data was analyzed, the velocity was assumed to be given by the distance from the injection point divided by the through-flow time, which was taken as the time of occurrence of the peak concentration at the station in question. This means that the average velocity through the test reach was used. Also, the dispersion coefficient which was obtained was a measure of the average rate of dispersion in the test reach.

A further break-down may be made in these values of $E/R_H u_*$ since Godfrey and Frederick classified the rivers as either straight or crooked. No additional clarification was given for these terms. Since all of the data being referred to was for natural streams, one may be sure that the test reaches were not perfectly straight or uniform. They must have included some degree of curvature and irregularity in the plan view of the stream since all of the test sections were about 4 miles long. However, for the rivers classified as straight, $E/R_H u_*$ varied only from 36 to 50 (about twice the value of eqn. 3-6) while it was a "crooked" river that gave $E/R_H u_*$ of 80.

On the basis of this limited data and the data mentioned

previously for cross-country pipe lines, it appears that gentle curvature in either pipes or rivers causes the dispersion coefficients to be about twice that given by Taylor's analysis (eqn. 3-6).

3.3) Estuaries

3.3.1) Fresh Water Region

In section 2 (eqn. 2-24) it was pointed out that the velocity in the constant density region of an estuary may generally be represented by

$$U_{xt} = U_{f_x} + U_{T_x} \sin \sigma (t - \delta) \qquad 3\text{-}17$$

where U_f is the velocity associated with the river discharge into the estuary and U_T is the velocity due to tidal motions. Non-uniformities may cause U_f and U_T to be functions of x. Also, frictional damping will cause U_T to decrease in the upstream direction. As far as is known, no basic investigation has been made into the fundamental relation between dispersion coefficients and the hydraulic parameters in flows of this type, even with U_f and U_T assumed to be constant.

Harleman (ref. 29, chap. N) treated this problem in an approximate way by writing a dispersion coefficient from eqn. 3-10 with the velocity U replaced by the average of the oscillatory velocity during half a period. This average is $2U_T/\pi$ so that eqn. 3-10 becomes

$$E_A = 77 \frac{n}{R_H^{1/6}} \left(\frac{2}{\pi} U_T\right) R_H \qquad 3\text{-}18$$

where n is Manning's roughness and R_H is the hydraulic radius. This coefficient was then used in an expression similar to eqn. 2-26 which represents concentration changes from one period to the next. Thus, as has already been indicated by using the notation E_A in eqn. 3-18, this equation would correspond to the average value of E during a period of oscillation. By analogy to eqn. 3-11, Harleman also wrote E_A as

$$E_A = \left[\frac{20.2g^{1/6}}{C_c^{1/3}}\right] R_H^{4/3} G_A^{1/3} \qquad 3\text{-}19$$

where G_A is the average rate of energy dissipation per unit mass of fluid and is due primarily to tidal motions. The implication of these expressions is that the average rate of dispersion is due to the velocity distribution and turbulent diffusivity associated with the oscillatory tidal velocity rather than with the steady fresh water velocity U_f. This is reasonable since U_T is many times greater than U_f in most estuaries. These expressions also tacitly assume that the velocity distribution and lateral mixing result from boundary shear. Hence, equations 3-18 and 3-19 should not be expected to apply in the salinity intrusion region of an estuary since internal density currents contribute significantly to transport in this region.

As reported in ref. 29, chap. N, eqn. 3-18 was found to be in good agreement with experiments made in a tidal flume at the Corps of Engineers Waterways Experiment Station. The comparison was based on values of E_A at the downstream end of the tidal flume. This rectangular flume was made of plastic and was 9" wide and 327 ft. long. The mean water depth was 6". Roughness elements were placed on the flume sides (not on the bottom). This roughness undoubtedly greatly increased the "side wall" effects and added to the three dimensionality of the velocity distribution. This probably accounts for the good numerical agreement between eqn. 3-18 and the experiments. (Recall that the coefficient 77 in eqn. 3-18 ultimately came from Taylor's calculation for a pipe and that in some cases Taylor's coefficient did not agree with experiments in open channels.) The functional agreement between eqn. 3-18 and experiments seem even more significant than the numerical agreement <u>per se</u>. This functional agreement shows that the average dispersion coefficient is related to the oscillatory velocity (U_T) and not the through-flow velocity (U_f).

Much of the work on mixing processes in both the fresh water portion and the salinity portion of estuaries has been based on model studies (ref. 2-6, 21, 28, 30, 31, 35, 42, 43). A detailed analysis of the interpretation of these model results is presented in the next section.

For the present, the model results may be viewed as experiments with estuary type flow in non-uniform channels.

Some of the results for experiments conducted in the fresh water portion of the Delaware estuary model were analyzed by O'Connor (ref. 35, 36). These were experiments with instantaneous dye releases. It was observed that dye was absorbed by the surface of the model. In previous reports on these experiments (ref. 5, 31) an approximate adjustment was made in the observed concentrations to account for this absorption. O'Connor was able to show that this absorption could be accounted for by a loss term in the differential mass balance equation. Thus, assuming uniform flow, O'Connor wrote

$$\frac{\partial C_s}{\partial t} + U_f \frac{\partial C_s}{\partial x} = E_A \frac{\partial^2 C_s}{\partial x^2} - KC_s \qquad 3\text{-}20$$

where K represents the rate of absorption. (C_s, U_f and E_A have been used to be consistent with the present notation.) In the experiments, dye was released at high water and spatial concentration distributions were measured at 5 period intervals up to 50 tidal periods after release. O'Connor found good agreement between the solution to eqn. 3-20 and the experimental concentration distributions. He concluded that the measured dispersion coefficients showed no correlation with the through-flow velocity U_f. It was also concluded that the dispersion coefficient decreased with distance downstream. When more data from this same set of experiments (ref. 5) was analyzed as part of the present work, scatter was noted but there was not a consistent tendency for E_A to decrease with distance. (See section 8.2.) These values of E_A are correlated with the tidal parameters in section 8.

O'Connor (ref. 36) also reported two values of E_A from prototype measurements in the James River (Virginia). These values were based on 1951 measurements of sulfate ion in industrial waste. It was concluded that E_A increased with river flow (Q_f). For one experiment Q_f was 35% greater than for the other, and E_A was found to be 28% greater in the former case. However, in view of the limited data that led to this conclusion and in view of the discussion above, this change in E_A is probably due to some influence other than Q_f. The tidal conditions were not given. Thus, it is not possible to compare the experimental E_A with eqn. 3-18.

3.3.2) Salinity Intrusion Region

In the salinity intrusion region of an estuary, internal density currents cause a mean circulation pattern as shown in fig. 1-1. Thus, the velocity distribution (fig. 3-1) and u'' depend strongly on the salinity gradients. This means that the velocity variations (u'') from the sectional

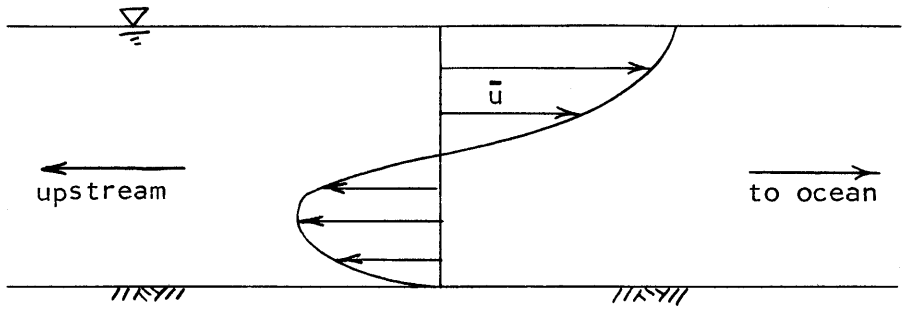

Fig. 3-1: Mean velocity distribution in the salinity region of an estuary

mean will generally be greater than would result from boundary shear alone. Also, the vertical density gradients tend to suppress vertical mixing. This means that c'' will be greater than in absence of density effects. In accordance with the definition of the dispersion coefficient (eqn. 2-14 and eqn. 2-17), one would expect the dispersion coefficient in a given estuary to be larger in the salinity intrusion region than in the constant density regions. This trend has been observed, as discussed below.

In section 2 it was pointed out that both turbulent diffusion and longitudinal dispersion are actually convective transport. Likewise, in ref. 16, it was reasoned and shown empirically that the effects of gravitational convection in the salinity region of an estuary may be treated as a one dimensional diffusive transport. In the salinity region, the dispersion coefficient was given the symbol E'_{xt} to indicate that gravitational effects were included in E. Thus, the mass balance equation (eqn. 2-18) now becomes

$$\frac{\partial C}{\partial t} + U_{xt} \frac{\partial C}{\partial x} = \frac{1}{A} \frac{\partial}{\partial x} \left(E'_{xt} A \frac{\partial C}{\partial x} \right) \qquad 3\text{-}21$$

Or by analogy to eqn. 2-26, the equation

$$\frac{1}{T}\frac{\partial C_s}{\partial n} + U_{f_x}\frac{\partial C_s}{\partial x} = \frac{1}{A}\frac{\partial}{\partial x}\left(E'_{A_x} A \frac{\partial C_s}{\partial x}\right) \qquad 3\text{-}22$$

represents the concentration changes from one period to the next if T is the period and n = 1, 2, 3 . . . Even for a uniform estuary, E'_A should be expected to vary with x since the strength of the gravitational convection due to salinity difference decreases in the upstream direction.

As part of the treatment of this problem by Ippen, Harleman, and others (ref. 16-18, 27, 29), experiments were conducted in an idealized estuary which was rectangular in cross section (16" wide, 7" water depth). Vertically oscillating screens were substituted for mixing due to tidal motion. Thus, the one dimensional diffusive type transport was due to turbulent diffusion and gravitational convection. In recognition of the fact that there was no shear-flow velocity distribution involved in the process, the apparent diffusion coefficient is given the symbol e_x'. For those tests made with no gravitational convection (i.e., no density difference), the diffusion coefficient was independent of x and is called $e°$.

The experiments showed that $e_x'/e°$ correlated with a dimensionless stratification parameter $G_A/(gCU_f)$ where g is the acceleration of gravity, C is the concentration of salt at any point in the estuary, U_f is the fresh water velocity, and G_A is the mean rate of turbulent energy dissipation per unit mass of fluid. The ratio $e_x'/e°$ represents the increase in longitudinal diffusion due to gravitational effects. The stratification parameter represents the ratio of the rate of turbulent energy dissipation to the rate of gain of potential energy of the fresh water as it moved toward the ocean. As the stratification parameter increases, the degree of stratification in the estuary decreases. Thus, large values of $e_x'/e°$ were found to correspond to small values of $G_A/(gCU_f)$.

Density differences between fresh and ocean water varied from 0 to 2% in the experiments. At high degrees of statification, it was found that the gravitational effects caused $e_x'/e°$ to be as great as 1000.

In general, this ratio of diffusion coefficients was found to be

$$\frac{e_x'}{e^o} = 1700 \left(\frac{G_A}{gCU_f} \right)^{-3/4} \qquad 3\text{-}23$$

For an estuary, interpreting this in terms of dispersion due to tidal motion and gravitation convection (i.e., E'_{A_x}) and using eqn. 3-19, it was concluded that the general functional relationship for E'_{A_x} should be

$$\frac{E'_{A_x}}{R_H^{4/3} G_A^{1/3}} = f \left(\frac{G_A}{gCU_f} \right) \qquad 3\text{-}24$$

Kent (ref. 30, 31) analyzed results from the Delaware model for an instantaneous release of tracer in the salinity region. He observed that the rate of decrease of the maximum concentration (dC_{max}/dt) of the tracer increased the further downstream the injection point was. From eqn. 5-7, it can be seen that this rate of decrease depends on the dispersion coefficient. Thus, Kent's observation is in accordance with an increasing value of E'_A in the downstream direction. The primary reason for this increase is probably the increasing gravitational convection. A smaller contribution would be the fact that the tidal velocity (U_T) increases in the downstream direction. This increase (or the decrease in the upstream direction) is due to frictional damping.

Kent also analyzed the results of three tests with different Q_f's in the Corps of Engineers tidal flume which was previously mentioned. (See the paragraph following eqn. 3-19.) The results showed that E'_A at a given point decreases as Q_f increases. For the fresh water portion, it was reasoned above that E_A should be independent of Q_f. In the salinity region, however, the intruded salt will be pushed downstream as Q_f is increased. As the pattern of gravitational convection is shifted downstream, the gravitational effects at a given point will decrease. Thus, E'_A will decrease also. This effect is accounted for in eqn. 3-24, which shows E'_A to be a function of U_f.

O'Connor (ref. 36) applied the one dimensional mass balance equation to non-conservative substances (BOD and dissolved oxygen) in the

salinity portion of estuaries. In all cases, the dispersion coefficient was assumed to be independent of x. This paper contained work on the James and the Delaware estuaries. For the James, he used the previously mentioned dispersion coefficients. For the Delaware, dispersion coefficients as determined from the model were used.

4) ESTUARY MODELS

4.1) Introduction

In the region of salinity gradients in prototype estuaries, the salt may be viewed as a natural conservative tracer and salt concentrations may be used to determine dispersion coefficients. These coefficients can then be used to predict concentration distributions of other substances which may be introduced into the saline region. However, in constant density regions (either all fresh water or all salt water), there are usually no natural concentration gradients which may be used to find dispersion coefficients. This means that direct prototype determination of dispersion coefficients is more difficult and expensive in constant density regions. Thus, distorted models are often used to study pollution distribution problems in estuaries. In using such models, one must determine the ratio or relation between model and prototype concentrations.

Since the models must reproduce tidal motions, they are constructed and operated according to Froude scaling which considers similitude of inertial and gravitational forces. However, because of the large length and relatively small depth of estuaries, the models must be distorted vertically. (The distortion of the Delaware model is 10 to 1.) Because of this distortion, the models must be verified. This verification is usually accomplished by adjusting local roughness in the model until certain quantities scaled from the model are in agreement with prototype observations. (In the Delaware model, the roughness was adjusted by placing vertical strips in the flow.) The quantities usually used for verification of models are tidal elevation and phase, magnitude and direction of velocity, and longitudinal and vertical salinity distributions. The velocities are usually measured at the surface, middepth, and near the bottom. (In the Delaware model, the furthest point upstream that was used in the original verification was just above Philadelphia. Thus, 125 ft. of the model or about 25 prototype miles were verified only for tidal stage and phase.)

Since the salinity distribution is largely a result of longitudinal circulatory motions induced by longitudinal density gradients, the model adjustments constitute a verification of the density induced circulatory motions in the salinity region. In Section 3.3.2, it was pointed out that these circulatory (gravitational) motions exerted the dominant influence in the dispersion process. Thus, concentration gradients measured in the region of the salinity distribution in the model may be used directly in prototype scale to determine prototype dispersion coefficients. Even more important and more directly to the point, the model verification implies that there is a one to one correspondence of concentrations (of salinity or other substances) in the model and prototype at geometrically similar points in the region where salinity gradients exist.

In the constant density regions of an estuary, the dispersion process depends on the velocity distribution resulting from boundary shear stress (not gravitational effects) and on lateral concentration distributions resulting from lateral turbulent diffusion. (See Sections 2.5 and 3.3.) The detailed velocity distribution and turbulent diffusion are not verified in the model. Thus, the question is raised concerning the relation between model and prototype dispersion coefficients and concentration distributions for constant density regions of an estuary. As far as is known, all modelling of the dispersion process in constant density portions of estuaries has assumed a one to one correspondence between concentration ratios (i.e. relative concentrations) at geometrically similar points in model and prototype. In fact, this assumption is invalid and has lead to incorrect values of predicted prototype concentrations. Most of the remainder of Section 4 is devoted to an examination of the scaling of dispersion coefficients and concentrations from model to prototype for constant density portions of distorted Froude models.

For the numerical examples, the scale ratios of the Delaware model will be used. A scale ratio is defined as a given model quantity divided by the corresponding prototype quantity. Using the subscripts m, p, and r to indicate model, prototype, and ratio, respectively, the scale ratio of a general quantity B is $B_r = B_m/B_p$. For the Delaware model, the following ratios exist:

horizontal length	$- L_r = 1/1000$
vertical length	$- Y_r = 1/100$
flow area	$- A_r = L_r Y_r = 1/100,000$
horizontal velocity	$- U_r = Y_r^{\frac{1}{2}} = 1/10$
discharge	$- Q_r = L_r Y_r^{3/2} = 1/1,000,000$

Also, it is assumed that the ratio of the hydraulic radii (R_{H_r}) is approximately equal to Y_r.

4.2) Concentration Similitude

The mass balance equation represents the influences which govern the concentration distribution for either model or prototype. For a conservative tracer, the one dimensional form of the mass balance equation is given by Eqn. 2-29 as

$$\frac{\partial C}{\partial t} + U \frac{\partial C}{\partial x} = \frac{1}{A} \frac{\partial}{\partial x} (EA \frac{\partial C}{\partial x}) \qquad 4\text{-}1$$

where the subscripts are omitted from the dispersion coefficient E and the velocity U for the time being. Eqn. 4-1 may be written in dimensionless form by defining the following reference quantities (subscript "o") and dimensionless quantities (subscript "1"):

$$C_1 = C/C_o$$

$$x_1 = x/L_o, \quad (x_o = L_o)$$

$$U_1 = U/U_o$$

$$t_1 = U_o t/L_o, (t_o = L_o/U_o)$$

$$A_1 = A/A_o$$

$$E_1 = E/E_o$$

After introducing these dimensionless quantities and rearranging, Eqn. 4-1 may be written as

$$\frac{U_o L_o}{E_o}\left[\frac{\partial C_1}{\partial t_1} + U_1 \frac{\partial C_1}{\partial x_1}\right] = \frac{1}{A_1}\frac{\partial}{\partial x_1}\left(A_1 E_1 \frac{\partial C_1}{\partial x_1}\right) \qquad 4\text{-}2$$

Past practice for the interpretation of model results has assumed that $(C_1)_m = (C_1)_p$ or that $(C_1)_r = 1$ (i.e. a one to one correspondence of concentrations). It has been pointed out in Section 4.1 that this assumption is valid in the region of longitudinal salinity gradients by virtue of model verification. The validity of this assumption (i.e. $(C_1)_r = 1$) for constant density regions may be investigated on the basis of Eqn. 4-2. Modelling theory states that if the coefficient $U_o L_o / E_o$ in Eqn. 4-2 is the same in model and prototype, then the concentration ratio C_1 is the same in model and prototype. This condition may be stated as,

$$\frac{U_r L_r}{E_r} = 1 \qquad 4\text{-}3$$

For a given Froude model, U_r and L_r will be known. The question arises as to the value of E_r. The value of E_r must be found from an expression which represents the fundamental process involved in producing dispersion. An equation such as Eqn. 4-1 may not be used to find E_r since Eqn. 4-1 represents the effects of dispersion, not the cause of it. On the other hand, the analytical work of Aris and Taylor shows that consideration of the fundamental definition of dispersion (Section 2.5) leads to the conclusion that E is proportional to $R_H u_*$ for uniform flow. Assuming that the same relation holds for constant density regions of estuaries, (see sections 6, 8, 9), then

$$E_r = (R_H\, u_*)_r \qquad 4\text{-}4$$

Or, using Harleman's equivalent expression (Eqn. 3-18),

$$E_r = \frac{n_r}{R_{H_r}^{1/6}}\, U_r\, R_{H_r} \qquad 4\text{-}5$$

Using the relations $R_{H_r} \approx Y_r$, $U_r = Y_r^{1/2}$, and $n_r = Y_r^{2/3}/L_r^{1/2}$ (from Manning's equation), then

$$E_r = Y_r^2/L_r^{1/2} \qquad 4\text{-}6$$

and

$$\frac{U_r L_r}{E_r} = \left(\frac{L_r}{Y_r}\right)^{3/2} \qquad 4\text{-}7$$

This shows clearly that the condition of Eqn. 4-3 is not satisfied for distorted models and that it is therefore invalid to assume a one to one correspondence of concentration ratios in model and prototype. (On the other hand, Eqn. 4-7 also shows that $(C_1)_r = 1$ for undistorted models since Y_r equals L_r in these models.)

The lack of one to one correspondence of concentration ratios in constant density regions of distorted estuary models may also be demonstrated by an example. In Section 6 (Eqn. 6-52) the solution is presented for the case of a continuous injection of a tracer into uniform estuary type flow. The concentration distributions shown in Fig. 4-1 were calculated from Eqn. 6-52 for a quasi-steady state condition with model and prototype flow parameters which might correspond to a 10:1 distorted Froude model. Prototype values were taken similar to those which might exist in the Delaware estuary:

U_f = fresh water velocity = 0.0290 fps
(Q_f = fresh water discharge $\approx$ 5000 cfs)
U_T = maximum tidal velocity = 2.82 fps
b = tidal excursion = 40,000 ft = 7.57 miles
E = average dispersion coefficient during a period = 22.8 ft^2/sec

The corresponding model values of velocities, discharge, and excursion can be found from the scale ratios given at the end of Section 4.1.

However, it is necessary to use Eqn. 4-6 to obtain an estimate of the corresponding dispersion coefficient for the model. This gives E_m of 0.0720 ft^2/sec. Thus, in dimensionless form, the parameters which were used were

$$\left(\frac{U_f T}{b}\right)_{m,p} = 0.0323$$

$$\left(\frac{U_T T}{b}\right)_{m,p} = 3.14$$

$$\left(\frac{E}{U_f b}\right)_p = 0.0197$$

$$\left(\frac{E}{U_f b}\right)_m = 0.619$$

Uniform flow was assumed for both model and prototype. Since the curves are plotted versus a dimensionless length scale, the two curves would coincide if $(C_1)_r = 1$. The concentration in the prototype is less spread out than in the model. Thus, if it were assumed that $(C_1)_r = 1$, the dispersion calculated for the prototype would be too large, as indicated in Section 4.4, below.

4.3) Example of Actual Concentration Ratio

The previous paragraphs have demonstrated that a one to one correspondence of concentration ratios does not exist in distorted Froude models. An example will now be presented to show what the actual concentration ratio is for a particular case.

Eqn. 2-38 is the mass balance equation for a quasi-steady state concentration distribution of a conservative substance. (The term quasi-

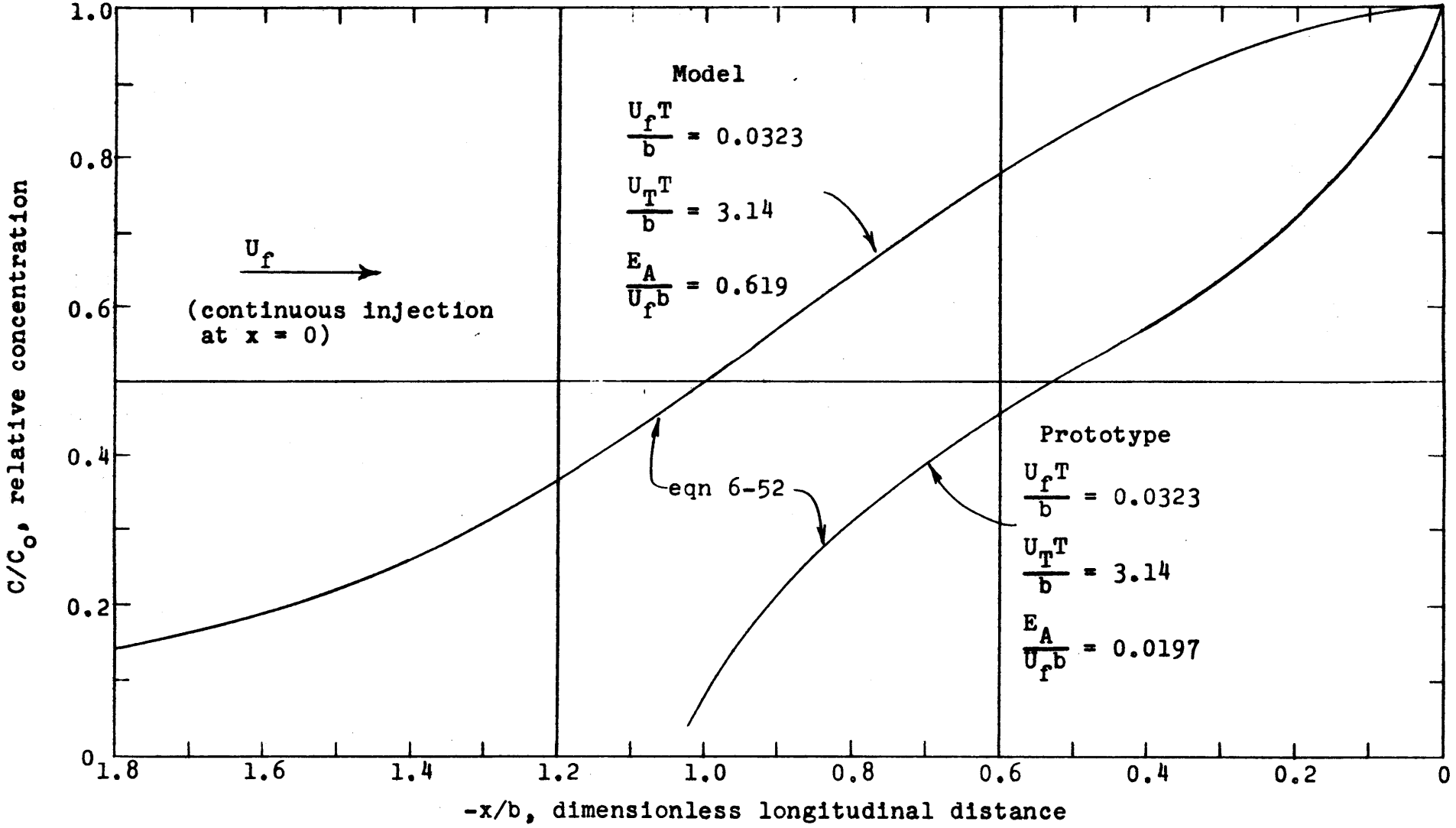

Fig. 4-1a: Theoretical concentration distributions in model and prototype at high water slack (linear scales)

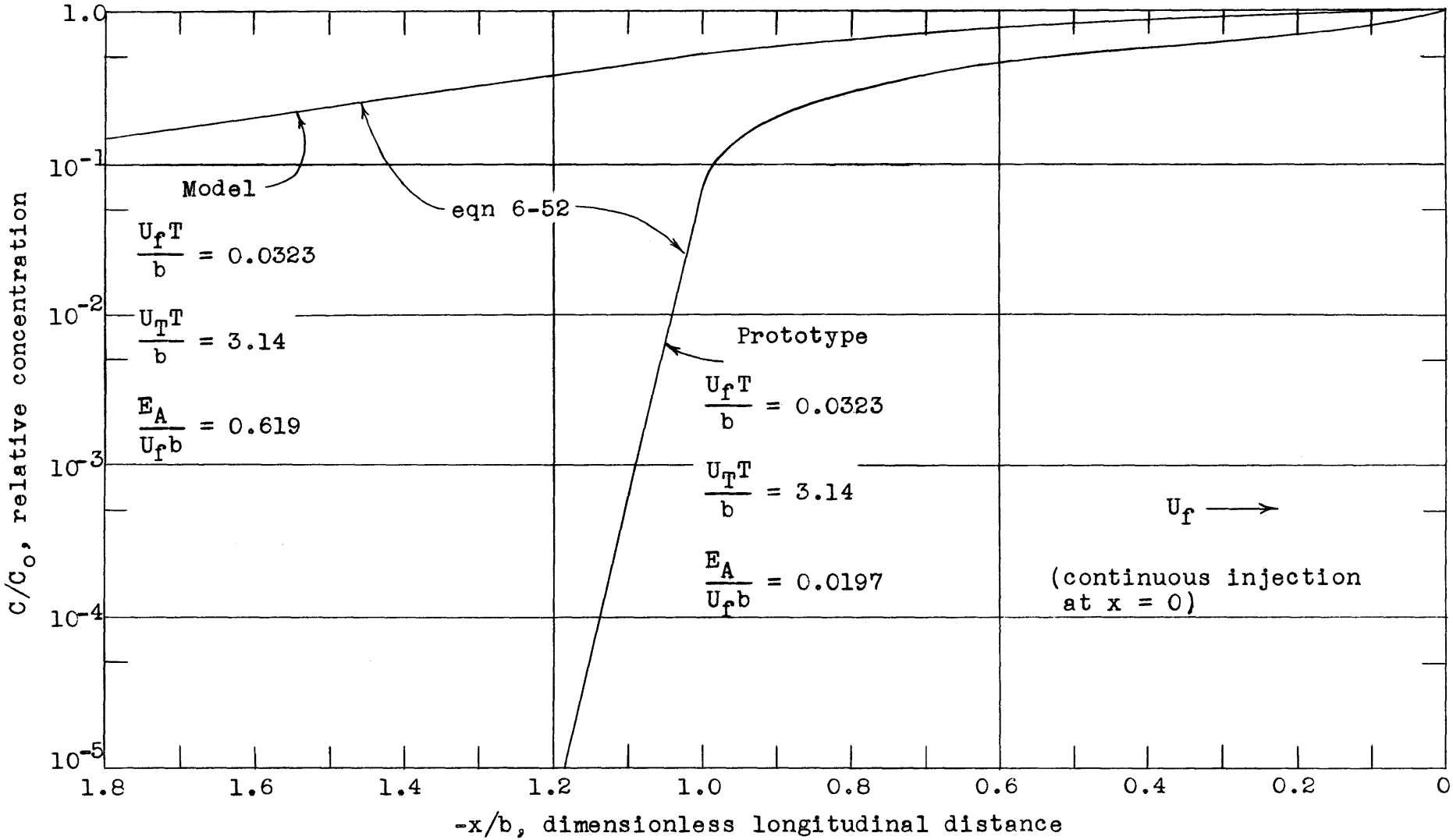

Fig. 4-1b: Theoretical concentration distributions in model and prototype at high water slack (semi-logarithmic plot)

steady refers to conditions when the concentration at a given point does not change at times differing by one tidal period.) For the model, this equation may be written as

$$\frac{dC_m}{C_m} = \frac{U_{f_m}}{E_{A_m}} dx_m \qquad 4\text{-}8$$

If C_{om} is the concentration at x_{om}, Eqn. 4-8 may be integrated to give

$$\ell n \frac{C_m}{C_{om}} = \int_{x_{om}}^{x_m} \frac{U_{f_m}}{E_{A_m}} dx_m \qquad 4\text{-}9$$

Using the relations that $U_{fr} = Y_r^{1/2}$, $E_{Ar}^2 = Y_r^2/L_r^{1/2}$, and $dx_m = L_o\, dx_p$, Eqn. 4-9 may be converted to

$$\ell n \frac{C_m}{C_{om}} = \left(\frac{L_r}{Y_r}\right)^{3/2} \int_{x_{op}}^{x_p} \frac{U_{f_p}}{E_{A_p}} dx_p \qquad 4\text{-}10$$

Eqn. 4-8 may also be written independently for the prototype. After integrating, one would obtain

$$\ell n \frac{C_p}{C_{op}} = \int_{x_{op}}^{x_p} \frac{U_{f_p}}{E_{A_p}} dx_p \qquad 4\text{-}11$$

Dividing Eqn. 4-11 by Eqn. 4-10,

$$\frac{\ell n \frac{C_p}{C_{op}}}{\ell n \frac{C_m}{C_{om}}} = \left(\frac{Y_r}{L_r}\right)^{3/2} \qquad 4\text{-}12$$

or

$$\frac{C_p}{C_{op}} = \left(\frac{C_m}{C_{om}}\right)^{(Y_r/L_r)^{3/2}} \qquad 4\text{-}13$$

For a model with a 10 to 1 vertical distortion, Y_r/L_r is 10 and

$$\left(\frac{C_p}{C_{op}}\right) = \left(\frac{C_m}{C_{om}}\right)^{31.6} \qquad 4\text{-}14a$$

or, equivalently,

$$(C_1)_r \equiv \frac{(C_m/C_{om})}{(C_p/C_{op})} = \left(\frac{C_m}{C_{om}}\right)^{-30.6} \qquad 4\text{-}14b$$

Thus, it is seen that the assumption of a one to one correspondence of concentration ratios (i.e. $(C_1)_r = 1$) is incorrect. Furthermore, $(C_1)_r$ is not constant but rather depends on the relative concentration. From Eqn. 4-14a, if C_m/C_{om} of 0.90 is observed at some point in the model, then at the equivalent point in the prototype C_p/C_{op} is 0.036.

Some observations about Eqn. 4-13 should be made. First of all, this equation does not give a direct concentration scale ratio (i.e., C_m/C_p). Rather, it gives the comparative ratios to some reference concentration for model and prototype (i.e., C_{om} and C_{op}). Thus, it is still necessary to have some means of determining this reference concentration in both model and prototype. Also, the equation which was used to write Eqn. 4-8 is

$$U_f C = E_A \frac{\partial C}{\partial x} \qquad 4\text{-}15$$

In applying this equation to a given one dimensional element of fluid, it is implied that, from one period to the next, mass enters or leaves this element only by convection or by dispersion. Eqn. 4-15 and hence Eqn. 4-13 do not apply to any of the fluid elements into which tracer is injected during a period of oscillation. For the example shown in Fig. 4-1, Eqn. 4-14 can not be applied in the region $-1.0 < (x/b) < 0$ (since the distributions are shown at high water). That is, the fluid in this region at high water is the fluid which oscillates past the injection point. At low tide, Eqn. 4-13 does not apply in $0 < (x/b) < 1.0$. The fact that Eqn. 4-13 does not apply in $-1.0 < (x/b) < 0$ at high water is easily observed from the figure. For the model, C/C_o is 0.90 at $x/b = -0.32$. At the same x/b for the prototype, C/C_o is 0.62 rather than the 0.036 cited immediately following Eqn. 4-14b. However, if C'_{om} and C'_{op} were taken as those values at $x/b = -1.0$, then Eqn. 4-13 would apply upstream from this point. For example, at $x/b = -1.0$,

$$\frac{C_m}{C_{om}} = \frac{C'_{om}}{C_{om}} = 0.500$$

$$\frac{C_p}{C_{op}} = \frac{C'_{op}}{C_{op}} = 0.080$$

and at $x/b = -1.05$,

$$\frac{C_m}{C_{om}} = 0.465$$

$$\therefore \quad \frac{C_m}{C'_{om}} = \frac{C_m/C_{om}}{C'_{om}/C_{om}} = 0.930$$

$$\left(\frac{C_p}{C'_{op}}\right) = \left(\frac{C_m}{C'_{om}}\right)^{31.6} = (0.930)^{31.6} = 0.101$$

$$\frac{C_p}{C_{op}} = \frac{C_p}{C'_{op}} \cdot \frac{C'_{op}}{C_{op}} = 0.0081$$

This agrees with the value found directly from Eqn. 6-52, as shown in Fig. 4-1.

4.4) Error in Prototype Dispersion Coefficients

The procedures which have been used in the past assumed that Eqn. 4-3 was valid. Thus, effectively, E_r has been assumed to be

$$E_r = Y_r^{1/2} L_r \qquad 4\text{-}16$$

(from Eqn. 4-3 with $U_r = Y_r^{1/2}$). For the Delaware model, Eqn. 4-16 gives $E_r = 1/10{,}000$. Under the assumptions which have been made above, E_r is actually given by Eqn. 4-6 which gives $E_r = 31.6/10{,}000$. Thus, for a given dispersion in the model, the procedures which have been used in the past give a dispersion coefficient for the prototype which is 31.6 times too large.

4.5) Discussion of Scale Ratio for Dispersion Coefficient

All of the development of this section has been based on a particular expression for E_r. (See Eqn. 4-4, 4-5, and 4-6.) While it is

certain that E_r is not given by Eqn. 4-16 (as past practice has implied), there are some questions about the complete accuracy of Eqn. 4-6 which was used for E_r.

The work discussed in Section 3 indicated that the dispersion coefficient may be given by

$$E = mR_H u_* \qquad 4\text{-}17$$

where m is nearly constant for a given stream but varies from stream to stream in general. In writing Eqn. 4-4 it was implied that m is the same for model and prototype. In Section 3 it was seen that one of the things which might cause m to change was a varying degree of "side wall" effects. In distorting a model, the relative effects of the side walls are increased over that for the prototype. In addition, the strips used to adjust the roughness during model verification would influence the velocity distribution and thus possibly change m.

It is true that the model may be verified for tidal velocities at three different depths. However, these three measurements do not assure the verification of the entire velocity distribution, and Eqn. 2-26 shows that the entire distribution contributes to the dispersion process. Even if the entire velocity distribution were verified, it must be remembered that the lateral diffusivity influences dispersion also and would need to be verified.

The existence of a laminar sublayer likewise influences dispersion. Natural roughness in the prototype probably excludes the chance of a sublayer. However, the model surface is usually smoother (as evidenced by the need for roughness strips) and a sublayer may exist. Also, to get from Eqn. 4-4 to Eqn. 4-6, Manning's equation was used to determine the roughness ratio n_r. In view of the adjustment of roughness which takes place during verification and the fact that the flow is unsteady, one could question the validity of expressing n_r as was done.

4.6) Conclusions About Modelling

It appears that the interpretation of model concentrations for pollution studies in the constant density portions of distorted estuary models has been incorrect. The analysis presented in this section should be much more nearly correct, but there is still room for question concerning the expression used for the ratio of dispersion coefficients. It would be helpful if the results of model dispersion studies could be checked against prototype results for the constant density portions of estuaries to investigate the validity of the assumptions made in the present work. In Section 6 of the present work, an analysis is presented which allows the dispersion coefficient to be calculated for uniform flow of the type found in constant density regions of estuaries (i.e. estuary type flow). In Section 8, experiments are described which were used to check the analysis of Section 6 for a specific boundary configuration, namely a circular pipe.

The verification of distorted models usually includes verification of salinity gradients. This effectively constitutes a verification of the dispersion process for the portion of the estuary where salinity gradients exist. Thus, concentrations measured in this portion of the model may be taken as applying directly to the geometrically similar points in the prototype.

5) SOLUTIONS FOR ONE DIMENSIONAL DISPERSION EQUATIONS IN STEADY FLOW

This section is concerned primarily with uniform flow since it is seldom possible to obtain an analytical solution to a dispersion equation for non-uniform flow. Nevertheless, much can be learned about the characteristics of the dispersion process by looking at some of the solutions which can be obtained for uniform flow. At the end of the section, an indication is given of how solutions may be obtained for non-uniform flows by use of finite difference equations.

It has previously been shown (eqn. 2-19) that the one dimensional equation for the conservation of a conservative substance in uniform flow is

$$\frac{\partial C}{\partial t} + U_t \frac{\partial C}{\partial x} = E_t \frac{\partial^2 C}{\partial x^2} \qquad 5\text{-}1$$

where C is the concentration of the substance, U_t is the one dimensional velocity, E_t is the coefficient of longitudinal dispersion, t is time, and x is the longitudinal space coordinate in the flow direction.

In the discussion which follows, the substance which is being transported by the fluid will be assumed to be a tracer with the same density as the flowing fluid. The mathematical solutions, however, will closely approximate the dispersion of any conservative substance whose concentration is low enough so that it does not appreciably affect the flow pattern.

5.1) Steady, Uniform Flow

If the flow is steady as well as uniform, then the velocity and the dispersion coefficient are constant so that U_t and E_t may be written respectively as U and E. Therefore,

$$\frac{\partial C}{\partial t} + U \frac{\partial C}{\partial x} = E \frac{\partial^2 C}{\partial x^2} \qquad 5\text{-}2$$

5.1.1) Instantaneous, Point Injection

Consider an instantaneous injection of tracer at x = 0 and

$t = 0$. The injection is assumed to be uniform over the cross section at $x = 0$. For simplicity, this will be called an instantaneous, point injection. If M is the mass of tracer which is injected, A is the cross sectional flow area, and $\delta(x)$ is the Dirac delta function, then the initial and boundary conditions for the solution of eqn. 5-2 are

$$C(x,0) = \frac{M}{\rho A}\,\delta(x)$$
$$C(\pm\infty,t) = 0 \qquad 5\text{-}3$$

The Dirac delta is a function which is defined as zero for all values of its argument (x) except zero. Also, the integral of the function is unity:

$$\int_{-\infty}^{\infty} \delta(x)\,dx = 1$$

Thus, at $x = 0$, $\delta(x)$ represents a "spike" of infinitestimal width and unit area. The spike initial condition is indicated on fig. 5-1. By introducing the change of variables

$$\bar{x} = x - Ut$$
$$\bar{t} = t \qquad 5\text{-}4$$

eqn. 5-2 becomes

$$\frac{\partial C}{\partial \bar{t}} = E\,\frac{\partial^2 C}{\partial \bar{x}^2} \qquad 5\text{-}5$$

which is the familiar "heat equation". The solution to eqn. 5-5 (ref. 9) under the conditions of eqn. 5-3 is

$$C = \frac{M}{\rho A\sqrt{4\pi E\bar{t}}}\,\exp\left(-\frac{\bar{x}^2}{4E\bar{t}}\right)$$

(This may be verified by substituting it into eqn. 5-5 and by observing that the conditions of eqn. 5-3 are satisfied.) After returning to the original variables x and t, the solution is

$$C = \frac{M}{\rho A\sqrt{4\pi Et}}\,\exp\left[-\frac{(x - Ut)^2}{4Et}\right] \qquad 5\text{-}6$$

The characteristics of this solution are discussed below and are shown in fig. 5-1 and fig. 5-2.

Eqn. 5-6 indicates that the tracer has a normal or Gaussian distribution in the x direction for all time. The maximum concentration is always at $x = Ut$ and decreases with time according to

$$C_{max} = \frac{M}{\rho A\sqrt{4\pi E t}} \qquad 5\text{-}7$$

The centroid of the dispersing tracer is also at $x = Ut$, and the variance (second moment, eqn. 7-2) of the tracer distribution is given by $\sigma^2 = 2Et$. Thus, the tracer is continually being spread out longitudinally due to dispersion. These characteristics of the spatial distribution are shown in fig. 5-1.

Consider the concentration distribution which will be obtained by observing the tracer as it passes a fixed x. The observed distribution will be skewed (fig. 5-2) even though the x distribution is normal at each instant. This skewness is due to the dispersion which takes place as the tracer passes the observation point.

It is generally more practical to observe a tracer as it passes a fixed point rather than to sample the spatial distribution at a fixed time. Thus, the spatial distribution for a fixed x will be investigated further.

By differentiating eqn. 5-6 with respect to t, the time of occurrence (t_p) of the peak concentration on a time record of concentration at any x_i may be found to be

$$t_p = \frac{x_i}{U}\left[\sqrt{1 + \left(\frac{E}{Ux_i}\right)} - \frac{E}{Ux_i}\right] \qquad 5\text{-}8$$

This shows that the peak concentration on a time record occurs after the time of mean flow (x_i/U) from the injection point to the station where measurements are being made. The difference between t_p and x_i/U decreases as x_i increases. For steady flow in a pipe of radius a, using Taylor's expression for E (eqn. 3-4) and taking a Darcy-Weisbach friction factor (f) of 0.02,

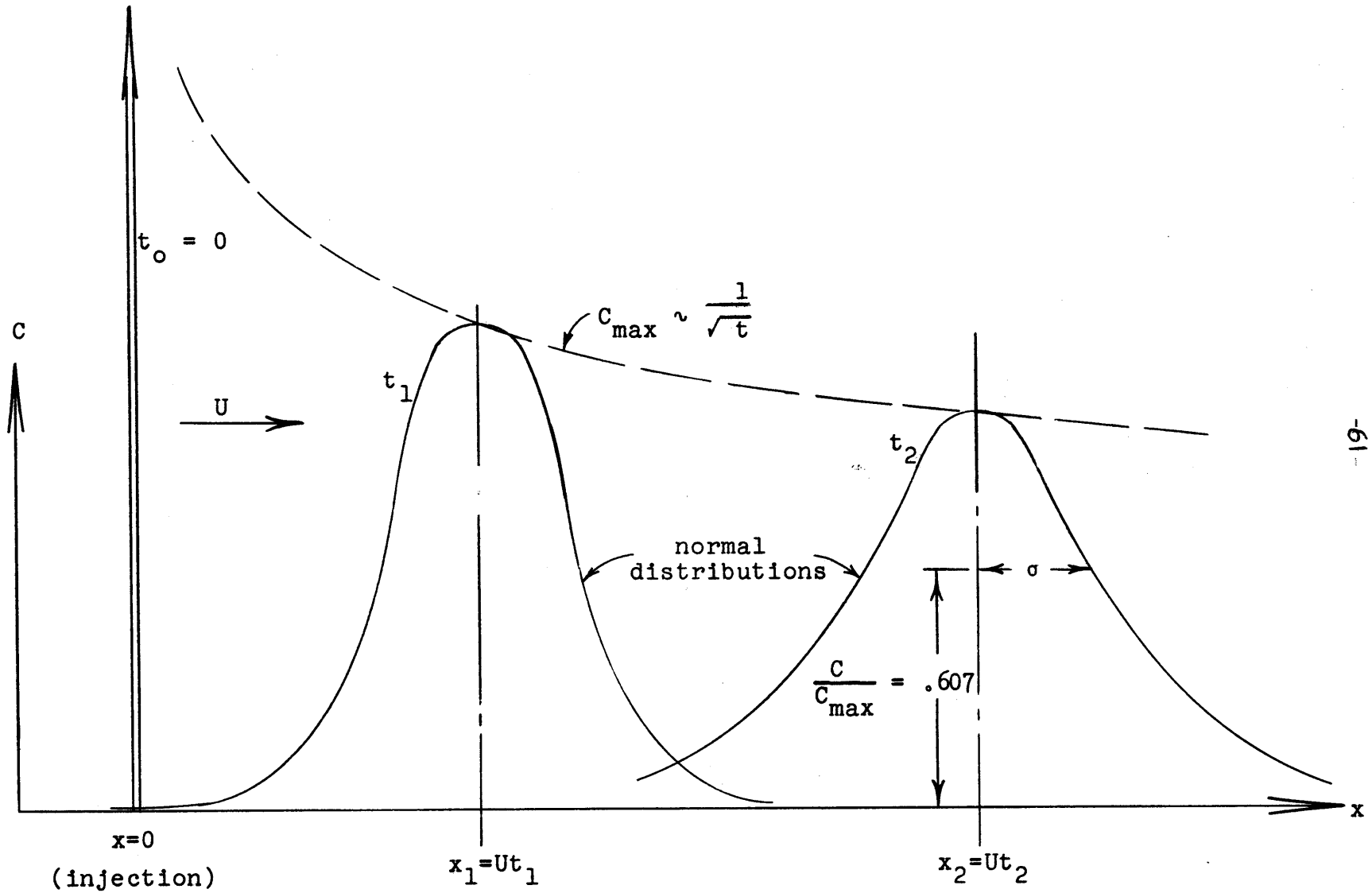

Fig. 5-1: Characteristics of spatial concentration distributions for an instantaneous, point injection of tracer

$$\frac{E}{Ux_i} \approx 4\frac{a}{x_i} \qquad 5\text{-}9$$

Thus, if x_i/U is large, t_p will be essentially equal to x_i/U, the mean flow time from the injection point to x_i. (The term "maximum concentration" will be used for a spatial distribution, and "peak concentration" will be used for the temporal distribution observed at a fixed x.)

In connection with the spatial distribution, it was pointed out that the mean (first moment) of the spatial distribution was at $x = Ut$ and that the variance (second moment) was related to E. Similar relationships can be derived for a temporal distribution.

Define the $p^{\underline{th}}$ time moment of the concentration distribution as

$$\mu_p = \int_0^\infty C\ t^p\ dt \qquad 5\text{-}10$$

In general, this integration can not be carried out directly using eqn. 5-6 to find the μ_p's. However, eqn. 5-2 may be converted into an equation for the μ_p's, and the moments may be found from solving this differential equation. (The general method for converting a differential equation into an equation for moments is demonstrated in appendix B in connection with obtaining eqn. B-4 from eqn. 6-13.) In this manner, it is found that

$$\mu_o = \frac{M}{\rho AU} \qquad 5\text{-}11$$

$$\mu_1 = \mu_o\left[\frac{x_i}{U} + \frac{2E}{U^2}\right] \qquad 5\text{-}12$$

$$\mu_2 = \mu_o\left[\frac{x_i^2}{U^2} + 6\frac{Ex_i}{U^3} + 12\frac{E^2}{U^4}\right] \qquad 5\text{-}13$$

These moments are taken about the origin of time, i.e., the time of injection. Define μ_2^p and μ_2^i as the second moments about t_p (eqn. 5-8) and about $t_i = \mu_1/\mu_o$, respectively. Note that t_i is the time of occurrence of the centroid of the temporal distribution at x_i. These two forms of the second moment are

$$\mu_2^p = \mu_o \left[2 \frac{Ex_i}{U^3} + 12 \frac{E^2}{U^4} \right] \qquad 5\text{-}14$$

$$\mu_2^i = \mu_o \left[2 \frac{Ex_i}{U^3} + 8 \frac{E^2}{U^4} \right] \qquad 5\text{-}15$$

For two stations x_i and x_j, let the times of occurrence of the centroid be t_i and t_j. From eqn. 5-12, it may be seen that $(t_i - t_j)$ is equal to the flow time between x_i and x_j. However, t_i is not equal to the mean flow time from the point of injection to x_i. This results from the fact that upstream dispersion causes the time μ_1/μ_o at the point of injection to be different from t = 0, the time of injection. Perhaps this can be seen more clearly from fig. 5-2, which shows some of the characteristics of temporal concentration distributions.

Equations 5-14 and 5-15 indicate that, if the second moment is taken about either t_p or t_i, then the rate of change of the second moment from one x to another is linearly related to the dispersion coefficient. That is,

$$\frac{2E}{U^3} = \frac{d}{dx}\left(\frac{\mu_2^p}{\mu_o}\right) = \frac{d}{dx}\left(\frac{\mu_2^i}{\mu_o}\right) \qquad 5\text{-}16$$

5.1.2) Continuous, Point Injection

Since eqn. 5-2 is linear, superposition of solutions may be used. In many cases, the way in which a tracer is introduced into the flow may be described as an integral of Dirac delta functions. If this is the case, the solution to eqn. 5-2 can be given as an integral of the concentration distribution as given by eqn. 5-6.

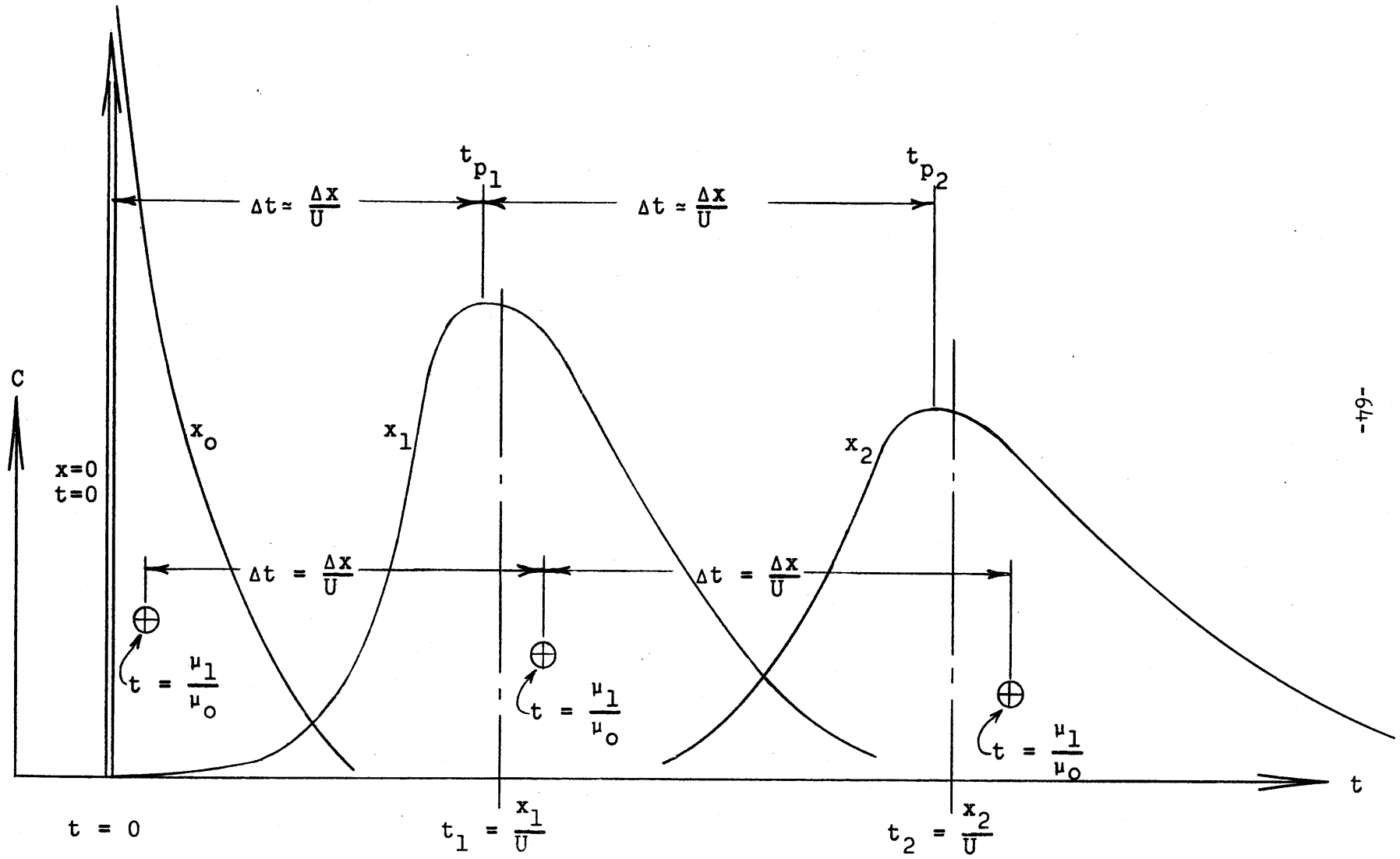

Fig. 5-2: Characteristics of temporal concentration distributions for an instantaneous, point injection of tracer.

For example, consider the case where a tracer is injected at a constant rate at x = 0 during a time interval $0 \leq \tau \leq t_1$. Thus, the injection condition could be written as an integral of delta functions for τ varying from zero to t_1. At any time t, the increment of concentration (dC) due to the increment of tracer (dM) which was injected at time τ is given by

$$dC = \frac{dM}{\rho A\sqrt{4\pi E(t-\tau)}} \exp - \frac{[x - U(t-\tau)]^2}{4E(t-\tau)} \qquad 5\text{-}17$$

if t is measured from the beginning of the injection. If the mass rate of injection is Q_m, then $dM = Q_m d\tau$ and for $t \geq t_1$

$$C = \int_o^{t_1} \frac{Q_m}{\rho A\sqrt{4\pi E(t-\tau)}} \exp - \frac{[x - U(t-\tau)]^2}{4E(t-\tau)} d\tau \qquad 5\text{-}18$$

(This solution is presented in ref. 9 and 29.)

By letting

$$a = \frac{Ux}{4E} \qquad b = \frac{U}{2}\sqrt{\frac{t-\tau}{E}}$$

$$B = \frac{U}{2}\sqrt{\frac{t}{E}} \qquad B_1 = \frac{U}{2}\sqrt{\frac{t-t_1}{E}}$$

eqn. 5-18 may be written as

$$C = \frac{2Q_m}{\rho AU\sqrt{\pi}} \exp \frac{Ux}{2E} \int_{B_1}^{B} \exp - \left(b^2 + \frac{a^2}{b^2}\right) db \qquad 5\text{-}19$$

In practice, it is impossible to obtain a truly instantaneous injection of tracer as was assumed in section 5.1.1. Hence, let us investigate the error which is introduced by assuming an instantaneous injection in a practical case.

Consider the case where tracer is actually injected during some time t_1 at the rate Q_m. When t becomes large relative to t_1, it would be expected that the concentration distribution would be about the same as for

an instantaneous injection of the same mass (i.e., $M = Q_m t_1$). Let C_1 be the concentration resulting from the injection during time t_1, and let C_2 be the concentration resulting from the instantaneous injection. Eqn. 5-18 may be used to obtain an approximation of the time required for C_1 and C_2 to agree to within some desired degree. From eqn. 5-6, one may write

$$\frac{C_2 \rho A \sqrt{\pi}}{M} \sqrt{4Et} \quad \exp \left(-\frac{Ux}{2E}\right) = \exp \left[- \left(B^2 + \frac{a^2}{B^2}\right) \right] \qquad 5\text{-}20$$

From eqn. 5-19, one may also write

$$\frac{C_1 \rho A \sqrt{\pi}}{M} \sqrt{4Et} \quad \exp \left(-\frac{Ux}{2E}\right) = \frac{2}{B\zeta} \int_{B\sqrt{1-\zeta}}^{B} \exp \left[-\left(b^2 + \frac{a^2}{b^2}\right) \right] db \qquad 5\text{-}21$$

where $\zeta = t_1/t$. Hence, the question concerning the agreement of C_1 and C_2 reduces to the question of agreement between the right-hand sides of eqn. 5-20 and eqn. 5-21. From eqn. 5-20, let

$$Y_2 = \exp - \left(B^2 + \frac{a^2}{B^2}\right) \qquad 5\text{-}22$$

and from eqn. 5-21, let

$$Y_1 = \frac{2}{B\zeta} \quad I\,(a, B, \zeta) \qquad 5\text{-}23$$

where

$$I\,(a, B, \zeta) = \int_{B\sqrt{1-\zeta}}^{B} \exp - \left(b^2 + \frac{a^2}{b^2}\right) db \qquad 5\text{-}24$$

The function I may be expanded in a Taylor series about $\zeta = 0$. When this is done, it is found that

$$Y_1 = Y_2 \left[1 + \zeta \left(B^2 - \frac{a^2}{B^2} - \frac{1}{2}\right) \right] + \begin{matrix} \text{terms of} \\ \text{order } \zeta^2 \end{matrix} \qquad 5\text{-}25$$

Since the same mass was assumed to be injected in both cases and since this mass will be more spread out when the injection time is longer, Y_1 will be less than Y_2 in the region near the maximum concentration. If it is desired to have Y_1 and Y_2 (thence C_1 and C_2) agree to within Δ%, then it must be that

$$\zeta \left(B^2 - \frac{a^2}{B^2} - \frac{1}{2}\right) \leq \frac{\Delta}{100} \qquad 5\text{-}26$$

Consider the point $x = Ut$. This point is the centroid of the dispersing tracer, and at this point a^2 equals B^4. Thus, as a first approximation, it may be concluded from eqn. 5-26 that if

$$t > \frac{50\ t_1}{\Delta} \quad , \quad \Delta \text{ in \%}, \qquad 5\text{-}27$$

C_1 and C_2 will agree within approximately Δ %.

This type of approach has been useful to obtain the approximation contained in eqn. 5-27. However, to find the concentration due to an injection for $0 \leq \tau \leq t_1$, eqn. 5-19 may be integrated in terms of error functions, which are defined by

$$\text{erf } z = \frac{2}{\sqrt{\pi}} \int_0^z \exp\ (-q^2)\ dq \qquad 5\text{-}28$$

Note that in general (ref. 24, 44),

$$\frac{2}{\sqrt{\pi}} \int_k^{\ell} \exp - \left(s^2 + \frac{n^2}{s^2}\right) \qquad 5\text{-}29$$

$$= \frac{1}{2}\, e^{2n} \left[\text{erf } \left(\ell + \frac{n}{\ell}\right) - \text{erf } \left(k + \frac{n}{k}\right)\right]$$

$$+ \frac{1}{2}\, e^{-2n} \left[\text{erf } \left(\ell - \frac{n}{\ell}\right) - \text{erf } \left(k - \frac{n}{k}\right)\right]$$

Then, from eqn. 5-19,

$$C = \frac{Q_m}{2\rho AU}\left[\operatorname{erf}\left(\frac{x-U(t-t_1)}{2\sqrt{E(t-t_1)}}\right) - \operatorname{erf}\left(\frac{x-Ut}{2\sqrt{Et}}\right)\right. \qquad 5\text{-}30$$

$$\left. - \exp\left(\frac{Ux}{E}\right)\left\{\operatorname{erf}\left(\frac{x+U(t-t_1)}{2\sqrt{E(t-t_1)}}\right) - \operatorname{erf}\left(\frac{x+Ut}{2\sqrt{Et}}\right)\right\}\right]$$

Up to this point, no restriction has been imposed that would require t_1 to be a constant. Thus, let $t_1 = t$. This corresponds to a continuous, constant rate of injection. Then, from eqn. 5-30, the concentration is

$$C = \frac{Q_m}{2\rho AU}\left[\pm 1 - \operatorname{erf}\left(\frac{x-Ut}{2\sqrt{Et}}\right) - \exp\frac{Ux}{E}\left\{\pm 1 - \operatorname{erf}\left(\frac{x+Ut}{2\sqrt{Et}}\right)\right\}\right] \qquad 5\text{-}31$$

where the plus sign applies for positive x's and the minus sign for negative x's.

If we further consider the steady state which is approached as t approaches infinity, it is found that

$$C = \frac{Q_m}{\rho AU} \quad \text{for} \quad x > 0$$

$$C = \frac{Q_m}{\rho AU} \exp\frac{Ux}{E} \quad \text{for} \quad x < 0 \qquad 5\text{-}32$$

if U is positive. This steady state solution is shown in the sketch below. Notice that for positive x, the

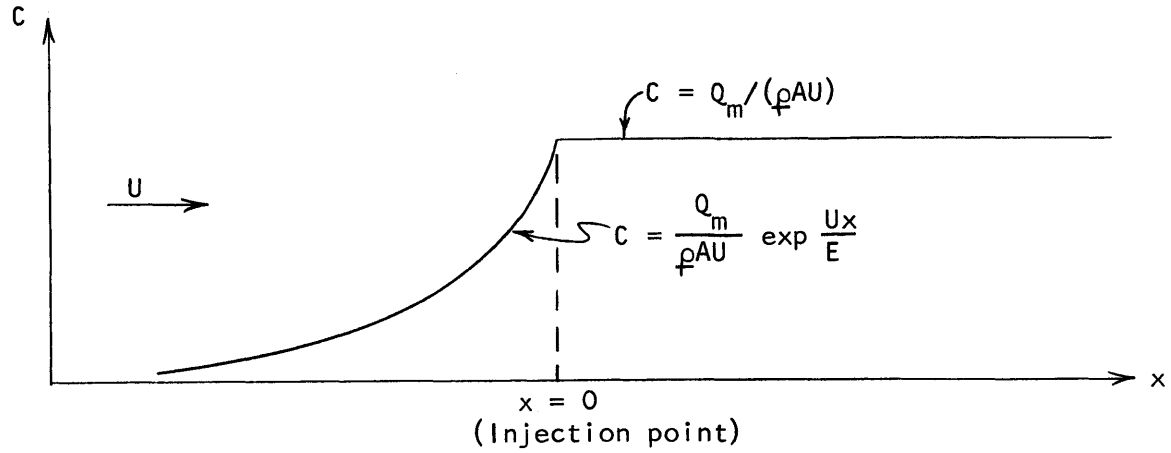

concentration is just given by the dilution ratio between the rate of injection of tracer and the total rate of fluid flow.

5.1.3) Step Function Initial Condition

Consider another case where the tracer concentration is given initially by the step function

$$C(x, 0) = 0 \quad \text{for} \quad 0 < x$$
$$C(x, 0) = C_o \quad \text{for} \quad x < 0 \qquad 5\text{-}33$$

This condition might be realized, for example, when the fluid being pumped through a pipe line is instantaneously changed to another fluid with similar flow properties. The initial condition of eqn. 5-33 represents an initial concentration distribution (i.e., at t = 0) as shown in the sketch.

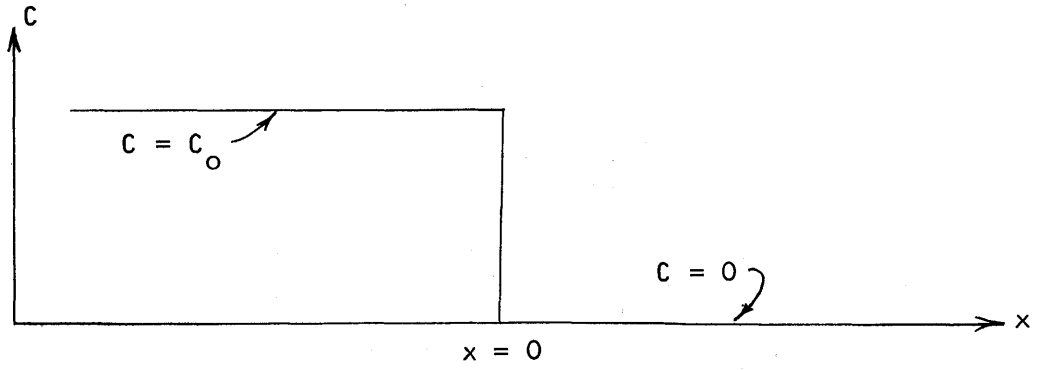

Eqn. 5-33 may also be written as

$$C\ (x,\ 0) = 0 \quad \text{for} \quad 0 < x$$
$$C\ (x,\ 0) = C_o \int_{-\infty}^{o} \delta\ (x - x')\ dx' \quad \text{for} \quad x < 0 \qquad 5\text{-}34$$

By comparison with equations 5-3 and 5-6, the solution for the concentration distribution is given by

$$C = C_o \int_{-\infty}^{o} \frac{1}{\sqrt{4\pi E t}} \exp - \frac{(x - x' - Ut)^2}{4Et}\ dx' \qquad 5\text{-}35$$

By introducing the change of variables

$$Z = \frac{x - x' - Ut}{2\sqrt{Et}} \qquad 5\text{-}36$$

one finds that eqn. 5-35 may be integrated in terms of an error function so that

$$\frac{C}{C_o} = \frac{1}{2} \left[1 - \text{erf} \left(\frac{x - Ut}{2\sqrt{Et}} \right) \right] \qquad 5\text{-}37$$

This solution is shown in the accompanying sketch.

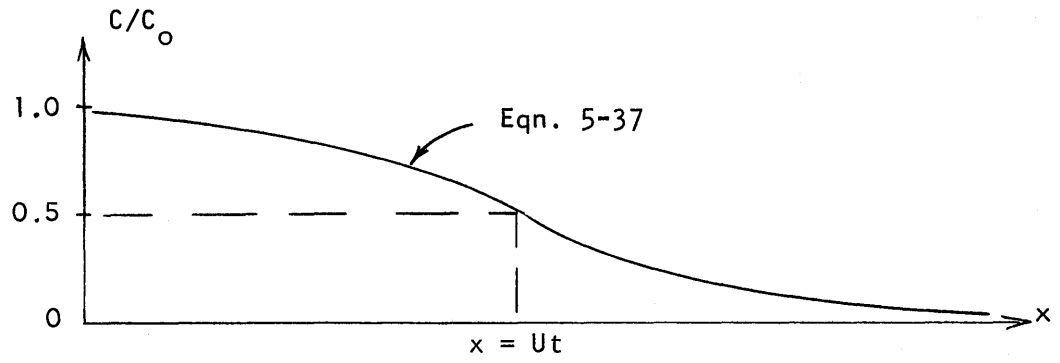

The concentration $C_o/2$ moves downstream with the velocity U. As time progresses, the concentration distribution becomes more and more spread out, while remaining an error function, as indicated by eqn. 5-37.

5.1.4) Constant Concentration at x = 0

If C_o exists for all time at x = 0 and if the initial and boundary conditions are

$$C(0, t) = C_o$$
$$C(x, 0) = 0, \quad x > 0 \qquad 5\text{-}38$$
$$C(\infty, t) = 0$$

then, for positive x, the solution to eqn. 5-2 is

$$\frac{C}{C_o} = \frac{1}{2}\left[1 - \text{erf}\left(\frac{x - Ut}{2\sqrt{Et}}\right) + \exp\frac{-Ux}{E}\left\{1 - \text{erf}\left(\frac{x + Ut}{2\sqrt{Et}}\right)\right\}\right] \qquad 5\text{-}39$$

This condition might come about, for example, when a pipe or stream flows into or out of a large reservoir which effectively has an infinite supply of fluid at concentration C_o, as shown in the sketch below.

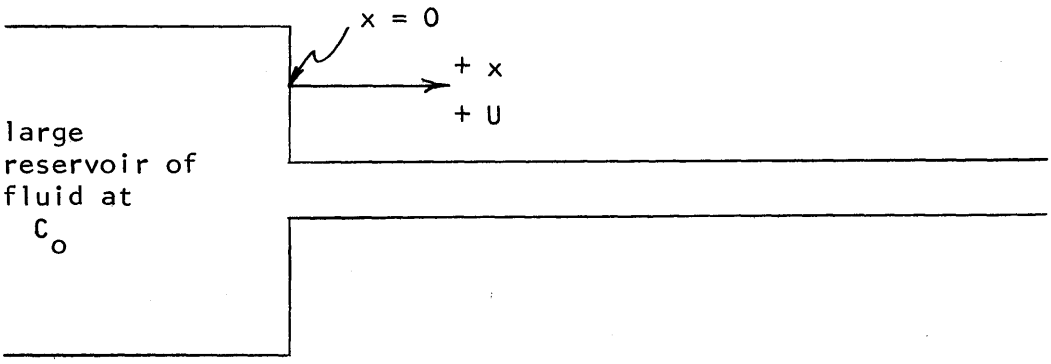

The details of obtaining this solution are presented by Ogata and Banks (ref. 37). If U is negative, then eqn. 5-39 has a steady state form which is

$$\frac{C}{C_o} = \exp\frac{Ux}{E} \qquad 5\text{-}40$$

for positive x's. This is identical to the steady state form of eqn. 5-31 for negative x with $Q_m/(\rho AU)$ replaced by C_o. Ref. 37 further shows that errors of less than 3% are introduced by using

$$\frac{C}{C_o} = \frac{1}{2}\left[1 - \text{erf}\ \frac{x - Ut}{2\sqrt{Et}}\right] \qquad 5\text{-}41$$

in place of eqn. 5-39 when Ux/E is greater than 500. Referring again to eqn. 5-9 (which gives an approximate value of E/Ux in a pipe), x must be greater than 2000 times the pipe radius for eqn. 5-41 to apply for flow in a pipe.

5.2) Steady, Non-uniform Flow - Finite Difference Equations

For cases of non-uniform flow when a closed-form mathematical solution cannot be obtained, there are several approximate methods which may be used to solve the mass balance equation. Among these methods are (a) the finite difference equation, (b) the relaxation method, (c) the method of iteration, and others. All of these methods fall into the general category of numerical solutions of partial differential equations. (See, for example, ref. 33, 48.) Solution of the mass balance equation by the finite difference method will be outlined in this section.

The mass balance equation may be viewed as an equation in x-t space, and this space may be divided into a grid as shown in fig. 5-3. The differential form of the mass balance equation may be written as a finite difference equation by writing approximate (finite difference) expressions for the derivatives. These finite difference expressions are

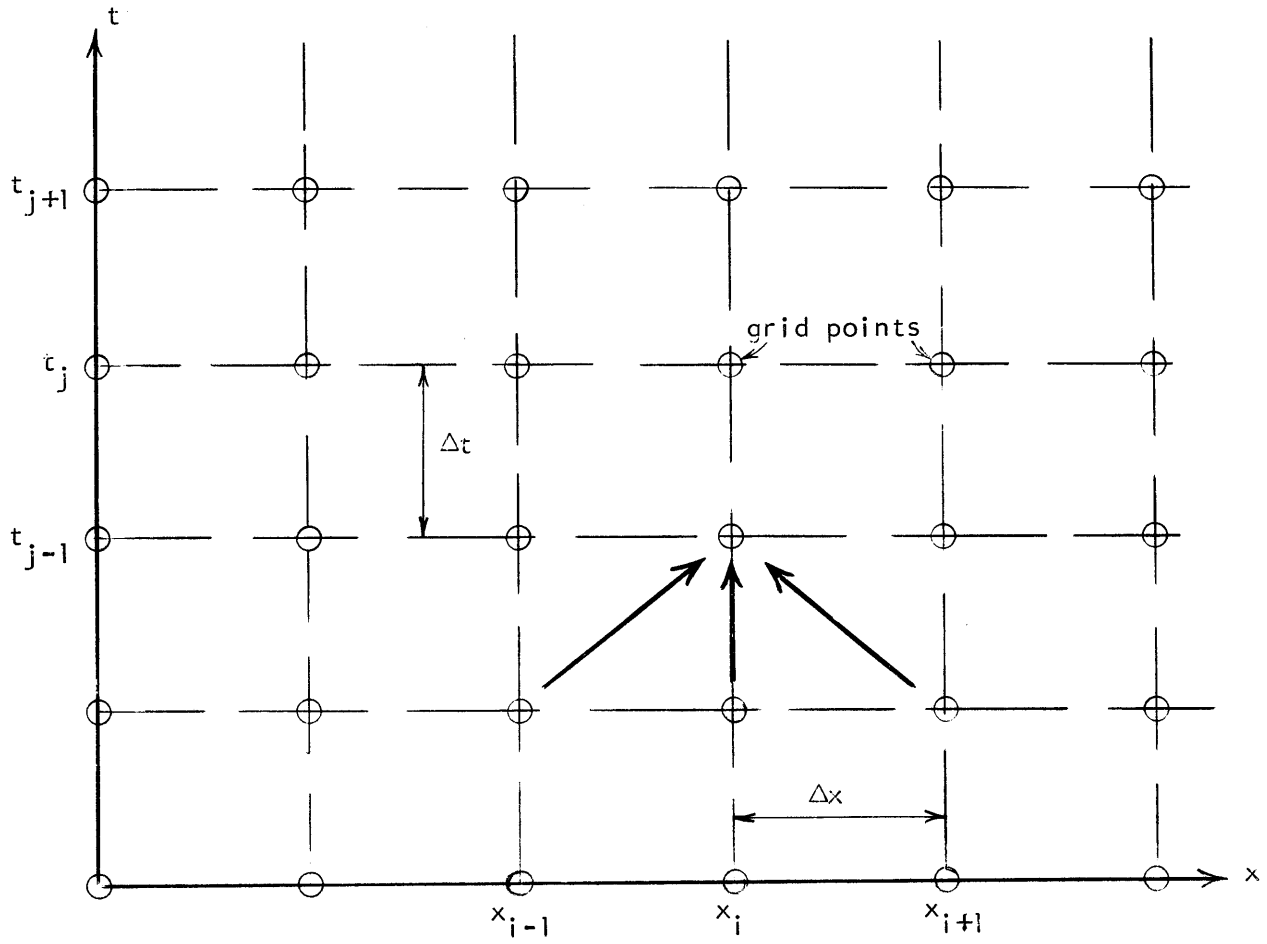

Fig. 5-3: Finite difference grid in x-t space

---

written in terms of the values at the grid points. For present purposes, it will be convenient to write the general one dimensional mass balance equation (eqn. 2-29) as

$$\frac{\partial C}{\partial t} + U_x \frac{\partial C}{\partial x} = E_x \frac{\partial^2 C}{\partial x^2} + \frac{1}{A} \frac{\partial (E_x A)}{\partial x} \frac{\partial C}{\partial x} \qquad 5\text{-}42$$

Using a forward difference and using the subscripts i and j to indicate the values of x and t at which the various parameters are to be evaluated, one may write

$$\left(\frac{\partial C}{\partial t}\right)_{i,j} = \frac{C_{i,j+1} - C_{i,j}}{\Delta t}$$

$$\left(\frac{\partial C}{\partial x}\right)_{i,j} = \frac{C_{i+1,j} - C_{i,j}}{\Delta x}$$

$$\left(\frac{\partial (E_x A)}{\partial x}\right)_{i,j} = \frac{(E_x A)_{i+1,j} - (E_x A)_{i,j}}{\Delta x}$$

Also, using a forward then a backward difference, one may write

$$\left(\frac{\partial^2 C}{\partial x^2}\right)_{i,j} = \frac{C_{i+1,j} - 2C_{i,j} + C_{i-1,j}}{(\Delta x)^2}$$

Inserting all of these, eqn. 5-42 may be written as

$$C_{i,j+1} = C_{i,j} + \Delta t \left[- U_{x_{i,j}} \left\{ \frac{C_{i+1,j} - C_{i,j}}{\Delta x} \right\} \right.$$

$$+ E_{x_{i,j}} \left\{ \frac{C_{i+1,j} - 2C_{i,j} + C_{i-1,j}}{(\Delta x)^2} \right\} \qquad 5\text{-}43$$

$$\left. + \frac{1}{A_{i,j}} \left\{ \frac{(E_x A)_{i+1,j} - (E_x A)_{i,j}}{\Delta x} \right\} \left\{ \frac{C_{i+1,j} - C_{i,j}}{\Delta x} \right\} \right]$$

As is indicated in fig. 5-3 by the arrows, it is necessary to know the conditions at three adjoining values of x for a given t in order to find one additional value of concentration. Nevertheless, for given initial and boundary conditions, eqn. 5-43 may be used to find the solution for the concentration in x-t space.

In section 2, it was mentioned that the finite difference approach is greatly simplified when a steady state concentration distribution is obtained so that $\partial C/\partial t$ is zero. In this case, eqn. 2-33 applies. Again using the forward difference for $\partial C/\partial x$, eqn. 2-33 may be written as

$$C_{i+1} = C_i \left[\frac{\Delta x}{E_{x_i}} \cdot U_{x_i} + 1 \right] \qquad 5\text{-}44$$

The accuracy of any finite difference solution will depend on the grid size (Δx and Δt) which is used and on the accuracy of the calculations themselves since each step is built on the results of previous calculations.

6) MATHEMATICAL ANALYSIS OF LONGITUDINAL DISPERSION IN UNIFORM, UNSTEADY FLOW

6.1) Objective

The objective of this analysis is to obtain an analytical expression for the coefficient of longitudinal dispersion (E_t) in uniform, unsteady, turbulent, shear flow in a circular pipe. The E_t which is being sought is the dispersion coefficient as used in eqn. 2-19. The general assumptions and definitions are presented below. Most of the mathematical manipulations are contained in appendix B. After obtaining an expression for E_t for general unsteady flow, it will be applied to estuary type flow where the one dimensional velocity is given by

$$U_t = U_f + U_T \sin\left[\sigma\ (t-\delta)\right]. \qquad 6\text{-}1$$

U_f is the velocity corresponding to the fresh water flow into an estuary, and U_T is the maximum tidal velocity.

The analytical development essentially parallels part of the work of Aris (ref. 7). As shown by eqn. 2-14, it is necessary to know the variation of velocity (u'') and of concentration (c'') across the section in order to obtain an analytical expression for E. The velocity distribution gives u''. The two dimensional mass balance equation in radial coordinates (eqn. 3-3) may be used to find an expression equivalent to c'' so that an integration similar to eqn. 2-14 may be carried out to find E_t.

This analysis will show that the dispersion coefficient is a periodic function of time for estuary type flow. Next, the errors involved in replacing E_t by its time average E_A will be investigated. Also, it will be shown that a simplified mass balance equation may be used if it is desired only to represent the concentrations at "slack times".

6.2) Definitions and Assumptions

Consider turbulent flow in an infinitely long, straight, circular pipe with its axis parallel to the x-axis. Let the radius of the

pipe be a, and let the radial coordinate r be measured from the centerline of the pipe. Axial symmetry is assumed. Let $\bar{u}$ (r,t) be the time-averaged velocity in the x-direction (section 2-4), and let U(t) be the one dimensional velocity defined by

$$U(t) = \frac{1}{\pi a^2} \int_o^a \bar{u}\ (r,t)\ 2\ \pi\ r\ \ dr \qquad 6\text{-}2$$

The dimensionless distribution of the velocity defect may be written as

$$\lambda\ (r,t) = \frac{\bar{u}\ (r,t) - U(t)}{u_*(t)} \qquad 6\text{-}3$$

where $u_*(t)$ is the shear velocity. Assume that the longitudinal and lateral turbulent (mass) diffusivities are equal and are given by

$$e\ (r,t) = e_o\ \psi(r,t) \qquad 6\text{-}4$$

where e_o is a constant reference value of e and ψ is the dimensionless variation of e with respect to e_o.

Let a finite quantity of some conservative substance (tracer) P be introduced into the flow, and let $\bar{c}(x,r,t)$ be the time averaged concentration of P. It is assumed that P does not affect the established flow and that the substance is conservative. Then, the two dimensional mass-balance equation for P is

$$\frac{\partial \bar{c}}{\partial t} + \bar{u}\ (r,t)\ \frac{\partial \bar{c}}{\partial x} = e\ (r,t)\ \frac{\partial^2 \bar{c}}{\partial x^2} + \frac{1}{r}\frac{\partial}{\partial r}\ (re(r,t)\frac{\partial \bar{c}}{\partial r}) \qquad 6\text{-}5$$

with the general boundary and initial conditions

$$\begin{aligned} &\bar{c}\ (x,r,0) = \bar{c}^o\ (x,r) \\ &e\ (a,t)\ \frac{\partial\ \bar{c}}{\partial r} = 0 \quad \text{on } r = a \\ &\bar{c}\ (\pm\infty,\ r,t) = 0 \end{aligned} \qquad 6\text{-}6$$

The first condition represents the initial distribution of tracer; the second says that no tracer is diffused across the flow boundaries; the

third states that the concentration is zero as x approaches plus and minus infinity. This last condition results from the fact that only a finite amount of tracer is being considered. Define the following dimensionless quantities:

$$\xi = \frac{1}{a}\left[x - \int_o^t U(t)\, dt\right]$$

$$\rho = r/a$$

$$\tau = t/T_r \qquad 6\text{-}7$$

$$\eta = VT_r/a$$

$$F(\tau) = u_*(\tau)/V$$

$$\mu = e_o T_r/a^2$$

where T_r is an arbitrary reference time and V is an arbitrary reference velocity. In any specific case, T_r and V may be taken as quantities which are characteristic of the flow being considered. In changing from x to ξ, the coordinate system is changed to one which moves with the velocity U(t). Introduction of the above quantities into eqn. 6-5 gives

$$\frac{\partial \bar{c}}{\partial \tau} = \mu\psi(\rho,\tau)\frac{\partial^2 \bar{c}}{\partial \xi} + \frac{\mu}{\rho}\frac{\partial}{\partial \rho}\left[\rho\psi(\rho,\tau)\frac{\partial \bar{c}}{\partial \rho}\right] - \eta F(\tau)\lambda(\rho,\tau)\frac{\partial \bar{c}}{\partial \xi} \qquad 6\text{-}8$$

Notice that with the introduction of ξ and λ, the mass convection due to the mean velocity U(t) disappears in eqn. 6-8 since the coordinate system is now moving with the velocity U(t). The convection term $\eta F\lambda \frac{\partial \bar{c}}{\partial \xi}$ is now the convection relative to U, and this convection exists because of the velocity distribution. The other two terms on the right-hand side of eqn. 6-8 are the longitudinal and lateral diffusion. Thus, in accordance with the definition of longitudinal dispersion as given in section 2, the net or one-dimensional mass transport represented in eqn. 6-8 makes up the transport which is defined as dispersion. This fact is important in the analysis which follows.

At each time t, the one dimensional velocity in the pipe is given by U(t). For each instant, let it be assumed that the lateral distribution of velocity and of turbulent diffusivity are the same as they

would be if the flow were steady at the velocity U(t). This assumption should be a better approximation the slower the rate of change of U(t) is. On the basis of this assumption and from experimentally determined distributions of the velocity defect for steady, uniform flow (ref. 46, p. 197), it is implied that λ is a function of ρ only, i.e. $\lambda\ (\rho,\tau) \equiv \lambda_o(\rho)$. Also, for this to hold, U(t) must always be of one sign (i.e., either positive or negative). Otherwise, λ would change sign as U did (see sketch below), and λ would remain a function of τ.

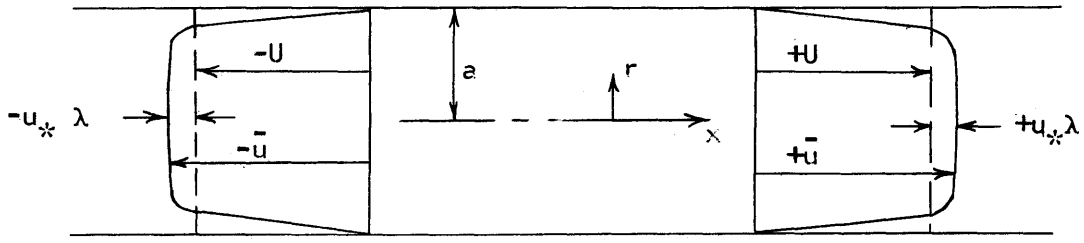

If it is assumed that Reynold's analogy is valid so that the mass diffusivity (e) equals the eddy viscosity (ϵ), then e may be written as

$$e\ (\rho,\tau) = e_o\ F(\tau)\ \left[\rho(1-\rho)\right] \qquad 6\text{-}9$$

if e_o is defined as κaV, where κ is von Karman's constant. This is the same e_o as in eqn. 6-7. Eqn. 6-9 is based on

$$\underline{\tau} = \underline{\rho}\ \epsilon\ \frac{\partial \bar{u}}{\partial r} \qquad 6\text{-}10$$

as the definition of ϵ and on the linear distribution of the shear stress ($\underline{\tau}$) across the section. Also, $\underline{\rho}$ is the fluid density. Eqn. 6-9 further makes use of von Karman's hypothesis which states

$$\frac{\partial \bar{u}}{\partial r} = \frac{1}{\kappa}\ \frac{u_*}{(a-r)} \qquad 6\text{-}11$$

The distribution of $\underline{\tau}$ and e are shown in fig. 6-1. Eqn. 6-9

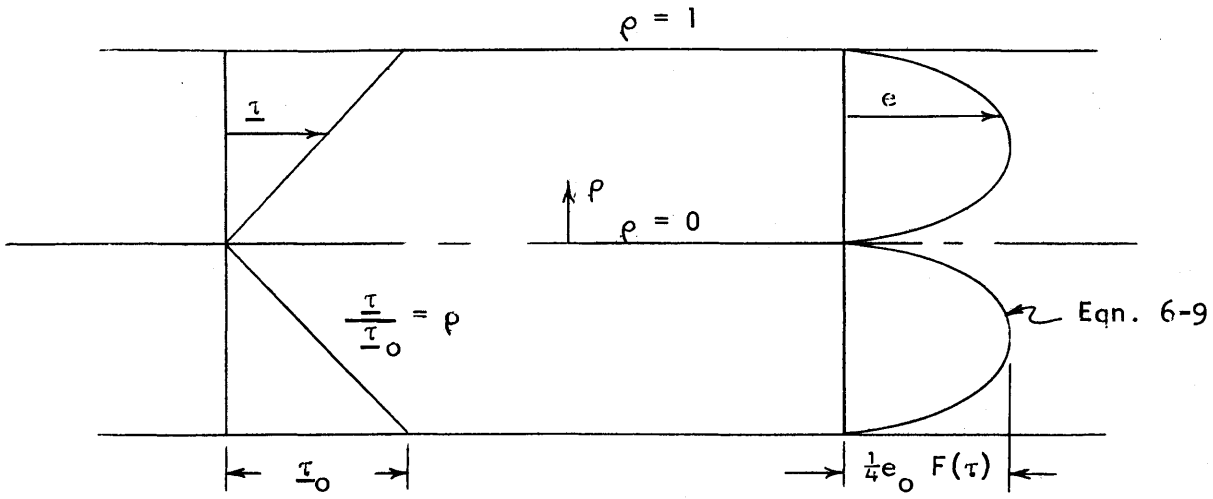

Fig. 6-1: Distribution of shear stress and turbulent diffusivity in a pipe

---

implies that $\psi\ (\rho,\tau)$ may be written as

$$\psi\ (\rho,\tau) = F(\tau) \cdot \psi_o\ (\rho) \qquad 6\text{-}12$$

where $\psi_o(\rho) = \rho(1-\rho)$. Now, from eqn. 6-8, the mass balance may be written as

$$\frac{\partial \bar{c}}{\partial \theta} = \mu\psi_o \frac{\partial^2 \bar{c}}{\partial \xi^2} + \frac{\mu}{\rho} \frac{\partial}{\partial \rho}\left[\rho\psi_o \frac{\partial \bar{c}}{\partial \rho}\right] - \eta\lambda_o \frac{\partial \bar{c}}{\partial \xi} \qquad 6\text{-}13$$

after letting

$$d\theta = F(\tau)\ d\tau \qquad 6\text{-}14$$

or

$$\theta(\tau) = \int_o^\tau F(\tau)\ d\tau\ . \qquad 6\text{-}15$$

Recall that $F(\tau) = u_*(\tau)/V$. Hence, $F(\tau)$ is always positive, so that the new variable θ is an increasing function of τ, i.e., as τ get large, θ will also.

In summary to this point, eqn. 6-13 now represents the mass balance equation in a dimensionless cylindrical coordinate system which moves with the velocity U(t). Certain assumptions have been made about the distributions of velocity and turbulent diffusivities to arrive at eqn. 6-13. Notice that the right-hand side of eqn. 6-13 is a function only of ξ and ρ (except for the dependent variable $\bar{c}(\xi,\rho,\tau)$, of course). Thus, on the basis of the assumptions which have been made, the effects of the unsteadiness of the flow are now embodied in the new variable θ.

In section 7, it is pointed out that the coefficient of longitudinal dispersion equals 1/2 the time rate of change of σ^2, where σ^2 is the spatial variance of the one dimensional concentration distribution. Appendix B is devoted to finding an expression for this variance, and thus for the dispersion coefficient, in pipe flow by operating on eqn. 6-13.

For unsteady flow, it has been assumed that the distributions of velocity and turbulent diffusivity are the same at each instant as for a corresponding steady flow. Since these are the factors which control longitudinal dispersion, one might expect to find that the longitudinal dispersion in unsteady flow would be the same at each instant as for a corresponding steady flow. Indeed, this is the conclusion which is reached in appendix B. However, <u>a priori</u>, it is by no means obvious though how the unsteadiness in the flow and the resulting unsteadiness in the concentration distribution will work together to influence the dispersion.

6.3) <u>Dispersion Coefficient for Uniform, Estuary Type Flow</u>

From appendix B (eqn. B-27), E_t may now be written as

$$E_t = 10.1 \left(\frac{u_*(t)}{V} \right) a V \qquad 6\text{-}16$$

for unsteady flow in a uniform pipe of a radius a. In this expression, $u_*(t)$ is the shear velocity as a function of time, and V is an arbitrary reference velocity. (Note that V could be cancelled from eqn. 6-16.

However, it is convenient to leave the equation in its present form for now). Eqn. 6-16 will now be applied to uniform estuary type flow where the one dimensional velocity is given by eqn. 6-1.

If U_f is less than U_T, then from eqn. 6-1, U varies with t as shown in fig. 6-2a, where T is the tidal period or period of oscillation. In obtaining eqn. 6-16, recall that it was assumed that U is always of one sign. It is reasonable also to assume that the flow which has a velocity as described by eqn. 6-1 will exhibit the same dispersion characteristics as the flow defined by

$$U(t) = \left| U_f + U_T \sin \sigma \ (t - \delta) \right| \qquad 6\text{-}17$$

where the vertical bars indicate absolute value. This velocity is always positive, as is shown in fig. 6-2b. At each instant, the absolute magnitude of the velocity is the same for both flows. Thus, the relative distribution of velocity defect and the turbulent diffusivity are the same for both flows. Since these are the factors involved in longitudinal dispersion, one would expect that the dispersion coefficient (E_t) should be the same for both flows.

In order to apply eqn. 6-16 to estuary type flow, a reference velocity V must be chosen, and u_* corresponding to the velocity of eqn. 6-17 must be found. It is desirable to find an expression for u_* in terms of other flow parameters which are more directly obtainable. Recall that

$$u_* = \sqrt{\frac{f}{8}}\, U = \sqrt{\frac{f}{8}} \left| U_f + U_T \sin \sigma \ (t - \delta) \right| \qquad 6\text{-}18$$

where f is the Darcy-Weisbach friction factor and is a function of time. In line with the previous assumption, it is assumed that eqn. 6-18 applies for the unsteady flow under consideration. Also, it is assumed that f at each instant may be taken to be the same as for steady flow at the velocity which exists at that instant.

A typical friction-factor diagram is shown in fig. 6-3. Note that this graph is shown on log-log paper and that lines of constant relative roughness are slightly curved except in the wholly rough region where f is a constant for a given relative roughness. If another

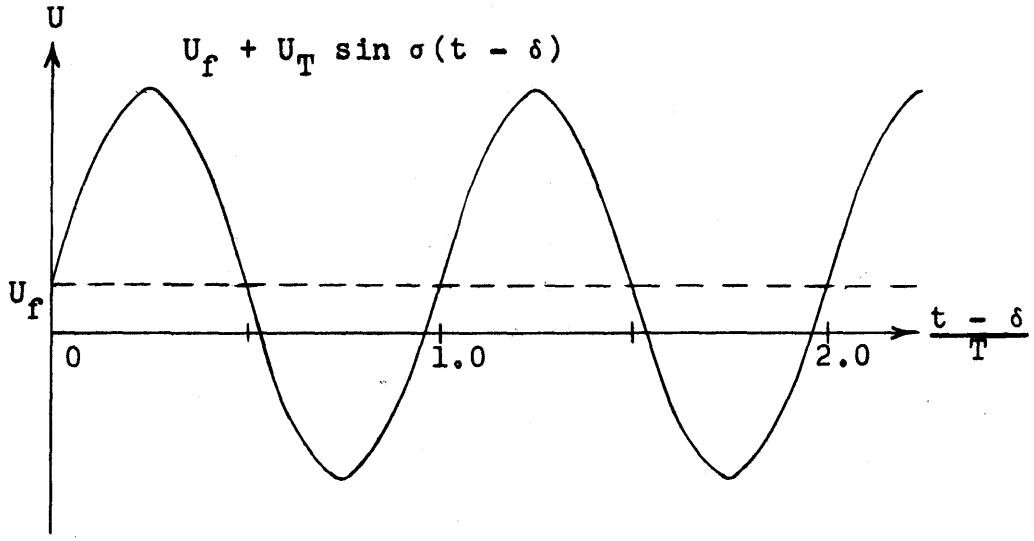

(a) Actual Velocity

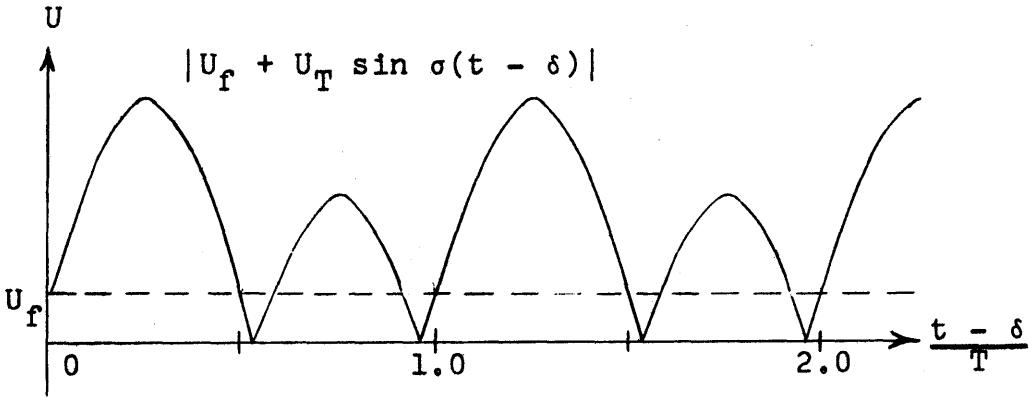

(b) Assumed Velocity

Fig. 6-2: Temporal velocity distribution for estuary type flow

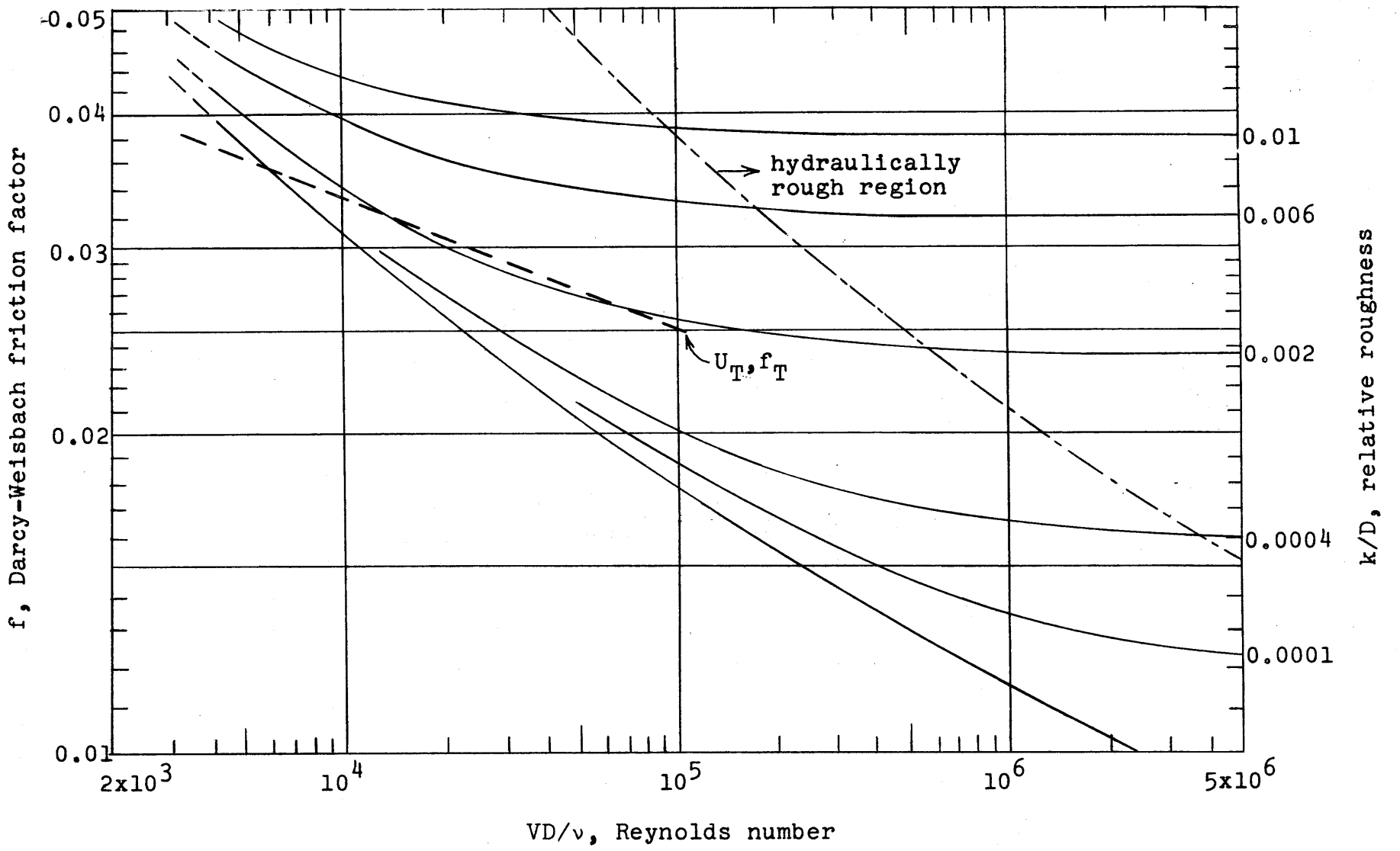

Fig. 6-3: Friction factor diagram for straight line approximation

assumption is made, u_* may be written in terms of the velocity variation and a constant, reference value of f. This assumption is that the curves of constant relative roughness on the friction-factor diagram may be approximated by a straight line in the region of interest. One such approximation is shown by the dashed line in fig. 6-3. For this line,

$$\frac{f}{f_T} = \left(\frac{\mathbb{R}}{\mathbb{R}_T}\right)^n = \left(\frac{|U|}{U_T}\right)^n. \qquad 6\text{-}19$$

$\mathbb{R}$ is the Reynolds number and f_T is the value of f on the straight line for $\mathbb{R}_T$, i.e., the Reynolds number corresponding to U_T. The constant n is determined by the slope of the dashed line. Note that n will be negative or zero in all cases. In general, the straight line can be drawn to give the best approximation to the curved line within just one log-cycle on the Reynolds number scale. The instantaneous Reynolds number for the flow will be within this log-cycle 90% of the time if the cycle is taken from $\mathbb{R}_{max}$ to 10% of $\mathbb{R}_{max}$.

From equations 6-18 and 6-19, u_* may now be written as

$$u_* = u_{*_T} \left[\left| \frac{U_f}{U_T} + \sin \sigma (t - \delta) \right|\right]^{1 + \frac{n}{2}} \qquad 6\text{-}20$$

where

$$u_{*_T} = \sqrt{\frac{f_T}{8}} \cdot U_T \qquad 6\text{-}21$$

i.e., the shear velocity corresponding to U_T. It will be more convenient to have u_* referred to u_{*A} (the average shear velocity during a period) rather than u_{*T}. By definition,

$$u_{*A} = \frac{1}{T} \int_t^{t+T} u_* \, dt \qquad 6\text{-}22$$

If u_* varied sinusoidally (that is, if U_f and n were zero) then u_{*A} would equal $2/\pi$ times u_{*T}. To take account of the effects of U_f and n, a factor B may be introduced, and u_{*A} may be written as

$$u_{*A} = \frac{2}{\pi} B u_{*T} \qquad 6\text{-}23$$

where

$$B = \frac{\pi}{2}\left[\frac{1}{T}\int_{t}^{t+T}\left\{\left|\frac{U_f}{U_T} + \sin\sigma\ (t-\delta)\right|\right\}^{1+\frac{n}{2}} dt\right] \qquad 6\text{-}24$$

This factor B, for values of n from zero to -0.25 is shown in fig. 6-4. For values of U_f/U_T from zero to 0.10, there was practically no change in B for a given n. Thus, only one curve is shown for this range of U_f/U_T. The range of n which is shown essentially covers the possible values. Thus, the effects embodied in B are, at most, 4% for the practical values of U_f/U_T which are encountered.

Eqn. 6-16 points out that E_t varies with time as $u_*(t)$ does. Thus, using the notation E_A for the average value of E_t during a period, this average is

$$E_A = 10.1\ a u_{*A} = 10.1a\ \left(\frac{2}{\pi} B u_{*T}\right) \qquad 6\text{-}25$$

Taking the reference velocity V as u_{*A} and recalling (eqn. 6-7) that $F(t) = u_*(t)/V$, the time variation of E_t may be referred to the average value by

$$E_t = F(t) \cdot E_A \qquad 6\text{-}26$$

where

$$F(t) = \frac{u_*(t)}{u_{*A}} = \frac{1}{\frac{2}{\pi}B}\left\{\left|\frac{U_f}{U_T} + \sin\sigma\ (t-\delta)\right|\right\}^{1+\frac{n}{2}} \qquad 6\text{-}27$$

If B equals one, then Harleman's expression for E_A (eqn. 3-18) is obtained from eqn. 6-25 when u_{*T} is replaced in terms of Manning's n, U_T, and the hydraulic radius. Thus, one may see the assumptions which are implicit in the writing of eqn. 3-18.

For future reference, it is well to recall at this point that

$$\theta(t) = \int_{o}^{t} F(t)\ dt \qquad 6\text{-}28$$

(See eqn. 6-15.) The variable θ is also used in the next sections. Fig. 6-5 shows the general variation of θ with t for $\delta = 0$. The

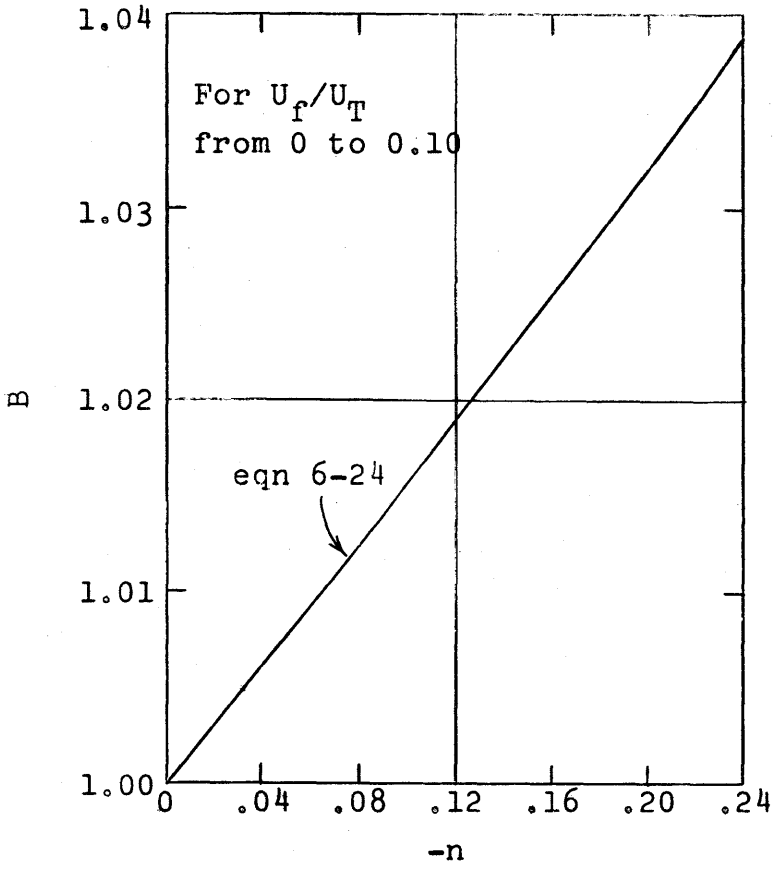

Fig. 6-4: Variation of factor B with n

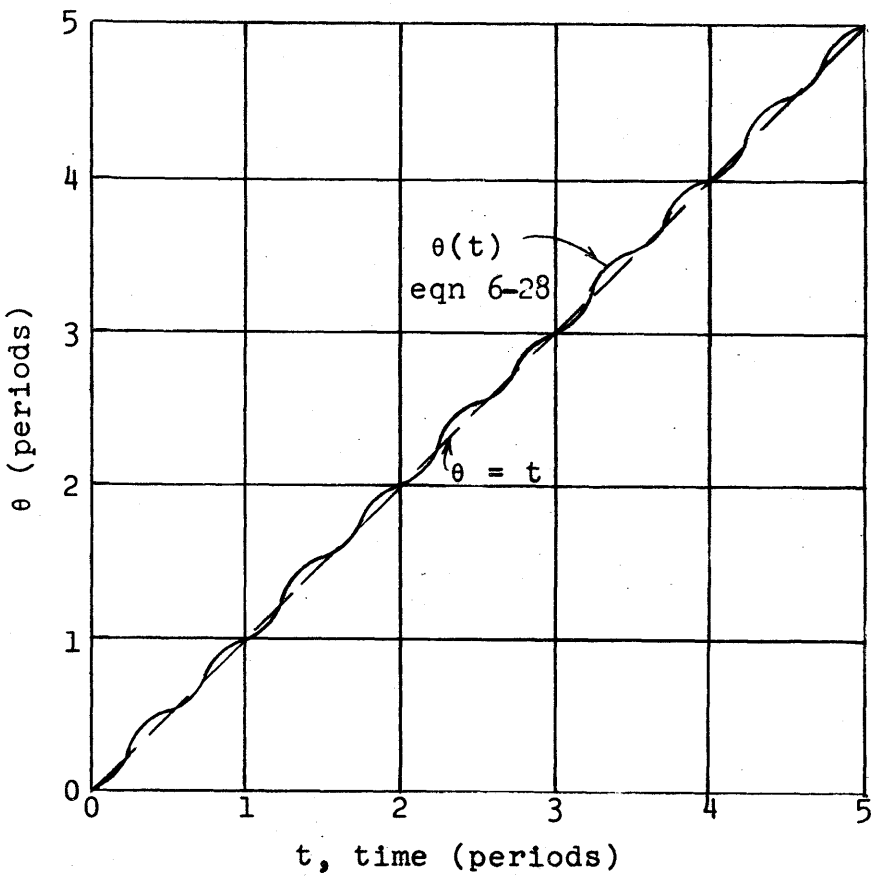

Fig. 6-5: Variation of θ with t

dashed line would apply if θ equalled t. The absolute deviation from the dashed line (i.e., θ - t) is the same in each period, but as t gets large, (θ - t)/t approaches zero due to the largeness of t. Thus, θ /t approaches unity as t get large. Also, θ equals t at the end of each period. If n = 0, then B equals one, and θ equals t at the middle of each period as well.

6.4) Assumption of Constant Dispersion Coefficient for Uniform Estuary Type Flow

Eqn. 6-26 and eqn. 6-27 give the time dependent dispersion coefficient for uniform, estuary type flow when the velocity is given by eqn. 6-1:

$$U_t = U_f + U_T \sin \sigma (t - \delta)$$

Since uniform flow is being considered, U_f and U_T are independent of x. The mass balance equation may be written as

$$\frac{\partial C}{\partial t} + \left[U_f + U_T \sin \sigma (t - \delta)\right]\frac{\partial C}{\partial x} = E_A F(t)\frac{\partial^2 C}{\partial x^2} \qquad 6\text{-}29$$

It is now desired to investigate the errors involved in taking the dispersion coefficient as constant and equal to E_A so that the mass balance equation may be written as

$$\frac{\partial C}{\partial t} + \left[U_f + U_T \sin \sigma (t - \delta)\right]\frac{\partial C}{\partial x} = E_A \frac{\partial^2 C}{\partial x^2} \qquad 6\text{-}30$$

(Note that this is equivalent to setting F(t) of eqn. 6-27 equal to unity).

The investigation of the errors introducted by using E_A will be based on the solution to eqn. 6-29 for an instantaneous injection of tracer which is made uniformly across a flow section. As was done in section 5, this will be referred to as an instantaneous, point injection. Most other solutions to eqn. 6-29 can be made up of various integrals of the solution for an instantaneous, point injection. Thus, the conclusions reached for this case should be generally applicable.

In the expressions for the velocity U, the term δ is the time shift between the origin of time and the time of zero velocity at the

upstream limit of the fluid excursion (high water in an estuary). It will be convenient to take the time origin at the time of injection for an instantaneous injection of tracer. If this is done, then for the example shown in fig. 6-6, δ equals -T/8, where T is the period of oscillation.

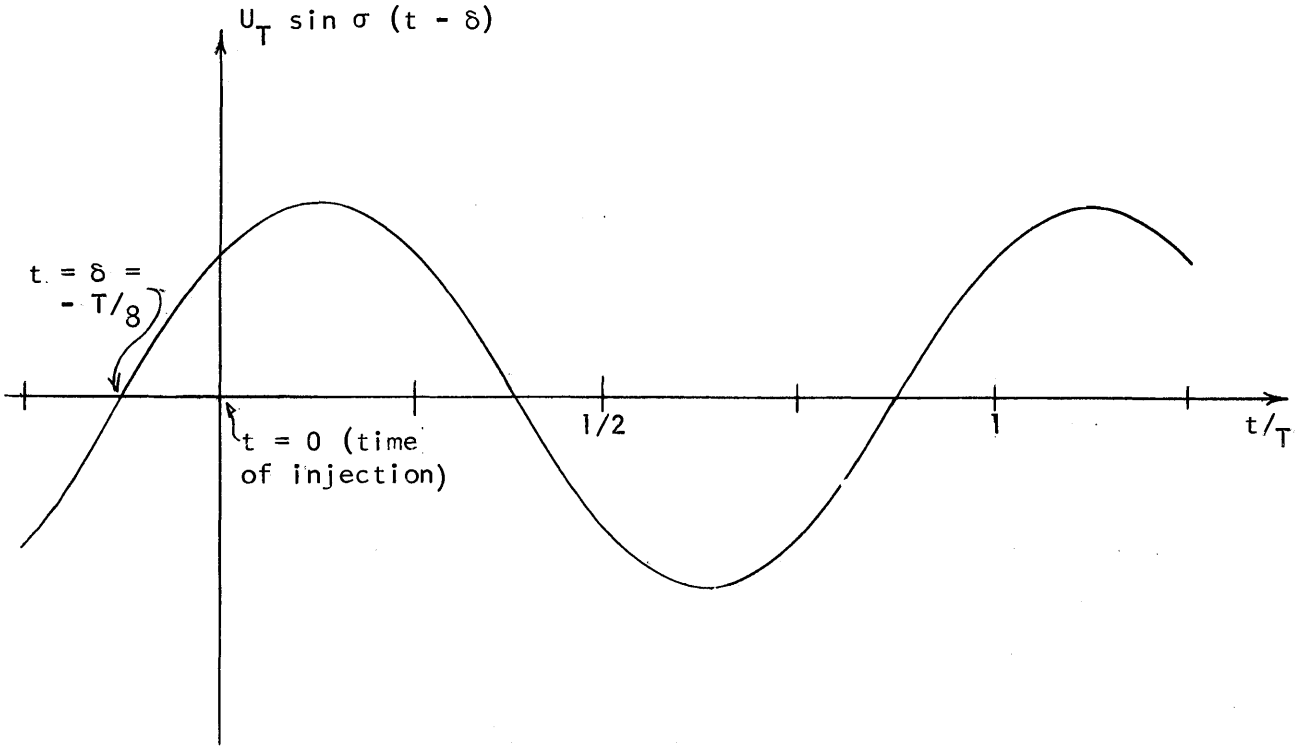

Fig. 6-6: Definition Sketch for Time Shift δ

Into eqn. 6-29, introduce the change of variables

$$\bar{x} = x - \int_o^t U \, dt$$

$$= x - U_f t + \frac{U_T}{\sigma} \left[\cos \sigma (t-\delta) - \cos \delta \right] \qquad 6\text{-}31$$

$$\theta = \int_o^t F(t) \, dt$$

Eqn. 6-29 then becomes

$$\frac{\partial C}{\partial \theta} = E_A \frac{\partial^2 C}{\partial \bar{x}^2} \qquad 6\text{-}32$$

which is again the "heat equation".

If the injection of tracer has mass M and if it is injected at $x = 0$ and $t = 0$ (i.e., $\theta = 0$), then the boundary and initial conditions of eqn. 5-3 apply. By analogy to the solution for steady flow, the solution to eqn. 6-32 is

$$C = \frac{M}{\rho A \sqrt{4\pi E_A \theta}} \exp - \frac{\bar{x}^2}{4E_A\theta} \qquad 6\text{-}33$$

or replacing $\bar{x}$ from eqn. 6-31,

$$C = \frac{M}{\rho A \sqrt{4\pi E_A \theta}} \exp - \frac{\left[x - U_f t + \frac{U_T}{\sigma}\left\{\cos \sigma\,(t-\delta) - \cos \delta\right\}\right]^2}{4E_A\theta} \qquad 6\text{-}34$$

At the end of section 6-3, it was pointed out that θ approaches t as t gets large. Thus, at large times after the injection of tracer, essentially no error would be introduced by replacing θ with t. From eqn. 6-28,

$$\theta = \int_o^t F(t)\, dt$$

Thus, setting θ equal to t is equivalent to taking F(t) equal to unity for large t's. Since $E_t = F(t) \cdot E_A$, replacing θ by t is also equivalent to taking E_A as the dispersion coefficient. This equivalence may also be seen by comparing eqn. 6-34 with the solution of eqn. 6-30 where F(t) has been set equal to unity (or the dispersion coefficient equal to E_A). This latter solution is

$$C = \frac{M}{\rho A \sqrt{4\pi E_A t}} \exp - \frac{\left[x - U_f t + \frac{U_T}{\sigma}\left\{\cos \sigma\,(t-\delta) - \cos \delta\right\}\right]^2}{4E_A t} \qquad 6\text{-}35$$

Hence, since θ is approximately equal to t for large values of t, the dispersion coefficient may safely be taken as E_A for large times after the injection.

It is still desirable to have an estimate of the effects of the time dependent dispersion coefficient at small times. Thus, let C_t be the concentration given by eqn. 6-34. This is the solution using E_t. Let C_A be the concentration given by eqn. 6-35, which is the solution using E_A. Also, let $\theta = Dt$, where D is a function of time. Eqn. 6-34 may be written as

$$\ell n \frac{C_t \rho A \sqrt{4\pi E_A D t}}{M} = - \frac{1}{D} \frac{[x - U_f t + \frac{U_T}{\sigma} (\cos \sigma (t-\delta) - \cos \delta)]^2}{4E_A t} \qquad 6\text{-}36$$

and eqn. 6-35 as

$$\ell n \frac{C_A \rho A \sqrt{4\pi E_A t}}{M} = - \frac{[x - U_f t + \frac{U_T}{\sigma} (\cos \sigma (t-\delta) - \cos \delta)]^2}{4E_A t} \qquad 6\text{-}37$$

Divide the second equation by the first and let Φ be defined by

$$\Phi = \frac{\rho A \sqrt{4\pi E_A t}}{M}$$

The result is

$$\frac{\ell n (C_A \Phi)}{\ell n (C_t \Phi \sqrt{D})} = D \qquad 6\text{-}38$$

or

$$\ell n (C_A \Phi) = \ell n (C_t \Phi \sqrt{D})^D \qquad 6\text{-}39$$

Take the inverse logarithm and divide both sides of the resulting expression by $C_t \phi \sqrt{D}$:

$$\frac{C_A}{C_t \sqrt{D}} = (C_t \phi \sqrt{D})^{D-1} \qquad 6\text{-}40$$

On replacing $C_t \phi \sqrt{D}$ from eqn. 6-34 and using the identity

$$\exp \frac{1}{D} X = (\exp X)^{1/D} ,$$

one obtains

$$\frac{C_A}{C_t} = \sqrt{D} \left[\exp - \frac{[x - U_f t + \frac{U_T}{\sigma} (\cos \sigma (t-\delta) - \cos \delta)]^2}{4 E_A t} \right]^{1-\frac{1}{D}} \qquad 6\text{-}41$$

This finally is the ratio of the concentrations obtained by taking the dispersion coefficient as either E_A or E_t.

The maximum of both C_A and C_t is always at

$$x = U_f t - \frac{U_T}{\sigma} (\cos \sigma (t-\delta) - \cos \delta) \qquad 6\text{-}42$$

From eqn. 6-41, the ratio of the maximum concentrations is given by the square root of D. Thus, the largest error in the maximum C_A (i.e. from E_A) compared to C_t results when D has its greatest deviation from unity. From fig. 6-5 (and equations 6-27 and 6-28), it can be seen that the general variation of

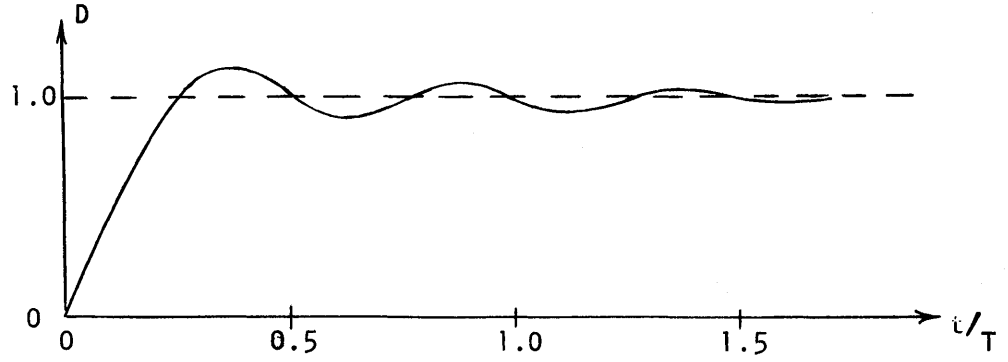

D is as shown in the accompanying sketch (for $\delta = 0$). (The exact values of D may be calculated using eqn. 6-27 and eqn. 6-28.) From the sketch, it is seen that D has its largest deviation from unity during the first quarter-period after the injection. During the second quarter-period, the maximum value of D is 1.15 if U_f/U_T is small. This means that there is only a 7% error in C_A compared to C_t. As t increases, D approaches unity and the error in C_A decreases. At $t/T = 9/8$, D is 0.96 and $C_A/C_t = 0.98$.

These values give an estimate of the errors to be expected by using E_A as the dispersion coefficient in place of $E_t = E_A F(t)$. Although the calculations above were based only on the maximum concentration, they indicate that by the second period of oscillation the difference between C_A and C_t has practically disappeared.

Thus, for most practical cases, the dispersion coefficient for estuary type flow may be taken as E_A, the average value of the dispersion coefficient, and eqn. 6-30 may be used as the mass balance equation. Because E_A is the average of E_t, it still depends most strongly on the oscillatory velocity ($U_T \sin \sigma t$) and not on the through-flow velocity (U_f), if U_f/U_T is small.

6.5) Mass Balance for "Slack Times"

In practice, concentration distributions are often sampled at "slack times". These are the times corresponding to high water slack (HWS, limit of upstream excursion) or low water slack (LWS, limit of downstream excursion). At the slack times, the oscillatory component of the velocity is zero, i.e.

$$U_T \sin \sigma (t - \delta) = 0 \qquad 6\text{-}43$$

Notice that HWS corresponds to

$$t - \delta = n T, \quad n = 0, 1, 2, \cdots \qquad 6\text{-}44$$

and LWS corresponds to

$$t - \delta = (n + \tfrac{1}{2}) T \qquad 6\text{-}45$$

where T is the period of oscillation.

Substitution of eqn. 6-43 into eqn. 6-30 yields a mass balance equation which describes the concentration changes from one slack time (either HWS or LWS) to the next. This new mass balance equation may now be written as

$$\frac{1}{T}\frac{\partial C_s}{\partial n} + U_f \frac{\partial C_s}{\partial x} = E_A \frac{\partial^2 C_s}{\partial x^2} \qquad 6\text{-}46$$

for uniform flow. The concentration has been written as C_s to emphasize that eqn. 6-46 only represents the concentrations at slack times. Also, the time derivative has been written as $\frac{1}{T}\frac{\partial C_s}{\partial n}$ to emphasize that this is the derivative for times differing by a full period. Also, at times differing by a full period, the net oscillatory convection will be zero. Thus, the convective term in eqn. 6-46 includes only the convection due to the fresh water velocity (U_f).

For an instantaneous, point injection of tracer at x = 0 and t = 0, the solution to eqn. 6-46 is

$$C_s = \frac{M}{\rho A \sqrt{4\pi E_A nT}} \exp - \frac{[x - U_f nT]^2}{4E_A nT} \qquad 6\text{-}47$$

This is exactly the same expression as would be obtained by substituting $t - \delta = nT$ (i.e. eqn. 6-44) into eqn. 6-35. This comparison further points up the validity of using eqn. 6-46 as the mass balance for slack times.

6.6) Solutions to Mass Balance Equation

6.6.1) Instantaneous, Point Injection

In section 6.4 (eqn. 6-34) the solution is presented for an instantaneous point injection into uniform estuary type flow. This solution was found using E_t (eqn. 6-26) as the dispersion coefficient, not E_A. The solution using E_A is eqn. 6-35.

Just as for steady flow, the concentration distribution (from either E_t or E_A) is normal with respect to x at each instant. The centroid of the distribution is always at

$$x = U_f t - \frac{U_T}{\sigma} \left[\cos \sigma (t-\delta) - \cos \delta\right] \qquad 6\text{-}48$$

and the variance (defined by eqn. 7-2) of the distribution is $\sigma^2 = 2E_A\theta$ (using E_t) or $\sigma^2 = 2E_A t$ (using E_A).

The concentration distribution undergoes an oscillatory convection as defined by the velocity of eqn. 6-1. Thus, the temporal concentration distribution observed at a fixed x_i is quite different from that observed for steady flow. One such temporal distribution was calculated from eqn. 6-34 (which is the solution based on E_t) and plotted in fig. 6-7. The time shift δ was taken as zero. The values of the various parameters were as shown on the figure. The same calculations were carried out using the solution based on E_A (eqn. 6-35). In the scale used to plot fig. 6-7, there was no distinguishable difference between the two solutions after the first period.

For the first seven periods, the majority of the concentration distribution moves past the measurement station on both the forward and the return excursion. Thus, there is part or all of two spikes within each of the first seven periods. Beginning with the fourth period, the downstream tail of the distribution does not move completely upstream of the observation station at the limit of the upstream excursion. This results from the distribution becoming more spread out due to dispersion and from the mean position of the distribution moving downstream due to U_f. By the eighth period, the convection due to U_f has moved the distribution so far downstream that only part of the upstream tail passes the observation station, even at the upstream limit of the excursion. Thus, from period eight on (for the example of fig. 6-7), the observed peaks do not correspond to the actual maximum of the concentration distribution, since the actual maximum is no longer passing the observation station. In general, the actual maximum and observed peaks will not be the same for t greater than x_i/U_f. Also, if x_i is greater than $(U_f t + U_T T/\pi)$, then the actual maximum will not reach x_i even at the

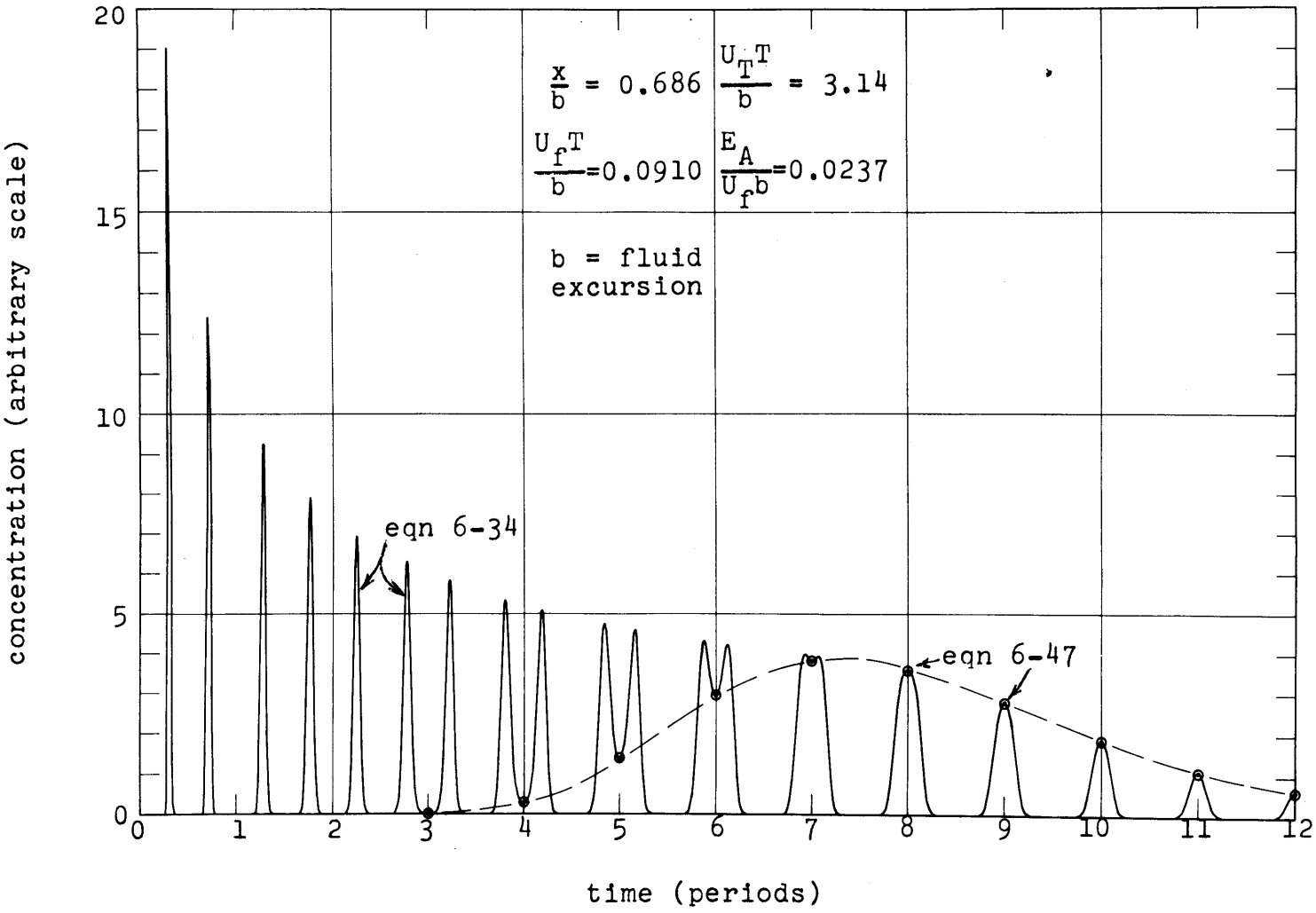

Fig. 6-7: Theoretical concentration distribution in estuary type flow for instantaneous, point injection

downstream limit of the excursion. ($U_T T/\pi$ is equal to the length of the fluid excursion.)

From eqn. 6-35, the actual maximum concentration decreases according to

$$C_{max} = \frac{M}{\rho A \sqrt{4\pi E_A t'}} \qquad 6\text{-}49$$

Also, the time (t_p) of occurrence of the peak concentration at x_i is given approximately by the solution of

$$x_i - U_f t_p + \frac{U_T}{\sigma} \left[\cos \sigma (t_p - \delta) - \cos \delta\right] = 0 \qquad 6\text{-}50$$

The degree of approximation in eqn. 6-50 is equivalent to saying that t_p equals x_i/U for steady flow. (See eqn. 5-8, eqn. 5-9, and the accompanying discussion.) For a pipe of radius a, if x_i/a is large, then eqn. 6-50 should be expected to give good results. In accordance with fig. 6-7, eqn. 6-50 gives more than one value of t_p. Also, when $U_f t$ becomes greater than x_i, no solution can be found for t_p from eqn. 6-50. This is in accordance with the previous observation that the actual maximum no longer passes x_i for $U_f t$ greater than x_i.

Fig. 6-7 is a continuous concentration distribution which was calculated for a particular set of circumstances. If this distribution were observed at one period intervals (say at HWS), then the circled points would represent the observed concentrations. These are the points which would be calculated from eqn. 6-47. If one were to draw a smooth curve through these points, the dashed line would be obtained. It is obvious from the figure that this line does not represent the concentration at x_i for all times. It is also interesting to note from fig. 6-7, that if the concentration were sampled at LWS, then zero concentration would be observed during the time interval represented on the figure.

6.6.2) Continuous, Point Injection

a) Exact solution: Again consider the case of a constant rate of injection, Q_m, at x = 0. Let the injection begin at the time of the upstream limit of the fluid excursion, and let time (t) be measured

from the beginning of the injection. Also, let the injection continue for $0 \leq \tau \leq t_1$. If it is assumed that the dispersion coefficient is constant and equal to E_A at all time, then C may be given as an integral of eqn. 6-35. For each increment of the continuous injection, dM equals $Q_m d\tau$; t of eqn. 6-35 now becomes $t-\tau$; and δ is now $-\tau$. For $t \geq t_1$,

$$C = \int_o^{t_1} \frac{Q_m}{\rho A \sqrt{4\pi E_A (t-\tau)}} \exp - \frac{[x - U_f(t-\tau) + \frac{U_T}{\sigma}\{\cos \sigma t - \cos \sigma\tau\}]^2}{4E_A(t-\tau)} d\tau \qquad 6\text{-}51$$

By letting $\eta = t-\tau$, the integral can be written as

$$C = \int_o^{t_1} \frac{Q_m}{\rho A \sqrt{4\pi E_A \eta}} \exp - \frac{[x - U_f\eta + \frac{U_T}{\sigma}\{\cos \sigma t - \cos \sigma(t-\eta)\}]^2}{4E_A\eta} d\eta \qquad 6\text{-}52$$

As far as is known, a closed form of this integral is not known at the present time. For a given set of conditions, the integral may be evaluated numerically to find C as a function of x and t.

If the injection in the above case is continuous so that $t_1 = t$, it would be expected that a quasi-steady state could be reached. That is, no change would take place in the concentration from one period to the next. Ippen and Harleman (ref. 28) have shown that in such cases, the problem of describing the concentration distribution may be separated into two parts. One part is equivalent to the application of eqn. 6-46 to find the concentration at $t = nT$. At steady state, $\partial C/\partial n = 0$ and this equation shows that from one period to the next there is a balance between convection due to U_f and dispersion represented by E_A. For the other part, Ippen and Harleman have shown that after a quasi-steady state is reached, the transport process during a period may be represented solely by the oscillatory convection; that is,

$$\frac{\partial C}{\partial S} + U_T \sin \sigma S \frac{\partial C}{\partial x} = 0 \qquad 6\text{-}53$$

where S is the time variable during a period so that S varies just in the interval $0 \leq S \leq T$. The solution of eqn. 6-53 gives the functional

variation of C:

$$C = f\left[x + \frac{U_T}{\sigma}\ (\cos \sigma S - 1)\right] \qquad 6\text{-}54$$

Thus, if the concentration is known as a function of x at any time during the period, the concentration can be found at any other time by eqn. 6-54. (See ref. 22.)

b) Approximate solution for quasi-steady state: An approximation to the quasi-steady state which eqn. 6-52 approaches may be obtained in the following way: Let the length of the fluid excursion during a half period be b. Since the injection of tracer is continuous at a fixed point, the tracer is introduced into a fluid volume of length b as the fluid moves past the injection point during the period. To account for this, assume that the injection is spatially distributed uniformly over a length b. Let the strength of the distributed injection be such that the total injection during a period is $Q_m T$, which is the actual mass injected during a period. This assumed condition may be used to find a steady-state solution of eqn. 6-46. If this solution is taken as representing the concentration distribution at some time during the period, then eqn. 6-54 can be used to find the concentration at other times.

The assumed injection condition is shown in the sketch below:

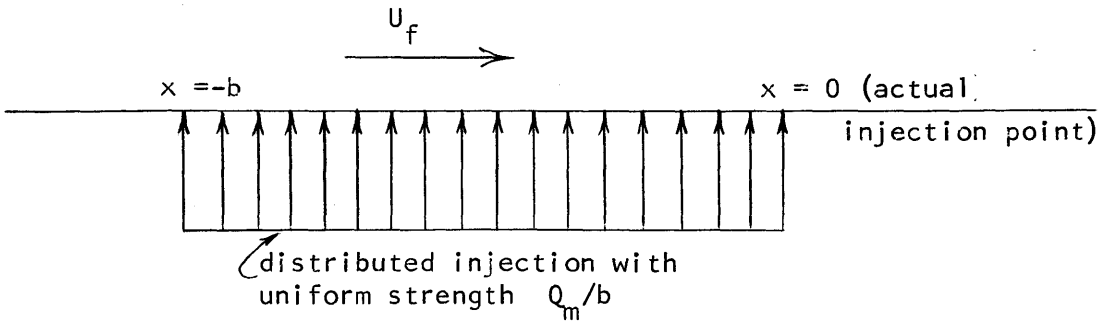

If x = 0 is the actual point of injection, the solution obtained from the assumed injection should approximate the solution at the time of the upstream limit of the fluid excursion since all of the region into which tracer is being injected has effectively been assumed to be

upstream from the actual injection point.

Recall that the steady-state solution for a continuous injection into steady flow was given by eqn. 5-32. By comparing eqn. 6-46 with eqn. 5-2, it is seen that the desired solution of eqn. 6-46 can be made up by integrating concentrations of the type given by eqn. 5-32. In general notation,

$$C = \int_{-b}^{o} f\,(x - x')\,dx'$$

where $f(x)$ is the concentration distribution given by eqn. 5-32. When this integration is carried out, it is found that

$$\frac{C}{C_o} = 1 \qquad \text{for} \quad 0 < x_H$$

$$\frac{C}{C_o} = \frac{x_H + b}{b} + \frac{E_A}{U_f b}\left(1 - \exp\frac{U_f x_H}{E_A}\right) \quad \text{for} \quad -b < x_H < 0$$

$$\frac{C}{C_o} = \frac{E_A}{U_f b}\left(\exp\frac{U_f(x_H + b)}{E_A} - \exp\frac{U_f x_H}{E_A}\right) \qquad 6\text{-}55$$

$$\text{for } x_H < -b$$

where $C_o = Q_m/(\rho A U_f)$. Note that C_o is again determined by the dilution ratio between the total rate of injection of tracer and the rate of fresh water flow. In eqn. 6-55, x_H is used to signify that this solution is being taken as the solution at HWS, the time of the upstream limit of the fluid excursion (i.e. $S = 0$ in eqn. 6-54). By applying eqn. 6-54 at $S = 0$ and $x = x_H$, then at any S and x, it is seen that the substitution

$$x_H = x + \frac{U_T}{\sigma}\,(\cos \sigma S - 1) \qquad 6\text{-}56$$

can be used in eqn. 6-55 to find the quasi-steady state concentration at any x and t (since S may now be replaced by t). Thus the final approximate solution is

$$\frac{C}{C_o} = 1 \quad \text{for } 0 < \left[x + \frac{U_T}{\sigma} (\cos \sigma t - 1)\right] \qquad 6\text{-}57$$

$$\frac{C}{C_o} = \frac{x + \frac{U_T}{\sigma}(\cos \sigma t - 1) + b}{b} +$$

$$\frac{E_A}{U_f b} \left(1 - \exp \frac{U_f \left[x + \frac{U_T}{\sigma} (\cos \sigma t - 1)\right]}{E_A}\right) \qquad 6\text{-}58$$

$$\text{for} \quad -b < \left[x + \frac{U_T}{\sigma} (\cos \sigma t - 1)\right] < 0$$

$$\frac{C}{C_o} = \frac{E_A}{U_f b} \left[\exp \frac{U_f \left[x + \frac{U_T}{\sigma}(\cos \sigma t - 1) + b\right]}{E_A} - \right.$$

$$\left. \exp \frac{U_f \left[x + \frac{U_T}{\sigma} (\cos \sigma t - 1)\right]}{E_A}\right] \qquad 6\text{-}59$$

$$\text{for} \quad \left[x + \frac{U_T}{\sigma} (\cos \sigma t - 1)\right] < -b$$

where $C_o = Q_m/(\rho A U_f)$. The regions where each of these three equations is valid are shown in fig. 6-8 as a function of time.

For two sets of conditions, the approximate solution given by equations 6-57, -58, and -59 was compared with the numerical integration of the exact solution as given in eqn. 6-52 for $t_1 = t$. This comparison is shown in fig. 6-9. The numerical integration of eqn. 6-52 was carried out with $\Delta t = 0.01T$. The upper limits of the integrations were taken as 600T and 600.5T. Thus, the distributions obtained correspond to the times of the upstream and the downstream limit of the excursion after 600 periods of oscillation. The integration to 600T effectively gave a quasi-steady state since 1.00 was obtained for downstream values of C/C_o. The steady state distribution perhaps could have been obtained with a smaller upper limit on the integration. This possibility was not investigated.

Only the distributions for the even period (600T) are shown in the figure. The numerical integration to 600.5T gave identical distributions shifted downstream by one excursion. This confirms Ippen and Harleman's statement that the concentration distribution

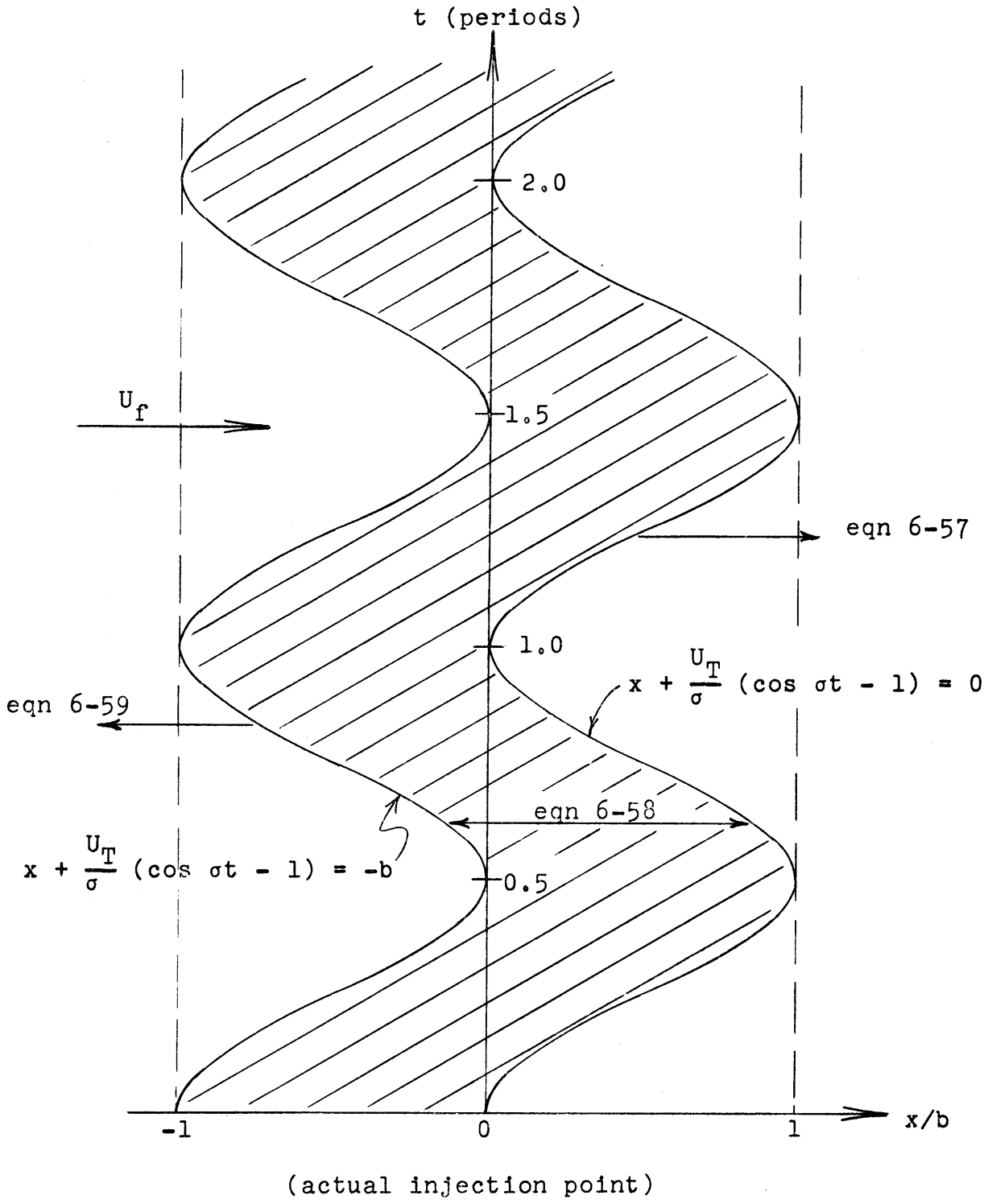

Fig. 6-8: Three regions involved in the approximate solution for a continuous injection into estuary type flow

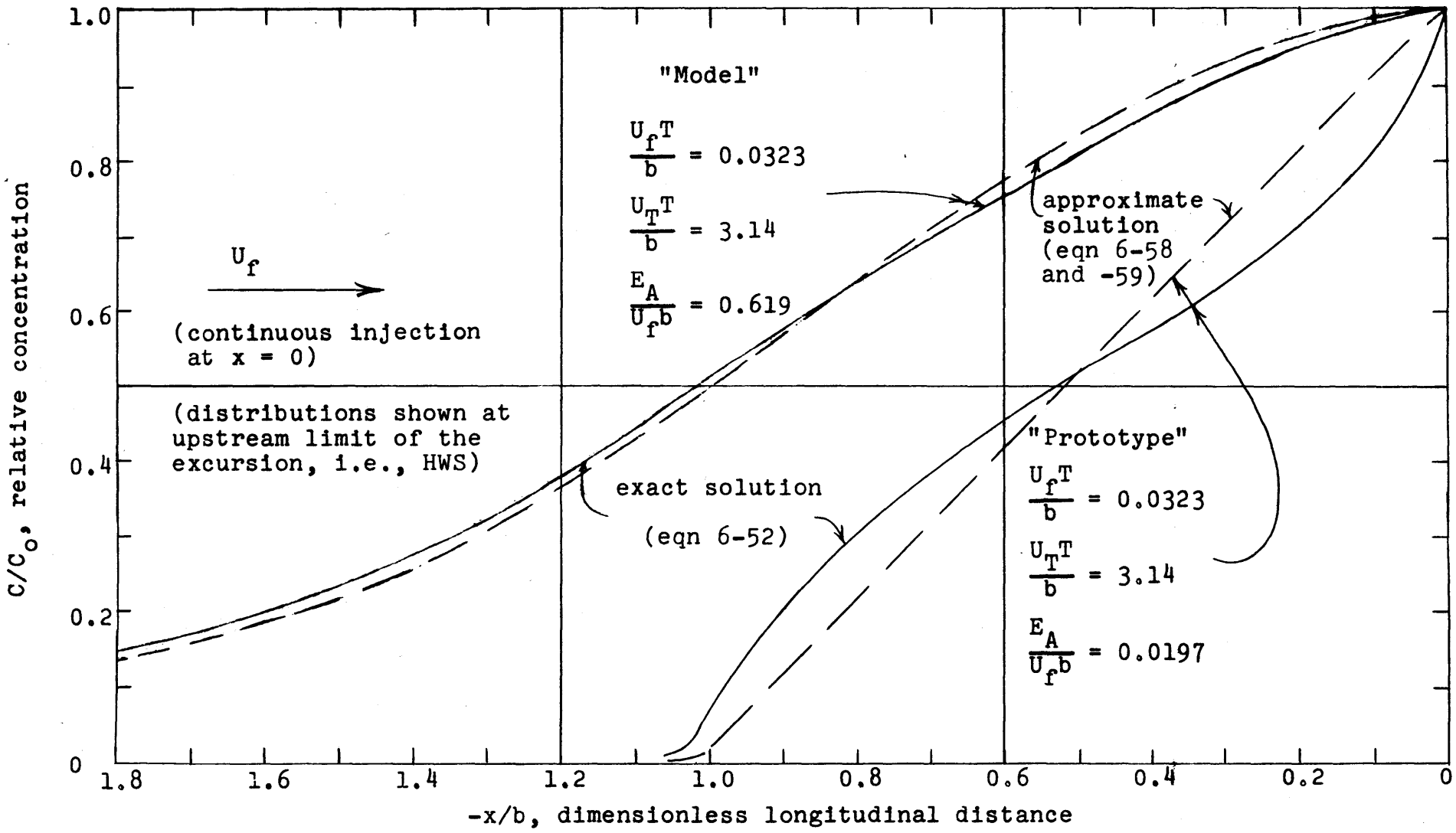

Fig. 6-9a: Exact and approximate solutions for continuous injection of tracer into estuary type flow (linear scales)

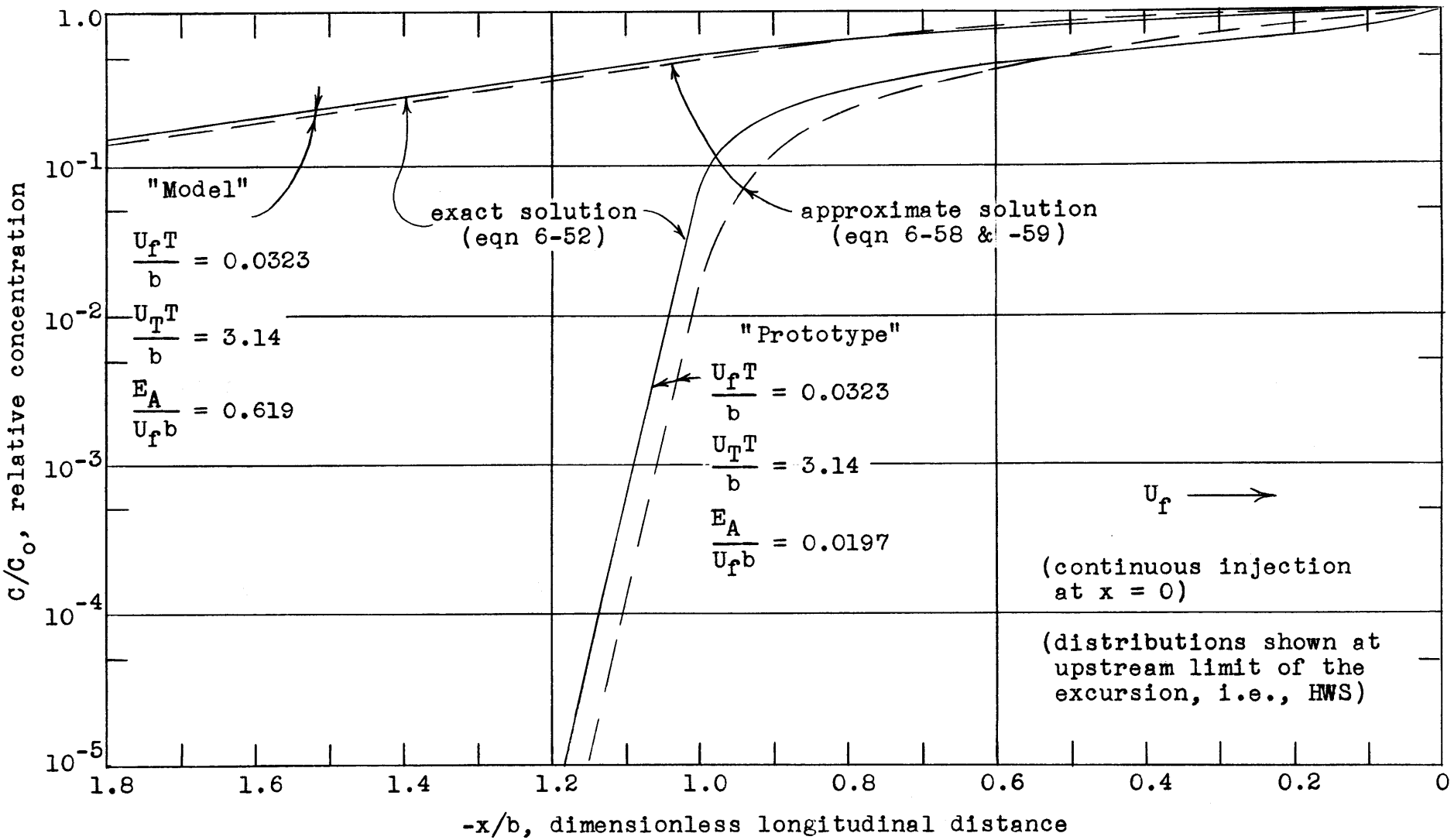

Fig. 6-9b: Exact and approximate solutions for continuous injection of tracer into estuary type flow (semi-logarithmic plot)

simply undergoes a one-dimensional convection during a period after a quasi-steady state is reached.

From fig. 6-9 it is seen that the approximate solution is a better approximation for the case where dispersion is relatively more important in the transport process. This is probably associated with the fact that a uniformly distributed injection was assumed for the approximate solution. This uniform distribution would correspond most closely to the actual case if the fluid moved past the true injection point with a constant, but reversing, velocity. However, the fluid moves past the true injection point with a sinusoidal velocity. If a spatial distribution were assumed so as to take account of this sinusoidal variation, then better agreement might be obtained for the case where dispersion is less significant. As the effects of dispersion increase, any non-uniformities in an assumed spatial distribution would tend to be smoothed out. This would seem to be a possible explanation for better agreement in one case than in the other.

For the case where dispersion is relatively less important, fig. 6-9 shows that dispersion still causes some upstream transport. Spread of the tracer in a region equal to the excursion length (i.e. $-1.0 < x/b < 0$ at HWS) would be expected just due to the fluid's moving back and forth past the injection point. However, tracer can move into the region $x/b < -1.0$ only by dispersion. In this same region, the concentrations given by the exact and approximate solutions do not agree. However, notice that the slopes of the exact and approximate solutions are the same for both cases presented in fig. 6-9. This indicates that the functional relationship of the approximate solution could be used to find the concentrations upstream of $x/b = -1.0$ if the concentration were known at that section.

From the two cases which were presented, it seems reasonable to say that the approximate solution gives an adequate representation of the concentration distribution when the relative importance of dispersion is such that an appreciable amount of the tracer becomes spread over a distance equal to two or more excursion lengths.

It should be pointed out that the dispersion equation and many sets of boundary conditions which arise are similar in mathematical form to heat flow problems and other types of diffusion problems. Thus, many more solutions for dispersion problems can be found in references such as ref. 9, 11, 26, 41.

7) SOME METHODS FOR EXPERIMENTAL DETERMINATION OF DISPERSION COEFFICIENTS

In the previous sections, several solutions were given for the dispersion equation under various sets of initial and boundary conditions. On the basis of these solutions, several methods are available for the calculation of dispersion coefficients. Recall that it was assumed that the introduction of a tracer into a given flow did not affect the flow pattern. Thus, since dispersion is related to the distribution of velocity and turbulent diffusivity, the same dispersion coefficient should be found for a given flow regardless of which set of boundary and initial conditions are used for the tracer.

7.1) Steady, Uniform Flow

7.1.1) Instantaneous Point Injection

Let the tracer be injected instantaneously and uniformly across the flow cross section at $x = 0$ and $t = 0$. For simplicity, this was called an instantaneous, point injection. For this injection condition and for steady, uniform flow the concentration distribution is given by eqn. 5-6. Three methods will be described for finding the dispersion coefficient under these conditions.

a) Spatial variance: If spatial distributions are available for fixed times, then the dispersion coefficient E may be found from the variance (σ^2) of the distribution since

$$E = \frac{\sigma^2}{2t} \qquad 7\text{-}1$$

(See section 5.1.1.) Basically, σ^2 is the second moment of the spatial distribution and is defined by

$$\sigma^2 = \frac{\int_{-\infty}^{\infty} (x - Ut)^2 C \, dx}{\int_{-\infty}^{\infty} C \, dx} \qquad 7\text{-}2$$

However, the normal distribution is also given by

$$\frac{C}{C_{max}} = \exp - \frac{\bar{x}^2}{2\sigma^2} \qquad 7\text{-}3$$

where $\bar{x} = x - Ut$, so σ^2 may be found directly from the spread of the distribution rather than by carrying out the integrations of eqn. 7-2. For example, at the level where $C/C_{max} = 0.5$ on the distribution, $\bar{x}_{0.5}$ may be found and σ^2 will be given by

$$\sigma^2 = - \frac{\bar{x}_{0.5}^2}{2 \ln 0.5} \qquad 7\text{-}4$$

See fig. 7-1. A similar calculation may be made for as many levels of C/C_{max} as desired. Then, using eqn. 7-1, E may be found.

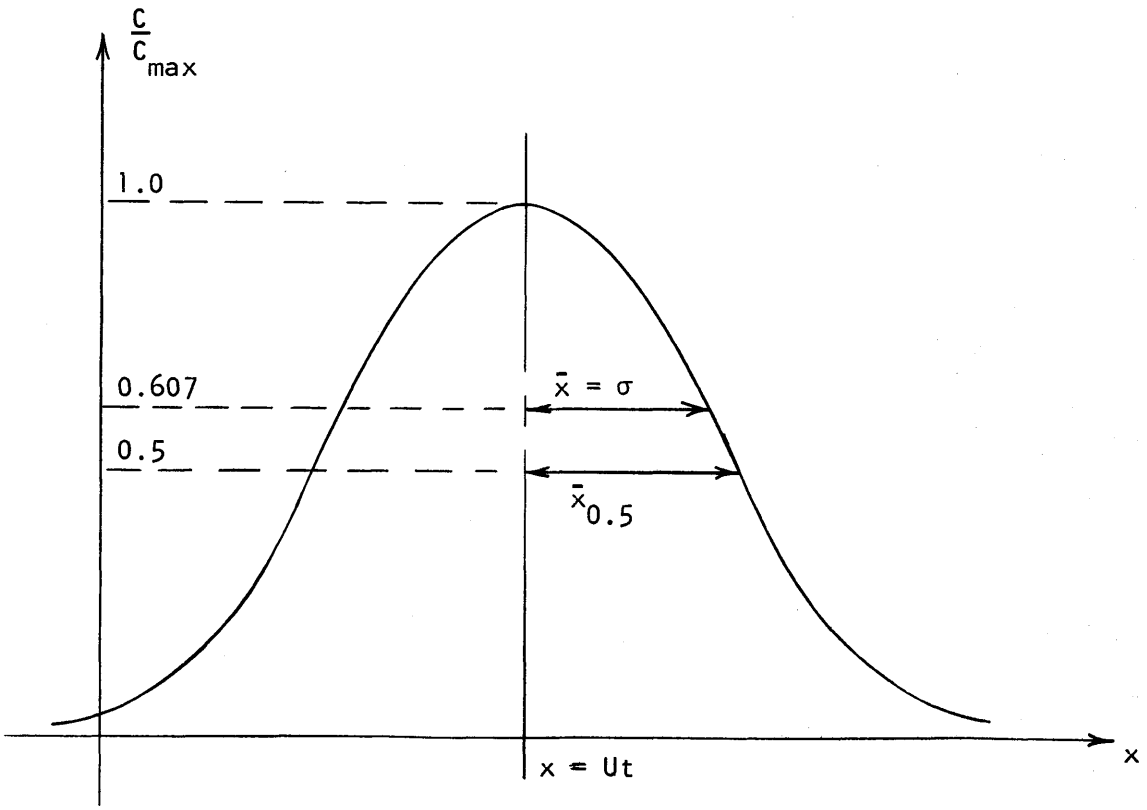

Fig. 7-1: Relation Between the Spread and the Variance of a Normal Distribution

Direct application of eqn. 7-1 assumes that the injection was made uniformly across the section. When this condition is not met, E may be found by taking the time rate of change of σ^2 after the tracer becomes uniformly mixed across the section. By differentiating eqn. 7-1 with respect to t, one finds that

$$E = \frac{1}{2} \frac{d\sigma^2}{dt} \qquad 7\text{-}5$$

This expression may also be used when the time and location of the injection are not known.

b) Temporal moments: For a temporal distribution, E is again related to the second moment (equations 5-14 and 5-15), but the second moment is not related in a simple way to the spread of the distribution. Thus, the distribution must be integrated to obtain the moments. From equations 5-14 and 5-15,

$$E = \sqrt{\left(\frac{Ux_i}{12}\right)^2 + \frac{U^4}{12} \frac{\mu_2^P}{\mu_o}} - \frac{Ux_i}{12} \qquad 7\text{-}6$$

or

$$E = \sqrt{\left(\frac{Ux_i}{8}\right)^2 + \frac{U^4}{8} \frac{\mu_2'}{\mu_o}} - \frac{Ux_i}{8} \qquad 7\text{-}7$$

where μ_2^P is the second moment about the peak of the distribution and μ_2' is about the centroid of the distribution. Again, if the initial condition is not known exactly, the change in the second moment may be used to find E. From eqn. 5-16 for either μ_2^P or μ_2',

$$E = \frac{U^3}{2\mu_o} \frac{d\mu_2}{dx} \qquad 7\text{-}8$$

It should be observed that it is necessary to know the entire concentration distribution rather accurately in order to carry out the integration to find μ_2. This is especially true of the tails of the distribution since these have the longest "moment arm" and this moment arm is squared to find μ_2. A slight error in the concentration can cause a large error in the moment and hence in E. The next method overcomes this difficulty.

c) Modified semi-log plot: Let C_* be a given concentration, say a value near the peak of the distribution, and let t_* be the time corresponding to C_* at x_i. From eqn. 5-6,

$$C_* = \frac{M}{\rho A \sqrt{4\pi E t_*}} \exp - \frac{(x_i - Ut_*)^2}{4Et_*} \qquad 7\text{-}9$$

Dividing eqn. 5-6 by eqn. 7-9, rearranging, and taking the natural log, one finds

$$\left[\ln \left(\frac{C}{C_*} \sqrt{\frac{t}{t_*}} \right) \right] = - \frac{1}{E} \left[\frac{(x_i - Ut)^2}{4t} - \frac{(x_i - Ut_*)^2}{4t_*} \right] \qquad 7\text{-}10$$

Thus, if the two bracketed quantities are plotted versus each other for the concentration distribution at x_i, the data should fall on the straight line whose slope is $-1/E$. If t_* is taken as x_i/U, then the second term in the right-hand bracket will be zero.

This method has the advantage that the straight line may be fitted to those points corresponding to concentrations in the upper part of the distribution. If this is done, inaccuracies in the measurement of the relatively low concentrations of the tracer do not influence the determination of E.

7.1.2) Other Injections

If tracer material is injected so that eqn. 5-30, 5-31,

or 5-39 gives the concentration distribution, there is no direct way of calculating E from the data acquired before a steady state is reached. However, if the distribution does come to steady state so that eqn. 5-32 or 5-40 applies, then E may be found from the slope of a semi-logarithmic plot of the relative concentration versus Ux. This requires that the spatial distribution of concentration be known, but for a steady state this does not present the problems that it does for an unsteady one.

If conditions are such that either eqn. 5-37 or 5-41 applies, then E can be obtained most directly by plotting C/C_o versus $(x_i - Ut)/(2\sqrt{t})$ on arithmetic-probability paper since these solutions involve error functions. E is then related to the slope of the straight line through the data points. If probability paper is not available, the same effect may be achieved in another way. For the cases being considered, the relative concentration may be written as

$$\frac{C}{C_o} = \frac{1}{2}\left[1 - \text{erf}\ \phi\right]$$

where

$$\phi = \frac{x - Ut}{2\sqrt{E\ t}}$$

For each C_j observed at the point x_i, a ϕ_j may be calculated just from C_j/C_o. Then, by taking x_i and t_j corresponding to C_j, the ϕ_j values may be plotted versus $(x_i - Ut_j)/(2\sqrt{t_j})$. The data should plot as a straight line whose slope is related to $\sqrt{E}$.

7.2) Uniform Estuary Type Flow

In estuary type flow, the time averaged dispersion coefficient (E_A) was shown to be the most significant dispersion parameter. (Section 6.) Thus, the methods discussed here deal only with finding E_A.

7.2.1) Instantaneous, Point Injection

For an instantaneous, point injection at x = 0 and

t = 0, eqn. 6-35 describes the concentration distribution when the dispersion coefficient is taken as E_A for all time. If the data is sampled at x_i at one period intervals after the time of injection, then eqn. 6-47 represents this selected data. Eqn. 6-47 is identical in form to eqn. 5-6. Thus, this selected data may be analyzed by spatial moments, temporal moments, or the modified semi-log plot just as described above. The dispersion coefficient which is obtained will be E_A. It must be remembered that the transport process represented by E_A is still strongly dependent on oscillatory velocity even though this velocity does not appear in eqn. 6-47.

If data is taken at one period intervals on the half period rather than the full period, then the data is represented by

$$C_s = \frac{M}{\rho A \sqrt{4\pi E_A (n+\frac{1}{2})T}} \exp - \frac{[(x - \frac{TU_T}{\pi}) - U_f(n+\frac{1}{2})T]^2}{4E_A(n+\frac{1}{2})T} \qquad 7\text{-}10$$

This data may be analyzed by the same methods if the effective value of x is taken as $(x-TU_T/\pi)$. (The quantity TU_T/π is the length of the fluid excursion.) It has also been assumed that $\theta = t$ at the half period in order to obtain eqn. 7-10. B (eqn. 6-24) must be unity and n must be zero for θ to exactly equal t at the half period.

7.2.2). Continuous, Point Injection

For a continuous, point injection there is apparently no direct method for calculating a dispersion coefficient on the basis of the exact solution as given by eqn. 6-52, even if a quasi-steady state is obtained. In section 6 it was pointed out that the approximate solution of equations 6-57, -58, and -59 is a better representation of the quasi-steady state in some cases than in others. If conditions are such that this approximate solution seems to apply, then it may be used to calculate an approximate value of the dispersion coefficient. Eqn. 6-58 may be differentiated and written as

$$\left[\ell n\ (1-b\cdot\frac{\partial(C/C_o)}{\partial x})\right] = \frac{U_f}{E_A}\left[x + \frac{U_T}{\sigma}\ (\cos\sigma t - 1)\right] \qquad 7\text{-}12$$

for the region

$$-b < \left\{x + \frac{U_T}{\sigma}(\cos\sigma t - 1)\right\} < 0$$

If the data for this region is plotted in terms of the bracketed quantities of eqn. 7-12, the points should fall on a straight line whose slope is U_f/E_A. Use of this method requires that enough data be available so that the gradients $\partial(C/C_o)/\partial x$ may be found.

For the region

$$\left[x + \frac{U_T}{\sigma}\ (\cos\sigma t - 1)\right] < -b$$

eqn. 6-59 may be written as

$$\frac{C}{C_o} = \left[\frac{E_A}{U_f b}\ (\exp\left\{\frac{U_f b}{E_A}\right\} - 1)\right] \exp\frac{U_f}{E_A}\left\{x + \frac{U_T}{\sigma}(\cos\sigma t - 1)\right\} \qquad 7\text{-}13$$

If $\ln(C/C_o)$ is plotted versus

$$\left\{x + \frac{U_T}{\sigma}\ (\cos\sigma t - 1)\right\}$$

the slope of the resulting straight line should be U_f/E_A. In connection with fig. 6-9 it was observed that the exact and approximate solutions gave the same slope of $\ln(C/C_o)$ vs. x/b in the region now under consideration. Thus, in this region, use of the method described above should give a value of E_A which would be as accurate as if the exact solution (eqn. 6-52) could be fitted to the data. (Note that the bracketed coefficient in eqn. 7-13 is a constant for a given set of flow conditions.)

7.3) Non-uniform Flow

In all of the cases which have been presented so far, it has been assumed that the flow was uniform so that the velocity, the flow area, and the dispersion coefficient were not functions of x. For cases where it is not reasonable to assume uniform flow, it has been shown that the mass balance equation may be written in finite difference form.

When a steady or a quasi-steady state is reached, the finite difference equation may be written as eqn. 2-34 or eqn. 2.40, using a central difference for the derivatives. (Eqn. 5-44 used a forward difference.) From eqn. 2-34 for steady flow, E_x is given as

$$E_{xi} = \frac{2\ (\Delta x)\ U_{x_i}\ C_i}{C_{i+1} - C_{i-1}} \qquad 7\text{-}14$$

For estuary-type flow (from eqn. 2-40),

$$(E_{Ax})_i = \frac{2\ (\Delta x)\ U_{f_{x_i}}\ C_{s_i}}{C_{s_{i+1}} - C_{s_{i-1}}} \qquad 7\text{-}15$$

Eqn. 7-15 may not be applied in regions where mass is added across the flow boundaries. (See discussion accompanying eqn. 4-15.) This equation is based on an expression which represents only the concentration changes of a conservative tracer from one period to the next. Thus, if a given fluid volume has mass added to it any time during a period, eqn. 7-15 cannot be applied to that fluid volume or across it. An example of this restriction is seen for the case of a continuous injection into estuary type flow. In this case, eqn. 7-15 may not be applied to any of the fluid which passes the injection station during an oscillation. Thus, eqn. 7-15 is applicable only in the region

$$\left[x + \frac{U_T}{\sigma}\ (\cos\ \sigma t - 1)\right] < -\ b$$

where b is the excursion length, U_T is the maximum oscillatory velocity, σ is the frequency of oscillation, and the injection is made at x = 0.

At the time of the upstream limit of the excursion ($t = nT$, $n = 0, 1, 2 \ldots$), the region of applicability is $x < -b$. At the downstream limit ($t = (n + 1/2)T$), the region is $x < 0$. In connection with eqn. 2-39, it is further pointed out that the fresh water discharge ($U_f A$) must be constant if eqn. 7-15 is to be applicable.

8) EXPERIMENTAL PROGRAM

8.1) M.I.T. Experiments

8.1.1) Objectives

The purpose of the experiments conducted at M.I.T. as part of the present work was to study longitudinal turbulent dispersion in both steady and unsteady, estuary type, shear flows. In the present sense, estuary type flow refers to flow where the velocity is the sum of two components--an oscillating component and a "through flow" component. (See eqn. 2-24.) It was convenient to make these studies in a pipe line in the laboratory. Thus, it was possible to have uniform flow for both the steady and the estuary type flows.

Naturally, it is recognized that uniform estuary type flow in a circular pipe is not a model of tidal flow in an estuary. It was not the purpose of this research to model tidal flows, but rather to study the fundamentals of dispersion in flows which were kinematically similar in most respects to estuary flow. Since the kinematics of turbulent flow in pipes and in open channels are similar, it is to be expected that the results obtained in the laboratory should apply in a functional way to open channels.

In order to study dispersion, it is necessary to be able to trace the movement of water particles. In these studies, salt (sodium chloride) in low concentrations was used as a tracer. Salt concentrations were measured with electrical conductivity probes.

8.1.2) Equipment

The dispersion studies reported in this section were conducted in a straight pipe line made up of standard 1-1/2" galvanized plain end pipe (1.610" I.D., 1.900" O.D.). The total length of the pipe line was 140 feet and it was supported at 15 ft. intervals by pipe-hangers attached to wall-brackets. In addition, supports from the floor to the pipe were placed half way between each pair of wall-

brackets, so that the pipe then had supports at 7-1/2 ft. intervals.

The pipe was placed on a uniform slope so that the downstream end was 2 in. higher than the upstream end. This slope was used so that no air pockets could remain in the pipe even at low flow rates. Sleeve-type couplings were used to join the pipe sections. The couplings were made of 6" long pieces of 1-7/8" I.D. radiator hose. Worm hose clamps were then used on the radiator hose to seal the joint.

At about 8" from the upstream end of each length of pipe and at about the center of each length of pipe, holes were drilled through the pipe wall and fittings were installed to allow instruments up to 5/16" dia. to be inserted into the flow (fig. 8-1). These fittings were intended primarily for the conductivity probes described below. Piezometer taps were installed 6" upstream from the end of each length of pipe. At each piezometer station, four 1/16" dia. holes were placed in the pipe wall at 90° intervals around the pipe. Fittings for plastic tubing were then soldered over each piezometer tap and interconnected (fig. 8-2). By placing the piezometer taps 6" from the end of the pipe sections, it was possible to clean the inside of the 1/16" holes after they were drilled.

The piezometer taps and the fittings for the probes were numbered from the upstream end of the pipe. The numbers for the piezometer taps were preceded with a "P" and those for the probe fittings, with an "M". The coordinates of the P and M stations along the pipe are tabulated in Table 8-1. These distances were measured from the upstream end of the pipe.

A schematic diagram of the test pipe and the associated equipment is shown in fig. 8-3. Upstream, the pipe line terminated in a closed, circular tank made from a piece of 12" I.D. pipe. This tank was used to assure that the water entered the straight test section without secondary motions due to pipe bends, etc. For steady flow experiments, the downstream end of the pipe line could be attached to a hose which led to a weighing tank (400 lb capacity) and to a drain. For the estuary type flow experiments, the pipeline terminated downstream in another 12" I.D. tank. This tank had a float-switch which was connected to a solenoid valve on the drain line from the tank. This drain line also went to the weighing tank.

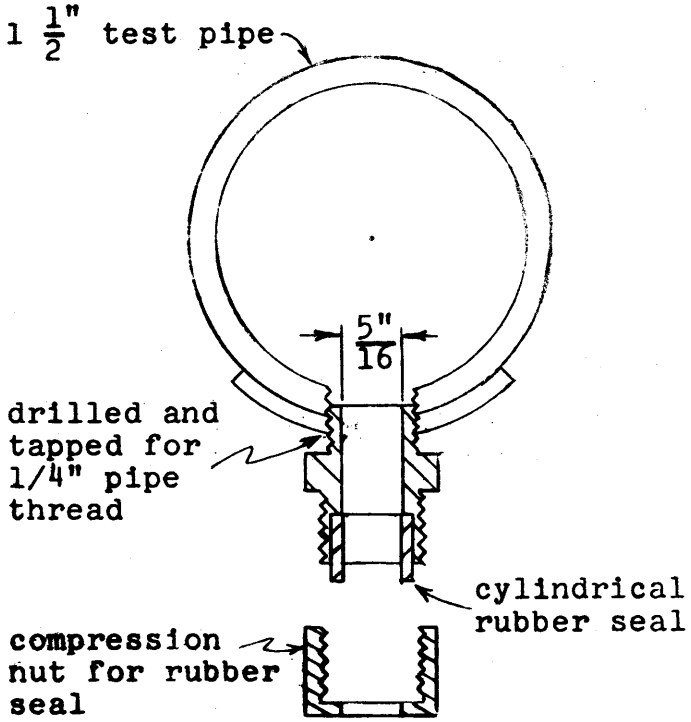

Fig. 8-1: Fittings for inserting instruments into pipe

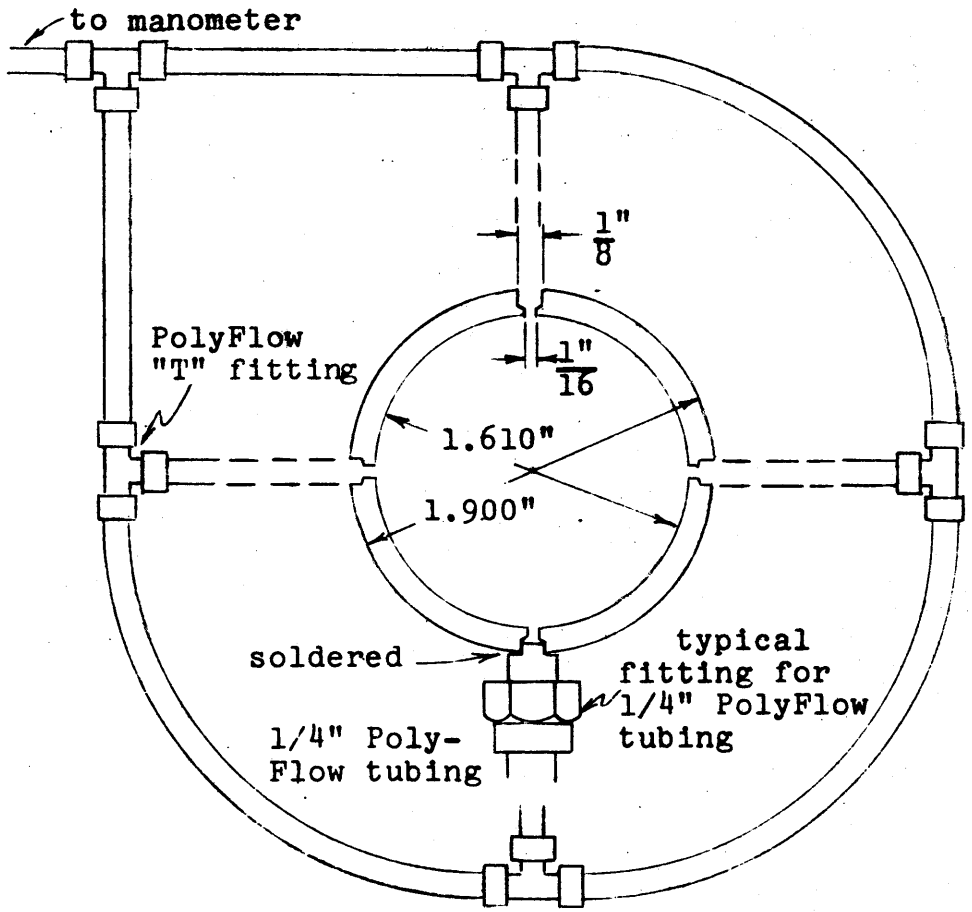

Fig. 8-2: Interconnected piezometer taps

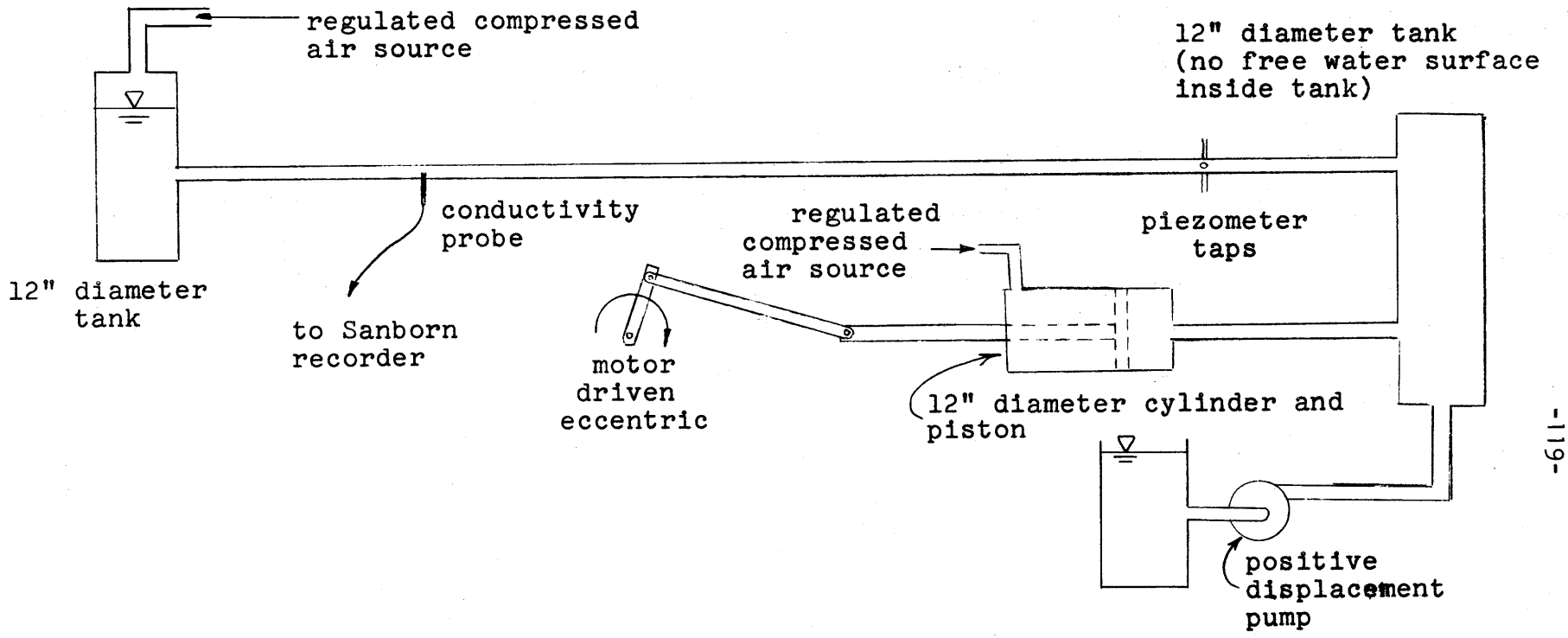

Fig. 8-3: Schematic diagram of test equipment

Table 8-1: Coordinates of Piezometric and Instrument Stations

Station Number	Longitudinal Distance from Upstream Tank (ft)
M1	1.21
M2	11.85
M3	22.22
M4	32.88
M5	43.24
M6	53.88
M7	64.26
M8	74.91
M9	85.26
M10	95.92
M11	106.33
M12	116.38
M13	127.38
M14	138.02
P1	21.39
P2	42.40
P3	63.42
P4	84.44
P5	105.50
P6	126.54

The upstream tank was connected so that it could be fed either by a centrifugal pump (for steady flow experiments) or by a hydraulic cylinder and piston apparatus (for estuary type flow experiments). The centrifugal pump was a Gould Close-Cupld 1 hp, 1750 rpm motor-pump rated at 100 gpm at 20 ft. The suction side was connected to the laboratory's main reservoir. Since the reservoir and the pump were in the basement of the laboratory, there was a static lift of 10 to 12 ft. to the pipe line. This pump was used for finding the relative roughness of the test pipe and for steady flow dispersion tests. To determine the roughness, the piezometer taps were connected to a manometer board. Then piezometer gradients were measured simultaneously with a gravimetric determination of the discharge. Typical piezometer gradients are shown in fig. 8-4. The results of all the head-loss tests are tabulated in appendix C, and the calculated friction factors are shown in fig. 8-5. A relative roughness of $k/D = 0.0013$ was taken for the pipe.

Oscillating flow was achieved in the pipe by a motor driven hydraulic cylinder and piston. The cylinder was a Hydroline (Rockford, Illinois) R2AW cylinder which had a 12" I.D. and a 12" maximum stroke. All parts of the cylinder and piston which were in contact with the water were chrome plated (CF 500). The power for driving the piston was supplied by a U. S. Electric Motors type VA-GWB motor with variable speed drive. The motor had a maximum output of 0.5 hp and the output speed ranged from 2.2 rpm to 20.6 rpm. The output speed was reduced by a 3/4" chain and sprocket drive. This additional reduction was 72:15. The chain drive was connected in turn to an adjustable eccentric mechanism on which the eccentricity could be varied continuously from zero to 6" (fig. 8-6). The eccentric was then connected by a 36" long drive arm to the piston rod. Thus, both the stroke and the frequency of oscillation of the piston could be varied from one run to the next. The ratio of the cylinder area to the pipe area shows that the fluid excursion in the pipe was 55.5 times the stroke of the piston. The objective of this type of drive was to obtain a sinusoidally varying velocity in the pipe. To obtain a true sinusoidal variation from a drive mechanism with a constant rotational speed, a scotch yoke mechanism is necessary. However, by using an

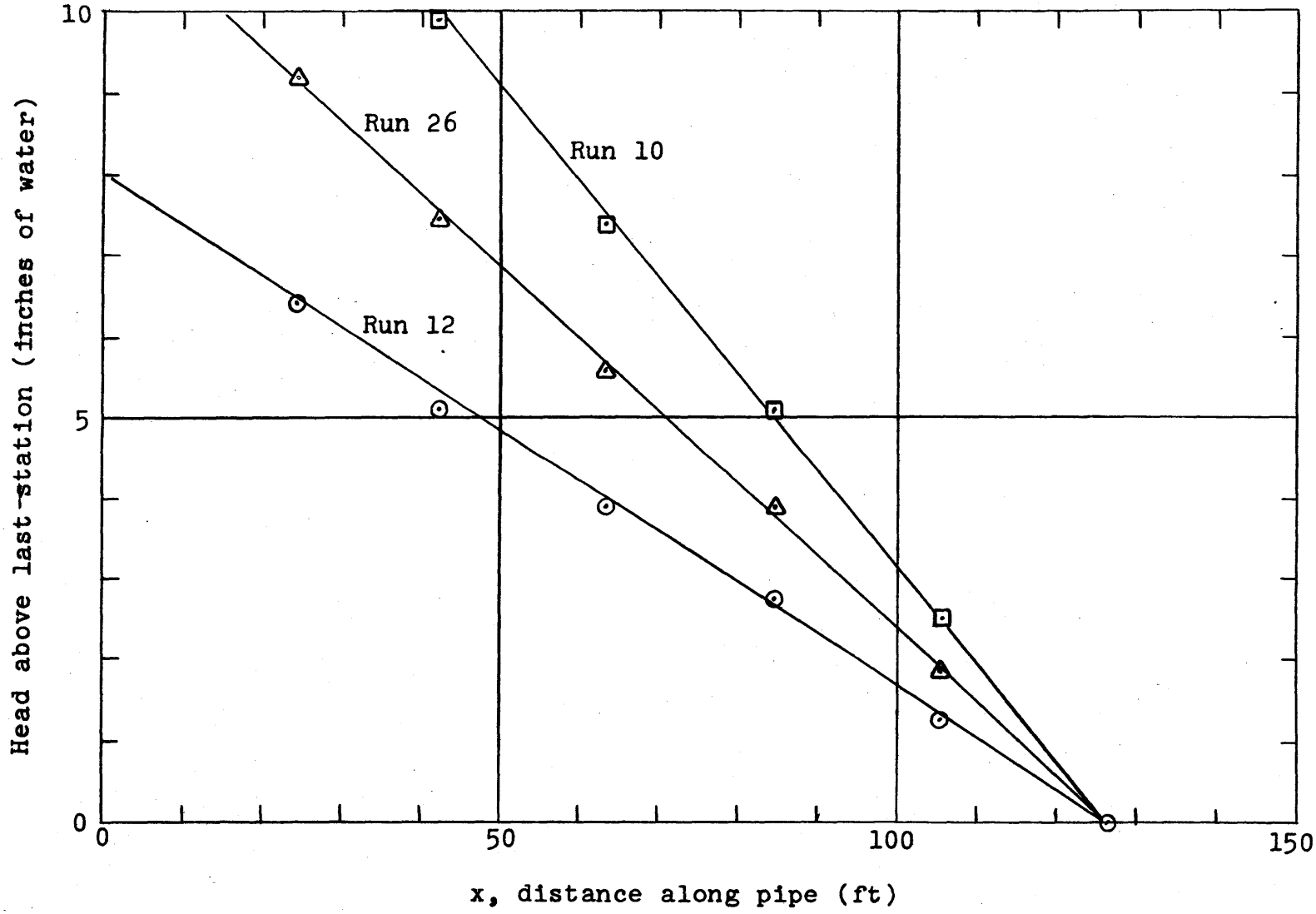

Fig. 8-4: Typical piezometric gradients

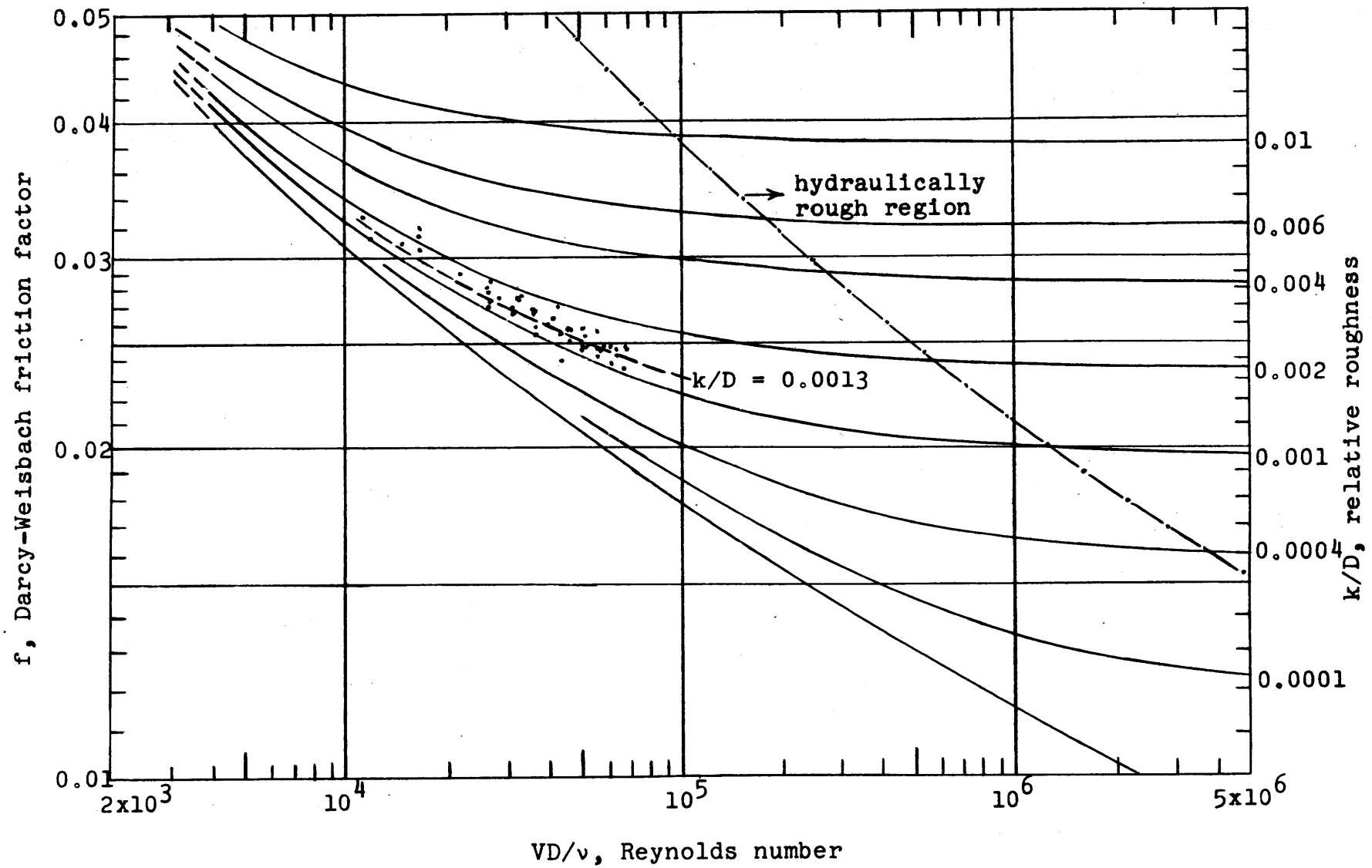

Fig. 8-5: Friction factors and relative roughness for test pipe

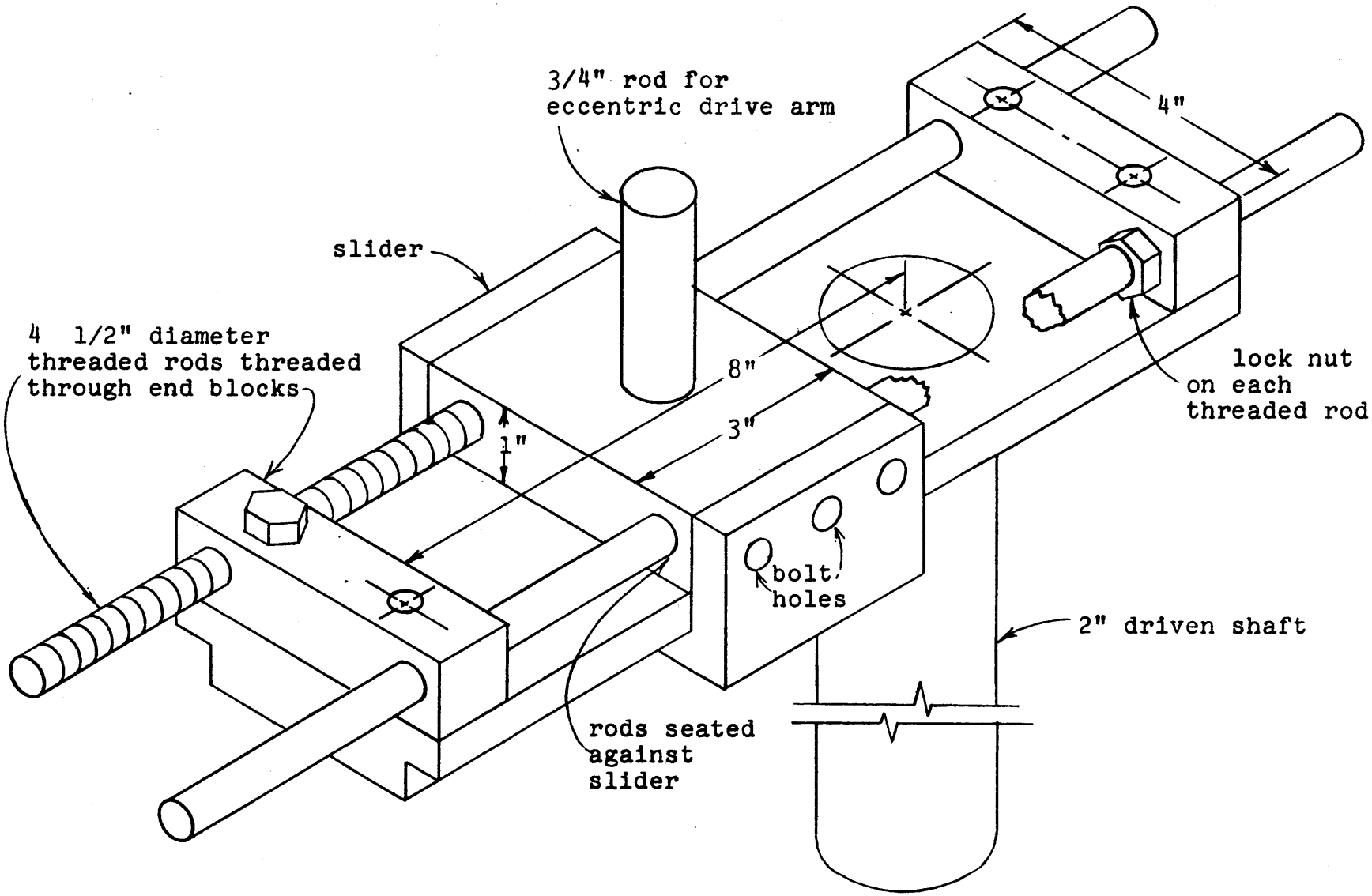

Fig. 8-6: Adjustable eccentric

eccentric drive and a drive arm which is arbitrarily long, a sinusoidal motion can be approximated to any desired degree. For the drive which was used the maximum deviation from the position given by a sinusoidal motion was 3.6% of the stroke.

If the downstream tank were open to the atmosphere, negative pressures would exist in the pipe and hydraulic cylinder during the reverse flow part of the oscillation. To avoid the negative pressures and the danger of air leaking into the system, the downstream tank was closed and pressurized to 15 psi. This was the maximum pressure change expected along the pipe during oscillatory flow. The motor and piston would have to work against this additional 15 psi if the back side of the piston were not pressurized also. Thus, a tank pressurized to 15 psi was connected to the back side of the piston. In addition the back side of the piston and the bottom of this pressurized tank were kept with water in them.

It was also desired to have a steady through-flow superimposed on the oscillating flow in the pipe. This through-flow was achieved by a positive displacement pump. This pump was Eastern Industries' model GW-2 gear pump which had a maximum discharge of 1.1 gpm at 1750 rpm and zero head. A positive displacement pump was used since it was discharging into a changing pressure caused by the oscillation of the piston and since it was desirable not to have the discharge change as the discharge head oscillated. The manufacturer's rating curve showed that the discharge at 1750 rpm dropped only to 1.05 gpm at 200 psi discharge pressure. Fig. 8-7, which is a calibration of the pump discharge vs. speed and discharge pressure, shows that the discharge actually dropped more than this for less pressure.

So that the through-flow rate could be changed from one run to the next, the pump was driven by a 1/8 hp variable speed D.C. motor with feed-back speed control. For the actual experiments, the through-flow was measured directly for each test rather than using the calibration curve.

As noted above, salt was used for a tracer in the dispersion studies. Salt concentrations were measured in the pipe by four conductivity probes which were constructed as shown in fig. 8-8. The body of the probes was a 5/16" O.D. glass tube through which two

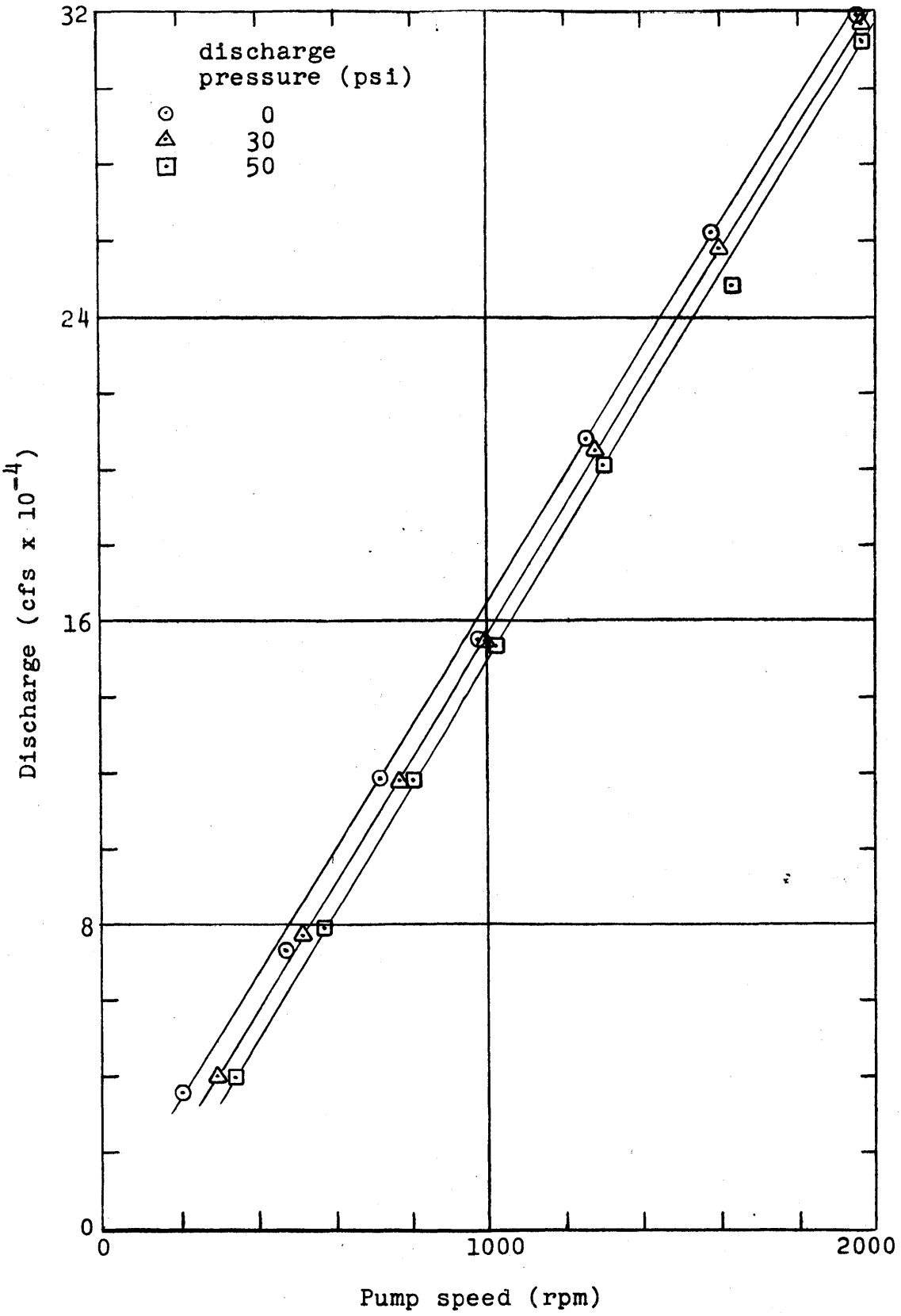

Fig. 8-7: Calibration of positive displacement pump

Note: Air inside of tube evacuated

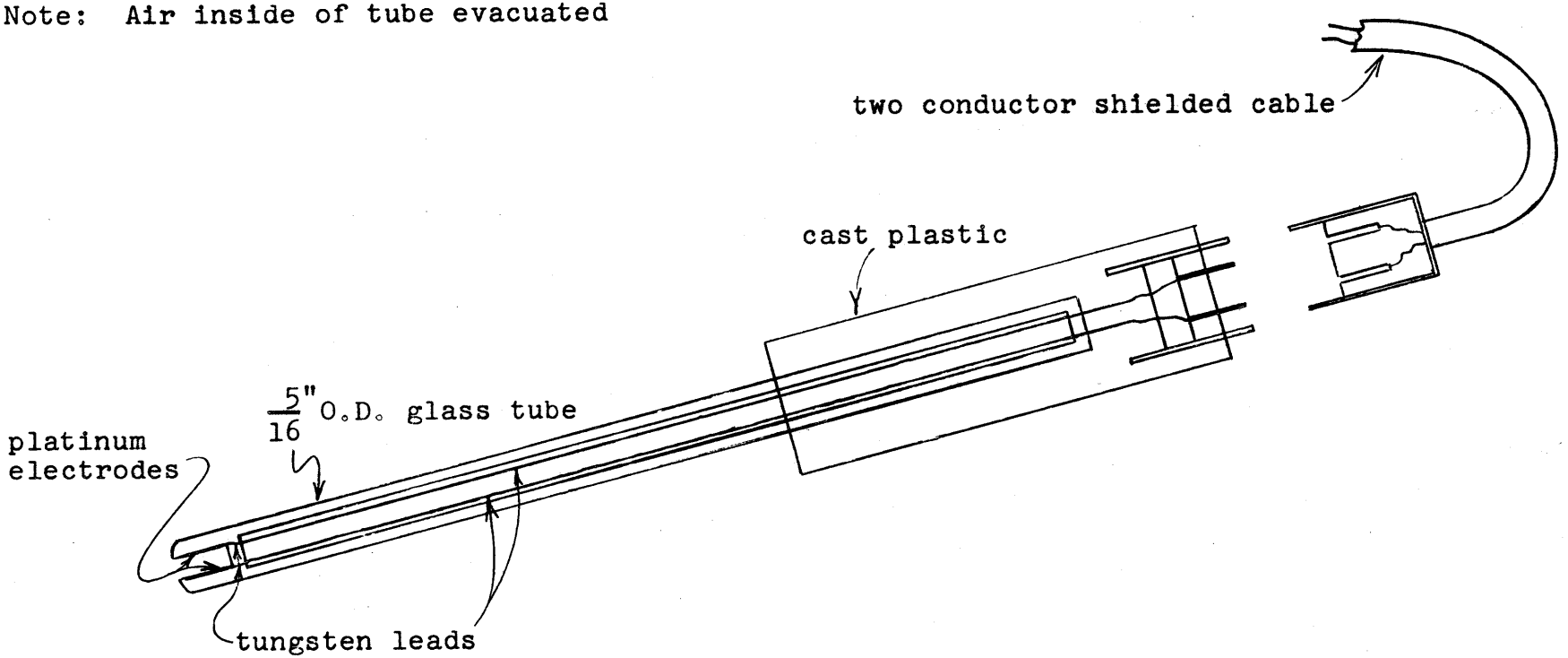

Fig. 8-8: Schematic diagran of conductivity probe

tungsten wires were placed. One end of the tube was formed into a U-shape with a gap of about 1/16" inside the U. Two platinum plates about 1/8" square were welded to the tungsten wires and placed on opposite sides of the inside of the U-shaped tip. The glass tip was then sealed against the back side of the platinum plates, and the glass tube was sealed around the wires at both ends of the tube. The tube was evacuated, and an electrical connector was placed on the tungsten wires. The upper part of the glass tube and the electrical connector were cast into molding plastic for added strength. The platinum plates were given a coat of platinum-black which was renewed about once a month.

Conductivity probes of this type have been used previously in the Hydrodynamics Laboratory (ref. 18, 19), as have probes of other types (ref. 16, 17, 19, 27). The sensing element, i.e., the two platinum plates, were placed inside the U-shaped tip to provide a more direct flow path for the electrical current. This direct path helped to minimize interference between probes and helped to prevent electrical losses to the galvanized pipe in which they were placed.

The glass probes were extremely fragile and had to be handled with great care. A similar probe could have been constructed with a plastic body. However, past experience in the Laboratory has shown that plastic probes are not as stable electrically as the glass ones due to absorption of water by the plastic. It is recommended that some stronger, but non-absorptive, material be investigated for future use. Perhaps a probe could be constructed with a ceramic body.

For salt (sodium chloride) solutions with concentrations less than 2% by weight, the specific conductance of the solution is essentially linearly related to the concentration, for normal temperatures, The conductance [mho] measured by a conductivity probe equals the specific conductance [mho/cm] of the solution divided by the cell constant [1/cm] of the probe. Calibrations such as that shown in fig. 8-9 verified that the probes were linear with concentration in the region of interest. It was found that the cell constants for the probes changed from week to week by as much as 20%. However, the experiments were conducted in such a way that only the relative concentrations at each probe needed to be known. Thus, it was not necessary to know the cell constants.

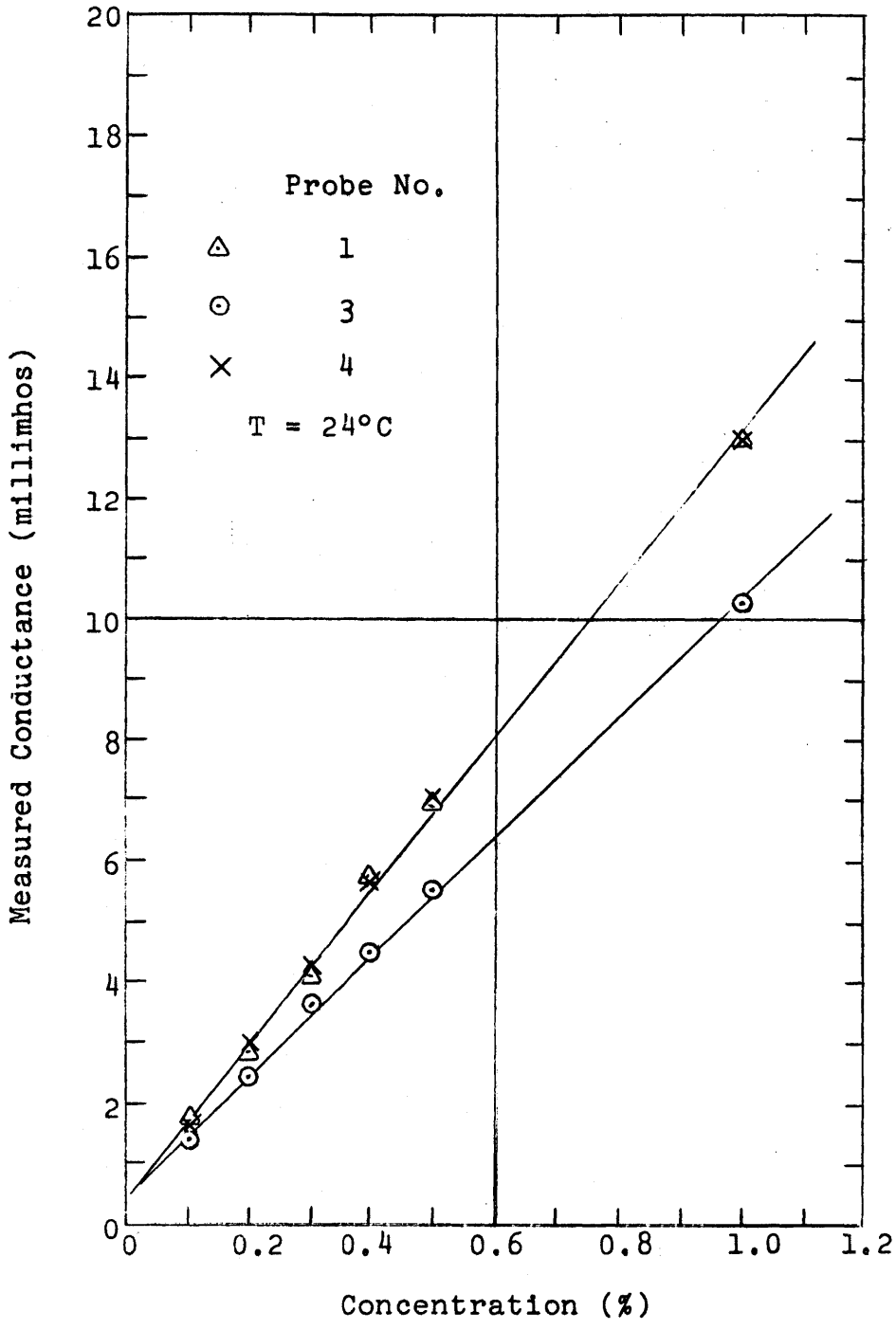

Fig. 8-9: Direct calibration of conductivity probe

As noted above, the probes gave a signal which was linearly related to conductivity. During experiments the signals were read-out on a four channel Sanborn recorder, model 154-100, which responded in a linear fashion to changes in resistance in one leg of a Wheatstone bridge. Thus, as shown in fig. 8-10, the Sanborn recorder did not give a signal which was linear with changing concentrations. By taking into account the electrical circuitry (fig. 8-11) by which the probes were connected to the recorder, it was possible to obtain a modified calibration curve which was linear (fig. 8-12, which is the same calibrations as fig. 8-10).

The probes were found not to be velocity sensitive. For constant salt concentrations between 0% and 5%, it was found that the conductivity of the probes did not change even though the velocity past the probe was varied from 0 to 6 fps.

The probes were placed in the pipe so that the sensing element was on the centerline of the pipe. Also, they were aligned so that the platinum electrodes were parallel to the pipe axis. This means that the U-shaped tips were open to the primary direction of flow and were continually being flushed by the flow.

The tracer (salt) solution was injected into the pipe through a set of the piezometer taps described above. Thus, the salt was introduced at four points around the circumference of the pipe. The salt injector is shown in fig. 8-13. It consisted of a vertical piece of 1-1/2" copper pipe about 6' long. At the bottom of the pipe, there was a 3/4" solenoid valve to which was connected a hose leading to the piezometer taps. At the upper end of the injector, salt solution could be placed into the injector, and the air space above the salt could be pressurized by a hose from the laboratory's central compressed air system. After the injector was pressurized, salt was introduced into the test pipe by a momentary switch connected to the solenoid valve. By using an oscilloscope, it was estimated that the switch was closed for about 20 millisec. For this switching time and with 100 psi air pressure in the injector, about 2.5 cu. in. (41 cc) of salt solution were introduced into the pipe. For an injection time of 20 milliseconds, eqn. 5-27 shows that after one second the concentration distribution is within

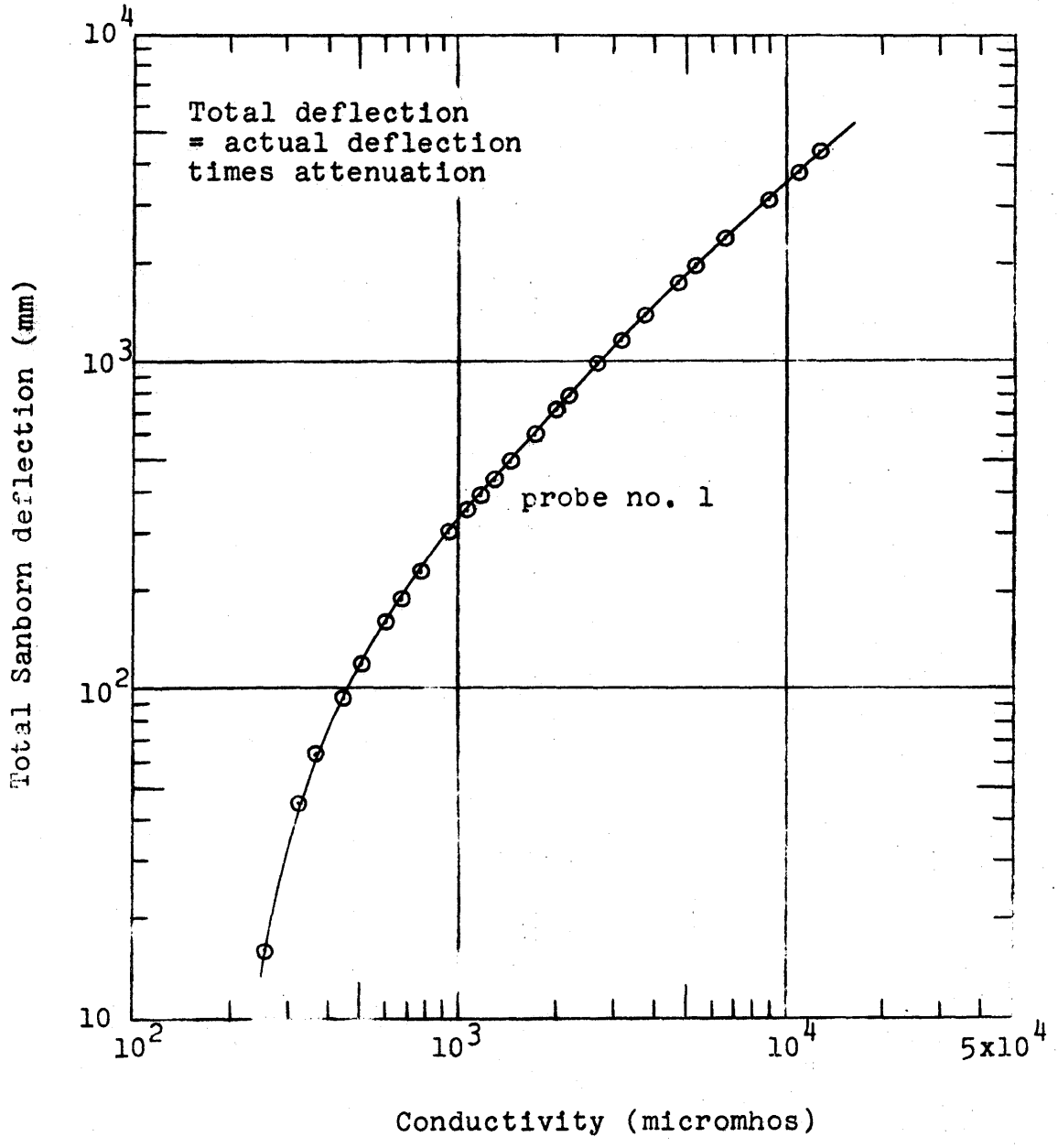

Fig. 8-10: Sanborn calibration of conductivity probe

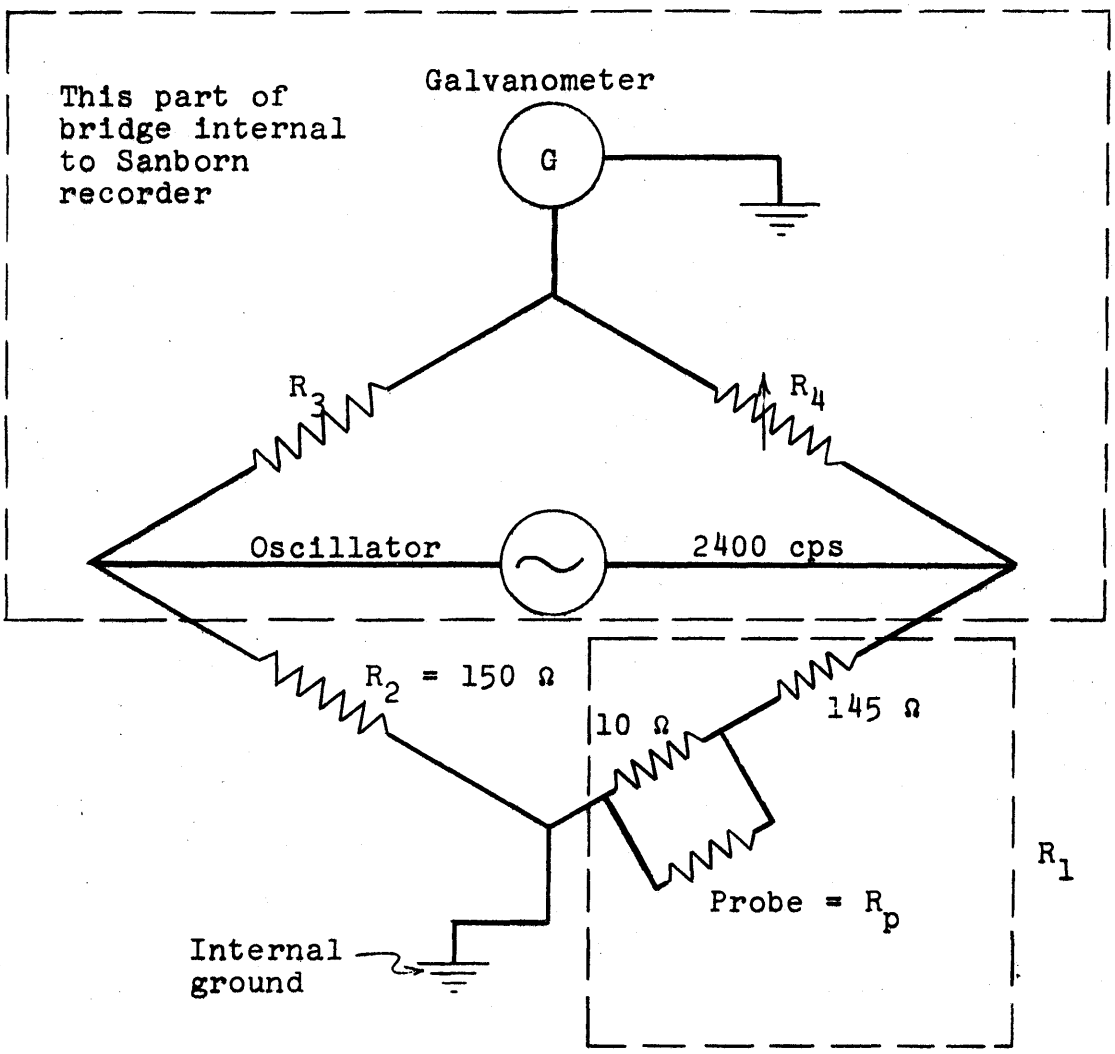

$R_{p_{bal}}$ = Probe resistance when Sanborn is balanced

$$\Delta R_1 = \frac{100\ \Delta R_p}{(10 + R_{p_{bal}})(10 + R_p)}$$

Fig. 8-11: Wheatstone bridge circuit for conductivity probe

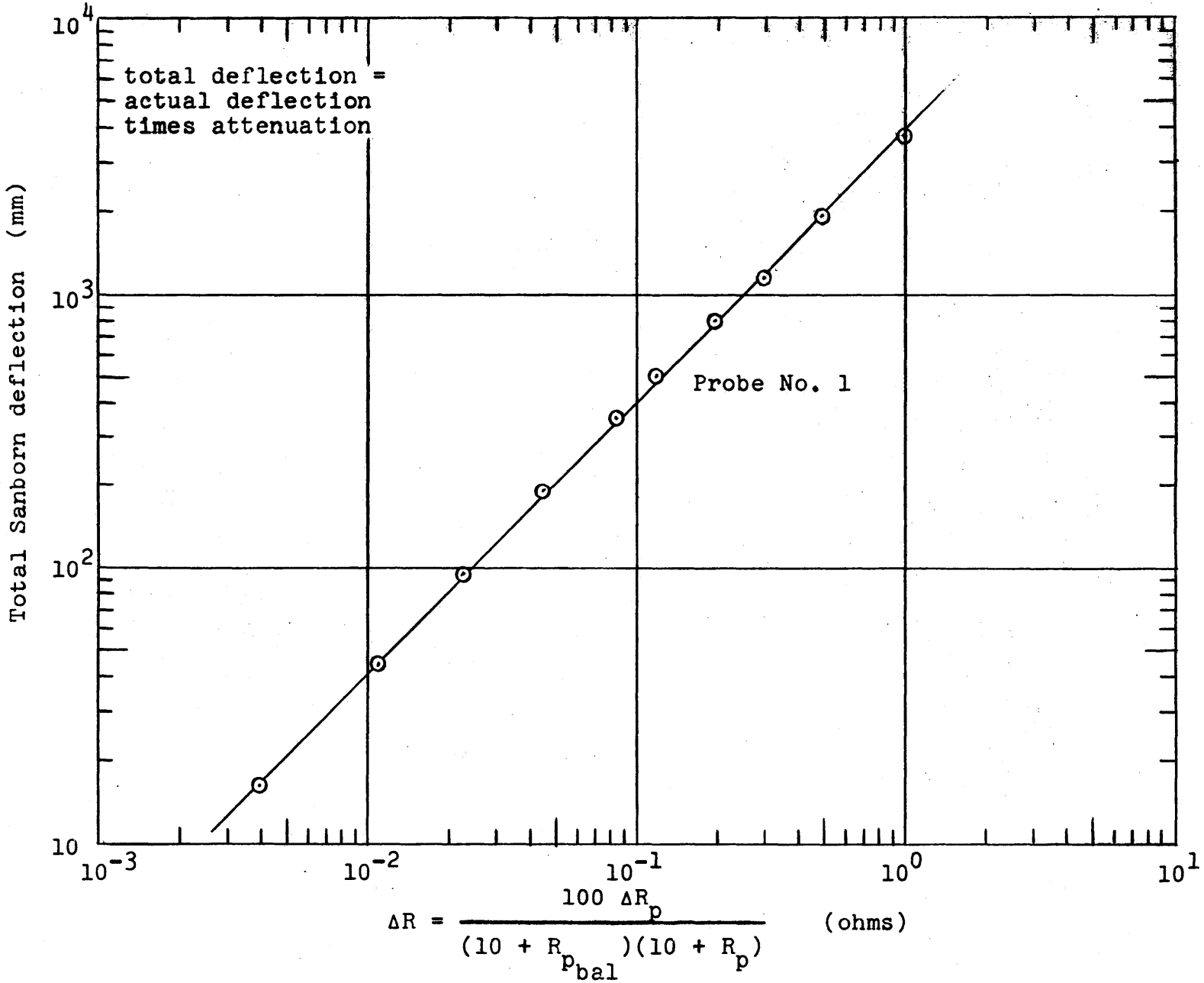

Fig. 8-12: Modified Sanborn calibration of conductivity probe

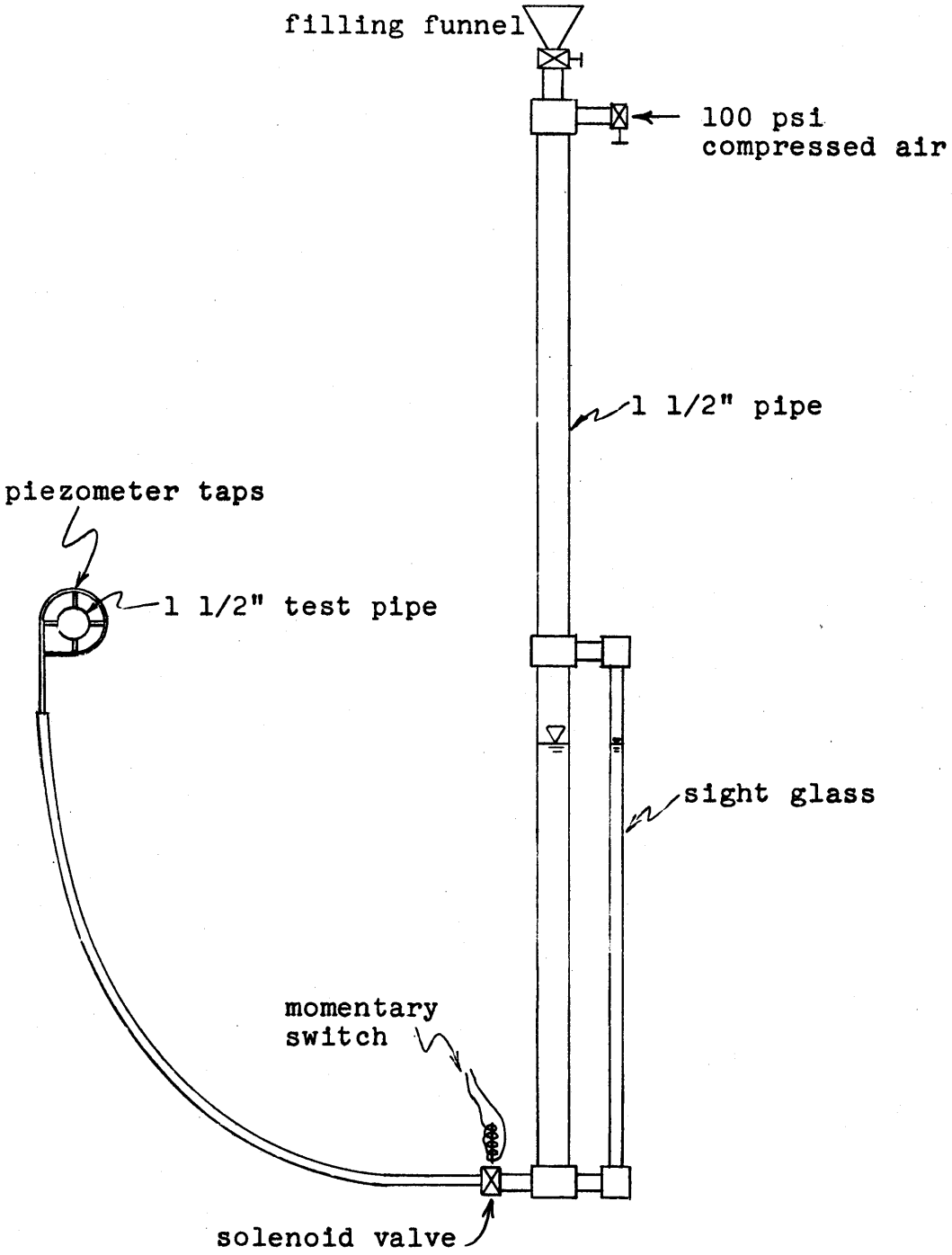

Fig. 8-13: Schematic diagram of salt injector

about 1% of that for a truly instantaneous injection. Thus, it was assumed that this injection was equivalent to an instantaneous injection. It was also assumed that the injection was made uniformly across the section.

8.1.3) Steady Flow

a) Objectives: The steady flow dispersion tests were conducted primarily for checking experimental techniques and methods of analysis of data. The attitude was taken that Taylor's theoretical prediction (ref. 53) of dispersion in steady flow in a pipe is correct. Thus, any technique or method of analysis which did not give results in reasonable agreement with Taylor's theory was considered to be incorrect.

b) Procedures and results: For these tests, salt was injected at P1 and the conductivity probes were placed at M11, M12, M13, and M14. (See Table 8-1 for station coordinates.) Thus, the first probe was 84.94 ft. downstream from the injection point. Typical "raw data" for a steady flow test is shown in fig. 8-14. This is a photograph of the Sanborn recording.

At first, the data was analyzed by taking the rate of change of the second moment (temporal moment) of the concentration distribution to find the dispersion coefficient. The relation between the second moment and the dispersion coefficient for steady uniform flow is given in eqn. 5-16 and 7-6. Typical results are shown in fig. 8-15. Ten runs with velocities from 2.4 to 5.6 ft/sec were analyzed by this method. The results were somewhat scattered, but the dispersion coefficients were consistently about 20% larger than Taylor's expression (eqn. 3-4).

It was mentioned in section 7 that it is necessary to know the entire concentration distribution accurately to use the moments-method of analysis. Elder (ref. 12) pointed out that a laminar sublayer tends to stretch out the upstream part of a concentration distribution. Since the flows in these tests were not in the wholly rough region, a laminar sublayer did exist. The fact

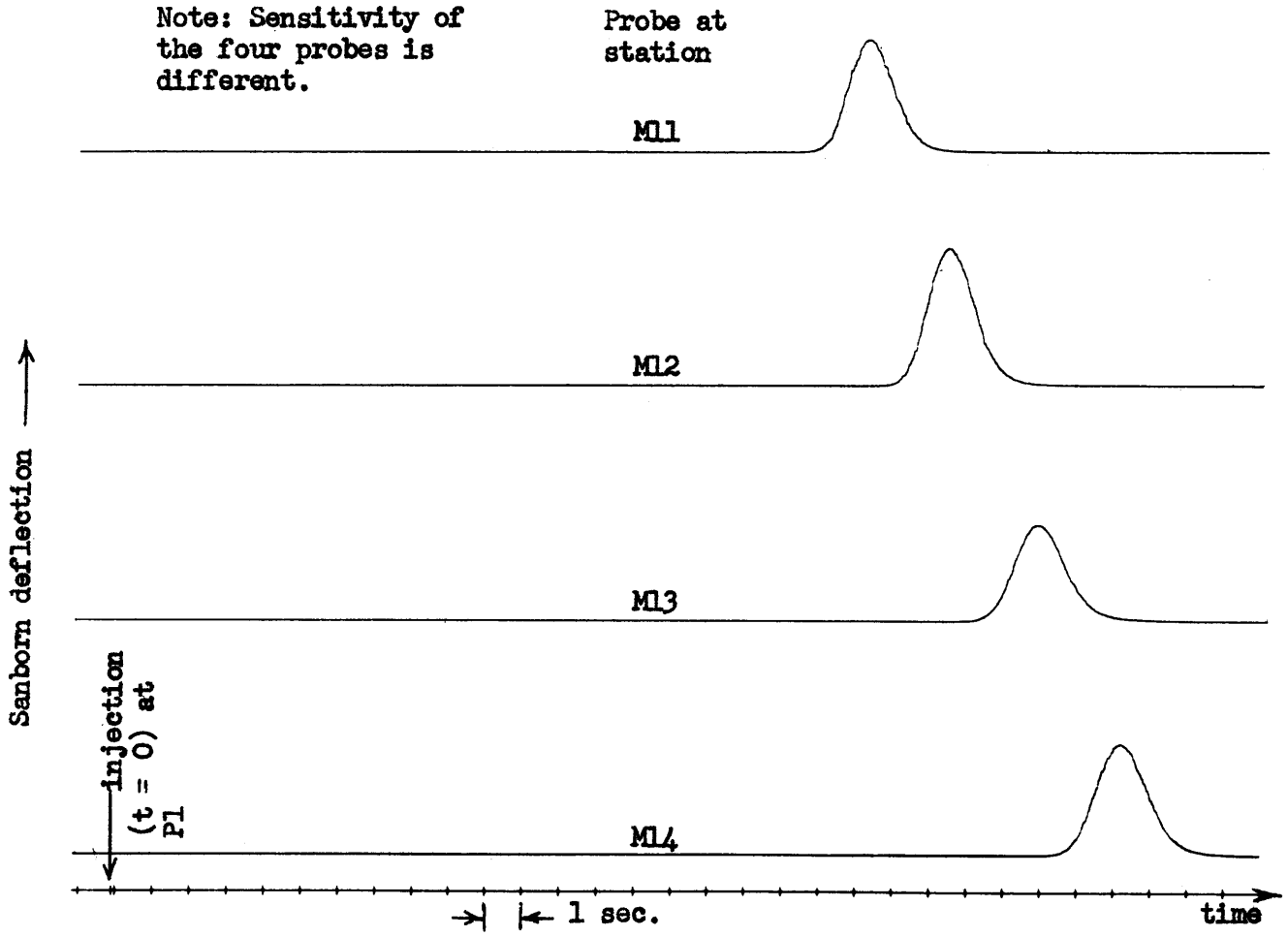

Fig. 8-14: Sanborn recording for a steady flow dispersion test

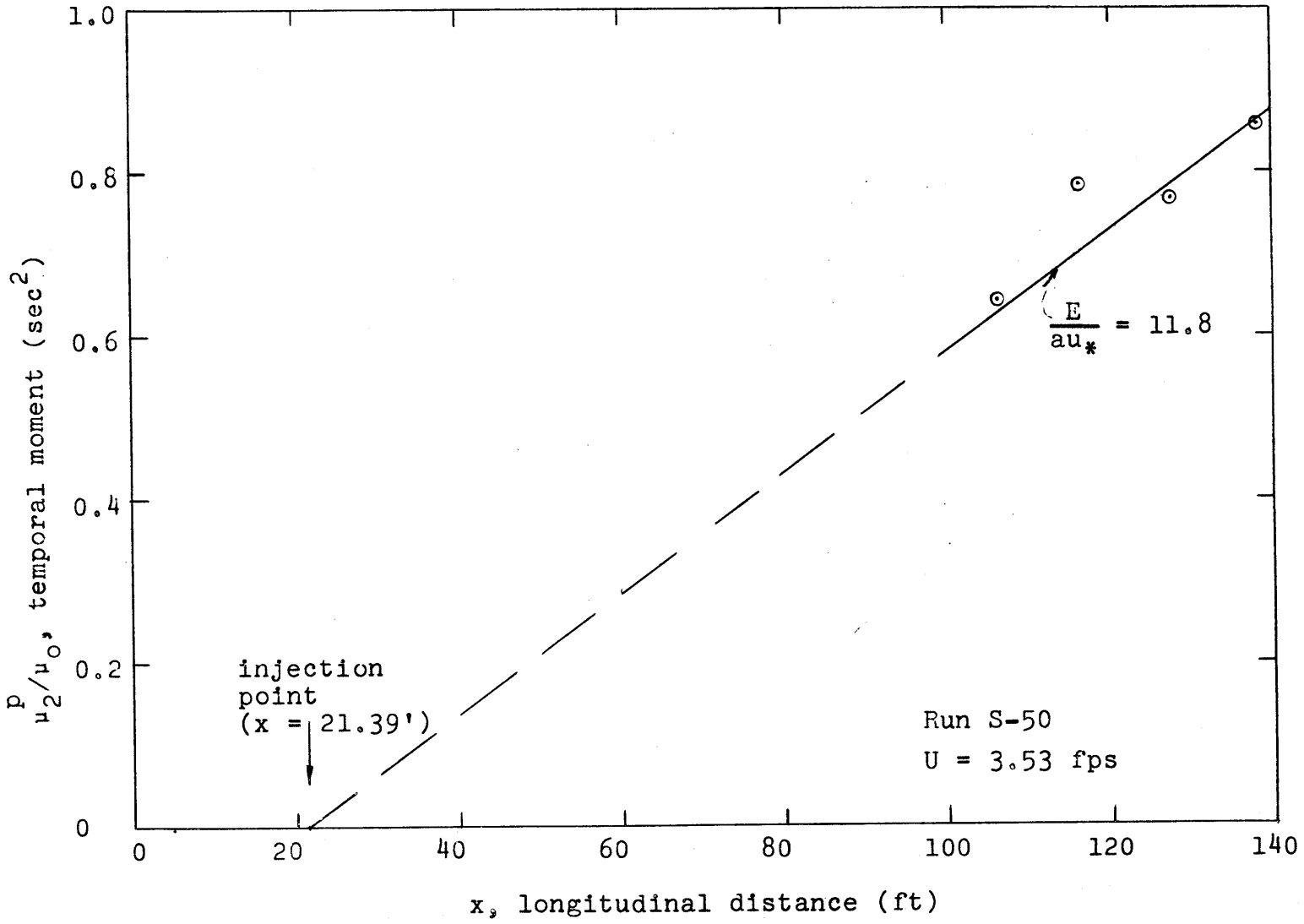

Fig. 8-15: Second temporal moments for a steady flow dispersion test

that the dispersion coefficients were too large was attributed to the effect on the second moment which resulted from the stretched out tail on the concentration distributions.

These same ten runs were next analyzed by the modified semi-log plot, as described in connection with eqn. 7-10. As shown in fig. 8-16, this method gave results which were generally in good agreement with Taylor's analysis (eqn. 3-4). With decreasing Reynolds number, there was an increasing trend for concentrations in the upstream part of the distribution to be higher than those given by the theory. Even for these cases, the dispersion coefficient given by Taylor's analysis gave good agreement with the downstream part of the concentration distributions. Thus, it was concluded that the modified semi-log analysis rather than the method of temporal moments should be used in further analysis. The agreement with Taylor's theory also substantiates the assumption that the salt was injected instantaneously and uniformly across the section.

For all of these ten tests which have just been discussed, 5% salt solution was injected with 100 psi air pressure in the injector. Next, the effects of varying the salt concentration and the air pressure in the injector were investigated. For salt concentrations from 1% to 20% and for air pressure from 20 psi to 100 psi, no consistent variation in the results could be detected. Thus, it was decided to use 5% salt and 100 psi in the remainder of the tests since this gave a signal from the conductivity probes which could easily be read on the Sanborn recorder.

c) Discussion of results: The results obtained for steady flow dispersion in the laboratory pipe line were generally in good agreement with Taylor's analysis (eqn. 3-4). The agreement was better at higher Reynolds numbers. The tests also show that concentrations in the upstream half of the concentration distribution were higher than predicted by the theory for an instantaneous injection (eqn. 5-6). This difference between theory and experiment was noticed by Elder (ref. 12). He attributed it to the influence of the laminar sublayer which was not included in the analysis. If this is the cause, then the difference between theory and experiment should

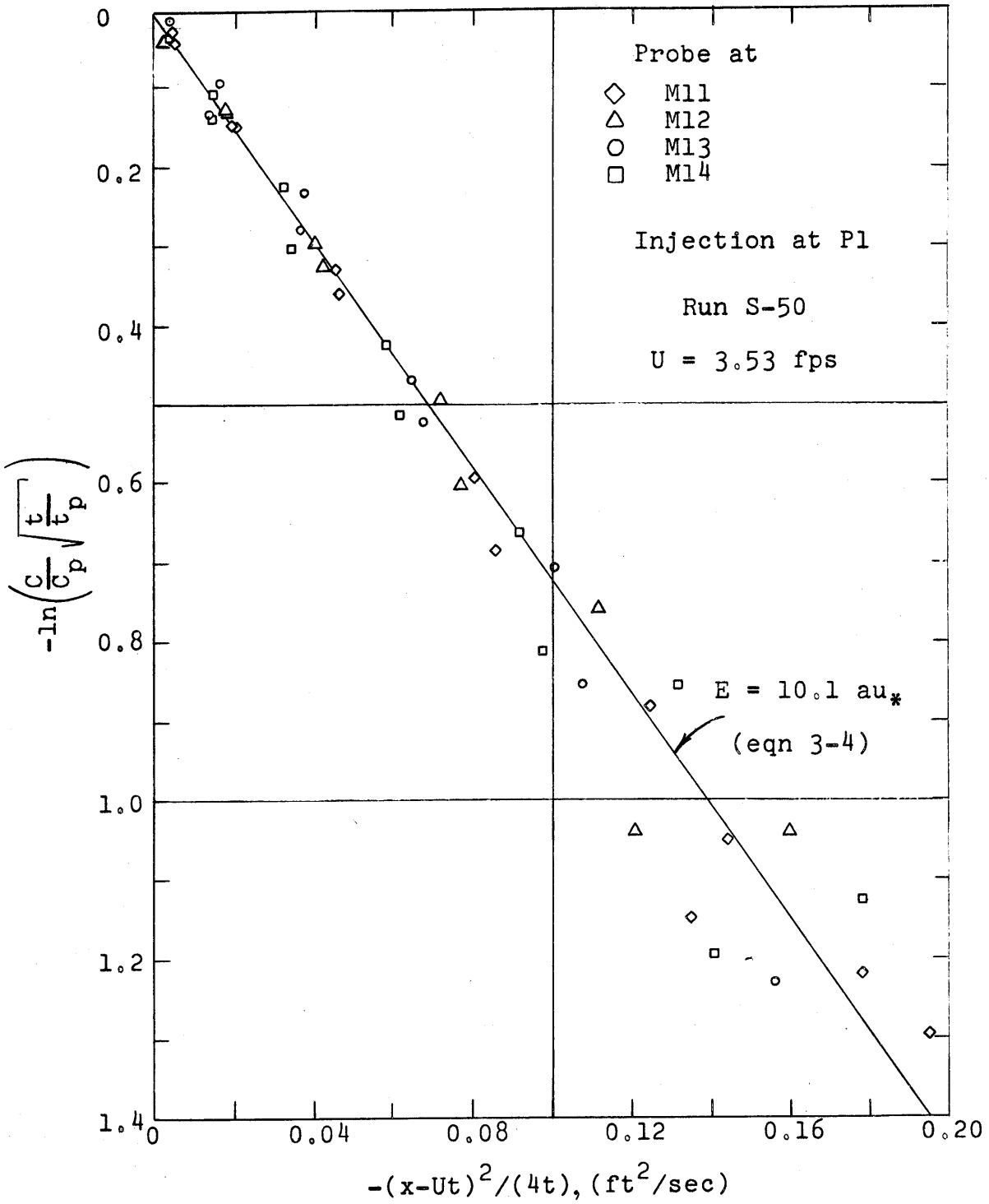

Fig. 8-16: Modified semi-log plot for a steady flow dispersion test

reduce as the sublayer thickness decreases (i.e., as the Reynolds number increase for a given relative roughness). For experiments made in the wholly rough region, there is no laminar sublayer so there whould be excellent agreement between theoretical and experimental concentration distributions.

Experimental results shown in fig. 8-17 are consistent with these trends. The experiments which are a part of the present work were conducted in the transition range between hydraulically smooth and wholly rough. Fig. 8-17 shows the upstream half of the concentration distribution for three of these experiments. The experimental concentrations are consistently higher than the theory, but the agreement between theory and experiment improves as the Reynolds number increases. Also, data from an experiment made in a rough pipe scatters about the theoretical line and shows no consistent tendency to be higher than the theory. The data for the rough pipe was taken from fig. 10 of Taylor's paper (ref. 53). This experiment was conducted in a 3/8" dia. pipe at a velocity of 146 cm/sec. The roughness was such that U/u_* was 6.73.

For the present work, the limits of the experimental equipment would not allow the Reynolds number to be increased enough to obtain flow in the wholly rough region. It would be helpful if a systematic set of experiments could be conducted in the hydraulically rough region of Reynolds numbers to further investigate the agreement between theoretical and experimental concentration distributions. However, on the basis of the evidence at hand now, it seems that Elder's explanation is correct and that the presence of a laminar sublayer does influence the concentration distribution. In section 3, it was noted that the sublayer effectively increases longitudinal dispersion over that indicated by Taylor's analysis. For run S-27 (as shown in fig. 8-17), a dispersion coefficient 31% higher than that given by Taylor's analysis is necessary to describe the experimental points in the upstream part of the distribution.

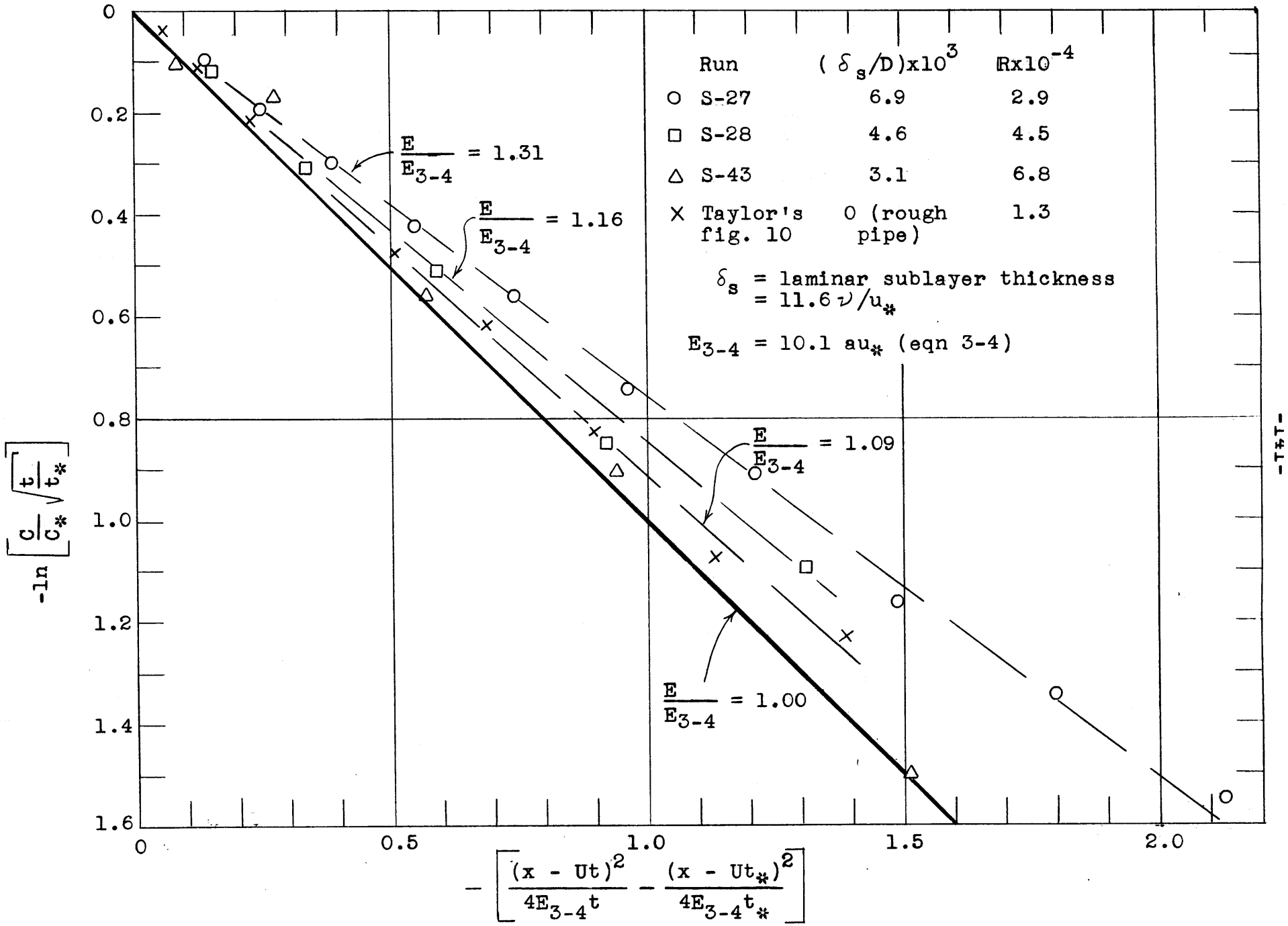

Fig. 8-17: Effect of laminar sublayer on dispersion coefficient in steady flow

8.1.4) Estuary Type Flow Tests

a) Objectives: The objective of the experiments in estuary type flow was to obtain a mean velocity in the pipe which followed the form

$$U = U_f + U_T \sin \sigma t \qquad 8\text{-}1$$

and to study longitudinal dispersion in this type of flow. In this expression, the U's are one dimensional velocities, U_f and U_T are independent of space and time, σ is the frequency of oscillation (i.e., $2\pi/T$ where T is the period), and t is time.

b) Procedures: U_T was determined from the eccentricity of the piston drive, the cylinder-to-pipe area ratio, and the period of oscillation. In more detail, the eccentricity (e) of the piston drive was measured. The stroke of the piston was equal to 2e. The excursion of the water in the pipe was equal to 2e times the area of the cylinder ($A_c = 0.785$ ft^2) divided by the area of the pipe ($A_p = 0.01414$ ft^2). The oscillating velocity averaged over a half cycle is the excursion divided by T/2. Since the amplitude of a sine wave is $\pi/2$ times the average over a half period, U_T is given by

$$U_T = \frac{\pi}{2} \left(\frac{2e\, A_c/A_p}{T/2} \right) = \frac{2\pi\, e\, A_c}{T\, A_p} \qquad 8\text{-}2$$

T was determined by a limit switch on the piston rod and the Sanborn recorder. A momentary micro-switch was attached to the piston rod so that it switched at the upstream limit of the excursion. The switch was then connected to the timing marker on the Sanborn recorder. The recorder also provided one-second marks on the timer. Thus, it was possible to find the period T.

U_f was determined gravimetrically. The float switch in the downstream tank activated the solenoid drain valve once each period as the water level in the tank rose due to the displacement of water by the piston. Since no water was being added to the system by the oscillating flow, the amount of water drained off each period was

equal to the through flow rate (Q_f) times the period. For each experiment which was made, this water was collected over three sets of 20 periods each and weighed to find Q_f. These values of Q_f were then averaged and divided by the pipe area to obtain U_f.

In all runs, 5% salt solution was injected at P1 at the time of the upstream limit of the excursion in the pipe. The injection was in the manner previously described for the steady flow tests and was assumed to be an instantaneous point injection. Since the injection was at the limit of the excursion, the oscillating component of the velocity was zero at the time of injection. In section 8.1.3b, it was pointed out that there were no noticeable density effects present in the steady flow experiments even with injection concentrations greater than 5%. Also in these tests in estuary type flow, density effects were negligible even though the injection concentration was 5%. The concentration of the tracer in the pipe line was much lower than 5% (of the order of hundredths of a percent) due to the dilution associated with longitudinal dispersion. Also, the lateral turbulent mixing in the pipe helps to suppress longitudinal spreading of the tracer due to density effects.

A photograph of the Sanborn record for an estuary type test is shown in fig. 8-18. Normally, the recorder paper was run at least five times as fast as that shown in the figure. Also, the one-second marks were omitted on this record. Notice that the attenuator setting was changed from time to time during the run. The total signal to the recorder was proportional to the measured deflection of the recorder pen multiplied by the attenuation.

In the section on experimental determination of dispersion coefficients, it was pointed out that concentration data could be taken at one period intervals in estuary type flow. Then, the data could be analyzed by the modified semi-log plot applied to eqn. 6-35 or 6-47. As was pointed out, it must be remembered that the dispersion still depends strongly on U_T, not U_f assuming that U_f is much less than U_T. It was also shown that if the data is taken at the time of zero oscillating velocity, then the dispersion coefficient which is found is the average value of the dispersion coefficient during a period.

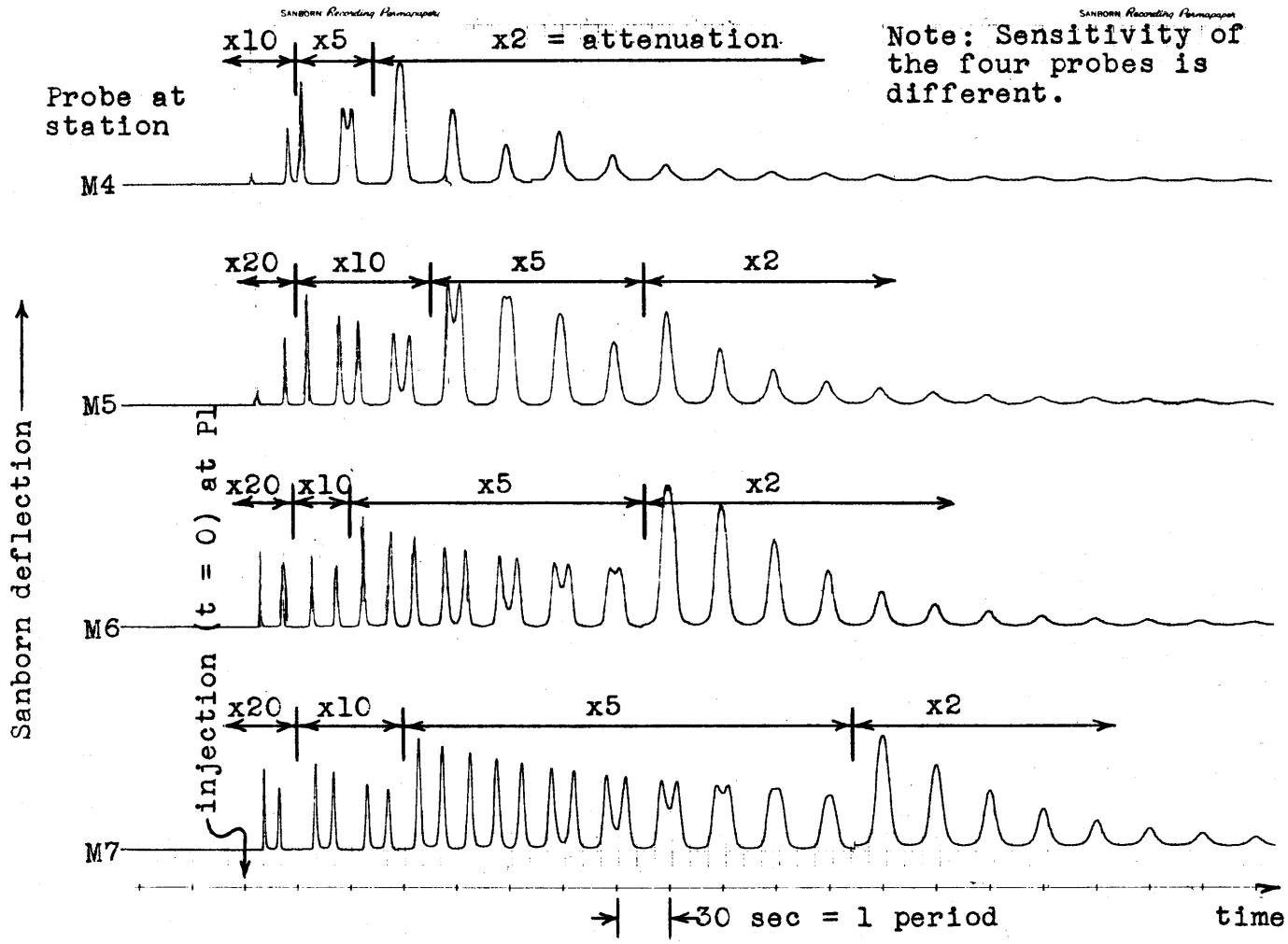

Fig. 8-18: Sanborn recording for an estuary type flow dispersion test

c) Results: The dispersion tests were analyzed by reading the concentration data at time increments of one period after the injection of the salt. Some data was also read for the half periods as well as the whole period. In either case, this selected data was analyzed by the modified semi-log plot. One such plot is shown in fig. 8-19. All of the results are tabulated in appendix E and are shown in fig. 8-20. In fig. 8-21, the experimentally observed dispersion coefficients ($E_{A_{obs}}$) are compared with the values ($E_{A_{calc}}$) calculated by eqn. 6-25. This comparison is discussed below.

No correlation was found between $E_{A_{obs}}$ and U_f. This was expected, as has been mentioned in sections 3.3 and 6.

Eqn. 6-35 predicts that the maximum concentration will decrease as $t^{-1/2}$ after an instantaneous injection into estuary type flow. The rate of decrease of the maximum concentration was checked for two runs (P-22 and P-23) and found to agree with the theory. The data for one of the runs is shown in fig. 8-23. Eqn. 6-35 also predicts that the maximum concentration will pass a fixed x at times given by

$$x - U_f t_p + \frac{U_T}{\sigma} (\cos \sigma t_p - 1) = 0 \qquad 8\text{-}3$$

for $\delta = 0$. For the same two runs, this equation was solved graphically for t_p and compared with the observed concentration distribution. Again, the agreement was good, as shown in fig. 8-22. The time t_p as given by eqn. 8-3 is controlled solely by the one-dimensional convection. The maximum concentration on a temporal distribution will actually occur slightly before t_p of eqn. 8-3 due to dispersion as the tracer is passing the measurement station. This was pointed out for steady flow in eqn. 5-8 and fig. 5-2.

Fig. 8-22 shows that the approximation made in using t_p from eqn. 8-3 does not lead to significant errors.

d) Discussion: For an instantaneous injection of tracer into estuary type flow, eqn. 6-35 adequately represents the one-dimensional concentration distribution as a function of space and time.

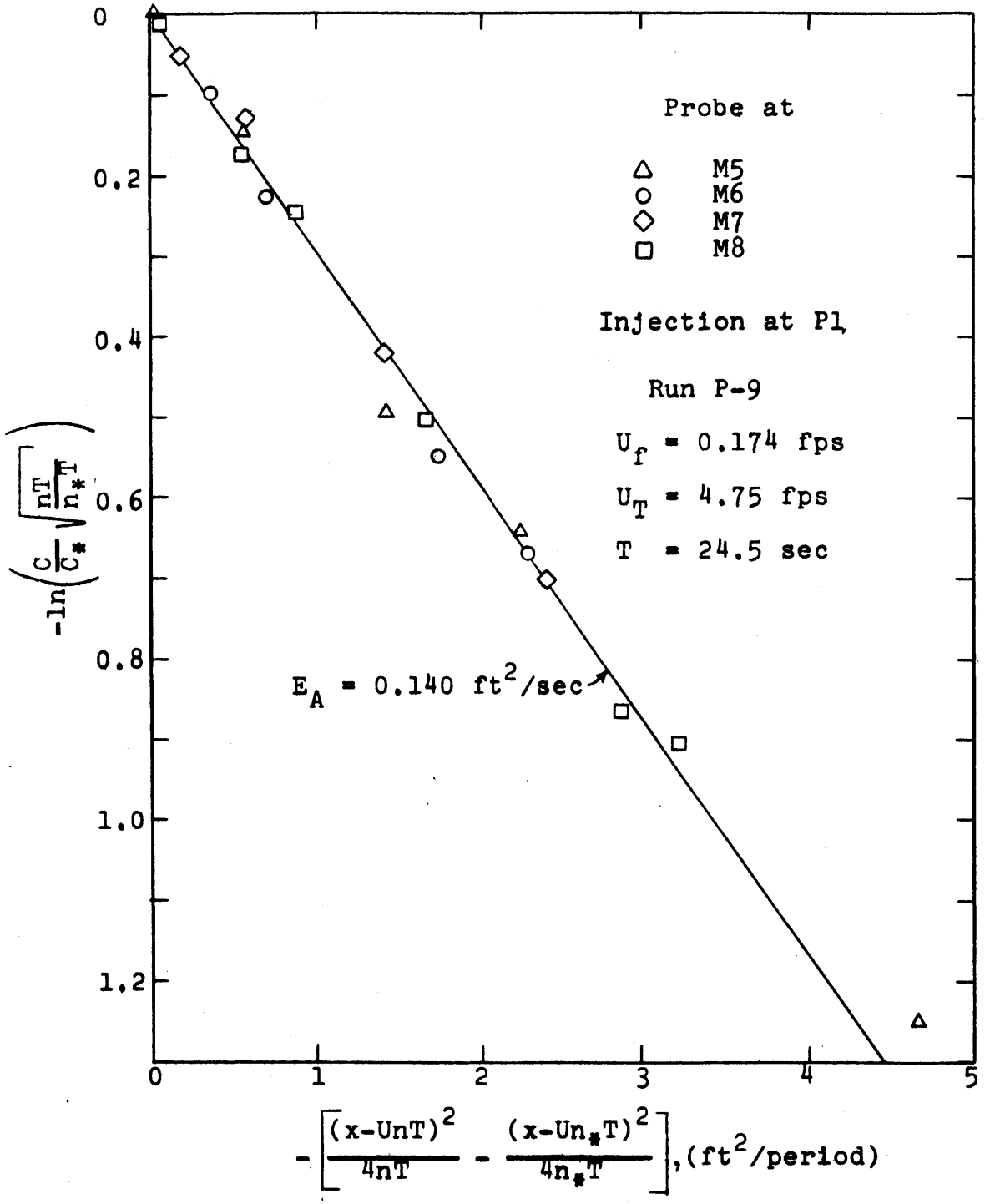

Fig. 8-19: Modified semi-log plot for an estuary type flow dispersion test

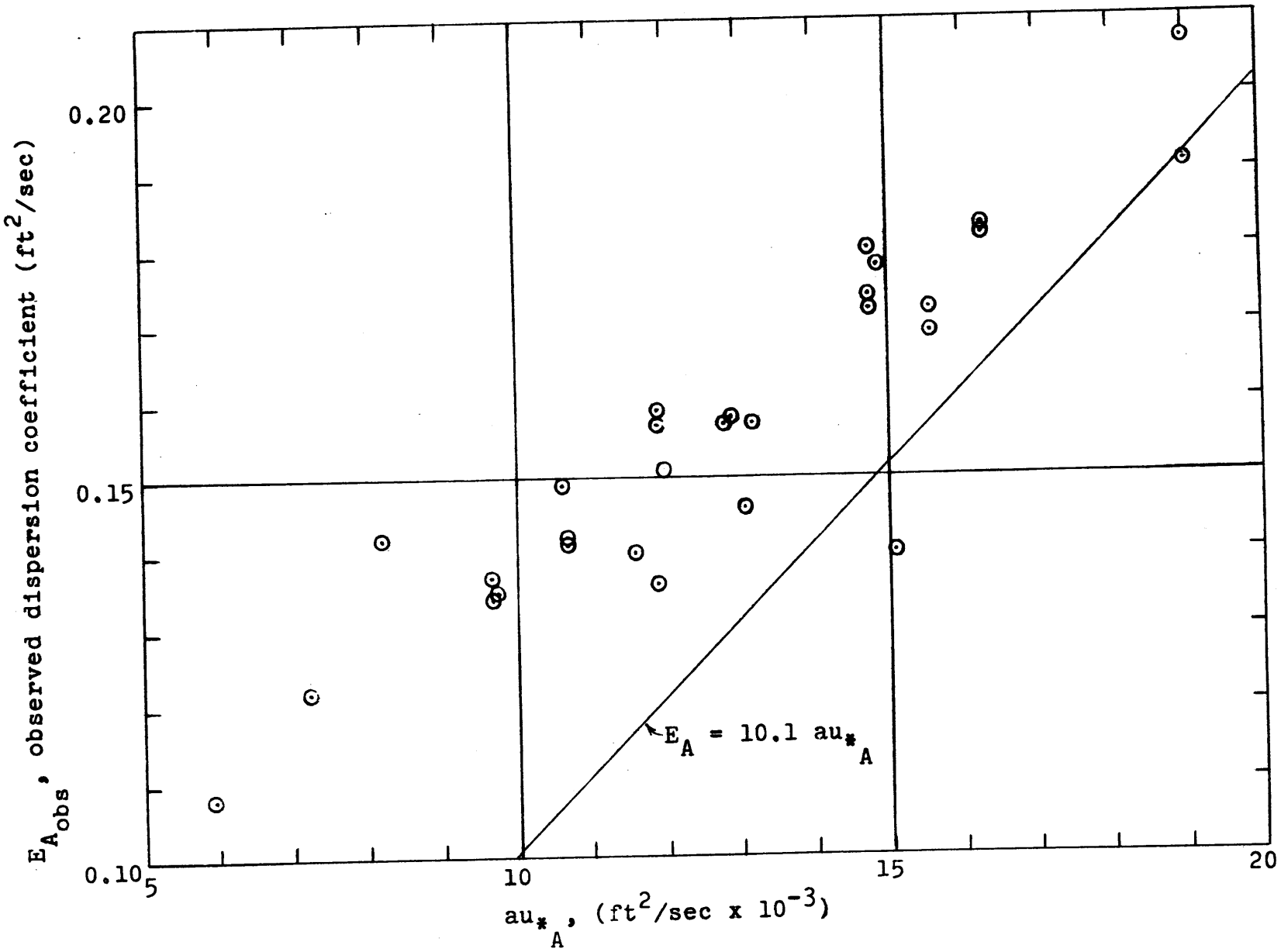

Fig. 8-20: Dispersion coefficients for estuary type flow

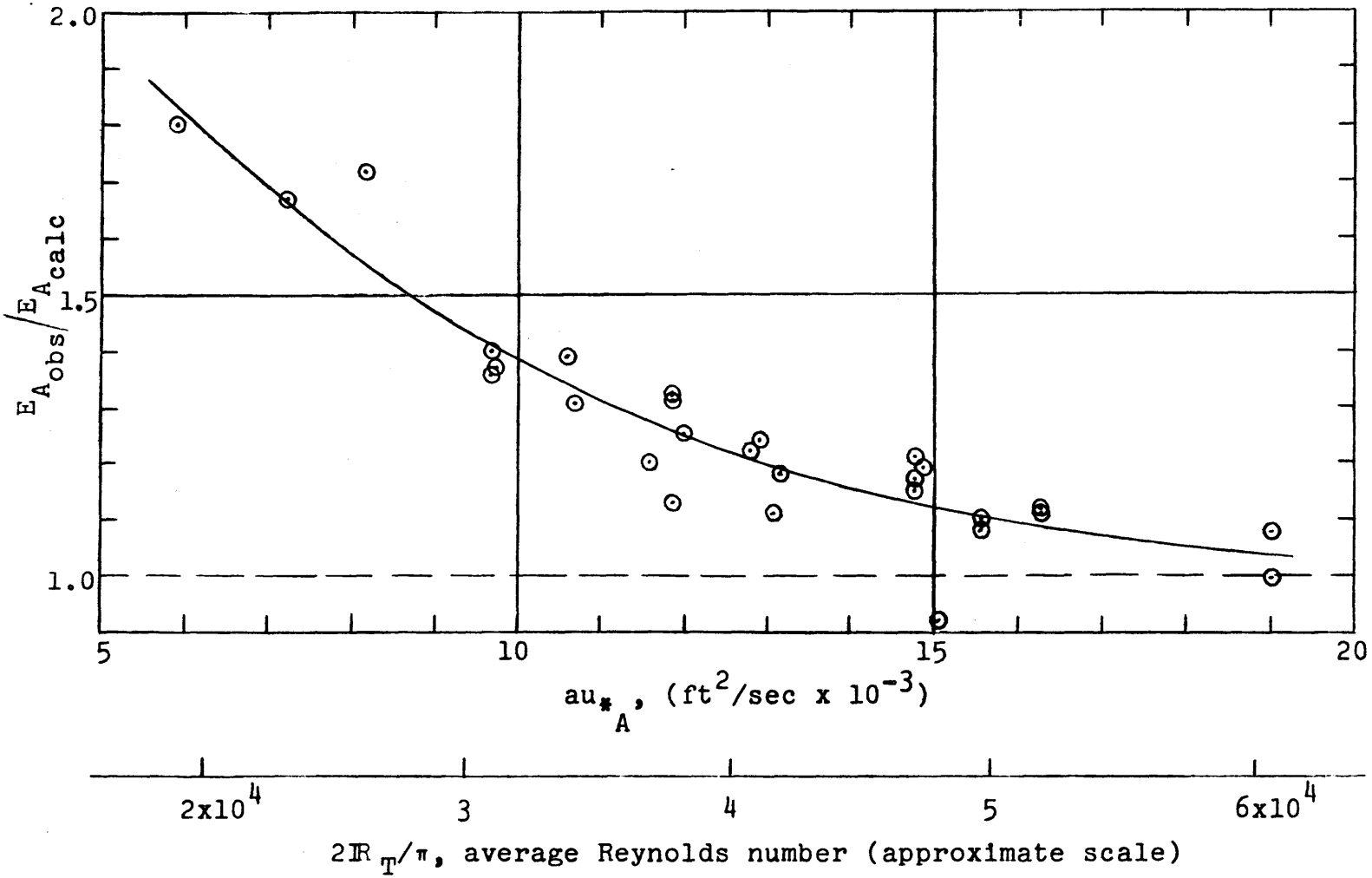

Fig. 8-21: Comparison of observed and calculated dispersion coefficients for estuary type flow

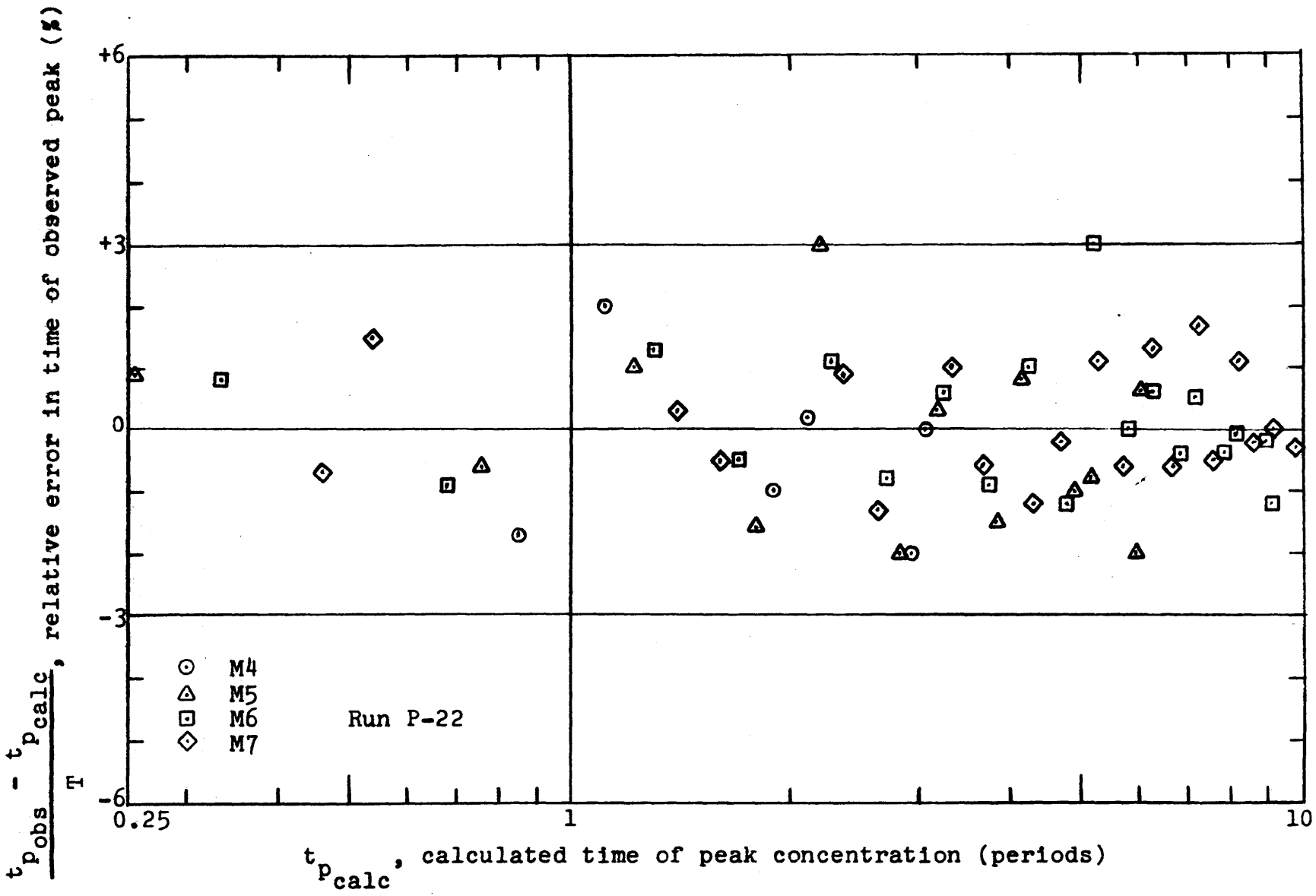

Fig. 8-22: Error in time of occurrence of peak concentration in estuary type flow

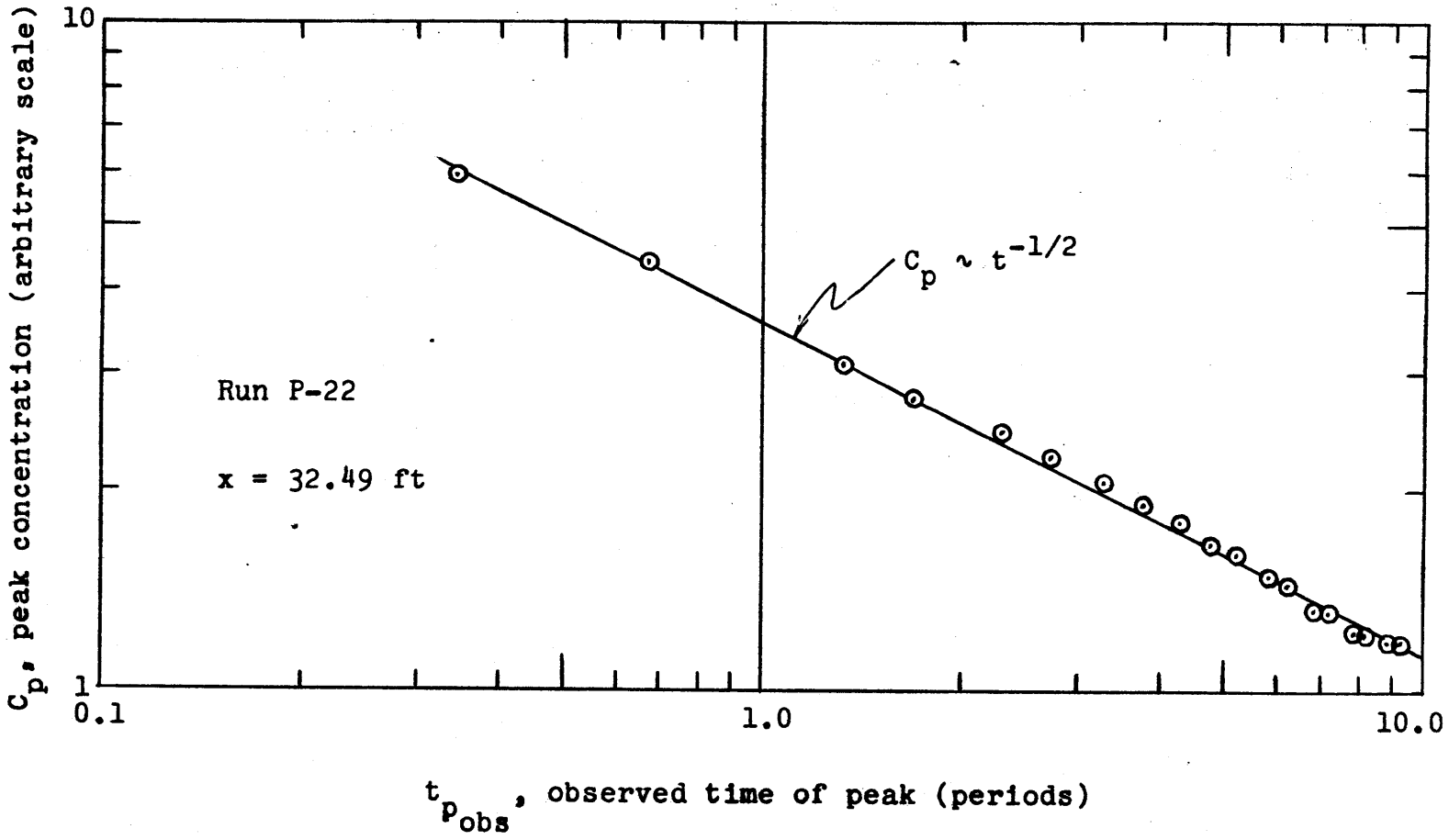

Fig. 8-23: Temporal decrease in peak concentration in estuary type flow

The validity of this equation was borne out by the modified semi-log plots used in analyzing the data, by the rate of decrease of the maximum concentration, and by the time of occurrence of the maximum concentration at a given station.

Fig. 8-21 indicates that agreement between dispersion coefficients calculated by eqn. 6-25 and experimental dispersion coefficients decreases as the average Reynolds number decreases. It is believed that this lack of agreement is due to the influence of the laminar sublayer which was not included in the analysis that led to eqn. 6-25. The lack of agreement can not definitely be attributed to the viscous sublayer until a more complete analysis is made so as to include the effects of the sublayer or until experiments are conducted in a hydraulically rough pipe. However, the following observations tends to indicate that the sublayer may be responsible for the lack of agreement.

The average Reynolds number (and the relative roughness) for all the tests with estuary type flow were such that the flow was in the transition range between hydraulically smooth and rough. Thus, a laminar sublayer was present. For the steady flow experiments, it was observed that the concentrations in the upstream part of the concentration distribution were higher than predicted. This was attributed to the sublayer. For estuary type flow, as the concentration distribution moves up and down the pipe, alternate ends of the distribution are effectively "upstream" during the forward excursion and during the return excursion. Thus, concentrations in both ends of the distribution might be expected to be higher than predicted from using the analytically obtained dispersion coefficient. Due to the reversing flow, the sublayer thus has a double opportunity to increase the longitudinal spread or dispersion. Also, in the steady flow tests, the tracer moves a total of about 100 ft. during an experiment. In the estuary type flow with an excursion of 40 ft., the tracer travelled 800 ft. during 10 periods. (The 40-ft. excursion and 10-period length of experiment represent an approximate average for the tests which were made.) Thus, the estuary type flow would again seem to have an increased opportunity for the effects of the sublayer to be felt. Finally, notice that for steady flow experiment S-27 at a

Reynolds number of 2.9×10^4, it was pointed out in connection with fig. 8-17 that a dispersion coefficient 31% higher than the predicted value was needed to describe the upstream portion of the concentration distribution. For estuary type flow, the experimental dispersion coefficient was 35% higher than the predicted value at an average Reynolds number of 3.0×10^4. The agreement between the 31% and the 35% indicates that for the steady flow and estuary type flow tests there is some degree of consistency in the general order of magnitude of non-agreement between experiment and analysis. Thus, it appears that the laminar sublayer may be responsible for this difference in estuary type flow as well as in steady flow. However, a firm answer as to the influence of the viscous sublayer must come from a more complete analysis which includes this influence and/or from experiments where no sublayer is present.

For estuary type flow there is a possibility that a reversal might take place in the velocity profile. In the analysis a smooth profile was assumed as shown in fig. 8-24a. If reversal were to occur, it would be because the period of oscillation was too small compared to the time required for turbulent diffusion of momentum to take place across the flow section. Let the period, T, be a characteristic time for the oscillation, and let $a^2/\bar{\bar{\epsilon}}_A$ be a characteristic time for lateral momentum diffusion (a = pipe radius, $\bar{\bar{\epsilon}}_A$ = lateral coefficient of turbulent diffusion of momentum, i.e., eddy viscosity averaged across the pipe and averaged during the period). If $T/(a^2/\bar{\bar{\epsilon}}_A)$ is large, i.e, if the period is long relative to the lateral diffusion time, no reversal would be expected to occur. For the present experiments taking $\bar{\bar{\epsilon}}_A = \frac{1}{15} a u_{*_A}$ where u_{*_A} is the average shear velocity during a period, this ratio was between 3 and 5 for all tests. Although not conclusive, this tends to indicate that no reversal took place.

Schultz-Grunow (ref. 50) measured velocity profiles in oscillatory flow in a 5.0 cm (1.97 in.) dia. pipe where the mean velocity was given approximately by

$$U = U_f + U_T \sin \sigma t$$

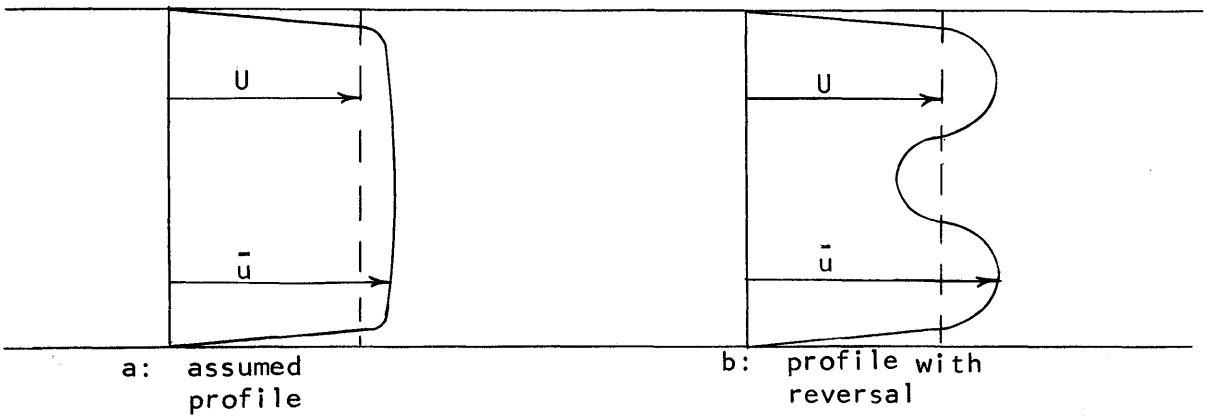

Fig. 8-24: Possible velocity profiles in estuary type flow in a pipe

---

but where U_f was greater than or equal to U_T. Thus, the velocity U never changed signs as it did in the present work. For T = 30 sec. and U_T = 58 cm/sec (1.9 ft/sec), no reversal was found in the velocity profile. This corresponds to a Reynolds number based on $\frac{2}{\pi} U_T$ of roughly 2×10^4, which is in the general range of the present experiments. Hence, this is another indication that probably no reversal existed in the velocity profile.

Again, if $T/(a^2/\bar{\bar{\epsilon}}_A)$ is taken as being characteristic of the degree of reversal in the velocity profile, then reversal can not account for the difference between the predicted and the experimental dispersion coefficients. Neglecting the small changes in the friction factor with changing Reynolds number, u_{*_A} is a constant fraction of U_T. Thus, $T/(a^2/\bar{\bar{\epsilon}}_A)$ is proportional to TU_T which is proportional to the fluid excursion during an oscillation. Thus, for a constant excursion, $T/(a^2/\bar{\bar{\epsilon}}_A)$ was approximately constant; thus, the degree of reversal, if any, should be constant. Yet, for a constant excursion, the ratio of the observed to the predicted dispersion coefficients varied from 1.08

to 1.80.

The analysis of appendix B and section 6 led to eqn. 6-25 and -26 for predicting the average dispersion coefficient in estuary type flow in a pipe. In this analysis it was assumed that turbulent flow existed throughout the period of oscillation. However, as the velocity approaches zero during each period, the instantaneous Reynolds number necessarily falls below the critical value (say 2000) above which turbulent flow exists. During the part of the period for which the instantaneous Reynolds number is less than 2000, it should be expected that the velocity distribution and lateral diffusion would be different from that assumed in the analysis. Also, the percentage of the period during which this difference existed would increase as the average Reynolds number decreases. Thus, this may help to account for the divergence between the observed and the predicted dispersion coefficients. The lowest average Reynolds number for the present experiments was 1.88×10^4 and at this Reynolds number there was an 80% difference between predicted and observed dispersion coefficients. During this experiment, the instantaneous Reynolds number was less than 2000 for about 4% of the period. It is difficult to conceive that variations during 4% of the period could fully account for an 80% difference between prediction and observation.

Whatever the cause of the disparity between predicted and observed values, this disparity decreases as the average Reynolds number increases. Thus, at the larger average Reynolds numbers and probably for hydraulically rough flow at the smaller average Reynolds numbers, eqn. 6-25 adequately predicts the average dispersion coefficient for estuary type flow in a pipe.

8.2) Estuary Model Experiments

It was pointed out previously that most of the studies of mass transport problems for estuaries have been conducted in distorted Froude models and that the interpretation of these model results has been incorrect for the fresh water portion of estuaries. Thus, there is no known data available for investigating the effects of non-uniformities in natural estuaries. However, the data for the

models may be used in model scale to investigate these effects.

The Corps of Engineers model of the Delaware estuary is constructed with a vertical length ratio (Y_r) of 1:100 and a horizontal length ratio (L_r) of 1:1000. Extensive studies have been made in this model. (Ref. 2-6, 21, 28, 30, 31, 35, 42, 43.) In particular, in ref. 5 some spatial concentration distributions were measured after an instantaneous, point injection of dye. The dye was injected at high water slack and the measurements were made at high and low water slack. The data tabulated in Tables IX-19, -20, and -21 of ref. 5 was taken for mean tide conditions and for fresh water flow rates of 3.4×10^{-3}, 7.0×10^{-3}, and 12.35×10^{-3} cfs. This gives mean velocities of 0.0046, 0.0096, and 0.017 fps at the point where the dye was released. For the mean tide, the maximum tidal velocity (U_T) is 0.22 fps and the average hydraulic radius (R_H) is 0.21 ft. (ref. 2, 29). From these values and by writing eqn. 6-25 in terms of the hydraulic radius, a dispersion coefficient could be calculated for the model if some information were available on the roughness of the model. Unfortunately, the roughness has apparently not been measured for the model. However, some approximate values may be assumed for Manning's n in order to get some idea of how the analysis compares with the data.

If f is the Darcy-Weisbach friction factor, then

$$u_{*_A} = \sqrt{\frac{f}{8}} \left(\frac{2}{\pi} U_T \right)$$

and

$$f = 116 \frac{n^2}{R_H^{1/3}}$$

For $n = 0.015$, $E_A = 0.044$ ft^2/sec is found from eqn. 6-25 (with $a = 2R_H$), and for $n = 0.025$, $E_A = 0.073$ ft^2/sec. These two values of probably bracket the actual value for the model. Note also that this calculation assumes that the amplitude of the tidal velocity and hydraulic radius are not functions of the longitudinal coordinate.

For the reported concentration data, values of E_A from

0.073 ft^2/sec to 0.083 ft^2/sec were found. The scatter in the observed E_A did not correlate with the fresh water flow rate. These values of E_A were found by plotting the spatial concentration distributions and reading the spread ($\bar{x}_{0.5}$) of the distribution at $C/C_{max} = 0.5$. Eqn. 7-4 states that the variance (σ^2) of the concentration distribution is given by

$$\sigma^2 = 0.721 \ \bar{x}^2_{0.5}$$

and eqn. 7-1 indicates that

$$\sigma^2 = 2 E_A t$$

Thus, σ^2 should be proportional to t with $2E_A$ as the constant of proportionality. Again, this assumes that E_A is not a function of x. Data for one of the runs is shown in fig. 8-25. The points are scattered but the general trend is for σ^2 to increase as t to the first power. Note that this data extends to the 30th period after the release of the dye. During this time, the centroid of the dye distribution had moved 60 ft downstream. In spite of the scatter of the data and the non-uniformities in this 60-ft reach, for most purposes it would be reasonable to take a constant value of E_A over reaches such as that represented by this data.

Ref. 4 reports concentration data for the same model and same tidal conditions, but for continuous injection of dye. Nine tests are reported for different combinations of dye discharge and fresh water flow. Test 7 was allowed to run for 240 tidal cycles and essentially came to a steady state. For this test, Q_f was 2.4×10^{-3} cfs; this gave a mean velocity of 0.0024 fps at the injection point. It would be expected that the concentration distribution could be represented by the exact solution of eqn. 6-52 or the approximate solutions of equations 6-57, 6-58 and 6-59. However, a river flows into the estuary just 20 ft. downstream from the dye-injection point. The dilution due to the increased Q_f causes the dye distribution to be distorted near the injection point. By considering only the points at distances greater than one excursion length upstream of the injection point, the diluting effects

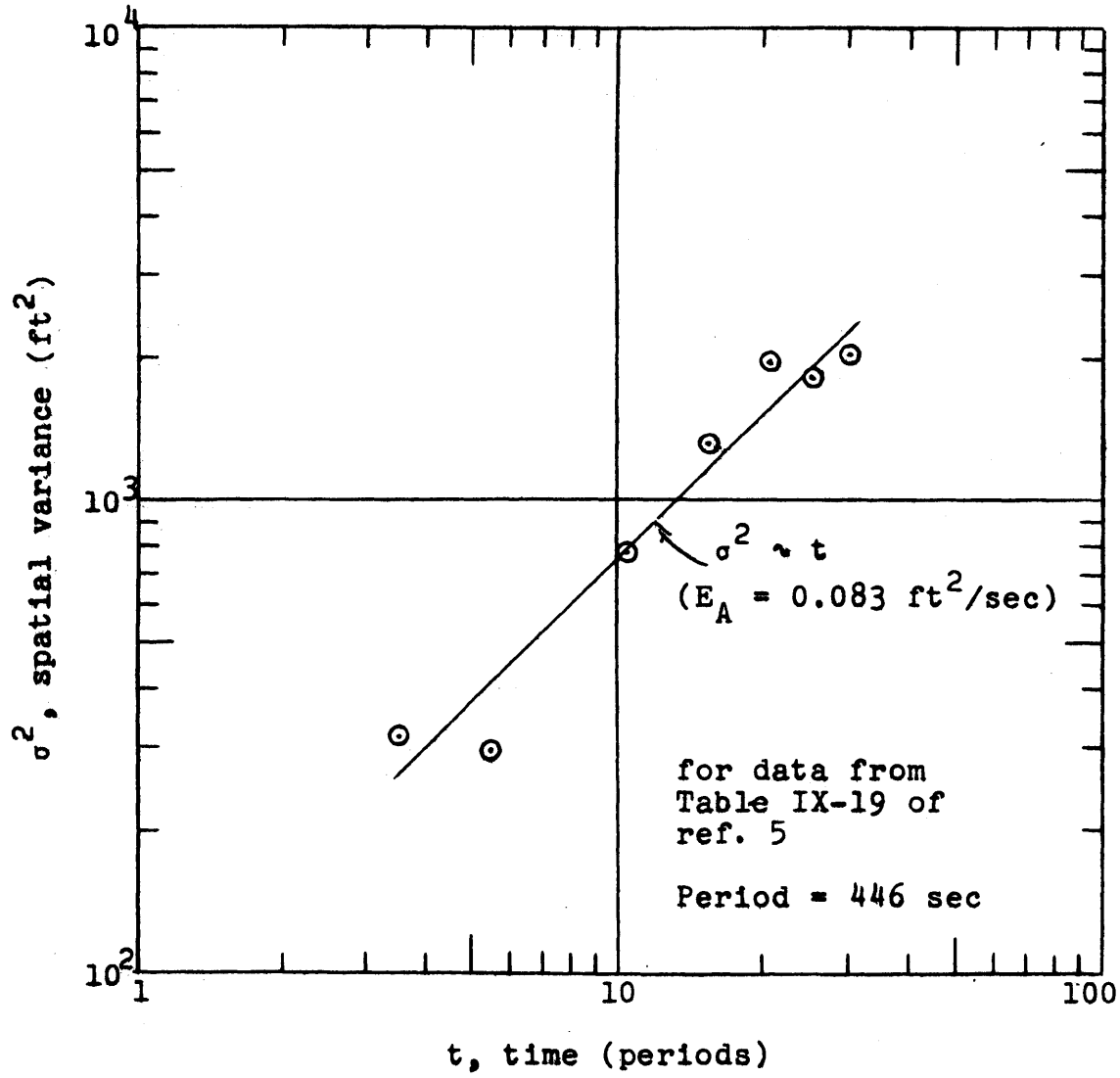

Fig. 8-25: Dispersion test for an instantaneous, point injection in Delaware estuary model

of the additional river flow are apparently no longer present. Thus, eqn. 7-13 may be used to find E_A, if it is again assumed that E_A is not a function of x. The data for test 7 was analyzed according to eqn. 7-13 and is shown in fig. 8-26. Again, it appears that the assumption of a constant E_A for this region is justified. The slope of the line gives $E_A = 0.083$ ft^2/sec, which is in good agreement with the values found in the tests with instantaneous dye release.

In the Delaware estuary model, by comparing calculated and observed values of E_A, it appears that the non-uniformities of the channel may cause E_A to be as much as twice that given by eqn. 6-25 (with $a = 2R_H$). However, use of eqn. 6-25 requires knowledge of the channel roughness, and it was necessary to assume a roughness coefficient in the calculations above. Thus, the conclusion as to the effects of non-uniformities is still open to question.

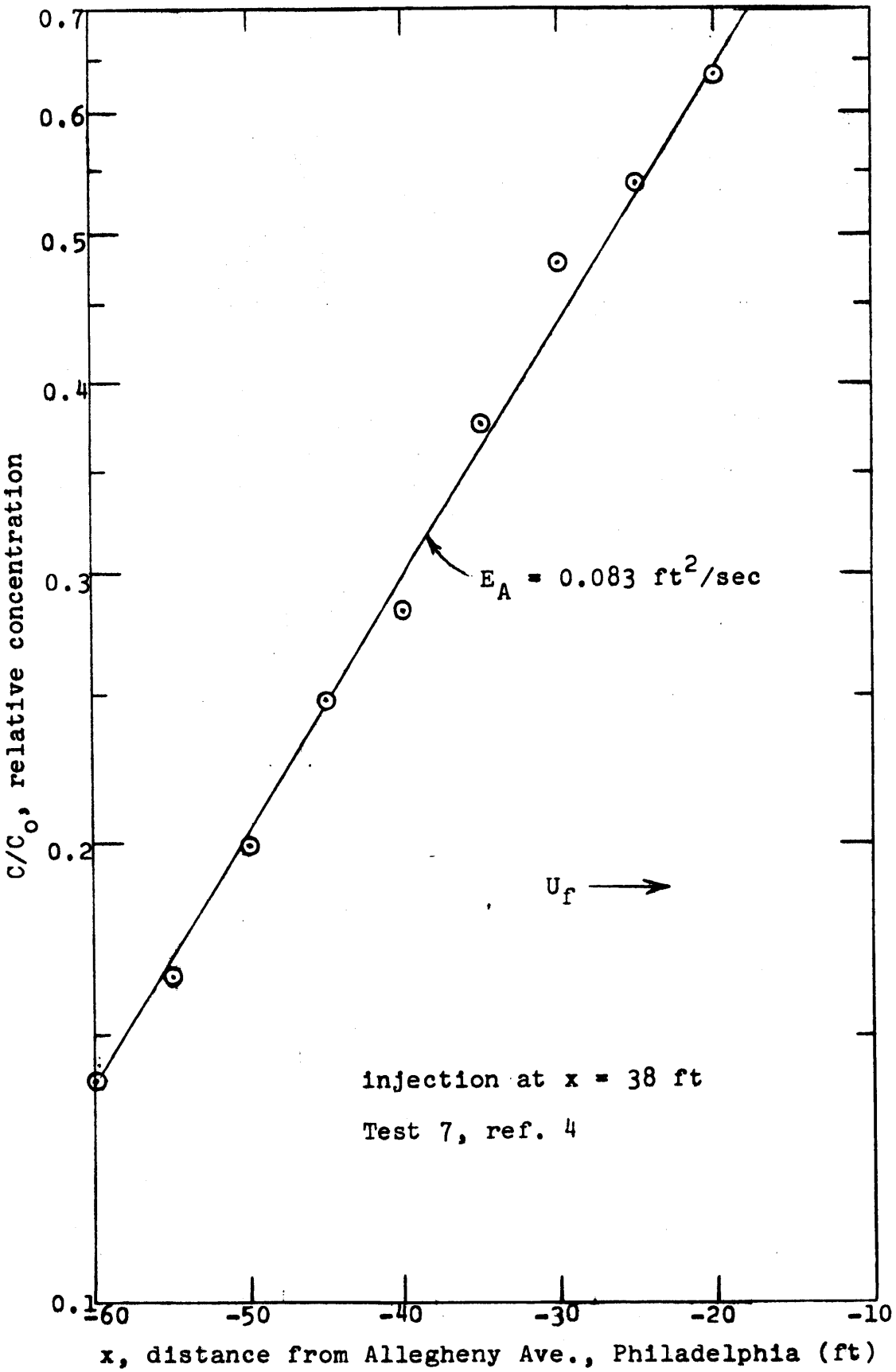

Fig. 8-26: Dispersion test for a continuous injection in Delaware estuary model

9) CONCLUSIONS

9.1) Concept of Longitudinal Dispersion and Its Importance in Mass Transport Problems

Practical considerations often lead to the necessity of taking a one-dimensional approach to pollution analysis in rivers and estuaries. In this approach, the convection with the one-dimensional or average velocity and longitudinal turbulent diffusion do not correctly describe the longitudinal mass transport. This inadequacy arises from the fact that the one dimensional convection (UC) does not account for variations of velocity and concentration across the section and these variations give rise to a net longitudinal mass transport. This transport is called longitudinal dispersion. For uniform flow, it has been shown that dispersion follows Fick's Law of diffusion with the diffusion coefficient replaced by a dispersion coefficient E. This dispersive transport must be included in the one dimensional mass balance equation to completely represent the longitudinal mass transfer. However, in any given situation, the importance of dispersion relative to convection depends not only on the magnitude of the dispersion coefficient relative to the one dimensional velocity but also on the concentration gradients for the substance which is being transported.

9.2) Dispersion in Steady Flow

For steady, uniform flow, Aris developed a general analytical expression by which the dispersion coefficient may be calculated for any uniform boundary configuration if the lateral distribution of velocity and turbulent diffusivity are known. Previous to Aris' work, Taylor presented an analysis which showed that $E = 10.1\, au_*$ for flow in a pipe of radius a where the shear velocity is u_*. For two dimensional channels of depth h, Elder showed that $E = 5.93\, hu_*$. Both Taylor's and Elder's calculations neglected the existence of a laminar sublayer for turbulent flows which are not in the hydraulically rough region. For the case of a slug injection of tracer, Elder observed that the influence of the sublayer causes concentrations in the upstream part of the distribution to be

greater than is predicted using the analytical dispersion coefficient. Thus, the sublayer effectively increases upstream dispersion.

For channels which are not infinitely wide (i.e. not two dimensional), the side walls affect the distribution of velocity and of turbulent diffusivity, and thus the longitudinal dispersion is affected. For example, in a trinagular flume where the hydraulic radius was R_H, $E/R_H u_*$ was found to be 18. For a smooth rectangular flume, $E/R_H u_*$ was 24. For the same flume, the bottom was roughened, thus reducing the relative effect of the side walls, and $E/R_H u_*$ was 13.

Natural streams have varying degrees of "side-wall effects". Also, they have bends and other non-uniformities, both of which increase dispersion above that given by the analytical expressions. On the other hand, natural streams are usually hydraulically rough so no influence from a laminar sublayer would be expected. From the scant data available for natural streams and cross-country pipe lines, $E/R_H u_*$ equal to 40 appears to be a good approximation for pipes and rivers with gentle curvature.

Further study is needed to clearly define the way in which bends and other non-uniformities affect dispersion and to obtain quantitative information on their effects.

9.3) Dispersion in Estuary Type Flow

Estuary type flow was defined as flow where the one dimensional velocity is given by

$$U = U_f + U_T \sin \sigma \quad (t - \delta) \qquad 9\text{-}1$$

In a natural estuary, U_f is the velocity associated with the river discharge and U_T is the maximum tidal velocity. (The term estuary type flow is used to refer to flow in regions where there are no longitudinal density gradients.)

An analysis similar to that of Aris has been presented. While Aris' work was for steady, uniform flow, the present analysis gives the dispersion coefficient for any unsteady, uniform flow in terms of the lateral distribution of velocity and turbulent diffusivity. This general

result was then used to obtain an expression for the dispersion coefficient as a function of time for estuary type flow. It was concluded that, after the first period or two, the dispersion process behaves essentially as if the dispersion coefficient were constant during the period and equal to E_A, the average during a period.

For times which differ by one period, the net effect of the one dimensional oscillatory convection is zero. Thus, for these times, the mass balance equation may be written with the convection given just by U_f, the constant through-flow velocity:

$$\frac{1}{T}\frac{\partial C_s}{\partial n} + U_f \frac{\partial C_s}{\partial x} = E_A \frac{\partial^2 C_s}{\partial x^2} \qquad 9\text{-}2$$

where T is the period and n = 1,2,3... The time variable t has been replaced by nT and C has been replaced by C_s to emphasize the fact that eqn. 9-2 represents only the changes from one period to the next and not the changes during the period. E_A is still the average dispersion coefficient associated with the oscillatory flow. In particular, eqn. 9-2 may be applied to the "slack times" i.e. times when the oscillating (tidal) component of the velocity is zero. For non-uniform flow, the equivalent to eqn. 9-2 is

$$\frac{1}{T}\frac{\partial C_s}{\partial n} + U_f \frac{\partial C_s}{\partial x} = \frac{1}{A}\frac{\partial}{\partial x}\left(E_A A \frac{\partial C_s}{\partial x}\right) \qquad 9\text{-}3$$

where A is the cross section area. Care must be used in applying either eqn. 9-2 or eqn. 9-3. These equations state that, from one period to the next, the changes in concentration for a given fluid element are due only to the net convection and to longitudinal dispersion. Thus, these equations may not be applied in differential or finite difference form to or across any fluid which has pollutants (or tracer) injected into it at any time during a period. On the other hand, if injection of pollutants is correctly represented in boundary conditions, then the solution to these equations will be valid for all fluid elements.

Dispersion experiments were made for estuary type flow in a uniform laboratory pipe line. The agreement between the analytical and the

observed dispersion coefficients was poor at low average Reynolds numbers, but the agreement increased with increasing Reynolds numbers. The lack of agreement is believed to be due to the effects of the laminar sublayer which were not included in the analysis.

No dispersion data was found for the fresh water portion of natural estuaries. Most of the studies for natural estuaries have been conducted in distorted Froude models. (Conclusions regarding the interpretation of model results are presented in section 4.6.) The model results were used in model scale to estimate the effects of non-uniformities on dispersion in estuary type flow. On the basis of estimated roughness coefficients for the Delaware estuary model, it was seen that the dispersion coefficient could be as great as twice that given by the analytical value (eqn. 6-25 with a replaced by $2R_H$). This is in good agreement with the difference between analytical and observed values for rivers of gentle curvature. (Estuaries should be expected to have only gentle curvature since they are in the late stages of river morphology.)

For natural estuaries, the physical size and the natural roughness almost always mean that the estuary is hydraulically rough. Thus, the problems which the laminar sublayer caused with the laboratory results would not be expected to arise in a natural estuary. However, just as for the case of steady flow, more work is needed to clearly define the effects of bends and non-uniformities on dispersion in estuary type flow.

For the region of longitudinal salinity gradients in an estuary, a circulatory gravitational convection exists. The effects of this convection may be included in the one dimensional dispersion process. When this is done, the dispersion coefficient is much larger than for the fresh water (constant density) portion of the estuary.

It has been demonstrated that it is difficult to correctly interpret the results of model studies of pollution transport problems in the constant density regions of estuaries. However, for these regions, the present study has demonstrated a way of estimating longitudinal dispersion coefficients when the one dimensional velocity is given by eqn. 9-1. Analysis of field and model data indicates that dispersion coefficients in natural estuaries tend to be about twice that given by the analytical value for uniform estuaries. Thus, a reasonable estimate of the average

dispersion coefficient (E_A) would seem to be

$$E_A = 40\ R_H\ u_{*A} = 40\ R_H\ \left(\sqrt{\frac{f}{8}}\ \frac{2}{\pi}\ U_T\right) \qquad 9\text{-}4$$

where R_H is the hydraulic radius, u_{*A} is the shear velocity (square root of boundary shear stress divided by fluid density) averaged during a tidal period, f is the Darcy-Weisbach friction factor, and U_T is the maximum tidal velocity. The dispersion coefficient estimated from eqn. 9-4 may be used in conjunction with a mass balance equation (e.g. eqn. 9-2 or 9-3) to calculate longitudinal distributions of pollutants introduced into an estuary. This approach may be used in place of model studies, and is much quicker and cheaper than model studies. The value of E_A from eqn. 9-4 would probably be accurate to within less than a factor of two. Even with this degree of uncertainty concerning E_A, the calculated concentration profiles would possibly be as accurate as the interpretation of model results for the constant density portion of estuaries in view of the difficulties which are inherent in this interpretation. (See discussion in section 4.)

REFERENCES

1) Allen, C. M. and E. A. Taylor, "A Salt Velocity Method of Water Measurement", Transactions, ASME, vol. 45, pp. 285-341, 1923.

2) Anon., "Delaware River Model Study; Report No. 1: Hydraulic and Salinity Verification", Technical Memorandum no. 2-337, U. S. Army Engineer Waterways Experiment Station, Vicksburg, Miss., 25 p, May 1956.

3) Anon., "Delaware River Model Study; Report No. 2: Salinity Tests of Existing Channel", Technical Memorandum no. 2-337, U. S. Army Engineer Waterways Experiment Station, Vicksburg, Miss., 38 p, June 1954.

4) Anon., "Dispersion of Effluent in Delaware River from New Jersey Zinc Company Plant", Technical Report No. 2-457, U. S. Army Engineer Waterways Experiment Station, Vicksburg, Miss., 18 p, June 1957.

5) Anon., "Dispersion Studies on the Delaware River Estuary Model and Potential Applications Toward Stream Purification Capacity Evaluations", Model Study Committee, Delaware State Water Pollution Commission et al, Dover, Delaware, 223 p, June 1961.

6) Anon., "DuPont Plants Effluent Dispersion in Delaware River", Miscl. Paper no. 2-222, U. S. Army Engineer Waterways Experiment Station, Vicksburg, Miss., 19 p, May 1957.

7) Aris, R., "On the Dispersion of a Solute in Fluid Flowing Through a Tube", Proceedings, Royal Society of London, Series A, vol. 235, no. 1200, pp. 67-77, April 10, 1956.

8) Bird, R. Byron et al, Transport Phenomena, John Wiley and Sons, New York, 1960.

9) Carslaw, H. S. and J. C. Jaeger, "Conduction of Heat in Solids", Oxford University Press, London, 1959.

10) Courant, R. and D. Hilbert, "Methods of Mathematical Physics", Interscience Publishers, New York, 1953.

11) Crank, J., "The Mathematics of Diffusion", Oxford University Press, London, 1956.

12) Elder, J. W., "The Dispersion of Marked Fluid in Turbulent Shear Flow", Journal of Fluid Mechanics, vol. 5, part 4, pp. 544-560, May 1959.

13) Glover, Robert E., "Dispersion of Dissolved or Suspended Materials in Flowing Streams", Geological Survey Professional Paper No. 433-B, U. S. Government Printing Office, 32 p, 1964.

14) Goda, Takeshi and Shoichi Nambu, "Some Considerations on River Pollution Mechanism", Memoirs, Faculty of Engineering, Kyoto University, vol. XXI, part 1, pp. 57-69, Jan. 1959.

15) Godfrey, Richard G. and Bernard J. Frederick, "Dispersion in Natural Streams", open file report, Geological Survey, Washington, D.C., 75 p, 1963.

16) Harleman, D. R. F. et al, "The Diffusion of Two Fluids of Different Density in a Homogeneous Turbulent Field", Technical Report 31, Hydrodynamics Laboratory, M.I.T., Cambridge, Mass., 93 p, Feb. 1959.

17) Harleman, D. R. F. et al, "An Analysis of One-dimensional Convective-Diffusion Phenomena in an Idealized Estuary", Technical Report no. 42, Hydrodynamics Laboratory, M.I.T., Cambridge, Mass., 31 p, Jan. 1961.

18) Harleman, D. R. F. et al, "Salinity Effects on Velocity Distribution in an Idealized Estuary", Technical Report no. 50, Hydrodynamics Laboratory, M.I.T., Cambridge, Mass., Jan. 1962.

19) Harleman, D. R. F. and R. R. Rumer, Jr., "Dynamics of Salt Water Intrusion in Porous Media", Technical Report no. 55, Hydrodynamics Laboratory, M.I.T., Cambridge, Mass., Aug. 1962.

20) Harleman, D. R. F., "The Significance of Longitudinal Dispersion in the Analysis of Pollution in Estuaries", unpublished paper, Hydrodynamics Laboratory, M.I.T., Cambridge, Mass., July 1964.

21) Harleman, D. R. F. and A. T. Ippen, "Longitudinal Dispersion in Constant Density Tidal Motion", draft for Technical Bulletin, Committee on Tidal Hydraulics, Corps of Engineers, Vicksburg, Miss., 22 p, 1964.

22) Hildebrand, Francis B., "Advanced Calculus for Applications", Prentice-Hall, Englewood Cliffs, New Jersey, 1963.

23) Hinze, J. O., "Turbulence", McGraw-Hill, New York, 1959.

24) Horenstein, W., "On Certain Integrals in the Theory of Heat Conduction", Appl. Math. Quart., vol. 3, pp. 183-187, 1945.

25) Hull, Donald E. and James W. Kent, "Radioactive Tracers to Mark Interfaces and Measure Intermixing in Pipe Lines", Industrial and Engineering Chemistry, vol. 44, no. 11, pp. 2745-2750, Nov. 1952.

26) Ingersoll, L. R. and O. J. Zobel, "An Introduction to the Mathematical Theory of Heat Conduction", New York, 1913.

27) Ippen, A. T. et al, "Turbulent Diffusion and Gravitational Convection in an Idealized Estuary", Technical Report no. 38, Hydrodynamics Laboratory, M.I.T., Cambridge, Mass., 33 p, March 1960.

28) Ippen, A. T. and D. R. F. Harleman, "One Dimensional Analysis of Salinity and Intrusion in Estuaries", Technical Bulletin no. 5, Committee on Tidal Hydraulics, Corps of Engineers, Vicksburg, Miss., 52 p, June 1961.

29) Ippen, A. T. (ed.), "Estuary and Coastline Hydrodynamics", Hydrodynamics Laboratory, M.I.T., Cambridge, Mass., 1963.

30) Kent, Richard, "Diffusion in a Sectionally Homogeneous Estuary", Proceedings, ASCE (Sanitary Engineering Division), paper no. 2408, SA2, pp. 15-47, March 1960.

31) Kent, Richard E., "Turbulent Diffusion in a Sectionally Homogeneous Estuary", Technical Report no. 16, Chesapeake Bay Institute, The Johns Hopkins University, ref. 58-1, 86 p, April 1958.

32) Krenkel, Peter A. and Gerald T. Orlob, "Turbulent Diffusion and the Reaeration Coefficient", Transactions, ASCE, vol. 128, part III, pp. 293-334, 1964.

33) Kunz, K. S., "Numerical Analysis", McGraw-Hill, New York, 1957.

34) Nejedly, Augùstin and Jiri Pelz, "Studie Podelneho Miseni", Vyzkumny Ustav Vodohospodarsky Prace a Studie, Sesit 112, Praha-Podbaba, 116 p, 1964.

35) O'Connor, Donald J., "Report on Analysis of Dye Diffusion Data in the Delaware River Estuary - Evaluation of Diffusion Coefficients", Manhattan College, New York, 14 p, Aug. 1962.

36) O'Connor, Donald J., "Oxygen Balance of an Estuary", Transactions, ASCE, paper no. 3230, vol. 126, part III, pp. 556-576, 1960.

37) Ogata, Akio and R. B. Banks, "A Solution of the Differential Equation of Longitudinal Dispersion in Porous Media", Geological Survey Professional Paper 411-A, Government Printing Office, Washington, 7 p, 1961.

38) Parker, Frank L., "Radioactive Tracers in Hydrologic Studies", Transactions, American Geophysical Union, vol. 39, no. 3, pp. 434-439, 1958.

39) Parker, Frank L., "Eddy Diffusion in Reservoirs and Pipe Lines", Proceedings, ASCE (Hydraulics Division), paper no. 2825, HY3, pp. 151-171, May 1961.

40) Patterson, C. C. and E. F. Gloyna, "Radioactivity Transport in Water - The Dispersion of Radionuclides in Open Channel Flow", Technical Report no. 2, Environmental Health Engineering Research Laboratory, University of Texas, 87 p, June 1, 1963.

41) Polubarinova-Kochina, P. Ya., "Theory of Ground Water Movement", (trans. by J. M. Roger de Wiest), Princeton University Press, New Jersey, 1962.

42) Pritchard, D. W., "A Study of Flushing in the Delaware Model", Technical Report no. 7, Chesapeake Bay Institute, The Johns Hopkins University, ref. 54-4, 143 p, April 1954.

43) Pritchard, D. W., "Computation of the Longitudinal Salinity Distribution in the Delaware Estuary for Various Degrees of River Inflow Regulation", Technical Report no. 18, Chesapeake Bay Institute, The Johns Hopkins University, ref. 59-3, 72 p, Sept. 1959.

44) Rieman, Bernard,"Partielle Differentialgleichungen und Deren Anwendung auf Physikalische Fragen", (prepared for publication by Karl Hattendorff), Friedrich Vieweg und Sohn, Braunschweig, 1882.

45) Rouse, H., "Advanced Mechanics of Fluids", Wiley, New York, 1959.

46) Rouse, H., "Elementary Mechanics of Fluids", Wiley, New York, 1957.

47) Rouse, H. (ed.), "Engineering Hydraulics", Wiley, New York, 1950.

48) Scarborough, James B., "Numerical Mathematical Analysis", The Johns Hopkins Press, Baltimore, 1958.

49) Schlichting, H., "Boundary Layer Theory", (trans. by J. Kestin), McGraw-Hill, New York, 4th edition, 1960.

50) Schultz-Grunow, F., "Pulsierender Durchfluss durch Rohre", Forschung auf dem Gebiete des Ingenieurwesens, Bd 11, Heft 4, pp. 170-187, July/Aug. 1940.

51) Simpson, E. S. et al, "Radiotracer Experiments in the Mohawk River, New York, to Study Sewage Path and Dilution", Transactions, American Geophysical Union, vol. 39, no. 3, pp. 427-433, 1958.

52) Smith, S. S. and R. K. Schulze, "Interfacial Mixing Characteristics of Products in Products Pipe Lines", The Petroleum Engineer, vol. 19, no. 13, pp. 94ff, Sept. 1948; vol. 20, no. 1, pp. 330ff, Oct. 1948.

53) Taylor, Geoffrey, "The Dispersion of Matter in Turbulent Flow Through a Pipe", Proceedings, Royal Society of London, Series A, vol. 223, no. 1155, pp. 446-468, May 20, 1954.

54) Thomas, H. A., Jr., "Radioactive Isotopes as Tools in Sanitary Engineering Research", Peaceful Uses of Atomic Energy, vol. 15, (Application of Radioactive and Fission Products in Research and Industry), United Nations, pp. 42-46, 1956.

BIOGRAPHY

The author was born in Atlanta, Georgia in 1936. During 1954-55, he attended David Lipscomb College in Nashville, Tennessee. From 1955 to 1960, he was enrolled in the Georgia Institute of Technology in Atlanta, and in 1960, received the Bachelor of Civil Engineering ("Cooperative Education Plan" and "With Highest Honor") and the Master of Science in Civil Engineering.

Since 1960, the author has been a graduate student at M.I.T. During the school years 1960-61 and 1961-62, he served as an instructor in fluid mechanics at the Lowell Institute School which is operated under the auspices of M.I.T.

Publications:

Harleman, Donald R. F. and E. R. Holley, Jr., Discussion of "Turbulent Diffusion and the Reaeration Coefficient" by Peter A. Krenkel and Gerald T. Orlob, Journal of Sanitary Engineering Division, Proceedings, ASCE, vol. 88, no. SA6, paper 3336, pp. 109-116, November, 1962.

Harleman, Donald R. F. and Edward R. Holley, Jr., John A. Hoopes, Ralph R. Rumer, Jr., "The Feasibility of a Dynamic Model of Lake Michigan", prepared for Corps of Engineers, U. S. Army, Contract no. DA-22-079-CIVENG-61-40, Waterways Experiment Station, Vicksburg, Mississippi, 93 p, November, 1961.

Harleman, D. R. F., E. R. Holley, Jr., J. A. Hoopes, and R. R. Rumer, Jr., "The Feasibility of a Dynamic Model of Lake Michigan", Proceedings, Fifth Conference on Great Lakes Research, Publication no. 9, Great Lakes Research Division, Institute of Science and Technology, The University of Michigan, Ann Arbor, pp. 51-67, 1962.

Memberships:

American Society of Civil Engineers, Boston
Society of Civil Engineers, Sigma Xi, Tau
Beta Pi, Phi Kappa Phi, Chi Epsilon

Appendix A: Spatial Averaging of Mass Balance Equation (Eqn. 2-10)

Introducing the expressions of Eqn. 2-12 into the left-hand side of Eqn. 2-10, expanding the products of sums, and taking the spatial average of the resulting expression, one obtains

$$\frac{1}{A}\int_A \frac{\partial[\rho\,(C + c'')]}{\partial t}\,dA + \frac{1}{A}\int_A \frac{\partial}{\partial x}\,[\rho U C]\,dA + \frac{1}{A}\int_A \frac{\partial}{\partial x}\,[\rho U c'']\,dA$$

$$+ \frac{1}{A}\int_A \frac{\partial}{\partial x}\,[\rho u'' C]\,dA + \frac{1}{A}\int_A \frac{\partial}{\partial x}\,[\rho u'' c'']\,dA + \frac{1}{A}\int_A \frac{\partial}{\partial y}\,[\rho v'' C]\,dA$$

$$+ \frac{1}{A}\int_A \frac{\partial}{\partial y}\,[\rho v'' c'']\,dA + \frac{1}{A}\int_A \frac{\partial}{\partial z}\,[\rho w'' C]\,dA + \frac{1}{A}\int_A \frac{\partial}{\partial z}\,[\rho w'' c'']\,dA \qquad \text{A-1}$$

$$= \frac{1}{A}\int_A \frac{\partial}{\partial x}\,[\rho(D_m + e_x)\,\frac{\partial \bar{c}}{\partial x}]\,dA + \frac{1}{A}\int_A \frac{\partial}{\partial y}\,[\rho(D_m + e_y)\,\frac{\partial \bar{c}}{\partial y}]\,dA$$

$$+ \frac{1}{A}\int_A \frac{\partial}{\partial z}\,[\rho(D_m + e_z)\,\frac{\partial \bar{c}}{\partial z}]\,dA + N_P$$

where N_P is the spatial average of $\bar{n}_P$. (Throughout this appendix, U and A may be functions of both x and t.) In performing the temporal averaging to obtain Eqn. 2-7, it was possible to interchange the order of integration and differentiation. However, since the area A may be a variable, it is not possible to make a simple interchange in the order of integration and differentiation in Eqn. A-1. Still, it is desirable to have the mass balance written in terms of the spatial average of the velocity and concentration, rather than the spatial average of their derivatives, as indicated in Eqn. A-1. Thus, consider the following:

Let Φ be a function of x, y, z, and t. Actually the integration over the area is more accurately expressed as in Eqn. A-2:

$$\int_A \frac{\partial \Phi}{\partial x}\,dA = \int_{z_1(x,t)}^{z_2(x,t)} \int_{y_1(x,z,t)}^{y_2(x,z,t)} \frac{\partial \Phi}{\partial x}\,dy\,dz \qquad \text{A-2}$$

where $y_2(x,z,t)$ and $y_1(x,z,t)$ are the equations of the upper and lower boundaries of the area A, and $z_2(x,t)$ and $z_1(x,t)$ are the coordinates of the lateral extremities of A. (See the sketch below).

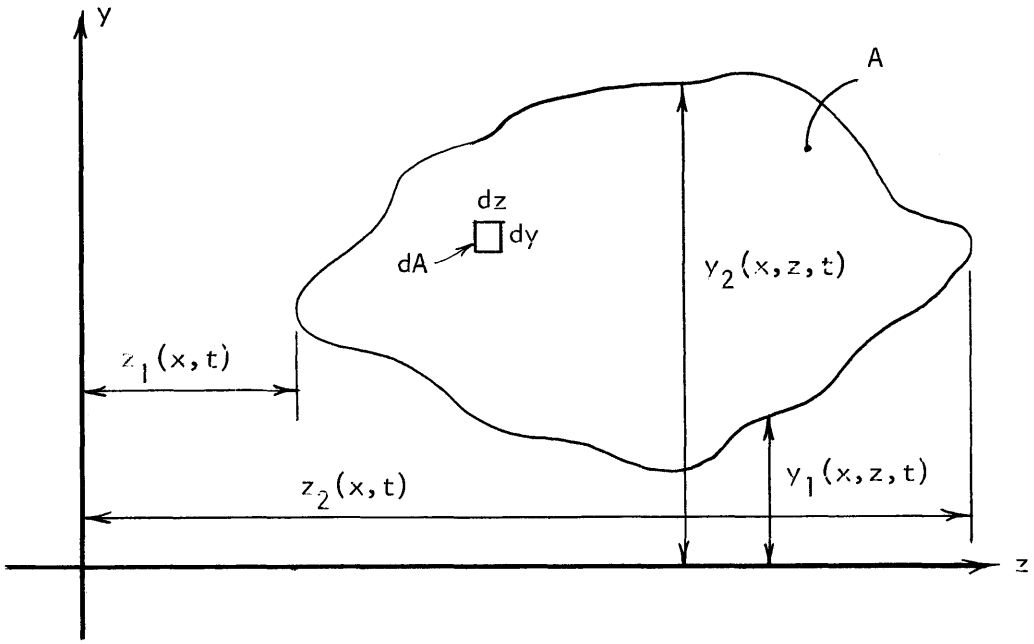

Fig. A-1: Definition Sketch

In general,

$$\frac{\partial}{\partial u}\int_{a(u)}^{b(u)} f(t,u)\,dt = \int_{a(u)}^{b(u)} \frac{\partial f(t,u)}{\partial u}dt + f[b(u),u]\frac{db(u)}{du} \qquad \text{A-3}$$

$$- f[a(u),u]\frac{da(u)}{du}$$

(This is known as Leibniz's formula.) Thus,

$$\frac{\partial}{\partial x}\int_{y_1}^{y_2} \phi\, dy = \int_{y_1}^{y_2} \frac{\partial \phi}{\partial x}dy + \phi_{y_2}\frac{\partial y_2}{\partial x} - \phi_{y_1}\frac{\partial y_1}{\partial x} \qquad \text{A-4}$$

where ϕ_{y_2} means ϕ evaluated at y_2, i.e. $\phi_{y_2} = \phi(x,y_2,z,t)$. Integrate with respect to z:

$$\int_{z_1}^{z_2}\left[\frac{\partial}{\partial x}\int_{y_1}^{y_2}\phi dy\right]dz = \int_{z_1}^{z_2}\int_{y_1}^{y_2}\frac{\partial \phi}{\partial x}dy\,dz + \int_{z_1}^{z_2}\phi_{y_2}\frac{\partial y_2}{\partial x}dz \qquad \text{A-5}$$

$$- \int_{z_1}^{z_2}\phi_{y_1}\frac{\partial y_1}{\partial x}dz$$

Let

$$\psi = \int_{y_1}^{y_2} \phi \, dy \qquad \text{A-6}$$

and consider that from Eqn. A-3

$$\int_{z_1}^{z_2} \frac{\partial \psi}{\partial x} \, dz = \frac{\partial}{\partial x} \int_{z_1}^{z_2} \psi dz - \psi_{z_2} \frac{\partial z_2}{\partial x} + \psi_{z_1} \frac{\partial z_1}{\partial x} \qquad \text{A-7}$$

But

$$\psi_{z_2} = \int_{y_1(z_2)}^{y_2(z_2)} \phi \, dy = 0$$

since $y_1(z_2) = y_2(z_2)$. Similarly,

$$\psi_{z_1} = 0$$

From Eqn. A-6 and A-7,

$$\int_{z_1}^{z_2} \frac{\partial}{\partial x} \int_{y_1}^{y_2} \phi \, dy = \frac{\partial}{\partial x} \int_{z_1}^{z_2} \int_{y_1}^{y_2} \phi \, dy \qquad \text{A-8}$$

Combining Eqn. A-8 with Eqn. A-5 and re-arranging,

$$\int_{z_1}^{z_2} \int_{y_1}^{y_2} \frac{\partial \phi}{\partial x} dy \, dz = \frac{\partial}{\partial x} \int_{z_1}^{z_2} \int_{y_1}^{y_2} \phi \, dy \, dz$$

$$- \int_{z_1}^{z_2} \phi_{y_2} \frac{\partial y_2}{\partial x} dz + \int_{z_1}^{z_2} \phi_{y_1} \frac{\partial y_1}{\partial x} dz$$

or

$$\int_A \frac{\partial \phi}{\partial x} dA = \frac{\partial}{\partial x} \int_A \phi \, dA - \int_{z_1}^{z_2} \phi_{y_2} \frac{\partial y_2}{\partial x} dz + \int_{z_1}^{z_2} \phi_{y_1} \frac{\partial y_1}{\partial x} dz \qquad \text{A-9}$$

Note that if y_2 and y_1 are independent of x, then Eqn. A-9 shows that the order of integration and differentiation may be interchanged since

$$\frac{\partial y_2}{\partial x} = 0 = \frac{\partial y_1}{\partial x}$$

in that case.

Eqn. A-9 may be applied directly to the second through the fifth terms of the left-hand side of Eqn. A-1:

$$\int_A \frac{\partial}{\partial x} [\rho UC]dA = \frac{\partial}{\partial x} \int_A \rho UC dA - \int_{z_1}^{z_2} \rho UC \frac{\partial y_2}{\partial x} dz + \int_{z_1}^{z_2} \rho UC \frac{\partial y_1}{\partial x} dz$$

$$= \frac{\partial}{\partial x} (\rho UC \int_A dA) - \rho UC \int_{z_1}^{z_2} (\frac{\partial y_2}{\partial x} - \frac{\partial y_1}{\partial x}) dz$$

$$= \frac{\partial}{\partial x} (\rho UCA) - \rho UC \int_{z_1}^{z_2} \frac{\partial}{\partial x} (y_2 - y_1) dz$$

By virtue of Eqn. A-7 and the fact that $y_2(z_2) = y_1(z_2)$ and $y_2(z_1) = y_1(z_1)$, then

$$\int_{z_1}^{z_2} \frac{\partial}{\partial x} (y_2 - y_1) dz = \frac{\partial}{\partial x} \int_{z_1}^{z_2} (y_2 - y_1) dz = \frac{\partial A}{\partial x}$$

since

$$\int_{z_1}^{z_2} (y_2 - y_1) dz = A \qquad \text{A-10}$$

Therefore,

$$\int_A \frac{\partial}{\partial x} [\rho UC]dA = \frac{\partial}{\partial x} (\rho UCA) - \rho UC \frac{\partial A}{\partial x}$$

$$= [A \frac{\partial}{\partial x} (\rho UC) + \rho UC \frac{\partial A}{\partial x}] - \rho UC \frac{\partial A}{\partial x}$$

$$\frac{1}{A}\int_A \frac{\partial}{\partial x} [\rho UC]dA = \frac{\partial}{\partial x} (\rho UC) \qquad \text{A-11}$$

whether A is constant or not.

Next,

$$\int_A \frac{\partial}{\partial x} [\rho Uc'']dA = \frac{\partial}{\partial x}\int_A \rho Uc''dA - \int_{z_1}^{z_2} (\rho Uc'')_{y_2} \frac{\partial y_2}{\partial x}dz$$

$$+\int_{z_1}^{z_2} (\rho Uc'')_{y_1} \frac{\partial y_1}{\partial x}\, dz$$

$$= \frac{\partial}{\partial x} (\rho U \cancel{\int_A c''dA}^{\,0}) - \rho U \int_{z_1}^{z_2} (c''_{y_2} \frac{\partial y_2}{\partial x} - c''_{y_1} \frac{\partial y_1}{\partial x}) dz\,.$$

$$\frac{1}{A} \int_A \frac{\partial}{\partial x} [\rho Uc'']dA = - \rho \frac{U}{A} \int_{z_1}^{z_2} (c''_{y_2} \frac{\partial y_2}{\partial x} - c''_{y_1} \frac{\partial y_1}{\partial x}) dz \qquad \text{A-12}$$

Also,

$$\int_A \frac{\partial}{\partial x} [\rho u''C]dA = \frac{\partial}{\partial x}\int_A \rho u'' CdA - \int_{z_1}^{z_2} (\rho u''C)_{y_2} \frac{\partial y_2}{\partial x}\, dz$$

$$+ \int_{z_1}^{z_2} (\rho u''C)_{y_1} \frac{\partial y_1}{\partial x} dz$$

$$= \frac{\partial}{\partial x} (\rho C \cancel{\int_A u''dA}^{\,0}) - \rho C \int_{z_1}^{z_2} (u''_{y_2} \frac{\partial y_2}{\partial x} - u''_{y_1} \frac{\partial y_1}{\partial x}) dz$$

$$\frac{1}{A}\int_A \frac{\partial}{\partial x}[\rho u''C]dA = -\rho\frac{C}{A}\int_{z_1}^{z_2}(u''_{y_2}\frac{\partial y_2}{\partial x} - u''_{y_1}\frac{\partial y_1}{\partial x})dz \qquad \text{A-13}$$

Taking the next term from Eqn. A-1,

$$\int_A \frac{\partial}{\partial x}[\rho u''c'']dA = \frac{\partial}{\partial x}\int_A \rho u''c''dA - \int_{z_1}^{z_2}(\rho u''c'')_{y_2}\frac{\partial y_2}{\partial x}dz + \int_{z_1}^{z_2}(\rho u''c'')_{y_1}\frac{\partial y_1}{\partial x}dz$$

$$= \frac{\partial}{\partial x}(\rho\int_A u''c''dA) - \rho\int_{z_1}^{z_2}[(u''c'')_{y_2}\frac{\partial y_2}{\partial x} - (u''c'')_{y_1}\frac{\partial y_1}{\partial x}]dz$$

$$\frac{1}{A}\int_A \frac{\partial}{\partial x}(\rho u''c'')dA = \frac{1}{A}\frac{\partial}{\partial x}(\rho\overline{\overline{u''c''}}A) - \frac{\rho}{A}\int_{z_1}^{z_2}[(u''c'')_{y_2}\frac{\partial y_2}{\partial x} - (u''c'')_{y_1}\frac{\partial y_1}{\partial x}]dz \qquad \text{A-14}$$

where the double bar indicates the spatial averaging as defined by Eqn. 2-11.

If x is replaced by t in Eqn. A-9, then the first term on the left hand side of Eqn. A-1 can be manipulated in the following way:

$$\int_A \frac{\partial[\rho(C+c'')]}{\partial t}dA = \frac{\partial}{\partial t}\int_A \rho(C+c'')dA - \int_{z_1}^{z_2}[\rho(C+c'')]_{y_2}\frac{\partial y_2}{\partial t}dz + \int_{z_1}^{z_2}[\rho(C+c'')]_{y_1}\frac{\partial y_1}{\partial t}dz$$

But

$$\frac{\partial y_2}{\partial t} = v''_{y_2}; \quad \frac{\partial y_1}{\partial t} = v''_{y_1}; \quad \int_A c''dA = 0$$

Thus

$$\frac{1}{A}\int_A \frac{\partial[\rho(C+c'')]}{\partial t}dA = \frac{1}{A}\frac{\partial}{\partial t}(\rho CA) - \frac{\rho C}{A}\int_{z_1}^{z_2}(v''_{y_2} - v''_{y_1})dz$$

$$- \frac{\rho}{A}\int_{z_1}^{z_2}[(c''v'')_{y_2} - (c''v'')_{y_1}]dz \qquad \text{A-15}$$

The sixth through the ninth terms on the left-hand side of Eqn. A-1 involve the spatial averaging of derivatives in the lateral directions. To treat these terms, consider the following:

$$\int_A \frac{\partial\phi}{\partial y}dA = \int_{z_1}^{z_2}\int_{y_1}^{y_2}\frac{\partial\phi}{\partial y}dy\,dz = \int_{z_1}^{z_2}\left[\int_{y_1}^{y_2}d\phi\right]dz$$

$$\int_A \frac{\partial\phi}{\partial y}dA = \int_{z_1}^{z_2}(\phi_{y_2} - \phi_{y_1})\,dz \qquad \text{A-16}$$

and

$$\int_A \frac{\partial\phi}{\partial z}dA = \int_{y_1}^{y_2}\int_{z_1}^{z_2}\frac{\partial\phi}{\partial z}dz\,dy = \int_{y_1}^{y_2}\left[\int_{z_1}^{z_2}d\phi\right]dz$$

$$\int_A \frac{\partial\phi}{\partial z}dA = \int_{y_1}^{y_2}(\phi_{z_2} - \phi_{z_1})\,dy \qquad \text{A-17}$$

(Note that Eqn. A-16 implies that the definitions of z_1 and z_2 have been interchanged with those of y_1 and y_2.) Thus, the sixth through the ninth terms may be written as

$$\frac{1}{A}\int_A \frac{\partial}{\partial y}(\rho v''C)\,dA = \frac{\rho C}{A}\int_{z_1}^{z_2}(v''_{y_2} - v''_{y_1})\,dz \qquad \text{A-18}$$

$$\frac{1}{A}\int_A \frac{\partial}{\partial y}\,(\rho v''c'')\,dA = \frac{\rho}{A}\int_{z_1}^{z_2}\left[(v''c'')_{y_2} - (v''c'')_{y_1}\right]dz \qquad \text{A-19}$$

$$\frac{1}{A}\int_A \frac{\partial}{\partial z}\,(\rho w''C)\,dA = \frac{\rho C}{A}\int_{y_1}^{y_2}\left(w''_{z_2} - w''_{z_1}\right)dy \qquad \text{A-20}$$

$$\frac{1}{A}\int_A \frac{\partial}{\partial z}\,(\rho w''c'')\,dA = \frac{\rho}{A}\int_{y_1}^{y_2}\left[(w''c'')_{y_2} - (w''c'')_{y_1}\right]dz \qquad \text{A-21}$$

Consider the sum of the second and third terms on the right-hand side of Eqn. A-1. By virtue of Green's theorem in the plane:

$$\int_A\left\{\frac{\partial}{\partial y}\left[\rho(D_m+e_y)\,\frac{\partial \bar{c}}{\partial y}\right] + \frac{\partial}{\partial z}\left[\rho(D_m+e_z)\right]\right\}dA =$$

$$\oint_\gamma\left\{-\left[\rho(D_m+e_z)\,\frac{\partial \bar{c}}{\partial z}\,dy\right] + \left[\rho(D_m+e_y)\,\frac{\partial \bar{c}}{\partial y}\,dz\right]\right\} \qquad \text{A-22}$$

where the path γ for the line integral is the perimeter of the area A. The two terms making up this line integral represent the lateral diffusion at the flow boundaries. If lateral diffusion is taking place at the flow boundaries, then substance is either being added to or removed from the flow by diffusion (usually molecular diffusion or absorption). The line integral of Eqn. A-22 represents the net lateral flux of substance across the boundaries, and the sign is such that it represents the flux into the flow. For present purposes, it is convenient to write a general term (M_P) for this rate of addition of mass by molecular diffusion or absorption. M_P is then analogous to N_P which represents the rate of production of the substance P.

Considering the first term on the right-hand side of Eqn. A-1 and again using Eqn. A-9,

$$\int_A \frac{\partial}{\partial x}\left[\rho(D_m+e_x)\frac{\partial \bar{c}}{\partial x}\right]dA = \frac{\partial}{\partial x}\left\{\int_A \rho(D_m+e_x)\frac{\partial \bar{c}}{\partial x}dA\right\} \qquad \text{A-23}$$

$$- \int_{z_1}^{z_2}\left[\rho(D_m+e_x)\frac{\partial \bar{c}}{\partial x}\right]_{y_2}\frac{\partial y_2}{\partial x}dz + \int_{z_1}^{z_2}\left[\rho(D_m+e_x)\frac{\partial \bar{c}}{\partial x}\right]_{y_1}\frac{\partial y_1}{\partial x}dz$$

The second and third terms on the right-hand side of Eqn. A-23 will usually be negligible compared to the first term since e_x at y_1 and y_2 will usually be zero or very small. The quantity in braces in the first term is the total rate of diffusive transport in the x direction. By analogy to Fick's law (Eqn. 2-3), define an average diffusion coefficient $\bar{\bar{e}}_x$ so that the total or one dimensional diffusive transport may be represented by

$$\int_A \rho(D_m+e_x)\frac{\partial \bar{c}}{\partial x}dA = \rho\bar{\bar{e}}_x A\frac{\partial C}{\partial x} \qquad \text{A-24}$$

(The contribution of D_m to $\bar{\bar{e}}_x$ will usually be negligible.) Thus,

$$\frac{1}{A}\int_A \frac{\partial}{\partial x}\left[\rho(D_m+e_x)\frac{\partial \bar{c}}{\partial x}\right]dA = \frac{1}{A}\frac{\partial}{\partial x}\left(\rho\bar{\bar{e}}_x A\frac{\partial C}{\partial x}\right)$$

In view of all the manipulations above, Eqn. A-1 may now be written as

$$\frac{1}{A}\frac{\partial}{\partial t}(\underline{\rho}CA) - \frac{\underline{\rho}C}{A}\int_{z_1}^{z_2}(v''_{y_2} - v''_{y_1})\,dz - \cancel{\frac{\underline{\rho}}{A}\int_{z_1}^{z_2}[(c''v'')_{y_2} - (c''v'')_{y_1}]dz} \text{ cancels}$$

$$+\frac{\partial}{\partial x}(\underline{\rho}UC) - \frac{\underline{\rho}U}{A}\int_{z_1}^{z_2}(c''_{y_2}\frac{\partial y_2}{\partial x} - c''_{y_1}\frac{\partial y_1}{\partial x})\,dz - \frac{\underline{\rho}C}{A}\int_{z_1}^{z_2}(u''_{y_2}\frac{\partial y_2}{\partial x} - u''_{y_1}\frac{\partial y_1}{\partial x})\,dz$$

$$+\frac{1}{A}\frac{\partial}{\partial x}[\underline{\rho}\overline{\overline{u''c''}}A] - \frac{\underline{\rho}}{A}\int_{z_1}^{z_2}[(u''c'')_{y_2}\frac{\partial y_2}{\partial x} - (u''c'')_{y_1}\frac{\partial y_1}{\partial x}]dz \qquad \text{A-25}$$

$$+\frac{\underline{\rho}C}{A}\int_{z_1}^{z_2}(v''_{y_2} - v''_{y_1})\,dz + \cancel{\frac{\underline{\rho}}{A}\int_{z_1}^{z_2}[(v''c'')_{y_2} - (v''c'')_{y_1}]dz} \text{ cancels}$$

$$+\frac{\underline{\rho}C}{A}\int_{y_1}^{y_2}(w''_{z_2} - w''_{z_1})\,dy + \frac{\underline{\rho}}{A}\int_{y_1}^{y_2}[(w''c'')_{z_2} - (w''c'')_{z_1}]dy$$

$$= \frac{1}{A}\frac{\partial}{\partial x}(\underline{\rho}\bar{\bar{e}}_x A\frac{\partial C}{\partial x}) + M_P + N_P$$

Eqn. 2-6 is the three dimensional form of the equation of continuity for the solution under consideration. Eqn. 2-6 is

$$\frac{\partial \underline{\rho}}{\partial t} + \frac{\partial}{\partial x}(\underline{\rho}u) + \frac{\partial}{\partial y}(\underline{\rho}v) + \frac{\partial}{\partial z}(\underline{\rho}w) = 0 \qquad \text{A-26}$$

Taking the time average of this equation, one obtains

$$\frac{\partial \underline{\rho}}{\partial t} + \frac{\partial}{\partial x}(\underline{\rho}\bar{u}) + \frac{\partial}{\partial y}(\underline{\rho}\bar{v}) + \frac{\partial}{\partial z}(\underline{\rho}\bar{w}) = 0 \qquad \text{A-27}$$

(See Section 2-4.) Eqn. A-27 may be spatially averaged across the flow section. By going through manipulations similar to those used to obtain Eqn. A-25, the spatial average of Eqn. A-27 is found to be

$$\frac{1}{A}\frac{\partial}{\partial t}(\rho A) - \frac{\rho}{A}\int_{z_1}^{z_2}(v''_{y_2} - v''_{y_1})\,dz + \frac{\partial(\rho U)}{\partial x}$$

$$- \frac{\rho}{A}\int_{z_1}^{z_2}(u''_{y_2}\frac{\partial y_2}{\partial x} - u''_{y_1}\frac{\partial y_1}{\partial x})\,dz + \frac{\rho}{A}\int_{z_1}^{z_2}(v''_{y_2} - v''_{y_1})\,dz \qquad \text{A-28}$$

$$+ \frac{\rho}{A}\int_{y_1}^{y_2}(w''_{z_2} - w''_{z_1})\,dy = 0$$

If Eqn. A-28 is multiplied by C and the result is subtracted from Eqn. A-25, one finds after dividing by ρ that

$$\frac{\partial C}{\partial t} + U\frac{\partial C}{\partial x} - \frac{U}{A}\int_{z_1}^{z_2}(c''_{y_2}\frac{\partial y_2}{\partial x} - c''_{y_1}\frac{\partial y_1}{\partial x})\,dz$$

$$+ \frac{1}{A}\frac{\partial}{\partial x}[\overline{\overline{u''c''}}A] - \frac{1}{A}\int_{z_1}^{z_2}[(u''c'')_{y_2}\frac{\partial y_2}{\partial x} - (u''c'')_{y_1}\frac{\partial y_1}{\partial x}]\,dz \qquad \text{A-29}$$

$$+ \frac{1}{A}\int_{y_1}^{y_2}[(w''c'')_{z_2} - (w''c'')_{z_1}]\,dy = \frac{1}{A}\frac{\partial}{\partial x}(\bar{\bar{e}}_x A\frac{\partial C}{\partial x})$$

$$+ M_P/\rho + N_P/\rho$$

(Recall that only cases of constant density are being considered.)

In most cases of interest to civil engineers, w''_{z_2} and w''_{z_1}

will be zero. The term w'' represents the lateral horizontal velocity. Thus, in both pipes and open channels (even if the free surface is rising or falling), these values of w'' will be zero. The two remaining integral terms in Eqn. A-29 both involve $\frac{\partial y_2}{\partial x}$ and $\frac{\partial y_1}{\partial x}$, so that the integral terms will be zero if the flow area is constant with distance.

In cases where the area is not constant, it may be that the two remaining integral terms will be small enough to be neglected. Consider that u'' will be of the order of U (i.e. $u'' = \mathcal{O}(U)$). The uniformity of concentration which results from lateral turbulent diffusion will generally mean that c'' will be of the order of C or less. It has previously been shown that

$$\int_{z_1}^{z_2} \left(\frac{\partial y_2}{\partial x} - \frac{\partial y_1}{\partial x}\right) dz = \frac{\partial A}{\partial x}$$

Thus,

$$\frac{U}{A} \int_{z_1}^{z_2} \left(c''_{y_2} \frac{\partial y_2}{\partial x} - c''_{y_1} \frac{\partial y_1}{\partial x}\right) dz +$$

$$\frac{1}{A} \int_{z_1}^{z_2} \left[(u''c'')_{y_2} \frac{\partial y_2}{\partial x} - (u''c'')_{y_1} \frac{\partial y_1}{\partial x}\right] dz \qquad \text{A-30}$$

$$= \mathcal{O}\left(\frac{UC}{A} \frac{\partial A}{\partial x}\right)$$

If the changes in the area (i.e. ∂A) are small relative to the area itself (i.e. A), it may be reasonable to neglect the terms of Eqn. A-30 relative to the remaining terms of Eqn. A-29. If this is the case, then the one dimensional form of the mass balance equation becomes

$$\frac{\partial C}{\partial t} + U \frac{\partial C}{\partial x} + \frac{1}{A} \frac{\partial}{\partial x} \left(\overline{\overline{u''c''}} A\right) =$$

$$\frac{1}{A} \frac{\partial}{\partial x} \left(\bar{\bar{e}}_x A \frac{\partial C}{\partial x}\right) + M_p/\rho + N_p/\rho \qquad \text{A-31}$$

Appendix B: Mathematical Manipulations for Obtaining Eqn 6-16 from 6-13

This appendix picks up from eqn. 6-13 and presents the mathematical manipulations which produce an expression (eqn 6-16) for the time variant dispersion coefficient for uniform, estuary type flow.

Define c_p by

$$c_p\ (\rho,\tau) = \int_{-\infty}^{\infty} \xi^p\ \bar{c}\ (\xi,\rho,\tau)\ d\xi \qquad \text{B-1}$$

Hence, c_p is the p^{th} spatial moment of the concentration distribution in a filament along the pipe at some radius ρ. This moment is taken about $\xi = 0$, the origin of a coordinate system moving with the velocity $U(t)$. The term "filament" is used here to denote the volume obtained by projecting a differential element (annulus) of cross section area from $\xi = -\infty$ to $\xi = +\infty$, as shown in fig. B-1a. If the concentration distribution in this filament is interpreted as a geometric area as shown in fig. B-1b, then c_p is the p^{th} moment of this area about the origin of the moving coordinate system ($\xi = 0$).

Also define $m_p\ (\tau)$ as the average value of c_p across the flow section, i.e.

$$m_p\ (\tau) = \frac{1}{\pi}\int_0^1 c_p\ (\rho,\tau)\ 2\pi\rho\ d\rho \qquad \text{B-2}$$

Substituting eqn B-1 for c_p in eqn B-2 and interchanging the order of the two integrations, m_p may be written as

$$m_p\ (\tau) = \int_{-\infty}^{\infty} \xi^p \left[\frac{1}{\pi}\int_0^1 c\ 2\pi\rho\ d\rho\right] d\xi \qquad \text{B-3}$$

The quantity in brackets is the average concentration at a section. Hence, m_p may be interpreted as the p^{th} moment of the average concentration. Thus,

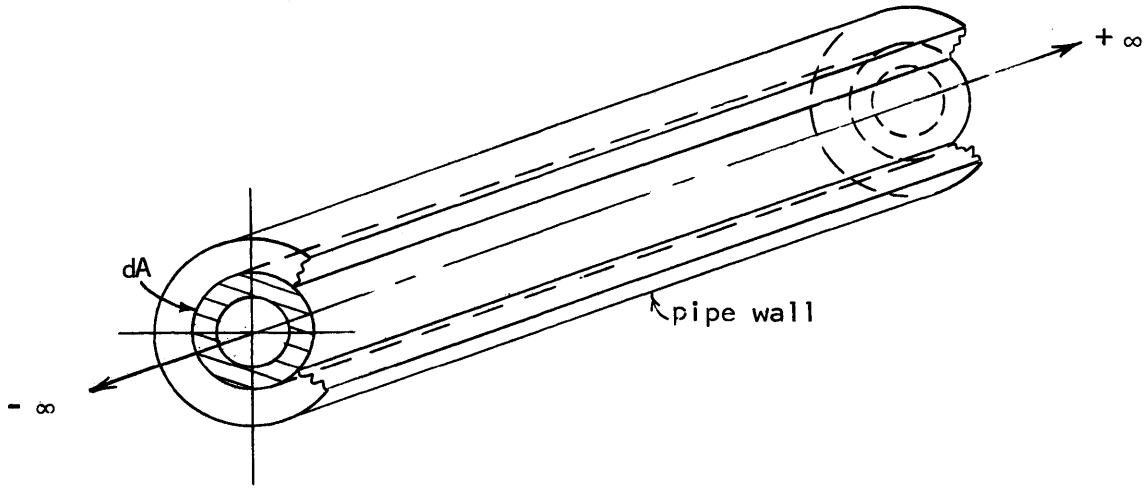

(a) Filament through pipe

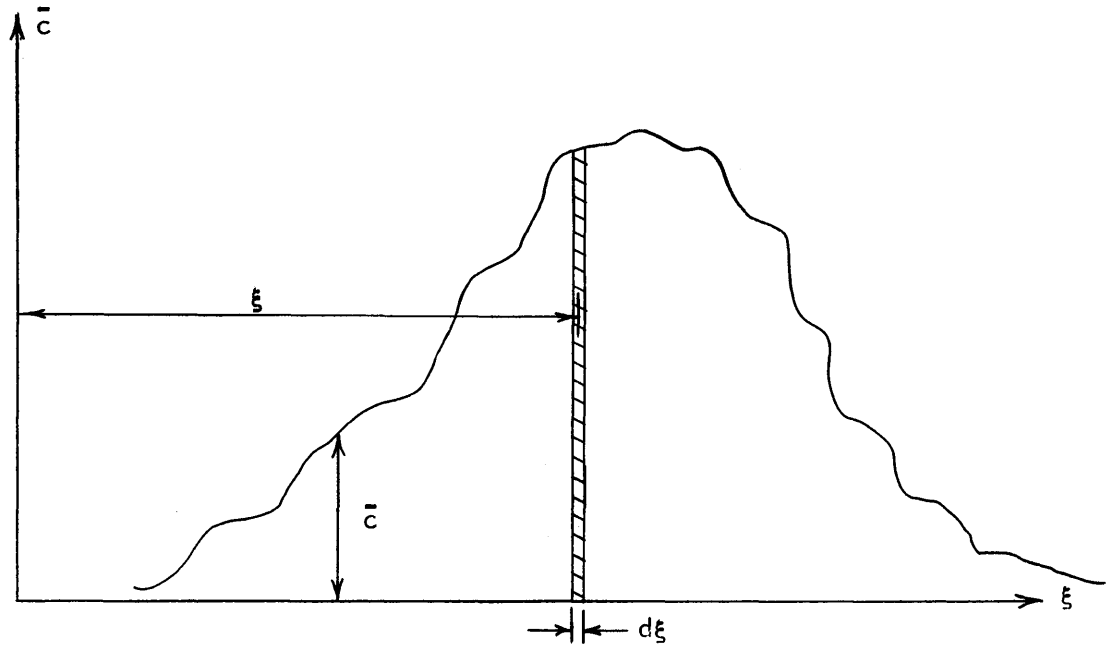

(b) Element in moment integral

Fig. B-1: Definition Sketch

in the development which follows, the information which the m_p's contain about the concentration distribution will be directly applicable to a one-dimensional analysis of transport problems. Specifically, since m_2/m_o is the dimensionless form of the variance, the dispersion coefficient will be related to the time rate of change of m_2/m_o. (See eqn 7-5.) Attention will now be given to obtaining a general expression for m_2. (The zeroth moment, m_o, is a constant since it is related to the total mass of dispersing substance.)

Multiply eqn 6-13 by ξ^p and integrate the result with respect to ξ from $-\infty$ to $+\infty$. This gives a differential equation for c_p:

$$\frac{\partial c_p}{\partial \theta} = \frac{\mu}{\rho} \frac{\partial}{\partial \rho} \left[\rho \psi_o \frac{\partial c_p}{\partial \rho} \right] = \mu p \, (p-1) \, \psi_o \, c_{p-2} + p \eta \lambda_o \, c_{p-1} \qquad \text{B-4}$$

The boundary and initial conditions (eqn 6-6) are now

$$c_p \, (\rho, 0) = c_p^o(\rho)$$

$$\psi_o \frac{\partial c_p}{\partial \rho} = 0 \quad \text{on } \rho = 1 \qquad \text{B-5}$$

In eqn B-4, c_{p-1} and c_{p-2} arise from integration by parts of $\xi^p \, \partial \bar{c}/\partial \xi$ and $\xi^p \partial^2 \bar{c} / \partial \xi^2$. If eqn B-4 is averaged over the cross section, it becomes

$$\frac{dm_p}{d\theta} = \mu p \, (p-1) \, \overline{\overline{\psi_o \, c_{p-2}}} + p \eta \, \overline{\overline{\lambda_o \, c_{p-1}}} \qquad \text{B-6}$$

with the initial condition

$$m_p(0) = m_p^o \qquad \text{B-7}$$

The first term on the right-hand side of eqn B-4 disappears under this

averaging process since $\psi_o \partial c_p/\partial\rho = 0$ on $\rho = 1$. In eqn A-6, the double bar signifies averaging over the cross section, as defined in eqn A-2, (i.e. $m_p = \bar{\bar{c}}_p$).

Equations B-4 and B-5, with p = 0, are

$$\frac{\partial c_o}{\partial \theta} = \frac{\mu}{\rho} \frac{\partial}{\partial \rho} \left[\rho \psi_o \frac{\partial c_o}{\partial \rho} \right] \qquad \text{B-8}$$

and

$$c_o (\rho, 0) = c_o^o(\rho)$$

$$\psi_o \frac{\partial c_o}{\partial \rho} = 0 \quad \text{on} \quad \rho = 1 \qquad \text{B-9}$$

Assume a separable solution for c_o, i.e.

$$c_o (\rho, \theta) = R(\rho) \cdot W(\theta)$$

Then, from eqn B-8,

$$\frac{1}{W} \frac{dW}{d\theta} = \frac{\mu}{\rho R} \frac{d}{d\rho} \left[\rho \psi_o \frac{dR}{d\rho} \right] = - \beta^2 \qquad \text{B-10}$$

where the minus β^2 is necessary for c_o to remain finite as θ increases. From eqn B-10,

$$\frac{dW}{d\theta} + \beta^2 W = 0$$

and

$$W = b \exp (-\beta^2 \theta)$$

where b is a constant. For the conditions being considered, there will be

an increasing sequence of eigenvalues, β_n^2, and a set of ortho-normal eigenfunctions, R_n, satisfying the remaining part of eqn B-10. Thus,

$$\frac{\mu}{\rho}\frac{d}{d\rho}\left[\rho\psi_o\frac{dR_n}{d\rho}\right] + \beta_n^2 R_n = 0$$

and

$$\psi_o\frac{dR_n}{d\rho} = 0 \quad \text{on} \quad \rho = 1$$

(ref. 7 and 10). The solution to eqn B-8 may now be written as

$$c_o(\rho,\theta) = k_1 + \sum_{n=1}^{\infty} b_n R_n(\rho) \exp(-\beta_n^2\theta) \qquad \text{B-11}$$

where the b_n's are defined by

$$c_o^o(\rho) = k_1 + \sum_{n=1}^{\infty} b_n R_n(\rho) \qquad \text{B-12}$$

The b_n's may be calculated from eqn B-12 by using the orthogonality of the R_n's. Note that as θ gets large, c_o approaches a constant value k_1, and is thus independent of ρ. Since c_o is the amount of the substance P in a filament within the pipe, this implies that P becomes uniformly mixed across the pipe as θ gets large. Thus, at large θ, c_o becomes its own average across the section. But m_o is also the average of c_o. Hence, k_1 equals m_o.

Introducing c_o from eqn B-11 into eqn B-6 with $p = 1$,

$$\frac{dm_1}{d\theta} = \eta\lambda_o\left[m_o + \sum_{n=1}^{\infty} b_n R_n \exp(-\beta_n^2\theta)\right] \qquad \text{B-13}$$

or

$$\frac{dm_1}{d\theta} = \eta\sum_{n=1}^{\infty} b_n \overline{\lambda_o R_n} \exp(-\beta_n^2\theta) \qquad \text{B-14}$$

since $\overline{\lambda_o m_o} = m_o\bar{\lambda}_o = 0$, λ_o being the velocity defect withrrespect to the one

dimensional velocity U. Integrating this expression with respect to θ from zero to infinity and interchanging the order of integration and summation,

$$m_1(\infty) - m_1(0) = \eta \sum_{n=1}^{\infty} b_n \overline{\overline{\lambda_o R_n}}\, \beta_n^{-2} \qquad \text{B-15}$$

In this summation, b_n and β_n are constants. R_n and λ_o are functions of ρ, but $(\lambda_o R_n)$ is averaged over the cross section. Thus, $m_1(\infty)$ is a constant. This implies that the center of gravity (i.e. the first moment of the concentration distribution) of the substance P ultimately moves with the mean fluid velocity U(t) since eqn B-15 is referred to a coordinate system moving with this speed.

Let

$$c_1(\rho,\theta) = \bar{\bar{c}}_1 + m_o\, \phi(\rho,\theta) = m_1 + m_o\, \phi(\rho,\theta)$$

Thus ϕ is related to the variation of c_1 with respect to its mean. Then, equations B-4 and B-5 with p = 1 become

$$\frac{\partial m_1}{\partial \theta} + m_o \frac{\partial \phi}{\partial \theta} = \mu \frac{m_o}{\rho} \frac{\partial}{\partial \rho} \left[\rho \psi_o \frac{\partial \phi}{\partial \rho} \right] + \eta \lambda_o \left[m_o + \sum_{n=1}^{\infty} b_n R_n \exp(-\beta_n^2 \theta) \right] \qquad \text{B-16}$$

and

$$\psi_o \frac{\partial \phi}{\partial \rho} = 0 \quad \text{on} \quad \rho = 1 \qquad \text{B-17}$$

Consider eqn B-16 as θ approaches infinity. It has been shown that $m_1(\infty)$ equals a constant (eqn B-15). Hence, as θ approaches infinity, $\partial m_1 / \partial \theta$ approaches zero. Also, the summation term will approach zero because of the exponential function. Furthermore, since eqn B-16 is a diffusion-type equation, it will only admit solutions for ϕ that are either increasing or decreasing in θ. Since only a finite amount of the substance P was introduced into the flow, c_1 and thence ϕ are finite. Thus, only the decreasing solution is allowed, and $\partial \phi / \partial \theta$ must equal zero as θ approaches infinity.

As a result, at large θ, ϕ is a function of ρ only. Equations B-16 and B-17 become

$$\frac{\mu}{\rho}\frac{d}{d\rho}\left[\rho\psi_o\frac{d\phi}{d\rho}\right] = -\eta\lambda_o \qquad \text{B-18}$$

and

$$\psi_o\frac{d\phi}{d\rho} = 0 \quad \text{on} \quad \rho = 1 \qquad \text{B-19}$$

after dividing through by m_o.

From this point forward, let considerations be limited to conditions as θ approaches infinity. Then

$$c_1 = m_1 + m_o\,\phi(\rho)$$

and eqn B-6 with p = 2 becomes

$$\frac{dm_2}{d\theta} = 2\mu\,\overline{\overline{\psi_o m_o}} + 2\eta\,\overline{\overline{\lambda_o(m_1 + m_o\,\phi(\rho))}} \qquad \text{B-20}$$

But

$$\overline{\overline{\lambda_o m_1}} = \overline{\overline{\lambda_o}}\,m_1 = 0$$

so

$$\frac{1}{2m_o}\frac{dm_2}{d\theta} = \mu\,\overline{\overline{\psi_o}} + \eta\,\overline{\overline{\phi\lambda_o}} \qquad \text{B-21}$$

Eqn B-21 is the expression which was being sought for the second moment ($\dot{m}_2$) of the one-dimensional concentration distribution. In the paragraphs which follow, it will be shown that $dm_2/d\theta$ is indeed related to the coefficient of longitudinal dispersion. In eqn B-21, the $\overline{\overline{\psi}}_o$ -term accounts for that part of dispersion due to longitudinal, turbulent diffusion and the

$\overline{\overline{\phi\lambda_o}}$ -term is that part due to the combined effects of the differential convection associated with the velocity distribution and to the lateral diffusion.

It will be noticed that eqn B-21 applies only as time approaches infinity, and it was stated above that this equation will be used to find the dispersion coefficient. At first, it may appear that the generality of the dispersion coefficient obtained in this manner will be limited. However, this conclusion is not valid for the following reason: In the preceding development, the time which approaches infinity is time measured from some arbitrary origin which is associated with the initial condition on the concentration $\bar{c}$. Also, it was assumed that the presence of the dispersing substance does not affect the flow pattern; thus, the substance does not affect the rate of dispersion either. This means that the dispersion process is independent of the measurement of time associated with the dispersing substance. Hence, eqn B-21 represents the rate of dispersive mass transport at the origin of time as well as at times approaching infinity.

Aris (ref. 7) shows that the longitudinal distribution of a dispersing substance in steady, uniform flow approaches normality as time (τ) approaches infinity. This conclusion is also applicable to the unsteady case since the mathematical proof is identical if the variable τ in Aris' work is replaced by θ. This normality implies that

$$C \sim \frac{1}{\sqrt{2\pi m_2/m_o}} \exp - \frac{[\xi - k_2]^2}{2m_2/m_o} \qquad \text{B-22}$$

where k_2 is a constant defined as the coordinate of the center of gravity of the normal curve and C is the average concentration at a given section. Eqn B-15 guarantees that k_2 is a constant. The second moment, m_2, is a linear function of θ defined by eqn B-21 and m_o is a constant since the zeroth moment is related to the total mass of dispersing substance. The fact that the concentration approaches normality implies that the dispersion process is behaving as a random diffusion process. This implication is also substantiated by the argument which follows:

Consider an arbitrary station ξ_o along the pipe. From eqn B-22, one can find the rate at which mass is being transported past this station due to dispersion. Call this transport rate q_p. At any time, the amount of mass in the region $\xi_o < \xi$ will be

$$A \int_{\xi_o}^{\infty} \rho \, Ca \, d\xi$$

where A is the cross sectional area of the pipe, a is the pipe radius which was used to non-dimensionalize the x coordinate, and ρ is the fluid density. Continuity requires that the time rate of change of this quantity be equal to q_p, i.e.

$$q_p = \frac{A}{T_r} \frac{\partial}{\partial \tau} \int_{\xi_o}^{\infty} \rho \, Ca \, d\xi$$

$$= \frac{A \, F(\tau)}{T_r} \frac{\partial}{\partial \theta} \int_{\xi_o}^{\infty} \rho \, Ca \, d\xi \qquad \text{B-23}$$

where T_r is the reference time used to non-dimensionalize t. Interchanging the order of differentiation and integration in eqn B-23, and then carrying out these operations using eqn B-22, one finds

$$q_p = - A \left[\frac{a^2}{T_r} \frac{F(\tau)}{2m_o} \frac{dm_2}{d\theta} \right] \rho \frac{\partial C}{\partial x} \qquad \text{B-24}$$

since $\partial C / \partial x$ equals $\partial C / \partial (a\xi)$. Comparison with eqn 2-3 shows that the rate of transport q_p follows a Fickian law if the dispersion coefficient as a function of time (i.e. E_t) is given by the bracketed quantity in eqn B-24. Thus,

$$E_t = \frac{a^2}{T_r} \frac{F(\tau)}{2m_o} \frac{dm_2}{d\theta} \qquad \text{B-25}$$

Eqn B-21 gives an expression for $dm_2/d\theta$, and eqn 6-7 defines $F(\tau)$. Also, from eqn 6-7 and from the definition of e_o following eqn 6-9, it can be seen that $\mu = \kappa\eta = \kappa V T_r / a$. Combining all these expressions, E_t may be written as

$$E_t = aV \left(\frac{u_*(\tau)}{V}\right) \left[\kappa\overline{\overline{\psi_o}} + \overline{\overline{\phi\lambda_o}}\right] \qquad \text{B-26}$$

(It will be convenient for further use to leave the quantity $u_*(\tau)/V$, i.e. $F(\tau)$, and not cancel the V's). Comparison with Aris (ref. 7) and Taylor (ref. 53) shows that the quantity in brackets was evaluated by Taylor and found to be 10.1 for the velocity distribution (λ_o) which he used. Because of the assumed similarities between steady and unsteady flow, eqn B-26 may now be written as

$$E_t = 10.1 \left(\frac{u_*(\tau)}{V}\right) aV \qquad \text{B-27}$$

Under the assumptions which have been made, this expression (with the V's cancelled) now bears out the fact that the dispersion coefficient in unsteady flow is the same at each instant as for a steady flow at the same velocity as exists at that instant. (Compare eqn B-27 and eqn 3-4.)

Table B-1: Velocity Distribution Used by Taylor (ref. 53)

$\rho = \frac{r}{a}$	$\frac{\bar{u}_{max} - \bar{u}}{u_*}$
0	0
0.10	0.059
0.20	0.236
0.30	0.530
0.35	0.750
0.40	1.01
0.45	1.29
0.50	1.62
0.55	2.00
0.60	2.42
0.65	2.89
0.70	3.40
0.75	4.05
0.80	4.80
0.85	5.79
0.90	7.10
0.92	7.66
0.94	8.37
0.96	9.36
0.97	10.11
0.98	11.12
0.99	12.85
1.00	∞

r = radial coordinate measured from centerline of pipe

a = pipe radius

$\bar{u}_{max}$ = maximum (centerline) velocity

u_* = $\sqrt{\tau_o / \rho}$

U = spatially averaged velocity = $\bar{u}_{max} - 4.25\ u_*$

Appendix C: Summary of Head Loss Results

Run No.	Date	Piezometric Gradient	Mean Velocity	Friction Factor X 100	Reynolds Number $X10^{-4}$
		ft/100 ft	fps		
1	Mar 7,'64	0.738	1.41	3.20	1.67
2		1.176	1.87	2.91	2.21
3		2.190	2.66	2.70	3.15
4		3.455	3.39	2.60	4.02
5		4.51	3.94	2.51	4.67
6		5.79	4.48	2.49	5.32
7		7.775	5.20	2.48	6.16
8	Mar 13,'64	2.41	2.79	2.67	2.79
9		2.41	2.70	2.86	2.70
10		0.990	1.65	3.14	1.65
11		0.990	1.678	3.04	1.68
12		0.530	1.181	3.28	1.18
13		0.530	1.208	3.13	1.21
14		3.335	3.23	2.76	3.24
15		3.335	3.24	2.74	3.26
16		4.15	3.65	2.69	3.65
17		4.15	3.66	2.68	3.69
18		5.27	4.16	2.63	4.21
19		5.27	4.16	2.64	4.21
20		6.37	4.18	3.15	4.26
21		7.58	5.14	2.48	5.25
22		7.58	5.08	2.54	5.19
23		8.74	5.53	2.47	5.65
24		8.74	5.53	2.47	5.65
25		3.41	3.265	2.77	3.35
26		0.748	1.440	3.11	1.48
27	May 5,'64	1.368	2.10	2.68	2.63
28		2.56	2.95	2.54	3.69
29		3.43	3.52	2.39	4.40

Run No.	Date	Piezometric Gradient	Mean Velocity	Friction Factor X 100	Reynolds Number $X10^{-4}$
		ft/100 ft	fps		
30	May 5,'64	4.61	4.03	2.45	5.04
31		5.81	4.55	2.42	5.69
32		6.74	4.94	2.38	6.17
33		7.95	5.39	2.36	6.74
34	May 6,'64	1.441	2.10	2.82	2.63
34a		1.441	2.14	2.72	2.68
35		2.64	2.92	2.67	3.66
35a		2.64	2.97	2.58	3.72
36		3.72	3.44	2.71	4.31
36a		3.72	3.54	2.56	4.43
37		4.77	4.00	2.58	5.01
37a		4.77	4.07	2.49	5.10
38		5.99	4.53	2.57	5.68
38a		5.99	4.58	2.46	5.74
39		7.40	5.11	2.46	6.40
39a		7.40	5.14	2.42	6.44
40	June 12,'64	1.825	2.43	2.67	3.16
41		3.85	3.59	2.58	4.67
42		5.57	4.42	2.46	5.75
43		7.90	5.24	2.48	6.82
44		1.499	2.17	2.75	2.82
45		3.71	3.52	2.58	4.58
46		5.93	4.53	2.49	5.90
47		8.12	5.33	2.47	6.93

Appendix D: Summary of Dispersion Tests for Estuary Type Flow

Run No.	U_f fps	U_T fps	T sec	$R_A \times 10^{-4}$	$f_T \times 10^2$	$E_{A_{calc}}$ ft^2/sec	$E_{A_{obs}}$ ft^2/sec	$\frac{E_{A_{obs}}}{E_{A_{calc}}}$
8	0.171	6.25	18.7	4.75	2.40	0.152	0.140	0.921
9	0.174	4.77	24.5	3.63	2.46	0.117	0.140	1.20
10	0.0467	6.18	18.9	4.70	2.40	0.152	0.178	1.19
11	0.0467	4.91	23.8	3.73	2.47	0.121	0.151	1.25
12	0.0467	3.945	29.6	3.00	2.53	0.0982	0.135	1.37
13	0.1022	6.15	19.0	4.94	2.38	0.149	0.172	1.15
14	0.1011	4.89	23.9	3.92	2.45	0.120	0.136	1.13
15	0.1011	3.92	29.8	3.15	2.52	0.0976	0.134	1.37
16	0.01372	6.15	19.0	4.81	2.38	0.149	0.174	1.17
17	0.01374	4.87	24.0	3.81	2.46	0.120	0.157	1.31
18	0.01401	3.92	29.8	3.06	2.53	0.0976	0.134	1.37
19	0.00980	6.15	19.0	4.94	2.38	0.149	0.180	1.21
20	0.01006	4.87	24.0	3.91	2.45	0.120	0.159	1.32
21	0.00996	3.92	29.8	3.15	2.52	0.0976	0.137	1.40
22	0.1780	6.83	19.2	5.48	2.36	0.164	0.183	1.12
23	0.1769	5.42	24.2	4.36	2.41	0.132	0.146	1.11
24	0.1766	4.375	30.0	3.52	2.49	0.108	0.141	1.31
25	0.1399	6.83	19.2	5.48	2.36	0.164	0.182	1.11
26	0.1383	5.44	24.1	4.37	2.41	0.133	0.157	1.18
27	0.1390	4.375	30.0	3.52	2.49	0.108	0.142	1.31
28	0.1747	5.29	30.3	3.94	2.45	0.130	0.158	1.22
29	0.1747	5.29	30.3	3.94	2.45	0.130	0.158	1.22
30	0.1739	6.51	24.6	4.86	2.38	0.157	0.172	1.10
31	0.1739	6.51	24.6	4.86	2.38	0.157	0.169	1.08
32	0.1719	8.05	19.9	6.01	2.33	0.192	0.191	0.995
33	0.1719	8.05	19.9	6.01	2.33	0.192	0.207	1.08
34	0.1061	5.27	30.4	4.24	2.43	0.129	0.157	1.22
35	0.1061	4.33	37.0	3.48	2.48	0.107	0.149	1.39

Run No.	U_f fps	U_T fps	T sec	$R_A \times 10^{-4}$	$f_T \times 10^2$	$E_{A_{calc}}$ ft^2/sec	$E_{A_{obs}}$ ft^2/sec	$\frac{E_{A_{obs}}}{E_{A_{calc}}}$
36	0.1060	3.52	45.5	2.83	2.55	0.0825	0.142	1.72
37	0.1054	2.90	55.4	2.33	2.63	0.0730	0.122	1.69
38	0.1065	2.34	68.5	1.88	2.70	0.0600	0.108	1.80

U_f = "through flow" velocity

U_T = maximum (amplitude) of oscillatory velocity

T = period of oscillation

R_A = average Reynolds number (based on $\frac{2}{\pi} U_T$)

f_T = friction factor corresponding to R_T (i.e. $\frac{\pi}{2} R_A$)

$E_{A_{calc}}$ = average dispersion coefficient calculated by eqn. 6-25

$E_{A_{obs}}$ = average dispersion coefficient observed in experiment (factor B = 11.03 for all runs)

Appendix E: Definition of Symbols

A	cross sectional area; subscript denoting average of a quantity during a period of oscillation	$[L^2]$
B	dimensionless factor	
C	average concentration at a section	
C_s	value of C at times differing by a full period	
D	pipe diameter	$[L]$
D_m	molecular (mass) diffusivity	$[L^2/T]$
E	longitudinal dispersion coefficient	$[L^2/T]$
E'	longitudinal dispersion coefficient in saline portion of an estuary (including effects of gravitational convection)	$[L^2/T]$
G	rate of turbulent energy dissipation per unit mass of fluid	$[M/L^2T]$
M_P	mass rate per unit volume of addition of substance P due to diffusion at the lateral flow boundaries	$[M/L^3T]$
N_P	average mass rate per unit volume of creation of substance P within one dimensional fluid element	$[M/L^3T]$
R_H	hydraulic radius	$[L]$
R	Reynolds number	
Q	volumetric fluid discharge rate (UA)	$[L^3/T]$
T	period of oscillation in estuary type flow; subscript denoting a quantity associated with U_T; temperature	$[T]$
U	velocity in x direction averaged over the cross section	$[L/T]$
U_T	amplitude of tidal or oscillatory component of velocity	$[L/T]$
V	velocity in the y direction averaged over the cross section	$[L/T]$
W	velocity in the z direction averaged over the cross section	$[L/T]$
a	pipe radius	$[L]$
b	a constant; fluid excursion during half a period of oscillation	$[L]$
c	concentration	
c_p	p^{th} moment of spatial concentration distribution in a filament in a pipe	
e	turbulent (mass) diffusivity	$[L^2/T]$
f	Darcy-Weisbach friction factor; subscript denoting a quantity associated with the fresh water flow in an estuary	
g	acceleration of gravity	$[L/T^2]$

h	depth of open channel flow	$[L]$
i	subscript in finite difference equation to indicate the value of x at which a quantity is to be evaluated	
j	mass rate of flux due to diffusion; subscript in finite difference equation to indicate the value of t at which a quantity is to be evaluated	$[M/T]$
k	a constant; equivalent sand grain roughness	$[L]$
m	subscript denoting a quantity associated with a model	
m_p	p^{th} moment of one dimensional spatial concentration distribution	
n	0,1,2,3,...; Manning's roughness parameter	$[L^{1/6}]$
n_p	mass rate per unit volume of creation of substance P within an elemental fluid volume	$[M/L^3T]$
o	subscript denoting a reference quantity	
p	subscript denoting quantity associated with the peak of a temporal concentration distribution; subscript denoting quantity associated with a prototype which is being modelled	
r	radial coordinate; subscript denoting ratio of a model quantity to the corresponding prototype quantity	$[L]$
t	time	$[T]$
u,v,w	fluid velocities in the x,y,z directions	$[L/T]$
u_*	shear velocity ($\sqrt{\tau_o/\rho}$)	$[L/T]$
x,y,z	Cartesian coordinate directions	$[L]$
δ	a constant representing the time shift between an arbitrary time origin and the time of zero oscillatory velocity	$[T]$
δ_s	laminar sublayer thickness	$[L]$
ϵ	eddy viscosity (turbulent momentum diffusivity)	$[L^2/T]$
κ	von Karman's constant (in logarithmic velocity distribution)	
λ	dimensionless distribution of velocity defect in shear flow	
μ	dimensionless constant	
μ_p	p^{th} moment of temporal concentration distribution	$[T^{p+1}]$
ν	kinematic viscosity	$[L^2/T]$
ξ	dimensionless longitudinal coordinate	
ρ	dimensionless radial coordinate	
ρ	fluid density	$[M/L^3]$

σ	frequency of oscillation	$[1/T]$
σ^2	spatial variance of concentration distribution	$[L^2]$
τ	time; dimensionless time	$[T]$
$\underline{\tau}$	shear stress	$[F/L^2]$
$\underline{\tau}_o$	boundary shear stress	$[F/L^2]$
ϕ	dimensionless function related to the distribution of concentration across a flow section; a variable	
ψ	dimensionless turbulent diffusivity	
$\bar{}$	time average	
$=$	average over cross sectional area	
$\approx$	approximately equal	
$\sim$	proportional to	
$'$	turbulent variation from time averaged quantity (except on E')	
$''$	spatial variation (within the cross section) from spatial average of a quantity at a cross section	

Appendix F: List of Figures and Tables